

PREFACE

The important role played by the platinum electrode surface in electrocatalytic reactions is now well known. In the oxidation of many organic compounds, the platinum surface provides sites for the dissociative adsorption of organic molecules with subsequent oxidation of the adsorbed species. The catalytic efficiency of the platinum surface in such reactions depends on the nature of any species already adsorbed on the surface, e.g. hydrogen or oxygen, which arise when an aqueous electrolyte is employed. The potential range over which the platinum surface in aqueous H_2SO_4 media is free from chemisorbed hydrogen or oxygen species is very limited, and as a result work has been performed on platinum electrodes in non-aqueous, aprotic solvents such as acetonitrile. Absence of water in the acetonitrile solvent system not only extends the potential range over which the platinum electrode is free from chemisorbed hydrogen or oxygen species, but it also allows the use of high cathodic or anodic potentials without the evolution of hydrogen or oxygen, respectively. Acetonitrile has thus been extensively employed in the study of organic redox reactions which often occur at very high cathodic or anodic potentials with passage of currents which are smaller than those which arise in the case of faradaic hydrogen or oxygen evolution.

Very little work has appeared regarding the electrochemical properties of acetonitrile itself, e.g. with regard to its possible influence on the platinum electrode surface. Where acetonitrile has been used as solvent, it has generally been assumed that it is inert towards the platinum surface and hence does not influence the kinetics and mechanism of the reaction under investigation. In the present work, the electroactivity of methanol and formic acid at platinum in anhydrous acetonitrile has been studied and an interpretation of the results follows after an investigation of the behavior of acetonitrile itself at platinum electrodes in aqueous media. Thus, the general assumption that acetonitrile is an inert solvent at platinum electrodes comes under careful and critical examination in Part I of Chapter III. A direct result of the work with acetonitrile in aqueous media was the discovery of the new anodic hydrogen displacement effect which is of general interest with regard to electrochemical hydrogenation of organic molecules and which is described in Part II of Chapter III.

There have been previous reports regarding the activating effects which several catalyst "poisons" have on the formic acid oxidation reaction at platinum; however, no reasons have been given for this unexpected result. In this work, the effect was also observed with acetonitrile and mercury, and an explanation is presented in terms of the formation of an inhibiting species derived from formic acid.

In fact, a considerable amount of research has been performed over the past fifteen years regarding the identity of the formic acid poison and a new possible identity is given in Part III of Chapter III which fits all of the experimental observations from this and related work.

The work presented in this thesis has either been published or is in course of publication as indicated below:

1. Reactivity of Surface Oxides in Fuel Cell Oxidations.
B.E. Conway, H.A. Kozłowska, B. MacDougall and B.V. Tilak, Proc. 2nd International Conference on Fuel Cells, 1968, publ. S.E.R.A.I., Brussels, 1969.
2. The Anodic H Displacement in Organic Adsorption at Platinum. B. MacDougall, H.A. Kozłowska and B.E. Conway, J. Electroanal. Chem., 32 (1971) 477 (App. 15).
3. Anodic Displacement of Adsorbed H in Electrochemisorption of Organic Molecules at Platinum. B.E. Conway, B. MacDougall and H.A. Kozłowska, Trans. Faraday Soc., accepted for publication (1972).
4. Electrochemisorption and Reactivity of Nitrites at Platinum Electrodes and the Anodic H Desorption Effect. B.E. Conway, B. MacDougall and H.A. Kozłowska, J. Electroanal. Chem., accepted for publication (1972).
5. Effects of Acetonitrile on the Oxidation of Formic Acid and Methanol in Aqueous Media. H.A. Kozłowska, B. MacDougall and B.E. Conway, J. Electrochem. Soc., in course of publication (1972).

6. Resolution of Reaction Charge Components by the Kinetic Relaxation Method. B. MacDougall, H.A. Kozłowska and B.E. Conway, J. Electroanal. Chem., in course of publication (1972).
7. Electrochemistry of Fuel Cell Processes. B.E. Conway, H.A. Kozłowska and B. MacDougall, D.R.B. Reports on Grant No. 5412-01, 1969, 1970, 1971.

For convenience, the page number for a figure given in the List of Figures refers to the nearest page of the text which follows the figure. For consistency, the same policy was adopted in the List of Tables.

ACKNOWLEDGEMENTS

The author wishes to thank Professor B.E. Conway for his direction and guidance throughout the course of this work. Dr. Conway was at all times willing and able to give assistance and suggestions when difficulties arose, no matter how busy he was himself. It was indeed a pleasure to work with such a capable and understanding person.

The author also wishes to thank Dr. H.A. Kozłowska, Senior Research Assistant in electrochemistry, who served as research director of the project during the year 1969-1970 in the absence of Dr. Conway who was Commonwealth Visiting Professor. She took a deep interest in the work and continued its supervision, in collaboration with Professor Conway, until its completion. Her instruction in electrochemistry was fundamental to the successful conclusion of this work.

The author thanks the graduate students and post-doctoral fellows of lab 151 for assistance in many ways during the course of this work. Also, the members of the teaching staff of the Department of Chemistry at the University of Ottawa were always available for discussion on many matters of chemistry.

The work of Mrs. E. Storto in typing the thesis and Mrs. E. Szabo in drawing most of the diagrams is also acknowledged.

TABLE OF CONTENTS

	<u>Page</u>
PREFACE	i
ACKNOWLEDGEMENTS	v
TABLE OF CONTENTS	vi
LIST OF FIGURES	xiii
LIST OF TABLES	xxiv
ABSTRACT	xxv

CHAPTER I

INTRODUCTION

1. Oxidation Processes on Platinum Anodes	1
(a) Electrocatalysis	1
(b) Nature of the platinum electrode surface in contact with aqueous solution	3
(c) Oxidation of simple organic molecules at platinum electrodes	8
(d) Inhibition effects in organic oxidation reactions at platinum electrodes	15
(e) Use of non-aqueous solvent systems with platinum electrodes	23
2. Choice and Basis of Experimental Methods Used in the Present Work for Studying Electrode Processes	27
(a) Steady-state method	27
(b) Non steady-state methods	29
(c) Controlled mass-transfer experiments	43
3. Aims of the Work	44

CHAPTER II

EXPERIMENTAL

1. Introduction	47
2. Preparation of Solutions	47
(a) Criteria of solution purity	47
(b) Purification of acetonitrile and organic reagents	50
3. Preparation of Electrode Metal Surfaces	52
4. Reference Electrodes	54
5. Gases	55
6. Cells	56
7. Electrical Circuits	58
8. Temperature	59
9. Experimental Procedures	59
(a) Steady-state measurements	59
(b) Potentiodynamic sweep measurements	60
(c) Evaluation of charge components for acetonitrile surface reactions at platinum	62

CHAPTER III

RESULTS AND DISCUSSION

Part I

Electrochemisorption and Reactivity of Nitriles at Platinum Electrodes	64
I.1 Behavior of Acetonitrile at Platinum in Aqueous H ₂ SO ₄ Solutions	64
(a) Introduction	64

	<u>Page</u>
(b) General behavior of acetonitrile at platinum as determined by the potentiodynamic sweep method	67
(c) Adsorption and reaction characteristics of acetonitrile in the double-layer region at platinum	68
(d) Electrode coverage by acetonitrile and blocking of hydrogen adsorption	72
(e) Reversibility of the acetonitrile reaction in the double-layer potential region	76
(f) Adsorption transients and the nature of acetonitrile chemisorption	78
(g) pH Dependence of the peak currents for acetonitrile reduction and oxidation	84
I.2 Involvement of the H Adsorption/Desorption Potential Region in the Acetonitrile Reactions at Platinum	84
(a) General observations	84
(b) Resolution of component currents and charges in the anodic and cathodic H regions by means of kinetic relaxation studies	85
(c) Kinetic heterogeneity in the double-layer potential region	90
(d) Dependence of acetonitrile oxidation charge on reversal potential in the cathodic-going sweep	91
(e) Evaluation of effects of holding the potential at the cathodic end of the sweep	96
I.3 Mechanism of Acetonitrile Adsorption and Reaction at Platinum	101
(a) Orientation, surface coverage and nature of the chemisorbed nitrile species	101
(b) Characterization of the slow component in acetonitrile reduction	104

	<u>Page</u>
(c) Mechanism of the surface reactions of acetonitrile at platinum	107
I.4 Involvement of Surface Oxide in Acetonitrile Reactions at Platinum	111
(a) Introduction	111
(b) Reaction of acetonitrile in the surface oxide region	112
(c) Relation between the behavior of adsorbed CH ₃ CN in the surface oxide region and that in the H region	119
(d) Identity and characterization of the B species	123
(e) Summary of the behavior of acetonitrile at platinum in aq. H ₂ SO ₄	126

Part II

Anodic Displacement of Adsorbed Hydrogen in Electrochemisorption of Organic Molecules at Platinum	130
(a) Introduction	130
(b) Chemisorption of sulfur compounds with anodic hydrogen displacement	131
(c) Anodic H displacement in relation to dissociative chemisorption	134
(d) Mechanism of sulfur compounds adsorption	136
(e) Adsorption of benzene in the hydrogen region at platinum	139
(f) Adsorption of nitriles in the hydrogen region at platinum	141
(g) Behavior of thiourea at nickel electrodes	146
(h) Summary of the anodic hydrogen displacement effect	147

Part III

Effects of Acetonitrile on the Oxidation of Formic Acid and Methanol in Aqueous Media	149
(a) Introduction	149
(b) Formic acid and methanol oxidation at platinum in the presence of acetonitrile	150
(c) Role of acetonitrile in formic acid oxidation	155
(d) Relation to mechanism of formic acid oxidation	161
(e) Time effects in the hydrogen region	164
(f) Effects of higher concentrations of acetonitrile	170
(g) Effects of mercury on the oxidation of formic acid at platinum	172
(h) Relation between the effects of mercury and acetonitrile	176
(i) Effect of solution impurity adsorption on the formic acid reaction	178
(j) Summary of the effects of acetonitrile on the oxidation of formic acid at platinum	182

Part IV

Studies Under Non-Aqueous Conditions	184
(a) Introduction	184
(b) Reference current-potential profiles in anhydrous acetonitrile in the absence of oxidizable substances	185
(c) Effects of additions of small quantities of water to the anhydrous system	186
(d) Oxidation of molecular hydrogen in acetonitrile	188

	<u>Page</u>
(e) Oxidation of molecular hydrogen in aqueous solutions	190
(f) Oxidation of formic acid in acetonitrile	192
(g) Oxidation of formaldehyde and methanol in acetonitrile	193
(h) Conclusions from the work in nominally anhydrous acetonitrile	193
(i) Summary of the results of non-aqueous studies	195
CLAIMS TO ORIGINAL RESEARCH	197
REFERENCES	200

LIST OF FIGURES

<u>Figure</u>		<u>Page</u>
1	Potentiodynamic current (i)-potential (V) profile for Pt in 1N H ₂ SO ₄ at (dV/dt) = 50 mV sec ⁻¹ in the potential range between appreciable hydrogen and oxygen evolution.	5
2	(a) Potentiodynamic i-V profile for Pt in 0.25M CH ₃ OH at dV/dt = 50 mV sec ⁻¹ ; potential range 0.05 to 1.5 V, E _H . (b) Potentiodynamic i-V profile for Pt in 0.25M HCOOH at dV/dt = 50 mV sec ⁻¹ ; potential range 0.05 to 1.5 V, E _H .	15
3	Photograph of the electrochemical cell frequently used for studies under aqueous conditions.	57
4	Electrical circuit for potentiostatic steady-state polarization.	59
5	Electrical circuit for potentiodynamic current-potential measurements.	59
6	Adsorption isotherm for thiourea (●), dimethylsulphide (x), acetonitrile (□), benzonitrile (■), and benzene (o) at Pt at 25°C, 1N H ₂ SO ₄ , represented in terms of their blocking effects on H electrochemisorption.	63
7	Potentiodynamic i-V profiles for adsorbed acetonitrile at platinum as a function of [CH ₃ CN] in relation to background curves for hydrogen and oxygen electroadsorption from 1N aq. H ₂ SO ₄ at (dV/dt) = 50 mV sec ⁻¹ . Also shown is the i-V relation for anhydrous CH ₃ CN + NaClO ₄ as electrolyte.	68
8	Dependence of peak currents, i _p , for acetonitrile oxidation at platinum in the double-layer region on sweep rate, (dV/dt), for various concentrations of acetonitrile. (∇) 2 x 10 ⁻⁵ M; (□) 2 x 10 ⁻⁴ M; (o) 2 x 10 ⁻³ M; (⊗) 2 x 10 ⁻² M; (∇) 2 x 10 ⁻² M with 90 sec cathodic holding. Potential range 0.06 to 1.4 V, E _H .	69


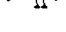
<u>Figure</u>		<u>Page</u>
9	Dependence of peak current, i_p , for acetonitrile oxidation at platinum in the double-layer region on square-foot of sweep rate, $(dV/dt)^{1/2}$, with $[CH_3CN] = 2 \times 10^{-5}M$. Potential range 0.06 to 1.4 V, E_H .	69
10	Dependence of peak current, i_p , for acetonitrile reduction (O) and oxidation (□) in the double-layer region at platinum on sweep rate, (dV/dt) , with $[CH_3CN] = 5 \times 10^{-3}M$. Potential range 0.06 to 1.4 V, E_H for the reduction peak.	70
11	Anodic and cathodic peaks in potentiodynamic i -V profiles for adsorbed acetonitrile at platinum showing the effect of the H-region and cathodic holding at 0.06 V, E_H on the reactions in the double-layer region; curve (a) for the double-layer region; curve (b) for double-layer and H regions; curve (c) with holding of potential at 0.06 V, E_H for 90 sec. $[CH_3CN] = 5 \times 10^{-3}M$, $dV/dt = 50 \text{ mV sec}^{-1}$.	71
12	Dependence of peak current, i_p , for acetonitrile reduction and oxidation in the double-layer region at platinum on sweep rate, (dV/dt) , for $[CH_3CN] = 5 \times 10^{-3}M$ with cycling restricted to the potential range 0.35 to 0.80 V, E_H .	71
13	Extent of adsorption of acetonitrile and corresponding apparent H blocking effects at platinum as a function of acetonitrile concentration; (a) in multisweep experiments; (b) after 90 sec cathodic holding at 0.06 V, E_H . The points, ●, represent expected continuation of $q_{a,d.l.}$ curve beyond L based on the assumption that $q_{a,H}$ should be constant if species "B" was not formed. $(dV/dt) = 50 \text{ mV sec}^{-1}$.	74
14	Dependence of peak current, i_p , for acetonitrile oxidation at platinum in the double-layer region on acetonitrile concentration, with (o) and without (□) solution stirring. Potential range 0.06 to 1.4 V, E_H ; $(dV/dt) = 50 \text{ mV sec}^{-1}$.	76

<u>Figure</u>		<u>Page</u>
15	Order of atomic hydrogen blocking at platinum by a series of nitriles at a concentration of $6.4 \times 10^{-4} \text{M}$ in $1 \text{N H}_2\text{SO}_4$ after 90 sec cathodic holding at 0.05 V, E_H . Potential range 0.06 to 1.4 V, E_H ; $(dV/dt) = 50 \text{ mV sec}^{-1}$.	76
16	i-V profiles taken on an oscilloscope at high sweep rates for $1 \text{M CH}_3\text{CN}$ at Pt in $1 \text{N H}_2\text{SO}_4$; $(dV/dt) = 5, 10, 20, 30, 40$ and 50 mV sec^{-1} . Potential range 0.05 to 1.25 V, E_H .	77
17	Anodic and cathodic peaks in potentiodynamic i-V profiles for adsorbed acetonitrile over various potential ranges obtained by reversing the direction of the sweep at different potentials in both the anodic-going and cathodic-going sweep; curve (a) for the double-layer region; curve (b) for double-layer and H regions, curve (c) with holding of potentials at 0.06 V, E_H for 90 sec. $[\text{CH}_3\text{CN}] = 5 \times 10^{-3} \text{M}$; $(dV/dt) = 50 \text{ mV sec}^{-1}$.	78
18	Change of peak potential in cathodic and anodic sweeps in the double-layer region with \log (sweep-rate) showing limit of reversibility of double-layer reduction/oxidation process.	79
19	Cathodic transient for acetonitrile adsorption at platinum at 0.40 V, E_H ; $[\text{CH}_3\text{CN}] = 5 \times 10^{-3} \text{M}$. Also shown are the first (-) and second (···) anodic and cathodic sweeps in the double-layer region after measurement of the transient.	80
20	(a) Cathodic transient for acetonitrile adsorption at platinum at ca. 0.45 V, E_H during an anodic-going potentiodynamic sweep; $[\text{CH}_3\text{CN}] = 5 \times 10^{-3} \text{M}$, $(dV/dt) = 50 \text{ mVsec}^{-1}$. First (1) and second (2) sweeps after adsorption of acetonitrile are shown in relation to the background sweep in the absence of acetonitrile.	81

<u>Figure</u>	<u>Page</u>	
20	(b) Potentiodynamic profile for $3 \times 10^{-3}M$ CH_3CN (---) and background (—) at 50 mV sec^{-1} together with typical anodic and cathodic transients which arise on potentiostatic adsorption at 0.11 or 0.26 V, E_H , with the anodic H displacement effect arising in the former case.	81
21	Transient adsorption charges, q_t (\square), from current transients for acetonitrile adsorption at Pt in relation to H blocking, Δq_H (\bullet), and total H coverage, q_H^0 (o), in absence of additive. The points \blacksquare represent q_t values before correction for slow reduction effects. q_r is as defined in the text. $[CH_3CN] = 3 \times 10^{-3}M$.	83
22	Effect on the hydrogen region of changing from slow (5 mV sec^{-1}) to fast (50 mV sec^{-1}) sweep rates during an anodic-going sweep. Pt, $1N H_2SO_4$.	88
23	(a) Resolution of the fast atomic hydrogen and acetonitrile processes obtained by initiating faster transients (50 mVsec^{-1}) on a slower anodic or cathodic-going one (5 mV sec^{-1}). (b) Resolution of fast H ionization process with transients at 500 mV sec^{-1} taken on a slower anodic sweep of 5 mV sec^{-1} .	89
24	Charges involved in reduction and oxidation of adsorbed acetonitrile determined in various potential ranges as a function of potential of sweep reversal in the cathodic-going sweep. Correction for acetonitrile reoxidation charge in the anodic H region was made and the true acetonitrile and hydrogen oxidation charges are shown (see Table 1 for definitions of charge quantities). $[CH_3CN] = 5 \times 10^{-3}M$, $(dV/dt) = 50 \text{ mV sec}^{-1}$.	94
25	As in Fig. 24 but with a modified potentiodynamic programme in which the surface oxide region is excluded.	95

<u>Figure</u>		<u>Page</u>
26	Effect of cathodic holding at various potentials on charge recoverable in the following anodic sweep in d.l. region ($q_{a,d.l.}$ and $q_{a,d.l.,h}$). Holding effect, corrected for additional charge involved in reoxidation (in the H region) of reduced CH_3CN species, is represented by the solid lines marked q_a and $q_{a,h}$. The (constant) cathodic charge, $q_{c,d.l.}$, for reduction in the double-layer region is also shown. $(dV/dt) = 50 \text{ mV sec}^{-1}$.	98
27	Repetitive sweep charges $q_{c,H}$, $q_{a,H}$ in the H-region and the anodic charge $q_{a,H,h}$ recovered after 90 sec holding at various cathodic end potentials. $q_{H^+}(h)$ and q_{H^+} are the corresponding charges for the resolved, fast H desorption component, (with and without cathodic holding), giving the true extent of H adsorption in repetitive sweep and holding experiments. q_{H^-} is the true charge for hydrogen deposition on the cathodic sweep; q_{H^0} is the H coverage in absence of acetonitrile as $f(V)$. $(dV/dt) = 50 \text{ mV sec}^{-1}$.	99
28	a) Lattice of Pt atoms on the 111 face showing maximum accommodation of CH_3CN and coadsorbed H. b) Orientation of CH_3CN on Pt 111 surface lattice. c) Orientation and shape of CH_3CN reduced by $1e$, $1H^+$ on Pt lattice. d) Orientation and shape of CH_3CN reduced by $2e$, $2H^+$ on Pt lattice.	104
29	a) Dependence of currents $i_{p,a,d.l.}$, $i_{p,H}$ and i_{min} , from the anodic $i-V$ profile in Fig. 29(b), on the potential region where slow cathodic sweeping was introduced into 100 mV sec^{-1} sweep. (This shows the relative effects of holding the potential almost constant in various 50 mV ranges of the cathodic sweep).	106

<u>Figure</u>		<u>Page</u>
29	b) Anodic-going potentiodynamic i-V profiles at 100 mV sec^{-1} taken after 50 sec periods of slow sweeping at 1 mV sec^{-1} over various potential ranges during a 100 mV, sec^{-1} cathodic-going sweep. Curve a: 0.33 to 0.38 V; curve b: 0.21 to 0.16 V; curve c: 0.15 to 0.10 V, E_H .	106
30	a) Resolution of component currents in the cathodic-going sweep in the H region by the method illustrated in Fig. 23a. $[\text{CH}_3\text{CN}] = 5 \times 10^{-3}\text{M}$. b) As in (a) but for the anodic-going sweep. c) Resolved current-potential profile for reoxidation of adsorbed acetonitrile reduced in a cathodic-going repetitive sweep up to 0.10 V, E_H and after holding for 90 sec at this potential.	107
31	Anodic (o) and cathodic (\square) charges in the surface oxide region at Pt as a function of CH_3CN concentration, together with the apparent charge (X) for blocking of oxide formation. Difference between (o) and (\square) points give q_{react} of Fig. 32. $(dV/dt) = 50 \text{ mV sec}^{-1}$; potential range 0.05 to 1.3 V, E_H .	114
32	Reaction charges q_{react} for oxidation of adsorbed CH_3CN species over the surface oxide region at Pt determined from the difference of anodic and cathodic oxide charges measured in this region (from Fig. 31) for various CH_3CN concentrations. $(dV/dt) = 50 \text{ mV sec}^{-1}$, potential range 0.05 to 1.3 V, E_H .	114
33	Dependence of acetonitrile reaction charge in oxide region, q_{react} , on sweep rate. $[\text{CH}_3\text{CN}] = 5 \times 10^{-3}\text{M}$, potential range 0.05 to 1.3 V, E_H .	117
34	Effect of different anodic termination potentials on the cathodic and anodic going i-V profile for acetonitrile at Pt in $1\text{N H}_2\text{SO}_4$. $[\text{CH}_3\text{CN}] = 5 \times 10^{-3}\text{M}$, $dV/dt = 50 \text{ mV sec}^{-1}$.	118

<u>Figure</u>		<u>Page</u>
35	Effect of cathodic holding for 30 sec at 0.05 V, E_H on the i-V profile of 1M CH_3CN at Pt in 1N H_2SO_4 at $(dV/dt) = 10 \text{ V sec}^{-1}$, potential range 0.05 to 1.3 V, E_H . Also shown is the effect on the i-V profile of cycling in a potential range which excludes the H region, i.e. 0.4 to 1.3 V, E_H .	120
36	(a) Effect of cathodic holding for 90 sec at 0.4 V, E_H on the i-V profile of 1M CH_3CN at Pt in 1N H_2SO_4 at $dV/dt = 10 \text{ V sec}^{-1}$. Potential range 0.4 to 1.3 V, E_H . (b) As in (a) but with 90 sec anodic holding at 1.3 V, E_H .	121
37	Dependence of peak current for oxide reduction on $[CH_3CN]$ for potential range 0.05 to 1.3 V, E_H with (□) and without (○) 90 sec cathodic holding and for potential range 0.4 to 1.3 V, E_H with (■) and without (●) cathodic holding. $(dV/dt) = 50 \text{ mV sec}^{-1}$.	123
38	Potentiodynamic current-potential profiles for Pt in the H and double-layer regions showing background curve (—) for 1N H_2SO_4 and corresponding curve (-.-.-) for addition of thiourea $3 \times 10^{-3}M$. Curves at r.h.s. are two (anodic) transients which arise when thiourea is added at 0.11 or 0.26 V, E_H .  - hatched area corresponds to quantity of H displaced by thiourea adsorbed at 0.11 V, E_H ;  - hatched area to that for thiourea adsorption at 0.26 V, E_H . $(dV/dt) = 50 \text{ mV sec}^{-1}$.	132
39	Anodic H desorption charges, q_t (□), from current transients for thiourea adsorption at Pt in relation to H blocking, Δq_H (⊙), and total H coverage q_H^0 (○), in the absence of additive.	132
40	Anodic H desorption charges, q_t (□), from current transients for dimethylsulfide adsorption at Pt in relation to H blocking, Δq_H (⊙), on both first and second anodic sweeps after adsorption, and total hydrogen coverage, q_H^0 (○), in the absence of additive.	134

<u>Figure</u>		<u>Page</u>
41	Anodic electrochemisorption transient for 0.5 M CH ₃ OH adsorption in the double-layer region (cf. ref. 17) and absence of transient in the H region. Note relative lack of adsorption of CH ₃ OH in 1st sweep after addition at 0.1 V, E _H in comparison with behavior in 2nd sweep. Potentiodynamic i-V profile at r.h.s. shows effect of methanol on the H region after dissociative adsorption at 0.4 V, E _H .	136
42	Potentiodynamic profile, as in Fig. 38, for background (—) and for addition of benzene (3 x 10 ⁻³ M, -·-·-) together with typical anodic transients which arise from benzene adsorption at 0.11 and 0.06 V, E _H . In the latter case, note increased steady-state cathodic current in the transient corresponding to benzene reduction.	140
43	Anodic H desorption charges, q _t (□), from current transients for benzene adsorption at Pt in relation to H blocking, Δq _H (●), and total hydrogen coverage, q _H ^o (o), in the absence of additive. Lower curve (q _r) represent difference of q _t and Δq _H due to electrochemical hydrogenation effects which increase as the potential becomes less positive.	141
44	Potentiodynamic profile, as in Fig. 38, for background and for addition of benzonitrile (3 x 10 ⁻³ M, -·-·-) together with typical anodic and cathodic transients for benzonitrile adsorption at 0.06 and 0.26 V, E _H , respectively. Note long-term cathodic reduction involving charge q _{t,-} at V _{ads} = 0.6 V, E _H after initial H displacement.	145
45	Transient adsorption charges, q _t (□), from current transients for benzonitrile adsorption at Pt in relation to H blocking, Δq _H (●), and total H coverage, q _H ^o (o), in the absence of additive. The points (■) represent the q _t values before correction for long-term reduction effects associated with charge q _{t,-} in Fig. 44.	145

<u>Figure</u>		<u>Page</u>
46	Potentiodynamic i-V profiles for 0.25M CH ₃ OH at platinum with various concentrations of acetonitrile. (dV/dt) = 50 mV sec ⁻¹ , potential range 0.05 to 1.5 V, E _H .	151
47	Dependence of peak current for the FA ₁ process, i.e. formic acid oxidation in the double-layer region (□) and methanol oxidation at ca. 0.9 V, E _H (○) on [CH ₃ CN]. The peak currents were determined from the potentiodynamic i-V profiles in Figs. 46 and 48. [HCOOH] and [CH ₃ OH] = 0.25M, (dV/dt) = 50 mV sec ⁻¹ .	151
48	Potentiodynamic i-V profiles for 0.25M HCOOH at platinum with various concentrations of acetonitrile. (dV/dt) = 50 mV sec ⁻¹ , potential range 0.05 to 1.5 V, E _H .	152
49	(a) Effect of cycling in a restricted potential range, in this case without the H region, on the i-V profile for 0.25M HCOOH at Pt. (dV/dt) = 50 mV sec ⁻¹ , potential ranges: (i) 0.05 to 1.5 V, E _H ; (ii) 0.4 to 1.5 V, E _H . (b) Dependence of (i _p) _{FA₁} on termination potential in the cathodic sweep for the same conditions as described in (a).	157
50	Anodic-going potentiodynamic i-V profiles resulting from HCOOH addition at 0.3 V, E _H on the cathodic-going sweep (a) and at 0.3 V, E _H on the anodic-going sweep (b). (dV/dt) = 25 mV sec ⁻¹ , potential range 0.05 to 1.5 V, E _H .	157
51	Dependence of (i _p) _{FA₁} for 0.25M HCOOH at Pt on [CH ₃ CN] when cycling is restricted to the range 0.4 to 1.5 V, E _H , i.e. in the absence of the H region.	158
52	Relation between steady-state point-by-point i-V curves for 0.25M formic acid oxidation in the presence and absence of CH ₃ CN (2 x 10 ⁻³ M in 1N aq. H ₂ SO ₄) and the corresponding potentiodynamic i-V profiles taken at 50 mV sec ⁻¹ over the same potential range in anodic-going direction.	159

<u>Figure</u>		<u>Page</u>
53	Anodic-going potentiodynamic i-V profiles for 0.25M HCOOH resulting from addition of 5×10^{-4} M CH ₃ CN at 0.3 V, E _H on the cathodic-going sweep (curve a) and 0.3 V, E _H on the anodic-going sweep (curve b). (dV/dt) = 25 mV sec ⁻¹ , potential range 0.05 to 1.5 V, E _H .	160
54	Peak current for FA ₁ process as a function of time t _H spent in the H region in potentiodynamic sweeps. [HCOOH] = 0.25M, (dV/dt) in FA ₁ region = 50 mV sec ⁻¹ , potential range 0.05 to 1.5 V, E _H .	165
55	Dependence of (i _p) _{FA₁} on termination potential in the cathodic sweep for various holding times, t _H , at that potential. Also shown on non-linear scale are the corresponding H coverages in 1N H ₂ SO ₄ at the different cathodic termination potentials. [HCOOH] = 0.25M, (dV/dt) = 100 mV sec ⁻¹ to minimize t _H effects in comparison with t _H in the H region, potential range to 1.5 V, E _H .	167
56	Progressive blocking of H adsorption peaks at Pt (but with maintenance of their resolution) upon electrodeposition of Hg from 3×10^{-6} M aq. HgSO ₄ during successive cathodic sweep in potential range 0.05 to 1.0 V, E _H . Quantitative oxidation of deposited Hg is measured in an anodic sweep taken to 1.4 V, E _H .	173
57	(a) Variation of potentiodynamic i-V profile for 0.25M HCOOH at Pt with Hg electrodeposition, as in Fig. 56. [HgSO ₄] = 10^{-6} M, (dV/dt) = 50 mV sec ⁻¹ , potential ranges 0.05 to 1.3 V, E _H and 0.05 to 1.05 V, E _H . (b) Variation of (i _p) _{FA₁} with H coverage, θ _H , at platinum controlled by Hg electrodeposition (as in Fig. 56). [HCOOH] = 0.25M, (dV/dt) = 50 mV sec ⁻¹ .	174

Figure

Page

- 58 Dependence of $(i_p)_{FA_1}$ on the apparent hydrogen coverage, θ_H , obtained with addition of various concentrations of acetonitrile (-●-, see text); potential range 0.05 to 1.5 V, E_H . Also shown is the increase of $(i_p)_{FA_1}$ as a function of apparent θ_H (see text) due to accumulation of adsorbed impurities during long-period cycling in a restricted potential range excluding surface oxidation (-■-), i.e. 0.05 to 0.9 V, E_H . For both cases, $[HCOOH] = 0.25M$, $(dV/dt) = 50 \text{ mV sec}^{-1}$. 178
- 59 Variation of $(i_p)_{FA_1}$ with progressively increasing reversal potential in the anodic sweep in the region of Pt surface oxidation. Initial condition of $(i_p)_{FA_1}$ at 0.9 V, E_H was achieved by extensive cycling in this restricted potential range with 0.25M HCOOH in the system. Critical surface cleaning effect arises at ca. 1.1 V, E_H leading to increase in coverage by adsorbed formic acid species. Also shown are the results of the same type of experiment but with $5 \times 10^{-3}M$ CH_3CN also present. $(dV/dt) = 50 \text{ mV sec}^{-1}$. The relative charge, Q_O/Q_H , for platinum surface oxidation is also given (Δ). 181
- 60 Potentiodynamic i-V profiles for Pt in acetonitrile with 0.5M $NaClO_4$ in the potential range 0.15 to 1.4 V, E_H showing the effects of various amounts of added water. Sweep profiles are shown in the case of multisweeps (—) and after 90 sec holding at the anodic termination potential (···). $(dV/dt) = 50 \text{ mV sec}^{-1}$. 187
- 61 (a) Potentiodynamic i-V profile for molecular hydrogen oxidation at Pt in 1N H_2SO_4 at electrode rotation rate of 4900 r.p.m. and $(dV/dt) = 50 \text{ mV sec}^{-1}$. Also shown is the background sweep obtained in the absence of hydrogen.
- (b) As in (a) but at a stationary platinum electrode, background not shown. 189

<u>Figure</u>		<u>Page</u>
62	Potentiodynamic i-V profile for molecular hydrogen oxidation at platinum in anhydrous acetonitrile containing 0.5M NaClO ₄ , (dV/dt) = 600 mV sec ⁻¹ . Also shown is the sweep obtained in the absence of hydrogen.	189
63	Potentiodynamic i-V profiles at 600 mV sec ⁻¹ for molecular hydrogen oxidation at platinum in anhydrous acetonitrile containing 0.5M NaClO ₄ and 1.0% (ca. 0.5M) water in two potential ranges: ----- -0.4 to 1.6 V, E _H ————— -0.4 to 2.6 V, E _H	189
64	Potentiodynamic i-V profiles for 0.25M HCOOH at Pt in acetonitrile/0.5M NaClO ₄ with two concentrations of water: (a) 0.1M H ₂ O (.2%); (b) 1.0M H ₂ O (2%). (dV/dt) = 50 mV sec ⁻¹ .	193
65	Potentiodynamic i-V profiles for acetonitrile/0.5M NaClO ₄ in the absence of (a) and in the presence of (b) 0.25M methanol, CH ₃ OH. (dV/dt) = 50 mV sec ⁻¹ .	194

LIST OF TABLES

<u>Table</u>		<u>Page</u>
I	Definitions of Charge and Other Quantities Discussed and Measured	73
II	Charge quantities involved in CH ₃ CN and H adsorption and their surface reactions at Pt (25°C, 1N aq. H ₂ SO ₄)	83

10

ABSTRACT

Part I

The electroactivity of acetonitrile at platinum electrodes in aqueous H_2SO_4 solutions has been investigated by the potentiodynamic sweep technique. It is shown that acetonitrile adsorbs on platinum electrodes and undergoes electrochemical reactions while in an adsorbed state on the platinum surface. The appearance of reduction-oxidation current peaks in the "double-layer" potential region is associated with a somewhat reversible, 2-electron reduction-oxidation of adsorbed acetonitrile, the primary reaction in the double-layer region being reduction.

The extent of acetonitrile adsorption can be determined from measurements of charge passed in the double-layer and H regions in potential sweep experiments and complementarily in potentiostatic current transients which are observed following adsorption of acetonitrile at potentials more negative than ca. $0.6 \text{ V}, E_{\text{H}}$. However, both reduction and oxidation of adsorbed acetonitrile extends into the H region so that the charge passed in this potential range contains components due both to electroactive acetonitrile and to hydrogen. The true coverage by hydrogen, and hence by acetonitrile, can be determined by utilizing the different kinetic relaxation characteristics of the two species. It is subsequently found that acetonitrile occupies three platinum sites per molecule

at adsorption saturation leaving 33% of the surface available for co-adsorption of hydrogen.

The stages of reduction and oxidation of the adsorbed acetonitrile species are considered in terms of a consecutive 2-electron process which involves a change of shape of the molecule leading to steric hindrance for completion of the reduction of the ad-layer at the least positive potentials.

The electrochemistry of acetonitrile in the platinum surface oxide region reveals the oxidative desorption of only a small fraction of the adsorbed species. In fact, inclusion of the surface oxide region in the potentiodynamic sweep program does not influence the charge for reoxidation of adsorbed acetonitrile determined on the next anodic-going sweep in the double-layer region. This behavior is to be contrasted with that observed over the H region, especially at high concentrations of acetonitrile, where another species appears on the electrode surface and decreases the coverage with the reactive species. The possible identity of this inhibiting species is discussed.

Part II

The adsorption of acetonitrile in the H region occurs by anodic displacement of previously adsorbed atomic hydrogen, if the adsorption is initiated at potentials less positive than ca. 0.11 V, E_H . This new electrochemical

adsorption effect also arises with thiourea, dimethylsulfide, benzene and benzonitrile upon adsorption in the H region. Anodic adsorption transients can be measured potentiostatically and the charges corresponding to quantities of atomic hydrogen displaced may be quantitatively related to the blocking of the surface for H adsorption as determined in subsequent cyclic voltammetry experiments. The effects are shown to be quite different from those previously described which result from dissociative chemisorption at electrodes where anodic transients arise from electrochemical ionization of adsorbed hydrogen atoms resulting from dissociation of the organic molecule itself, e.g. in the case of methanol adsorption in the double-layer region at platinum.

The anodic adsorption transients resulting from adsorption of thiourea and dimethylsulfide in the H region are only associated with H ionization. However, adsorption of nitriles and benzene in the H region gives an adsorption transient charge which is composed of an anodic charge due to H ionization and a cathodic charge due to electrochemical hydrogenation of the organic molecule. Separation of these component charges is discussed and, in the case of nitriles, the cathodic reduction charge can be divided experimentally into a fast and slow component.

Part III

The effects of such catalyst poisons as acetonitrile and mercury on the oxidation of formic acid and methanol at platinum was investigated by the potentiodynamic sweep technique. It is shown that the currents for formic acid oxidation, measured in the potential range 0.4 to 0.8 V, E_H , are substantially increased by the presence of these poisons. This result is in contrast with the auto-inhibition usually suffered during oxidation of fuel molecules when a build up of inhibiting species, referred to as p, occurs on the electrode surface. It is shown that acetonitrile and mercury increase the currents for formic acid oxidation at platinum in an indirect way by diminishing the extent of p formation. The formation of p is shown to be a slow reaction which occurs more readily at less positive potentials and a mechanism is proposed for p formation which involves dehydration between two adsorbed formic acid molecules. In this way, the adsorbed formic acid is tied up as an unreactive p species which blocks the surface for oxidation of the normal reactive species.

It is shown that accumulation of impurities from solution on the electrode surface, which is achieved by potentiodynamic cycling in the absence of the platinum surface oxide region, also gives rise to an increase in the formic acid oxidation currents in the double-layer potential region. The effect of acetonitrile on the peak current for various

other formic acid oxidation processes is described, together with an investigation of the effect of very high concentrations of acetonitrile on formic acid oxidation at platinum.

Part IV

The effect of trace quantities of water on the potentiodynamic i-V profiles for platinum in anhydrous acetonitrile was also investigated and the formation and reduction of surface oxides under these conditions is explained. The oxidation behavior of formic acid, methanol and molecular hydrogen at platinum in anhydrous acetonitrile is described. The lack of activity in the case of formic acid and methanol is interpreted in terms of the results given in Part I. Molecular hydrogen oxidation occurs over a wide potential range in anhydrous acetonitrile, this potential range being dependent on the extent of platinum surface oxide formation and hence on the quantity of water present in the system. Molecular hydrogen oxidation was also studied in aqueous media at platinum and the origin of the oxidation currents is discussed in relation to the currents arising from adsorbed hydrogen deposition or ionization.

CHAPTER I

INTRODUCTION

1. Oxidation Processes on Platinum Anodes

(a) Electrocatalysis

The electrochemical oxidation of organic molecules at platinum electrodes has been extensively studied in regard to (a) fundamental aspects of electrocatalysis and electrochemisorption; (b) applications in fuel-cell technology; and (c) in electrosyntheses, e.g., the Kolbe and Hofer-Moest reactions. In order to obtain optimum fuel-cell efficiency in the oxidation of organic molecules, an understanding of reaction mechanisms is necessary. The electrochemical oxidation of many organic molecules depends on the ability of the electrode to dissociate catalytically the molecule into smaller, adsorbed fragments which can be oxidized from the surface. The role of the electrode surface in providing sites where this dissociative adsorption can arise and where the intermediates resulting from this process can undergo electrochemical oxidation, has given rise to a new term, "electrocatalysis" (1). The catalytic efficiency of the surface depends on the nature of the electrode material and on the potential at which the electrode is held in a particular solution. This potential-dependent role of the electrode surface in the overall reaction mechanism and the coupling of

electrochemical with dissociative adsorption processes are the factors which distinguish electrochemical catalytic processes from ordinary catalyzed reactions.

The importance of the electrode material is well known in the case of the hydrogen evolution reaction. Conway and Bockris (2) showed that the electrochemical catalytic properties of a series of electrode materials, as indicated by the exchange-current densities for the hydrogen reaction, could be correlated with the %d character in the d^2sp^3 hybrid bonding in the metal lattice and in the surface. This arises because the metal electrodes, to be referred to generally as M, may act in an electrocatalytic role by forming a chemical bond with the atom of hydrogen to be discharged from H^+ to give a chemisorbed species, M-H. The reaction proceeds by the transfer of charge from the electrode to an activated state of the solvated proton in solution with the formation of a chemical bond, $M + H_3O^+ + e \rightarrow MH + H_2O$. The strength of this chemical bond is related to the adsorptive and catalytic properties of the electrode and is a major factor determining the mechanism of the reaction. In fact, the rate-determining step for the hydrogen evolution reaction and even the overall reaction pathway itself can depend upon the M-H bond strength, i.e., on the nature of the electrode material and its coverage by H.

The chemisorption of atomic hydrogen on an electrode surface at which H_2 evolution is occurring (3) is an example

of direct adsorption of an intermediate resulting from charge transfer. However, as mentioned above, the oxidation of many organic molecules proceeds by a prior dissociative chemisorption of reactant, followed by charge transfer. The dissociative chemisorption of methanol, formic acid and ethylene on a platinum electrode is well known and the electrochemical oxidation of molecular hydrogen proceeds by a similar mechanism on platinum, involving chemisorbed H atoms. Since the ability of the platinum electrode to dissociatively chemisorb organic molecules depends upon the condition of the electrode surface with regard to coverage by hydrogen or oxygen species, the nature of the platinum electrode surface in pure, aqueous solutions will first be discussed.

(b) Nature of the platinum electrode surface in contact with aqueous solution

The nature of any electrode surface depends upon the potential at which it is maintained and the solution with which it is in contact (4). For example, there exists only a relatively narrow range of potentials over which the platinum surface in aqueous solution is free of chemisorbed hydrogen or oxygen particles (see below). The dependence of reaction kinetics on the state of the electrode surface has often resulted in contradictions between the experimental data reported by different authors engaged in studying the same

reaction at the same electrode but under somewhat different conditions of the surface. It is therefore important to know the state of the electrode surface when investigating the kinetics of an electrochemical reaction.

The hydrogen and oxygen evolution reactions on platinum are examples of continuous faradaic processes, i.e., the reaction currents do not fall to zero upon potentiostatic polarization, and, as a consequence, these reactions can be studied by steady-state techniques. However, no continuous faradaic processes are possible on platinum in pure, aqueous solutions between the thermodynamic limits for hydrogen and oxygen evolution and the reactions occurring in that region, i.e., hydrogen and oxygen adsorption, must therefore be non steady-state processes. Since the currents arising from non steady-state processes fall to zero upon potentiostatic polarization, transient methods are required for their investigation.

One important transient method is the potentiodynamic sweep technique, developed by Will and Knorr (3), which consists of changing the potential in a controlled, usually linear, manner with time and recording the non steady-state currents which result. The potential is varied in a cyclic manner between certain limits, e.g., from the hydrogen reversible to the oxygen reversible potentials as shown in Fig. 1 for platinum in aqueous H_2SO_4 . The currents recorded during the potential sweep in Fig. 1 are the result of

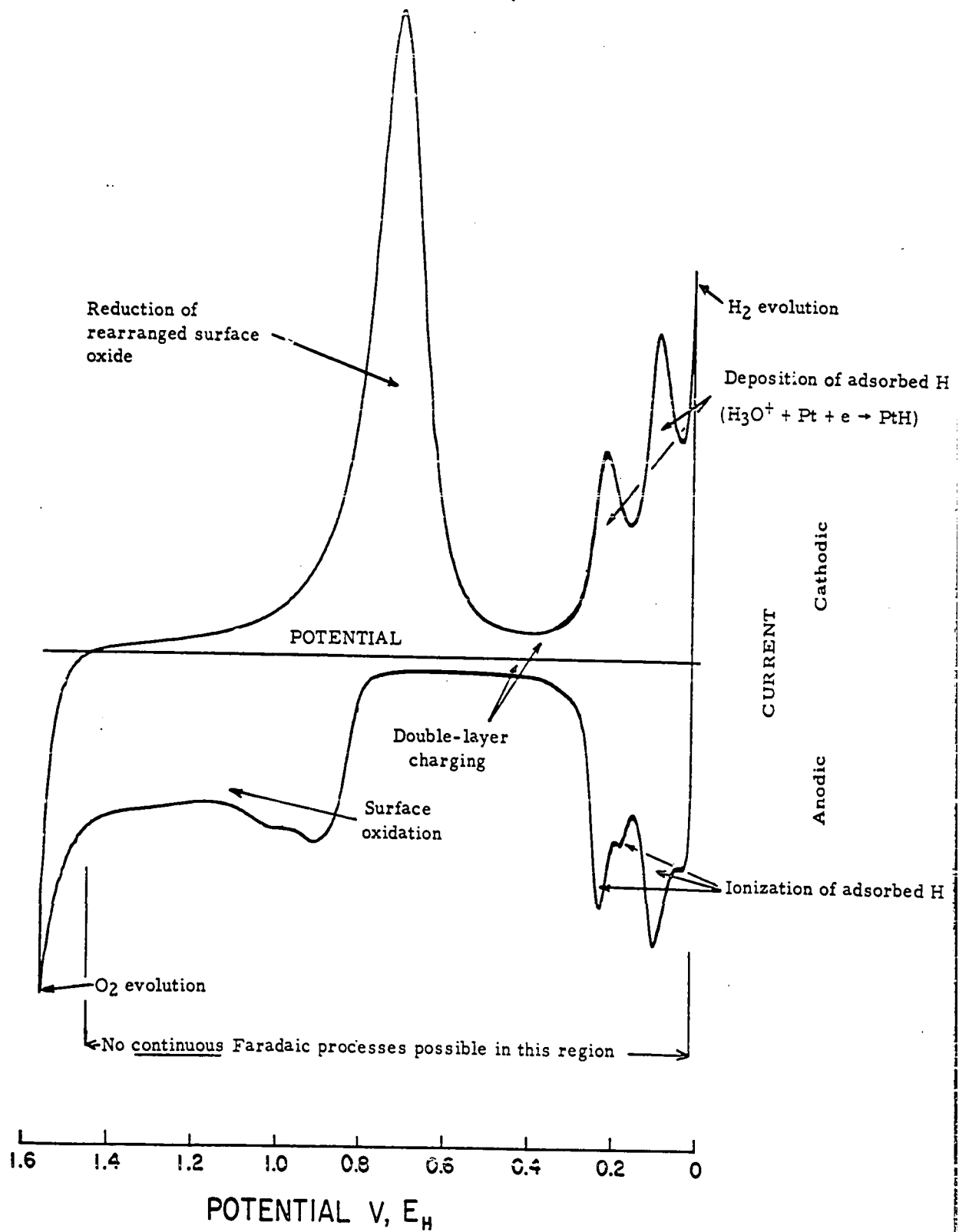


Fig. 1. Potentiodynamic current (*i*)-potential (V) profile for Pt in 1N H₂SO₄ at $(dV/dt) = 50 \text{ mV sec}^{-1}$ in the potential range between appreciable hydrogen and oxygen evolution.

(i) non steady-state, pseudo-faradaic reactions* involving only the formation and removal of a layer of adsorbed intermediates, and (ii) the non-faradaic reaction of charging the metal-solution double-layer (see below). For a pseudo-faradaic reaction, at each potential, there is a certain coverage of the electrode with adsorbed species corresponding to an equilibrium condition. If this coverage is attained and the electrode potential is not changed, e.g., upon potentiostatic polarization, the net electrochemical reaction ceases and the currents fall to zero.

The nature of the platinum surface in aqueous solution can be classified by reference to three distinct potential regions as shown in Fig. 1: (i) the adsorbed atomic hydrogen region; (ii) the double-layer region; and (iii) the surface oxide region. These three regions are observed during both the anodic and cathodic-going sweeps and their main features will now be discussed.

In a cathodic-going sweep over the potential region 0.05 to 0.35 V, E_H , pseudo-faradaic currents arise from deposition of atomic hydrogen onto the surface from solution ($Pt + H_3O^+ + e \rightarrow PtH + H_2O$); in the reverse direction of the sweep, ionization of adsorbed H from the surface occurs. The different peaks correspond to distinguishable states of atomic hydrogen adsorbed on the surface with different bond strengths.

* Pseudo-faradaic reactions are also referred to as electrochemical surface reactions. They cannot occur continuously as does a normal faradaic reaction.

For the two principal* H species on Pt, the difference of mean adsorption energy is ca. 3.5 kcal.mole⁻¹. An important characteristic of the reactions of atomic hydrogen on platinum is that they are reversible, the equilibrium coverage at any potential being attained almost instantaneously.

Between the hydrogen and oxygen adsorption regions, i.e., 0.35 to ca. 0.8 V, E_H, the platinum surface is free from chemisorbed particles although oriented solvent molecules are ubiquitously present. In this region, changes of surface charge on the metal change the electrode potential and give rise to a different distribution of anions and cations at the metal-solution interface. This is a non-faradaic process in the sense that no electrons flow across the double-layer between solution and metal, i.e., the behavior is similar to that of charging a condenser. Behavior in this range of potential, to be referred to as the "double-layer" region, differs from that in the hydrogen adsorption region where electrons pass across the double-layer in the deposition or ionization of atomic hydrogen causing flow of non steady, pseudo-faradaic current.

At potentials more positive than ca. 0.8 V, E_H, the platinum surface oxidizes, the anodic current profile

* Three species can be distinguished in work carried out on clean surfaces in very pure solutions (see Chapter III).

exhibiting several reproducible peaks.* Reduction of surface oxide occurs in a single peak at more cathodic potentials than correspond to its formation (contrast the reversibility in the hydrogen region). The oxidation and reduction of the surface are slower, less reversible processes than the atomic hydrogen reactions and require time for reaching equilibrium at any potential.

Another method for studying non steady-state processes at electrodes is chronopotentiometry (7-11), i.e., the recording of changes of potential as a function of time which result when a constant charging current is applied to the electrode. The results obtained are related to those from the potentiodynamic sweep method (12) except that in the latter case there is more resolution of the processes that occur, e.g., in the hydrogen and oxygen adsorption regions. This is because the potentiodynamic method is essentially a differential method**. Similar resolution can, however, be obtained with the differential galvanostatic method (13).

* In work to be described elsewhere (5), it has been shown that the Pt surface undergoes several distinguishable stages of oxidation corresponding to development of sub-lattices of adsorbed OH ($\text{Pt} + \text{H}_2\text{O} \rightarrow \text{"PtOH"} + \text{H}^+ + \text{e}$) below full coverage by OH which occurs at ca. 1.1 V, E_{H} . Beyond this potential, the "PtOH" species becomes oxidized to "PtO" in a broad, less reversible region. For convenience in the following material, these various species covering the electrode surface will be referred to as "surface oxide" although it is probably only after "PtO" formation that the ad-layer approaches a 2-dimensional phase (6).

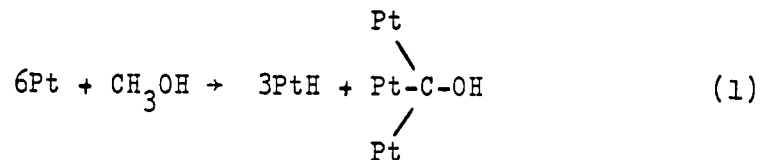
** The significance and origin of currents arising from electrochemical surface processes in the potentiodynamic method are discussed in Chapter I, section 2(b).

The d.c. methods discussed above for studying the nature of surface reactions at electrodes can be complemented by the a.c. capacitance method in which the capacitative component of the impedance of the electrode to an a.c. signal is derived as a function of frequency after allowance for diffusional effects (14-16). This method was employed by Breiter (16) in the case of platinum electrodes in aqueous solution, the capacity-potential profiles being compared with the potentiodynamic current-potential profiles. The results from the a.c. method are more difficult to interpret quantitatively than those from d.c. methods on account of the large frequency dependence of the capacity that usually arises.

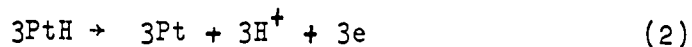
(c) Oxidation of simple organic molecules at platinum electrodes

The oxidation of simple organic molecules such as ethylene, formic acid, and methanol has been studied extensively and the special significance of platinum as an electrocatalyst material is now well known. The overall oxidation reaction of these organic molecules may be divided into two important steps: (i) adsorption on the electrode surface with the formation of a chemisorbed intermediate; (ii) anodic oxidation of the intermediate from the surface. The mechanism for the oxidation of methanol and formic acid at platinum electrodes will now be discussed with reference to the nature of the electrode surface, since these two molecules were involved in part of the original work to be reported later.

Methanol is a representative example of a molecule which dissociatively chemisorbs on platinum in the double-layer potential region; the three H atoms of the methyl group are split off and adsorbed together with a carbon containing residue (17); thus



The adsorbed hydrogen atoms then undergo rapid electrochemical ionization:



and reaction (2) gives rise to a non steady-state current which is initially observed after adsorption of methanol on platinum (17). The above mechanism for adsorption of methanol on platinum is supported by the fact that the charge for oxidation of the adsorbed hydrogen which has split from the molecule is equal to the charge associated with complete oxidation of the residue, this charge also being equal to the charge equivalent to the decrease in hydrogen coverage after adsorption due to the presence of $\equiv\text{C}-\text{OH}$ groups.

The ability of the surface to adsorb a reactant, e.g., methanol in reaction (1), depends on the energetics of bond breaking in the molecule and bond formation with the metal surface. The energy of the latter process depends on the nature of the surface and of any species already chemi-

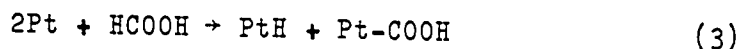
sorbed on the surface, e.g., electrosorbed oxygen or hydrogen species. For adsorption of methanol on platinum, the dependence of coverage by the organic species* on electrode potential has been determined experimentally by several workers (18-21). If methanol adsorption at each potential is allowed to occur on a clean platinum surface, i.e., free from any previously chemisorbed methanol, the coverage follows a dome-shaped curve with potential (18). Maximum coverage with methanol occurs between 0.35 and 0.55 V, E_H , i.e., in the double-layer potential region, where the platinum surface is free from adsorbed hydrogen or oxygen species.** If, on the other hand, methanol is initially adsorbed in the double-layer region and the electrode potential is then taken to cathodic values, no significant decrease in coverage with methanol species is observed (19). This is associated with the irreversibility of methanol adsorption, the adsorbed species being displaced only at more positive potential where they are oxidized from the surface (see reaction (4) below).

There has been considerable controversy concerning the electrochemisorption of formic acid on platinum. Its adsorption and oxidation appears to be more complicated than

* For an outline of the methods used in determining coverage by organic species, see p.41.

** A similar dome-shaped relationship was obtained for methanol adsorption on an iridium electrode (22) with maximum adsorption in the potential region 0.3 to 0.4 V, E_H where oxygen and hydrogen adsorption on iridium is minimal.

that of methanol due to the possibility of side reactions with formation of a co-adsorbed blocking species (23-26). Bagotsky and Vasiliev (27,28) believe that the mechanism for the adsorption of formic acid as a species, which is reactive in subsequent desorptive oxidation from the surface, involves dissociation of the molecule; thus



with the participation of two platinum atom sites. Like methanol, formic acid also displays a non steady current after adsorption on platinum in the double layer region because of the rapid electrochemical oxidation of atomic hydrogen. However, significant oxidation of the formic acid residue is also possible at these potentials; therefore, the charge associated with oxidation of adsorbed hydrogen split from the molecule cannot be easily evaluated. In this case, the dissociative adsorption mechanism is supported by (i) results obtained at a palladium bi-electrode (27) where some of the atomic hydrogen resulting from splitting of the molecule diffuses through the palladium and gives an anodic current on the opposite side of the membrane; and by (ii) equality of the charge for complete oxidation of the residue and the charge equivalent to the decrease in hydrogen coverage after adsorption (28).

For adsorption of formic acid on platinum, the dependence of coverage by organic species on electrode potential gives a dome-shaped curve with maximum surface

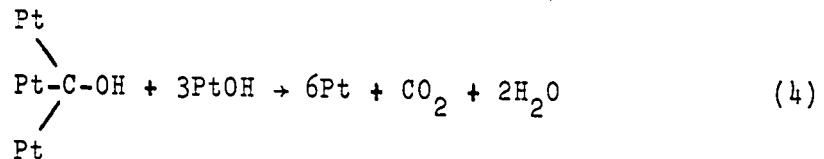
coverage by formic acid species at 0.2 V, E_H (23,28). The coverage by formic acid species is close to unity up to ca.

0.3 V, E_H , at which potential the coverage begins to decrease and eventually falls to zero at ca. 0.7 V, E_H because of electrochemical oxidation of the adsorbed species. The formic acid adsorption is not as irreversible as the methanol adsorption since oxidation of formic acid can occur, at least to a small extent, at potential less positive than 0.4 V, E_H and formic acid can adsorb on a surface partially covered by atomic hydrogen.

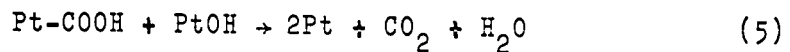
For both methanol and formic acid, the rate of oxidation of the adsorbed organic residue is a somewhat slow reaction which depends on (a) the coverage by organic residue; (b) the metal-solution potential difference and (c) the coverage by any other adsorbed species such as surface oxide. It is with regard to oxidation of the carbon residue that the methanol and formic acid reactions differ, the adsorption mechanism which gives the reactive species being similar for both molecules on platinum. In the case of methanol, the anodic current resulting from oxidation of the adsorbed species at a fixed potential increases with increasing coverage by methanol (17,27). This is to be contrasted with the result reported by Brummer (23,26) for formic acid where an increase in coverage by adsorbed species at a fixed potential results in a decrease in the anodic current. It has been proposed (26) that while all of the experimentally determined coverage of

adsorbed methanol species at platinum is involved in the main oxidation reaction, a large proportion of the species resulting from formic acid adsorption is not the main reactive species in reaction (3) but is an inhibitor resulting from a parallel side reaction. As the coverage by this inhibiting species increases, the currents for formic acid oxidation decrease.

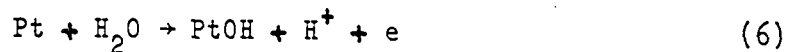
Oxidation of the methanol residue with platinum surface oxide at potentials $>0.9 \text{ V}, E_{\text{H}}$ may be written as follows (17):



while that for the formic acid residue in the main reaction path is:



In both cases, the anodic current for oxidation of the organic residue arises in the surface oxidation itself, thus:



with consumption of the electro-generated PtOH species through reaction (5).

Although steady-state Tafel plots are required for a full investigation of the charge-transfer events in organic reaction mechanisms, the rate of organic oxidation processes can in certain cases be followed conveniently with the potentiodynamic sweep method, as can the oxidation and

reduction of the platinum surface itself (Fig. 1). The potential-dependent currents observed in many organic reactions at platinum are fundamentally different from those observed in the background potentiodynamic sweep arising when only the "electro-inactive" supporting electrolyte itself is present. Whereas in the latter case only reactions of surface species at a finite coverage are involved, with methanol and formic acid the currents can be of a continuous faradaic nature, i.e., under controlled potential polarization conditions the currents will not usually fall to zero but will attain some steady, finite value corresponding to the activation and/or diffusion controlled rate of the reaction of species from the solution. It is often useful to compare the potentiodynamic current-potential curves for methanol or formic acid with that for the platinum surface reactions in the supporting electrolyte alone, (e.g., 1M aq. H_2SO_4 (Fig. 2) see also ref. 2). While, quantitatively, the coverage by surface oxide and hydrogen will be changed in the presence of the organic compounds, it is usually possible to gain qualitative information on the electrochemical surface reaction from such a comparison. The current densities for methanol and formic acid oxidation at any potential are substantially different (Fig. 2) because the oxidation rates for the two reactions at platinum differ appreciably due to different reaction mechanisms. From the oxidation peaks in the i-V profiles, both organic substances are seen to be reactive in

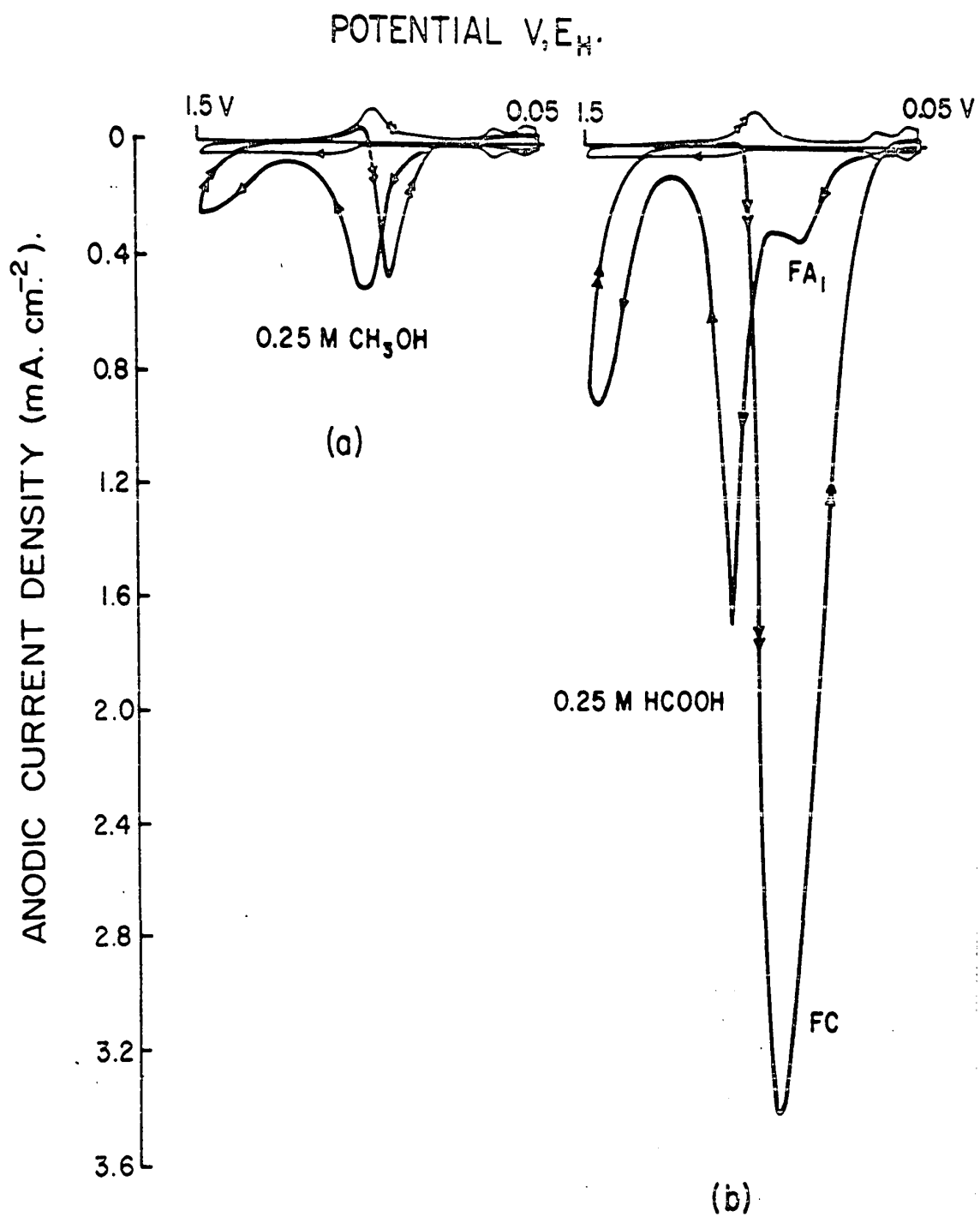
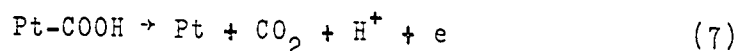


Fig. 2. (a) Potentiodynamic i - V profile for Pt in 0.25M CH_3OH at $dV/dt = 50 \text{ mV sec}^{-1}$; potential range 0.05 to 1.5 V, E_H .

(b) Potentiodynamic i - V profile for Pt in 0.25M HCOOH at $dV/dt = 50 \text{ mV sec}^{-1}$; potential range 0.05 to 1.5 V, E_H .

the same potential ranges except for an additional reaction which arises in the double-layer region in the case of formic acid. This reactivity of formic acid during a potentiodynamic sweep in the double-layer potential region may be associated with the fact that a mechanism of oxidation to CO_2 can be proposed for the formic acid residue without the participation of surface oxide:



whereas such a mechanism cannot easily be envisaged for methanol. However, the problem is complicated because of the existence of finite steady-state currents for methanol oxidation even at $0.5 \text{ V, } E_{\text{H}}$ (17), i.e., at potentials which are much less positive than those required for detectable surface oxide coverage.

(d) Inhibition effects in organic oxidation reactions at platinum electrodes

From potentiodynamic sweep experiments, both methanol and formic acid are seen to react differently as various stages of platinum surface oxidation are reached in the potential range 0.8 to $1.4 \text{ V, } E_{\text{H}}$ (Fig. 2); inhibition effects occur with increasing potential after initial reaction of the organic substance with the surface oxide. It has been suggested that the role of platinum surface oxide species in organic oxidations can be two-fold (4): (i) they can react with co-adsorbed organic molecules or derived adsorbed

intermediates as shown above; (ii) they can act as blocking species causing inhibition of organic oxidation. The mechanism by which platinum surface oxides inhibit the oxidation of hydrocarbons has been studied in some detail (29-33). Steady-state current-potential profiles for oxidation of an extensive series of organic substances (e.g., ethylene, methanol, formic acid, formaldehyde) at platinum show a general passivation region at 0.95 V, E_H , i.e., the inhibition takes the form of a slower rate of increase of current with potential which often leads to a reversal of direction of the current-potential profile. It has been suggested that the passivation can be due to the following factors: (i) adsorption of supporting electrolyte anions (34-36); (ii) self-inhibition by adsorbed intermediates produced in the reaction itself (37-38); (iii) formation of a surface oxide on the platinum electrode (29-33). The case of development of potential-independent currents also represents a decrease in the "rate of increase" of current with potential; however, this case arises when the reaction becomes completely diffusion controlled and it is not of fundamental mechanistic interest. The fact that there is very often a real reversal of direction of the current-potential curves (see Fig. 2), and not just development of a limiting current, indicates that diffusion control is not an important factor in such cases. With regard to (i), Schuldiner has suggested that the adsorption of SO_4^{2-} could give rise to passivation

in those systems where sulfuric acid was used as electrolyte. However, the coverage of platinum by SO_4^{2-} was found from radiotracer studies (39) to decrease at about 0.9 V, E_H , i.e., in the region where surface oxidation commences. Since the potential of passivation for oxidation of organic compounds is the same in HClO_4 and H_3PO_4 solutions, the perchlorate and dihydrogen-phosphate anions, like the sulfate anion, evidently play no direct role in the passivation.

In connection with (ii), it has been shown theoretically by Gilroy and Conway (39) that self-inhibition effects can arise in a reaction where electrochemical adsorption is followed by a heterogeneous chemical step involving production of species which occupy more surface sites than did the kinetically antecedent species. The resulting rate-equation involves a $\theta(1-\theta)$ term, θ being coverage by the reacting intermediate, i.e., the reaction requires both reactant coverage and free surface sites to proceed, a maximum rate occurring at $\theta = 0.5$. A somewhat different approach has been used to explain the inhibition of formic acid oxidation at platinum through coverage of the electrode by adsorbed species. It has been pointed out above that the formic acid oxidation is retarded by an intermediate derived from the reacting particles in a reaction step parallel to the main reaction sequence. This intermediate is a poisoning species^{*} and blocks a large

*The identity of this species will be discussed in Chapter III, Part III.

part of the electrode surface for the main oxidation reaction. The possibility also exists that self-inhibition can occur by the oxidation products themselves poisoning the electrode surface. Work by Dolin et al. (40) on the effect of irradiation on the oxidation rate of HCOOH and C₂H₅OH has shown that unstable oxidation products of a radical type are not responsible for the inhibition. The end oxidation product, CO₂, also has no effect on the passivation behavior.

With respect to (iii), Bagotsky and Vasiliev (22, 27,41) noted that the range of potentials of inhibition of organic reactions depends only on the nature of the electrode metal and the solution pH; hence, kinetic inhibition above 0.9 V, E_H is probably a result of a change in the state of the electrode surface brought about by the adsorption of oxygen species. Bockris et al (30) arrived at the same conclusion and were able to incorporate the surface oxidation reaction into the rate equation with reasonable results. Indeed, it is known that the presence of surface oxides affects the rate of simple electron transfer processes at platinum. Anson (42, 43) investigated the Fe(III)-Fe(II) couple at platinum and found the reaction to be less reversible on an oxide covered electrode than on a reduced electrode. Also, the reduction of molecular oxygen follows a different mechanism on oxide-free and oxide covered platinum surfaces (44-46). Oxide-free platinum is more active than oxide-covered platinum for oxygen reduction as indicated by the Tafel slope values of $\frac{RT}{F}$ and $2\frac{RT}{F}$, respectively, in dilute sulfuric acid.

Further support for the role of platinum surface oxides as inhibiting species for organic oxidations comes from the manner in which the rate of oxidation of organic substances follows the well-known hysteresis (47) in the electrodeposition and reduction of platinum surface oxide species. In potentiodynamic i - V profiles at Pt, oxidation of organic substances arises in the cathodic sweep only after free Pt sites appear on part of the surface through reduction of the oxide. In the same way that the potential for commencement of oxide reduction changes with the amount and type of oxide formed in the anodic sweep, the potential at which the organic oxidation reaction begins on the cathodic sweep depends on the prior anodic treatment of the electrode. Bagotsky and Vasiliev (27) found that as the termination potential on the anodic sweep was increased, the hysteresis in the steady-state polarization curve for methanol oxidation at platinum increased accordingly.

The inhibition resulting from surface oxide formation can be due to: (i) the amount of surface oxide, i.e., its coverage; and/or (ii) the type of surface oxide since various oxidation states of platinum are possible. Although most organic oxidation reactions in aq. medium at Pt probably occur with the participation of surface oxide as was shown on p.13 for methanol, the organic molecule must generally be in an adsorbed state on the electrode surface initially. The presence of O species can thus block surface sites for

adsorption of organic molecules and, at sufficiently high oxide coverages, inhibit the reaction. Increasing coverage of a surface with O species may also give rise to an increase in the standard free energy of adsorption for organic molecules on the existing free surface sites (cf. Temkin's isotherm), and hence decrease the extent of adsorption of the organic compounds in this way. As the anodic potential increases above 0.9 V, E_H , the electrode surface becomes progressively filled by oxide species and at the same time higher states of oxidation of the platinum surface are generated. These higher oxidation states can be unreactive toward organic molecules, i.e., the inhibition results more from the type of surface oxide rather than the coverage by surface oxide. Hence, it is often the species corresponding to lower states of oxidation (e.g., OH on Pt or Pt surface interstitial sites), at coverages which are not too high ($\theta_{OH} < 0.2$) that appear to react with the adsorbed organic molecules to give the oxidation current in the region of initial stages of surface oxide formation. One experimental fact which appears difficult to explain in terms of the theory of inhibition by oxides is that there is usually a region of reactivity of organic substance at about 1.3 V, E_H , i.e., at higher coverages of the initial surface oxide and/or coverage by higher oxide different from that causing the initial inhibition. This is seen from both potentiodynamic sweeps (Fig. 2) and steady-state polarization curves (e.g., for formic acid and methanol (27)). A possible explanation is that the reaction

mechanism changes at these more anodic potentials so that organic adsorption on free surface sites next to O-occupied sites (bifunctional mechanism (48)) is no longer a prerequisite for oxidation. For example, a change in the condition of the surface oxide at platinum at these potentials is a likely reason for this type of effect. Also, the changing anodic potential determines not only the type and coverage of oxide species but also the rate of charge transfer through the usual exponential factor in potential (see p.27). The reactivity at 1.3 V, E_H may partly be due to this exponential increase of charge transfer rate with increasing anodic potential; however, the fact that the oxidation current again decreases at ca. 1.5 V, E_H indicates another region of inhibition of the oxidation reaction. This must be the result of further change of the oxidized platinum surface with the formation of oxide species on which oxidation of the organic compounds cannot occur even at these high positive potentials.

The surface oxide may thus be considered a co-adsorbed species which can react with the adsorbed organic molecule and/or inhibit the organic oxidation reaction. Its coverage must therefore be taken into consideration in the rate equation for oxidation of the organic compound in the potential region of platinum surface oxidation. In the general case of competition of oxygen electrosorption with that of an intermediate produced in an anodic discharge reaction such as $Pt + X^- \rightarrow PtX + e$, the rate of the reaction is

affected by a potential dependent term $1-\theta = (1-\theta_{OH}-\theta_x)$, and θ will be mainly determined by θ_{OH} , the coverage by oxide species, PtOH, if θ_x tends to be small. This will be the case if the step of discharge of X^- is rate-determining with respect to a following desorption step and this example will be typical for organic oxidation reactions in the oxide region. The $1-\theta_{OH}$ term arises under both Langmuir and Temkin adsorption conditions (49) and results in the characteristic reversal of the current-potential curve at $\theta = 0.5$ over a breadth of potential determined by the Temkin heterogeneity/interaction parameter r (50). Theoretical calculations for reaction inhibition by surface oxide species on platinum can be fitted very closely (31) to the experimental i - V curves for the inhibited formate ion reaction at platinum in the potential region 0.8 to 1.2 V, E_H .

Molecular hydrogen oxidation at platinum also exhibits inhibition in the oxide region (51,52); however, unlike the case of organic oxidations, no further reaction occurs at potentials around 1.3 V, E_H . The inhibition occurs immediately at the onset of surface oxidation (see Fig.62) and has generally been attributed to blocking of sites required for H_2 dissociation and oxidation by formation of chemisorbed oxygen species (i.e., OH initially; see footnote on p. 7). The reaction of H_2 thus appears to be less complicated than most organic oxidations, the main role of surface oxide being that of a blocking species, since H_2

(or H) does not require co-adsorption of OH for its oxidation.

(e) Use of non-aqueous solvent systems with platinum electrodes

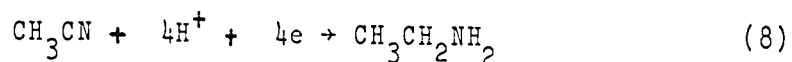
The complications associated with reactions at oxygen-covered platinum electrodes have lead to work being carried out under non-aqueous conditions (53-60). In such systems, the degree of surface oxidation can be controlled both by addition of known amounts of water and by control of the anodic end potential in a potentiodynamic sweep or step. Also, the relatively large background currents (i.e., peaks) associated with the formation or removal of adsorbed layers of hydrogen or oxygen on platinum can be avoided in a non-aqueous system. Although the currents associated with surface reactions at platinum may not substantially interfere with the interpretation of large, faradaic oxidation currents (e.g., for formic acid and methanol), some slow organic reactions at platinum give currents of the same order of magnitude as the background currents (e.g., benzene (30,61, 62) and most saturated aliphatic amines (63)). Non-aqueous solvent systems have also been used in organic polarography at both mercury and platinum electrodes where simple electron transfer reactions were being studied. Under such conditions the production of stable, free-radical cations or anions is possible from the oxidation or reduction of aromatic hydro-

carbons (64-66). Reduction reactions of aromatic hydrocarbons have also been conducted under non-aqueous conditions with aprotic organic solvents (67-70). The aprotic solvent allows electro-generated radical anion species to have relatively long lifetimes due to absence or slowness of protonation (cf. the very rapid protonation of radical anions in water (70)).

Acetonitrile has been extensively used as an aprotic, non-aqueous solvent in the study of electrochemical reactions (71). It is well known that acetonitrile is a difficult solvent to purify (72-78) and special attention is given to this matter in Chapter II. Depending on the water content and state of purity of acetonitrile and the supporting electrolyte, the potential range over which both faradaic and pseudo-faradaic processes (see p.5) are negligible can be several times that observed in the aqueous solvent system. Acetonitrile is thus said to be inert at platinum over an extended range of potentials and permits many reactions to be studied at high cathodic or anodic potentials without the participation of faradaic processes (79-81) involving the supporting electrolyte.

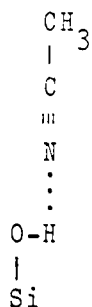
Although the physical properties of acetonitrile itself as a non-aqueous solvent have been studied at length, the effects of acetonitrile on the catalytic and electro-sorption properties of platinum electrodes have hitherto received little attention. Acetonitrile is known to retard the oxygen evolution reaction on platinum in aqueous media (82) and shifts the potential of the reversible hydrogen

electrode to some extent (83). However, reversibility of the hydrogen electrode is still maintained in acetonitrile even at 90% concentration with 10% water (84). The reduction of acetonitrile on a palladized platinum electrode at high cathodic potentials was performed in 1942 (85), with characterization of the resulting product as ethylamine:

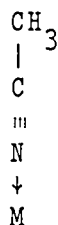


However, such studies have provided only limited and qualitative information on the effects of acetonitrile on the platinum electrode surface itself with no thought of the mechanisms of adsorption and poisoning. While the adsorption of acetonitrile and other nitriles onto a platinum surface may not significantly alter simple electron transfer processes, any reaction for which the surface acts directly as a catalyst, i.e., as a source of sites for the production and adsorption of intermediates in the reaction mechanism, must be affected by nitriles adsorbed on the surface.

Infrared spectroscopy has been used to study the adsorption of nitriles on various adsorbents from the vapor phase. Low and Bartner (86) examined the absorption of acetonitrile on porous glass and found a weak adsorption with only a very small change in the symmetric-stretching frequency, this being ascribed to hydrogen bonding with surface hydroxyl groups:



When the porous glass was impregnated with aluminium or zirconium, acetonitrile adsorption resulted in increases of $\Delta\nu_{\text{C}\equiv\text{N}}$ by 94 cm^{-1} and 38 cm^{-1} , respectively, for the symmetric mode of vibration due to electron donation from nitrogen to the metal atom with the molecule in the following orientation:



It is well known (87-89) that the formation of inorganic complexes by coordination through the nitrogen atom results in an increased $\nu_{\text{C}\equiv\text{N}}$, due to an increase in the $\text{C}\equiv\text{N}$ force constant upon coordination. In contrast, only a very limited number of inorganic complexes have been prepared which show a decrease in $\nu_{\text{C}\equiv\text{N}}$ upon coordination (90); acetonitrile complexed to ruthenium amines is nevertheless an example (91). However, the adsorption of gaseous nitriles onto silica-supported platinum surfaces results in a decrease of the $\text{C}\equiv\text{N}$ stretching frequency (92,93). This weakening of the $\text{C}\equiv\text{N}$ bond strength is believed to be due to back bonding of the d-electrons of platinum to the anti-bonding π^* orbitals of the nitrile.

2. Choice and Basis of Experimental Methods Used in the Present Work for Studying Electrode Processes

A number of complementary experimental methods were employed during the course of this work. The techniques involved in the various methods, their limitations, advantages and disadvantages will now be discussed.

(a) Steady-state method

In 1905 (94) Tafel noted that a relation existed between current and potential for an electrode reaction, this relation now being called the Tafel equation. In its simple (exponential*) form, the relation gives the current, i , as a function of potential, V . For a simple electron transfer process such as $O + e \rightarrow R$, where O and R are the reactant and product, respectively, in solution, the relation in terms of absolute rate theory is as follows:

$$i = F \frac{kT}{h} \left\{ \exp - \frac{\Delta G^{o\ddagger}}{RT} \right\} (C_o)_s \exp \left\{ - \frac{\beta F}{RT} V \right\} \quad (i)$$

where F is the faraday, $\frac{kT}{h} \left\{ \exp - \frac{\Delta G^{o\ddagger}}{RT} \right\}$ the chemical reaction rate constant, $\Delta G^{o\ddagger}$ the standard chemical free energy of activation, $(C_o)_s$ the reactant concentration at the electrode, β the symmetry factor and V is the metal-solution potential difference. ** The metal-solution potential difference, V , can be expressed in terms of the reversible potential for the reaction, V_r , and the overpotential, η :

* The original equation was given in the log form, $V = a - b \log i$.

** For a more complete discussion of these terms, see ref. (95).



$$V = V_r + \eta \quad (ii)$$

When equation (ii) is substituted into equation (i) and the constants are put together into an overall constant, the exchange current density i_0 , equation (iii) results:

$$i = i_0 \exp\left\{-\frac{\beta F}{RT} \eta\right\} \quad (iii)$$

Equation (iii) may be simplified to the following form:

$$\eta = \frac{RT}{\beta F} \ln i - \frac{RT}{\beta F} \ln i_0 \quad (iv)$$

hence, a plot of η against $\ln i$ gives the Tafel slope, $(RT/\beta F)$, usually denoted by b . If the reaction is more complex, e.g., $O + e \rightarrow I$; $I \rightarrow R$ where I is an intermediate that may be adsorbed on the electrode surface, i.e., the electrode is no longer simply a source or sink of electrons, equation (iii) must be modified to take into account free space $(1-\theta)$ and/or coverage, θ , by intermediate I on the electrode surface. If the coverage by the adsorbed intermediate is dependent on potential, the Tafel slope will not be $(RT/\beta F)$ but a new quantity, $(RT/\alpha F)$, where α , defined as the transfer coefficient, may differ from β , the symmetry factor, because the former term will contain a factor arising from the potential dependence of coverage by the adsorbed intermediate.

Steady-state current-potential curves can be obtained by (i) galvanostatic and (ii) potentiostatic polarization. In galvanostatic polarization, the potential is measured as a function of the controlled current supplied to the electrode system. In potentiostatic polarization, the current

is measured as a function of the controlled potential of the electrode system. In both cases, measurements are obtained while the reaction is in a steady-state condition, i.e., there are normally no further short-time fluctuations. Both methods provide experimental data from which polarization curves can be obtained and Tafel slopes measured for various reactions. In favorable cases, analysis of the Tafel slopes can lead to assignment of possible reaction mechanisms and, when used in connection with product yield and controlled potential reaction-order experiments, can give the actual reaction mechanism. Both methods should give the same results for a reaction which displays a simple, linear Tafel region. However, the potentiostatic method is more versatile since it can be used for reactions where passivation causes a change in direction of the current-potential profile. Under galvanostatic conditions, this region of reversal of the i - V relation is unstable due to its negative resistance characteristic.

The potentiostatic method was exclusively used in the present work since passivation effects by the surface oxides at platinum were of considerable importance.

(b) Non steady-state methods

In contrast to the steady-state methods mentioned above, non steady-state procedures can often be profitably employed to provide information not obtainable under steady-state conditions, particularly for reactions which involve only adsorbed species. In these methods, the electrochemical

system is not in an equilibrium state. One such method, the potentiodynamic procedure developed by Will and Knorr (3), was briefly discussed on p.4 for Pt in aq. H_2SO_4 . The method consists of varying the potential of the working electrode in a controlled manner by means of a repetitive or single triangular voltage-time signal and measuring the resulting currents which pass at the electrode. Although the sweep method can quickly give qualitative information about processes at electrodes, a quantitative interpretation of the experimental data is sometimes difficult because the currents observed are often the result of a number of different processes. These currents can contain components due to (a) non-faradaic; (b) pseudo-faradaic; and (c) faradaic processes occurring at the electrode. The non-faradaic contribution arises from charging of the double-layer, the so-called "pseudo-faradaic" processes are associated with surface reactions at the electrode and faradaic processes are those in which a net steady-state current can ultimately be sustained by reaction between the electrode interface and reaction components in the solution. The pseudo-faradaic and faradaic components can be either activation controlled or diffusion controlled, the latter processes depending on reactant concentration. The problem is further complicated by the fact that a particular electrode process which is activation controlled at one potential sweep rate, (dV/dt) , may become diffusion controlled at a faster sweep rate where higher

relaxation currents are demanded, and vice versa. When using the potentiodynamic method, it is thus necessary to work under well-defined conditions corresponding to either activation or diffusion control and to ascertain whether any change in the experimental variables causes a change in the rate determining step of the reaction mechanism.

A characteristic potentiodynamic i - V profile was shown in Fig. 1 for a platinum electrode immersed in 1N aq. H_2SO_4 with the potential varied between the limits for hydrogen and oxygen evolution. For this particular case, the electrode processes which occur between these potentials can only be the activation controlled "pseudo-faradaic" surface reactions corresponding to atomic hydrogen deposition and ionization, and to surface oxide formation and reduction, referred to on p.6. These processes are not continuous since they virtually cease as the fractional coverage, θ , by the adsorbed species reaches its equilibrium value at any potential. The transient currents, i_{ads} , which are observed during the potentiodynamic sweep, depend on the coverage by adsorbed species produced or stripped from a surface in an electrochemical reaction. The quantity which characterizes the potential dependence of coverage by the adsorbed species is the adsorption pseudo-capacitance, C_{ads} , and hence the transient currents will be related to this quantity.

The deposition or removal of adsorbed hydrogen is an example of a pseudo-faradaic process occurring reversibly

at the electrode surface. Since the adsorbed intermediates are formed in a charge transfer process, ($\text{Pt} + \text{H}_3\text{O}^+ + e \rightarrow \text{PtH} + \text{H}_2\text{O}$), each value of coverage, θ , corresponds to a charge, q , required to achieve that coverage from a condition where the electrode surface was previously uncovered, i.e., $q = k\theta$ where k is the charge needed to establish a monolayer of adsorbed species. The derivative dq/dV is defined as the adsorption pseudo-capacitance:

$$C_{\text{ads}} = \frac{dq}{dV} = k \frac{d\theta}{dV} \quad (\text{v})$$

since the electrode coverage, θ , is a function of potential. The potential dependence of coverage by an electroactive species in an electrode process is analogous to the pressure dependence of coverage in a gas/solid adsorption process. In the first case it is the electrochemical potential, $\bar{\mu}$, that is changed while in the latter case it is the chemical potential, μ , that is altered. Equation (v) also gives the dependence of transient current on adsorption pseudo-capacity since the charge, q , is simply the product of current and time. Thus

$$C_{\text{ads}} = \frac{dq}{dV} = \frac{d(i_{\text{ads}} t)}{dV} = i_{\text{ads}} \frac{dt}{dV} \quad (\text{vi})$$

$$\therefore i_{\text{ads}} = C_{\text{ads}} \frac{dV}{dt} \quad (\text{vii})$$

For simple, reversible electrochemical adsorption processes such as the stages of hydrogen deposition or removal,

kinetic equations give, at equilibrium,

$$\frac{\theta_H}{1 - \theta_H} = K_H C_{H^+} \exp(-VF/RT) \quad (\text{viii})$$

where $K_H = \frac{k_{H^+}}{k_H}$, i.e., the ratio of rate constants for electro-deposition and ionization, respectively, of hydrogen at the metal surface and C_{H^+} is the bulk concentration of the proton source. More explicitly

$$\theta_H = \frac{K_H C_{H^+} \exp(-VF/RT)}{1 + K_H C_{H^+} \exp(-VF/RT)} \quad (\text{ix})$$

so that the corresponding pseudo-capacitance, C_{ads} , is given by

$$C_{ads} = k \left(\frac{d\theta_H}{dV} \right) = \frac{kF}{RT} \frac{K_H C_{H^+} \exp(-VF/RT)}{|1 + K_H C_{H^+} \exp(-VF/RT)|^2} \quad (\text{x})$$

which is a symmetrical function in V with a maximum at $\theta_H = 0.5$. The pseudo-capacitance C_{ads} has the properties of a condenser exhibiting potential-dependent capacitance and hence the current flowing into it (or out from it) is a charging current. C_{ads} has limits of zero at $\theta=1$ or $\theta=0$ at high or low V , respectively. For a condenser of capacity C , the charging current for a linearly varying potential is $C(dV/dt)$. Hence, in a potentiodynamic sweep, a pseudo-faradaic current, $i_{ads} = C_{ads}(dV/dt)$, flows and has a maximum corresponding to the maximum in C_{ads} as $f(V)$ (Equation (vii)). The ideally reversible electrochemical adsorption case has been discussed here as an example. Other cases involving varying degrees of

reversibility of the reaction and heterogeneity of the surface have been treated in previous work by Gileadi and Conway (96,97). Some examples will be involved in the interpretation of results obtained in the present work.

Surface processes involving deposition or removal of an electroactive intermediate display a peak in the potentiodynamic current-potential profile since C_{ads} is a $f(V)$ exhibiting a maximum at $\theta = ca. 0.5$. It is convenient to consider, in particular, the current corresponding to the peak potential, V_p , the measured current being the peak current, i_p . If C_{ads} is independent of sweep-rate, i.e., for a relatively reversible electrochemisorption process such as that discussed above, the transient currents will be directly proportional to sweep rate. For the peaks in the hydrogen adsorption region on platinum, this criterion is fulfilled exactly since the reactions of adsorbed hydrogen at platinum are fast, reversible processes even at quite rapid ($>50 \text{ V sec}^{-1}$) sweep rates. This fact will be utilized later in distinguishing co-adsorbed organic species from hydrogen in the hydrogen adsorption region. The potentiodynamic peak current for a diffusion controlled process is, on the other hand, proportional to $(dV/dt)^{1/2}$ (98,99), and the peak current for any sweep rate will then also depend on reactant concentration.

The charge associated with the electrochemical deposition or removal of a layer of adsorbed intermediates over a potential range V_2-V_1 is given by the expression:

$$q = \int_{V_1}^{V_2} i dt = \int_{V_1}^{V_2} (C_{ads} \frac{dV}{dt}) dt \quad (xi)$$

and C_{ads} will usually be a function, often symmetrical (cf. Eqn. (ix)), of potential. The area under the i-V peak between the potential limits V_2-V_1 within which the electro-sorption reaction is occurring gives the charge passed to produce the adsorbed layer. The coverage of the electrode with adsorbed intermediates can then be obtained from the charge passed if information is available on the number of electrons involved in the adsorption or ionization process at each platinum atom site.

For hydrogen adsorption on platinum, the assumption* is usually made that one atom of adsorbed hydrogen is associated with one atom of platinum and one electron is involved in its adsorption or ionization. Hence, the total charge under the anodic or cathodic hydrogen peaks at platinum gives directly the hydrogen coverage while the charge at full hydrogen coverage can also be employed to provide a basis for estimation of the real area of the electrode (since the number of exposed platinum atoms is known per real cm^2 of any given

* The hydrogen atoms may, in fact, sit interstitially in the surface amongst groups of 3 or 4 platinum atoms (depending on the index of the crystal face) with multiple or delocalized bonding (cf. the conclusions of Mignolet (100) on the surface potential of chemisorbed hydrogen).

crystal face).^{*} The charge associated with the deposition or removal of adsorbed atomic hydrogen is found to be independent of sweep rate, the peak heights changing in exact proportion to $\frac{dV}{dt}$. This will be true for any activation controlled pseudo-faradaic process which is rapid enough to keep up with the rate of potential change in the sweep.

In the case of surface oxide formation on platinum, the oxide charge is not independent of sweep rate since the reaction is a relatively slow surface process requiring time for the equilibrium coverage, corresponding to any potential, to be attained. Coverage by adsorbed oxygen species is determined in the same manner as that for hydrogen; however, it is usually preferable to obtain this coverage by integration of the i-V peak for surface oxide reduction since this peak is not usually affected by impurities which, because of reaction with the surface oxide formed in the anodic sweep, change the charge passed in the anodic direction of the sweep. Some types of organic impurities may, however, react in the region of oxide reduction in the cathodic sweep, as well as on the anodic sweep, in which case this method for evaluation of surface oxide charge could be inaccurate.

This method for determining surface coverage cannot, of course, be applied to reactions where a net steady-state current is sustained since such reactions involve the formation of adsorbed species which are constantly removed from the

* A complete discussion on the relationship between hydrogen adsorption charge and area of the electrode is given in ref. (101).

surface by the reaction and permit more of the adsorbed species to form by continuing electrochemical reaction. Hence, the potentiodynamic sweep method cannot give direction information regarding the surface coverage by species such as formic acid, methanol, formaldehyde, etc. An indirect method for obtaining such coverages by the sweep method is, however, possible and is given below.

The information which can be obtained by the potentiodynamic sweep method may be summarized as follows:

1. Whether the reactants under investigation are adsorbed at platinum. In the case of aqueous H_2SO_4 as supporting electrolyte, adsorption of reactant species such as organic molecules will give rise to a new i - V profile different from the standard background i - V profile for deposition and removal of hydrogen and oxygen species at platinum.
2. In cases where the reactant molecule is electroactive in the adsorbed state, the manner in which it reacts over the various ranges of potential may be observed. Its electrochemical behavior in the hydrogen and oxygen adsorption regions (0.05 to 0.35 V, E_H and 0.8 to 1.5 V, E_H , respectively) and the cathodic and anodic double-layer regions may be readily distinguished.
3. By studying the reaction over various potential ranges, e.g., with or without the presence of surface oxide and/or adsorbed hydrogen, information can be obtained regarding electrochemical modifications of the reactant molecule that can occur in the different potential regions.

4. Distinction can be made between reactants which give faradaic or pseudo-faradaic currents since a faradaic process gives a finite, steady-state current on potentiostatic polarization. The currents will be independent of sweep rate if the faradaic process is not diffusion controlled and does not involve slowly produced intermediates; examples are the oxygen and hydrogen evolution reactions at platinum in aq. H_2SO_4 .
5. If the reaction is pseudo-faradaic, i.e., it involves electrochemical deposition or removal of an adsorbed species which does not undergo a continuous, faradaic reaction, and gives a peak in the current-potential curve, e.g., in the double-layer region, the sweep rate dependence of the peak current, i_p , and peak potential V_p , can be determined. For an activation controlled pseudo-faradaic process, $i_p \propto (dV/dt)$ and is independent of reactant concentration in solution. For a diffusion controlled process, $i_p \propto (dV/dt)^{1/2}$ and will also depend on reactant concentration in solution. A pseudo-faradaic process which is influenced by diffusion of reactant to the electrode surface will display an $i_p \propto (dV/dt)^x$ where x is between 1/2 and 1. If the process is fast and reversible, V_p should be independent of sweep rate while any dependence of V_p on sweep rate will indicate a degree of slowness and irreversibility in the reaction; dependence of V_p on $\log (dV/dt)$ can give Tafel parameters for the surface process.

In cases where the reaction gives rise to a peak in either the hydrogen or oxygen regions of the sweep, complications arise because the background currents of surface oxidation or reduction, and of H deposition or ionization, will also play a role. In general, the currents associated with pseudo-faradaic adsorption processes involving organic substances are of the same order of magnitude as those for the hydrogen and oxygen reactions arising from the supporting aqueous electrolyte; hence these background currents must always be taken into consideration together with the corresponding double-layer charging current. However, it is unlikely that these current contributions will be the same as they were in the absence of the adsorbing reactant, so that the correction to be employed may be unknown. Even when organic faradaic reactions are being investigated which exhibit large oxidation currents, the smaller background currents may complicate interpretation of the results. This difficulty does not arise with the steady-state method since currents for any background surface processes will have fallen to zero in the steady-state.

6. For a pseudo-faradaic process involving an electroactive adsorbed species, the fraction of electrode surface blocked by reactant adsorption can be determined from the decrease in atomic hydrogen coverage observed in the sweep. The coverage by adsorbed species, θ_R , is thus equivalent to $(1-\theta_H')$, θ_H' being the total hydrogen coverage after

reactant adsorption. For this method to give a reliable result, the only reaction in the hydrogen region should be atomic hydrogen deposition and ionization, i.e., no hydrogenation of the adsorbed species should be possible. For a diffusion controlled pseudo-faradaic process, this method cannot be employed since the coverage by reactant may be changing even during the sweep in the hydrogen region.

7. The role of protons in the mechanism of an electrochemical process displaying a current peak can be examined by varying the pH of the solution, as in pH studies in steady-state investigations (33). The pH dependence of the peak potential, V_p , will indicate whether protons are involved in the reaction and will also give the ratio of the number of protons to the number of electrons involved.
8. The potentiodynamic sweep method can also be used to give the i - V profile for the hydrogen and oxygen evolution processes at platinum. Although steady-state polarization plots are required for any mechanism study of the reactions, the general qualitative effects of additives on these faradaic processes can be quickly ascertained, e.g., whether inhibition of the reactions occurs and how such changes in the kinetics of these processes may be related to hydrogen and oxygen coverage.
9. In a similar manner, the potentiodynamic sweep method can be used to examine the faradaic currents associated with organic oxidations, e.g., methanol, formic acid and formaldehyde. The reactions of such organic molecules in

the various potential regions can be readily established (24,102) with regard to activation and inhibition effects. Although integration of the oxidation peak area does not, in this type of case, give the coverage of the electrode by the organic reactant, a method exists for determining the coverage at different potentials from the decrease in charge (area) for the atomic hydrogen reaction brought about by adsorption of the organic species in relation to the charge measured over the same potential range in the supporting electrolyte alone.

The method consists (24,103) of polarization at the potential of interest, followed by a very rapid cathodic sweep into the hydrogen adsorption region. The assumption is made that no further adsorption or desorption occurs during the rapid cathodic sweep; this assumption can be checked by varying the rate of the cathodic sweep into the hydrogen region. Usually low concentrations of reactant are employed to minimize continuing reaction in the transient.

In a similar fashion, the surface coverage with adsorbed organic species may be determined from the charge for complete oxidative desorption of the adsorbed species during a rapid anodic sweep to ca. 1.8 V, E_H (52). In order to evaluate surface coverage from oxidation charge by this procedure, information is required, or assumptions must be made, as to the number of electrons involved in the

oxidation of the adsorbed species per platinum atom. These procedures may be complemented by the technique of radioactive isotope labelling, which can give a direct measure of the degree of adsorption on the electrode surface in the case of suitable substances, e.g., C^{14} -ethylene, formic acid, benzene, etc. (102, 104-106).

10. The potentiodynamic sweep method is particularly well suited to the study of non-aqueous systems since it allows a rapid qualitative determination of the water content in the system. This method involves the reactivity of molecular hydrogen at the platinum electrode and further details will be given in Chapter III, part IV.

Another transient procedure consists in obtaining current-time transients after addition of various additives at potentiostatically controlled potentials. For an activation-controlled pseudo-faradaic process, i.e., one involving only electrochemical adsorption, the area under the current-time transient can sometimes give the equilibrium coverage of additive at the potential of addition (see p.79). The method may thus give the potential at which maximum adsorption of the additive in question occurs, provided no complications arise from other reactions on the surface. As with the potentiodynamic sweep method, fewer complications

will arise for reactions studied in the double-layer region than for reactions studied in the hydrogen or oxygen regions.

(c) Controlled mass-transfer experiments

It is usually desirable to study the kinetics of a reaction under activation control, if possible. However, for conditions where diffusion or mass-transfer effects cannot be avoided, the kinetic parameters (e.g., i_0 and the transfer coefficient^{*}) can usually be evaluated by appropriate choice of a non steady-state transient method (99). Alternatively, by forced convection, it is sometimes possible to change the conditions so that a process which was previously diffusion controlled becomes activation controlled. Thus, some reactions which are under diffusion control at a stationary electrode can be forced into activation controlled behavior at a rotating electrode (108). As the rotation speed of the electrode increases, reactant is transported to the surface more rapidly and the diffusion layer thickness effectively decreases. With some fast reactions, e.g., molecular hydrogen oxidation at platinum (108), a very high rotation rate results in reactant being transported to the surface sufficiently fast that it is consumed by the electrochemical reaction at a rate determined by the velocity of the activation controlled reaction at the electrode surface. The reaction is then no longer diffusion controlled.

For those reactions which do not become activation controlled, even at high rotation speeds, the diffusion layer

^{*}For definitions of the exchange current density, i_0 , and the transfer coefficient, α , see (107).

thickness can at least be kept constant and well-defined by means of the rotating electrode. Indeed, for reactions studied under diffusion control, the rotating electrode provides the only method for obtaining reproducible results, this method being greatly superior to solution stirring by nitrogen as a basis for providing a constant flow of reactant to the surface.

3. Aims of the Work

The aims of the present work were to investigate the role of a number of electrode poisons, acetonitrile in particular, in electro-catalytic organic oxidation reactions at platinum in relation to the dissociative chemisorption of organic molecules and H_2 . The extensive use of acetonitrile with various electrode materials as a non-aqueous solvent in electrochemistry over the past decade has not been complemented by any significant studies on its basic electrochemical properties at the electrode surfaces. Indeed, the substance has been assumed to be unreactive in the pure form at platinum except at extremes of potentials.

In the present work, acetonitrile is shown to be reactive at platinum electrodes in aqueous media and this behavior is used to explain the results obtained with acetonitrile under non-aqueous conditions.

The general aims of the work can be sub-divided into a number of sections as outlined below, covering specific areas of the investigation required to characterize the electrochemical properties and reactivity of acetonitrile and a number of other nitriles.

1. To investigate the possible reactivity of acetonitrile itself at platinum electrodes and the manner in which acetonitrile affects the normal surface reactions at platinum in aqueous medium between the potential limits of hydrogen and oxygen evolution. Also to investigate the mechanism of reactions which acetonitrile itself undergoes at a platinum electrode.
2. To determine the optimum procedure for purifying and drying acetonitrile for use as a non-aqueous solvent. The effects of low concentrations of water on the acetonitrile solvent system were investigated electrochemically in order to establish the effect, if any, of small amounts of water in the acetonitrile on its electrochemical reactivity.
3. To devise a reasonable, in situ, method of detecting the presence of trace quantities of water in the non-aqueous acetonitrile solvent system before an experiment was begun.
4. To investigate further the mechanisms of formic acid and methanol oxidation at platinum by working under non-aqueous conditions in acetonitrile. Also, to determine the effects of low concentrations of acetonitrile on methanol and formic acid oxidations at platinum and to correlate this information with that obtained at very high concentrations of acetonitrile (i.e., virtually non-aqueous conditions).

5. To investigate, in a general way, the mechanism by which both organic and inorganic poisons affect organic oxidations at platinum in relation to the manner in which surface oxides inhibit these reactions.
6. To elucidate further the role of platinum surface oxides in organic oxidations (as well as in molecular hydrogen oxidation) by working under conditions where the formation of such oxide species is either not possible, i.e., under non-aqueous conditions, or can be controlled independently by water content of the solvent.
7. To investigate the manner in which adsorption of organic or inorganic substances occurs on a platinum electrode surface partially or fully covered by atomic hydrogen and the relation between these processes and adsorption on a surface initially free from chemisorbed hydrogen or oxygen particles.

CHAPTER II

EXPERIMENTAL

1. Introduction

The electrochemical experiments carried out in the present work employed both steady-state and non steady-state techniques. Since the study of passivation effects and non-continuous faradaic processes was of particular interest, the electrochemical methods involved potential rather than current control. Measurements of current-time transients were made in determining the coverage by certain electroactive species at various controlled potentials. These procedures, as well as those involved with preparation of solutions and electrodes, will be described in detail below.

2. Preparation of Solutions

(a) Criteria of solution purity

Aqueous solutions were prepared from water that had been doubly distilled, the last stage of distillation being from an alkaline permanganate solution in an apparatus provided with three spray traps and baffles. Identical results were obtained from water which had undergone one further step of distillation without permanganate. Acidic solutions were prepared from B.D.H. micro-analytical grade sulfuric acid without any further purification being necessary. Pre-

electrolysis treatment of the solutions was employed where required, i.e., when the criteria of solution purity listed below were not satisfied. On the basis of results obtained by the potentiodynamic sweep method at a platinum electrode in aq. H_2SO_4 , the criteria for high solution purity were as follows:

- a) Resolution of the two cathodic and three anodic atomic hydrogen electrosorption peaks in the potential range 0.05 to 0.35 V, E_H .
- b) Resolution of the three anodic peaks for Pt surface oxidation* in the potential range 0.8 to 1.2 V, E_H .
- c) Independence of the charges and peak current/potential coordinates for the oxide and hydrogen peaks on solution stirring and linearity of the peak currents with sweep rate, indicating the occurrence of surface processes only.
- d) Equality of cathodic and anodic charges for the oxide and hydrogen regions to within 2% (contrast results of earlier work (110)).
- e) Reversibility to within 5 mV of the two main peaks for electrosorption of H.
- f) Maintenance of the charge associated with hydrogen coverage to within 95% of its initial value during

* These three peaks have received special attention and recognition in recent work (109) and are, in fact, only well resolved under conditions of highest purity.

cycling for one hour in the range 0.05 to 0.75 V, E_H , i.e., in the absence of formation of Pt surface oxides which otherwise leads to anodic oxidation of any accumulating impurities and cleaning of the electrode for H adsorption.

- g) Absence of any spurious peaks in the cathodic or anodic double-layer regions of the sweep.
- h) Constancy of the anodic double-layer charging current between 0.4 V and 0.75 V, E_H and observation of an equal cathodic double layer charging current at 0.4 V, E_H for anodic termination potentials in the sweep of up to 1.3 V, E_H .

Fulfillment of the above criteria not only indicates a high degree of purity of the electrolyte solution but also a very clean platinum electrode surface.* Before any experiments were performed with additives in the system, all the above criteria were fulfilled with the exception of (f), this extra criterion being employed only in those experiments which required cycling in a restricted potential range without formation of Pt surface oxide.

Alkaline solutions were prepared from B.D.H. AnalaR grade KOH recrystallized once from water.

* In other work in this laboratory, it has been shown by low energy electron diffraction that electrodes examined under the conditions mentioned above are exceptionally clean in relation to normally accepted standards in LEED work.

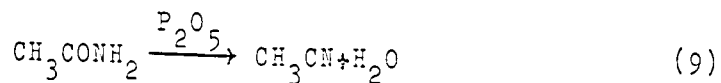
(b) Purification of acetonitrile and organic reagents

Purification of acetonitrile as an electrochemical solvent has received considerable attention in the literature because it is more difficult to purify than most other non-aqueous solvents (cf. dimethylsulfoxide, dimethylformamide, propylene carbonate) and, as a result, there are numerous procedures for acetonitrile purification (72-78). Coetzee et al (74) reviewed a number of the standard procedures and recommended a multi-stage refluxing and distillation operation employing CaH_2 and P_2O_5 . However, polymerization of the acetonitrile at each stage of this procedure results in a low percentage yield. In the present work, acetonitrile was purified by the procedure of Mann et al (73) using Union Carbide grade 98% acetonitrile as starting material. The acetonitrile was not subjected to a prior drying over CaSO_4 as suggested by these authors since traces of water were thought to be desirable in aiding the permanganate oxidation of olefinic impurities (84,111) which can cause difficulties (impurity current or inhibition effects) in the anodic potential region at platinum. The acetonitrile was distilled first from alkaline permanganate through a short column having 3 theoretical plates. This distillation was followed by acidification of the acetonitrile and a further distillation through a multi-plate column having ca. 30 theoretical plates. The "middle" 70% fraction was collected.

Gas chromatography on a Porapak column using a thermal conductivity detector showed this acetonitrile to contain less than 0.01% water and no detectable acrylonitrile. Gas chromatography, with high sensitivity hydrogen flame ionization detection, showed less than 5 p.p.m. of organic impurities. The purified acetonitrile was stored over a dry molecular sieve (B.D.H. type 4A) in all-glass containers and syphoned off as necessary. It was found that dry acetonitrile exposed to air picked up water rapidly, from less than 0.01% to 0.10% in four hours of exposure from a thin (ca. 1 cm. diam.) necked flask. The molecular sieve was found to be extremely effective in drying acetonitrile, the water content decreasing from 1.0% to less than 0.01% after half an hour of treatment with the molecular sieve (cf. 112).

For runs in anhydrous acetonitrile, a specially constructed platinum gauze bag electrode was filled with molecular sieve and immersed in the solution for prior, in situ drying and purification treatment. Although the Eastman "spectrograde" acetonitrile gave results identical with those obtained with the Union Carbide treated acetonitrile when added to aqueous solutions in small quantities, in the case of experiments conducted in almost 100% acetonitrile, the Eastman grade product gave difficulties in the high anodic potential region.

In order to check the results obtained using the various commercial grades of acetonitrile, a quantity of acetonitrile was prepared synthetically in the laboratory by dehydration of acetamide:



After distillation of the product, no differences were found between the behavior of this and the purified commercial acetonitrile.

Sodium perchlorate was used as the supporting electrolyte for the non-aqueous acetonitrile system.

"Anachemia" reagent grade material was recrystallized from water and dried in a vacuum oven at 80°C. The salt was stored in all-glass containers and dried again before use, great care being necessary at all times in handling the salt because of its hygroscopic nature.

Formic acid solutions were prepared from the "AnalaR" analytical reagent, and methanol and benzene solutions from Baker "Spectroanalyzed" reagents. Ethylamine, iso-butyronitrile, acrylonitrile and propionitrile were distilled through a three plate fractionating column while all other "reagent pure" chemical compounds were used without further purification. Acetonitrile was the only material which was used as a 100% non-aqueous solvent so that it was the only nitrile which required rigorous drying.

3. Preparation of Electrode Metal Surfaces

The platinum electrodes used in the present work were prepared from Johnson Matthey and Mallory spectroscopically pure platinum wire degreased for 24 hours in an

acetone-containing Soxhlet extractor. The platinum wire was then annealed for one hour in a quartz furnace at 900°C in an atmosphere of purified hydrogen and allowed to cool slowly. The annealed wire was then sealed into a specially prepared thin glass bulb under a hydrogen atmosphere (113); in this way, the electrodes could be stored without contamination until used in the experiment. The bulbs were subsequently broken in the solution being studied so that no prior atmospheric contamination occurred.

It was of particular importance in the non-aqueous runs to prepare platinum electrodes, the surface of which had not undergone any prior oxidation at elevated temperatures. Some large area platinum electrodes were also prepared, in this case with spectroscopically pure platinum foil, degreased, but not annealed in the manner described above. Such large area electrodes were used when results were required over ranges of potential where the surface oxide region was excluded in the experiments in aqueous media; they were never used in the non-aqueous systems because of the high resistance of such solutions.

In the case of the runs in aqueous solutions, a clean platinum electrode was found to continue to give reproducible potentiodynamic current-potential profiles for several weeks, fulfilling the criteria listed above, provided the electrode was washed thoroughly after each run with concentrated sulfuric acid and stored under doubly-distilled water. The various nitriles could be washed from the surface with some facility

but sulfur compounds (e.g. thiourea) used in part of the work required more rigorous cleaning coupled with anodic polarization in the oxygen evolution region in a separate cell in order to effect their complete removal. Nickel and gold electrodes were also investigated and were prepared in a manner identical with that for platinum, except that the annealing temperature for nickel was 600°C while that for gold was 550°C.

4. Reference Electrodes

Hydrogen reference electrodes were prepared by platinizing platinum gauze electrodes in an acidic solution of platinic chloride (114). The platinized platinum electrodes were frequently checked with other freshly prepared reference electrodes and were kept under double-distilled water between runs. The hydrogen reference electrodes were used in all aqueous runs and in those non-aqueous runs where exclusion of the last traces of water from the system was not necessary. The hydrogen reference electrode in highly concentrated acetonitrile solutions gave reproducible results (cf (84)) provided the solution in the reference compartment was made 0.25 M in HClO_4 . In those acetonitrile solutions where very low water contents were essential, a Ag/Ag^+ reference electrode was used, following the method of Billon (80). This reference electrode was prepared in situ by anodically polarizing a silver wire with a sufficient quantity

of electricity to give a 10^{-2} M Ag^+ solution in acetonitrile containing 0.5 M NaClO_4 . In addition to the normal stopcock between the reference and working electrode compartments, the silver wire and solution were enclosed in a small tube which was closed by means of a solution-wetted standard taper joint to minimize diffusion of silver ions to the working electrode compartment.

5. Gases

Hydrogen and nitrogen gases were passed through standard (dry) purification trains (113) before admission to the electrochemical cell. The gas purification trains consisted of (a) a mercury blow-off safety trap; (b) magnesium perchlorate and molecular sieve drying tubes; (c) a duel oven containing copper turnings and palladized asbestos maintained at 450°C to remove oxygen from the gases and (d) three traps maintained at liquid nitrogen temperatures, the last two containing activated charcoal covered by glass wool. Medical grade carbon dioxide employed in some experiments was used after passage through a trap maintained at the dry ice-acetone temperature (i.e., -78°C). Solution pre-saturator bubblers were used for both the working and reference electrodes so as to minimize solution evaporation and hence change of concentration during experiments.

6. Cells

Three different types of all-glass electrochemical cell were used in the present work; one for experiments in non-aqueous solutions, one for aqueous solutions and one for work with a rotating-disk electrode. The cell employed in the non-aqueous work was of the standard three-compartment design (115) with a large volume working electrode compartment, so that up to 250 ml of solution could be used with as many as six different platinum working electrodes without opening the working electrode compartment to the atmosphere. This was a great advantage in the non-aqueous acetonitrile work since vapor phase chromatography showed that even limited exposure to the atmosphere gave an increase in the water content (together with the usual danger of accumulation of traces of impurities from the atmosphere). This cell was equipped with a movable glass probe in the working compartment which could be used to break the electrode glass bulbs while they were immersed in the solution (116). Glass connections were also provided for transferring the solutions directly to the cell, after a prior distillation, without contact with the atmosphere.

The cell used for most of the work in aqueous solutions was entirely different from that described above and shown in Fig. 3. Special features to be noted are the movable beaker below the cell which serves as a counter electrode compartment and also facilitates changing of

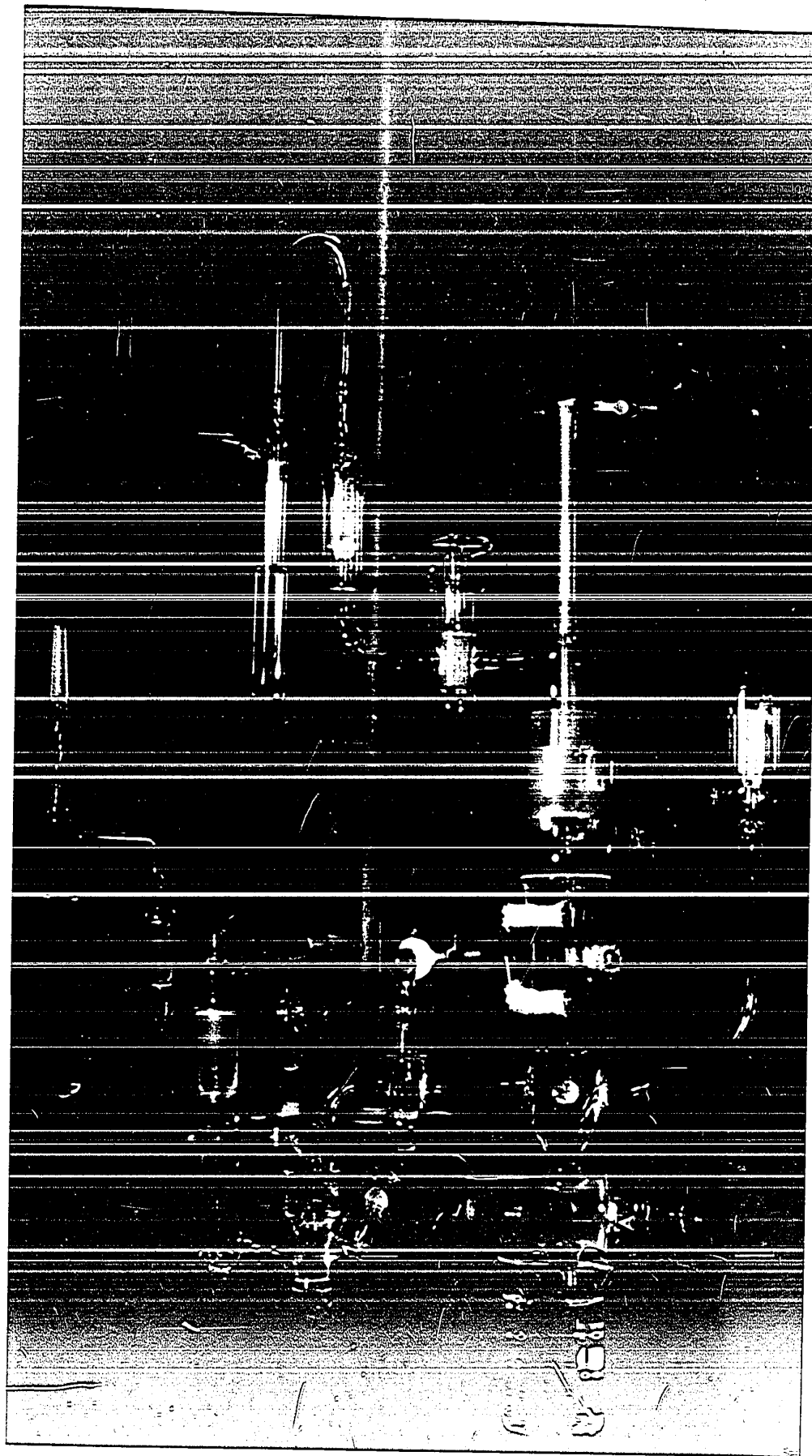


Fig. 3. Photograph of the electrochemical cell frequently used for studies under aqueous conditions.

solutions, a condition required in some runs. Also the reference electrode compartment is not permanently fixed to the working electrode compartment; the latter was designed for a small volume of solution only (20 to 40 mls) and there was accommodation at the top of the cell for two electrodes mounted in sliding sleeves. The nitrogen bubbled was introduced through the bottom of the cell to maximize efficiency of oxygen removal, such removal being easier in a cell of this design because of the lack of any dead-space or stagnant solution region associated with connection to a counter electrode compartment. This design of the cell made washing of the apparatus very easy since only the working compartment needed to be cleaned rigorously and frequently, this being an important and necessary requirement because of the large number of individual experiments which had to be performed on the various organic compounds in aqueous solutions.

The cell used for studies with the rotating disc electrode was of the standard three-compartment type with a working electrode compartment of large diameter. Since rotation speeds of up to 10,000 r.p.m. could be employed, turbulent flow could arise in a cell having an insufficiently large diameter compartment for the working electrode. The rotating electrode was of the ring-disc type and was fabricated, together with the support stand and motor, by Pine Instrument Company, N.J. The rotating electrode was located in the cell through a Teflon joint, the opening of which was

a millimeter greater than that of the electrode to prevent friction and heating at the fast rotation speeds employed. A stream of purified N_2 was passed over the solution and out through the loose Teflon bearing. This was found to be the best way of minimizing admission of oxygen.

7. Electrical Circuits

The circuit for potentiostatic steady-state polarization measurements is shown in Fig. 4. The potential between the working and reference electrodes was controlled with a Wenking potentiostat and the potential readings were taken on a potentiometer (Radiometer Model PHM-4b). The current was read from a Sensitive Research multi-range ammeter in series with the counter electrode.

The circuit used in obtaining potentiodynamic current-potential relations is shown in Fig. 5. In this case, the potentiostat is driven by a Servomex LF141 wave-form generator capable of giving single and multiple triangular potential-time functions. A Tacussel function generator was used for obtaining more complex potential sweep programmes, e.g., a programme where the rate of potential scan in the cathodic and anodic directions is different. The constantly varying potential between the working and reference electrodes results in a current which usually also varies in response to the potential. The resulting current-potential profile was recorded either on a Tektronix dual-beam oscilloscope or on a

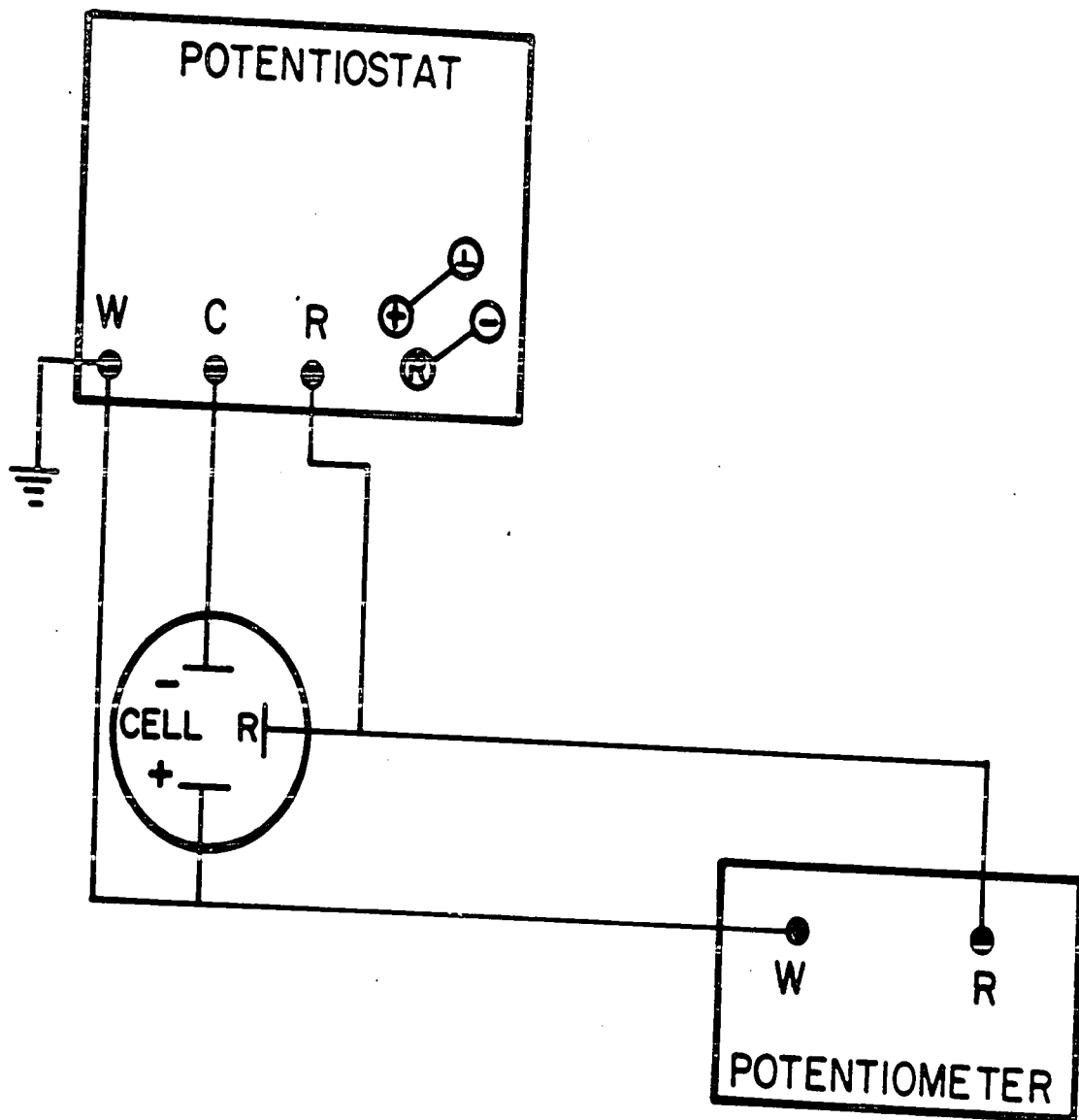


Fig. 4. Electrical circuit for potentiostatic steady-state polarization.

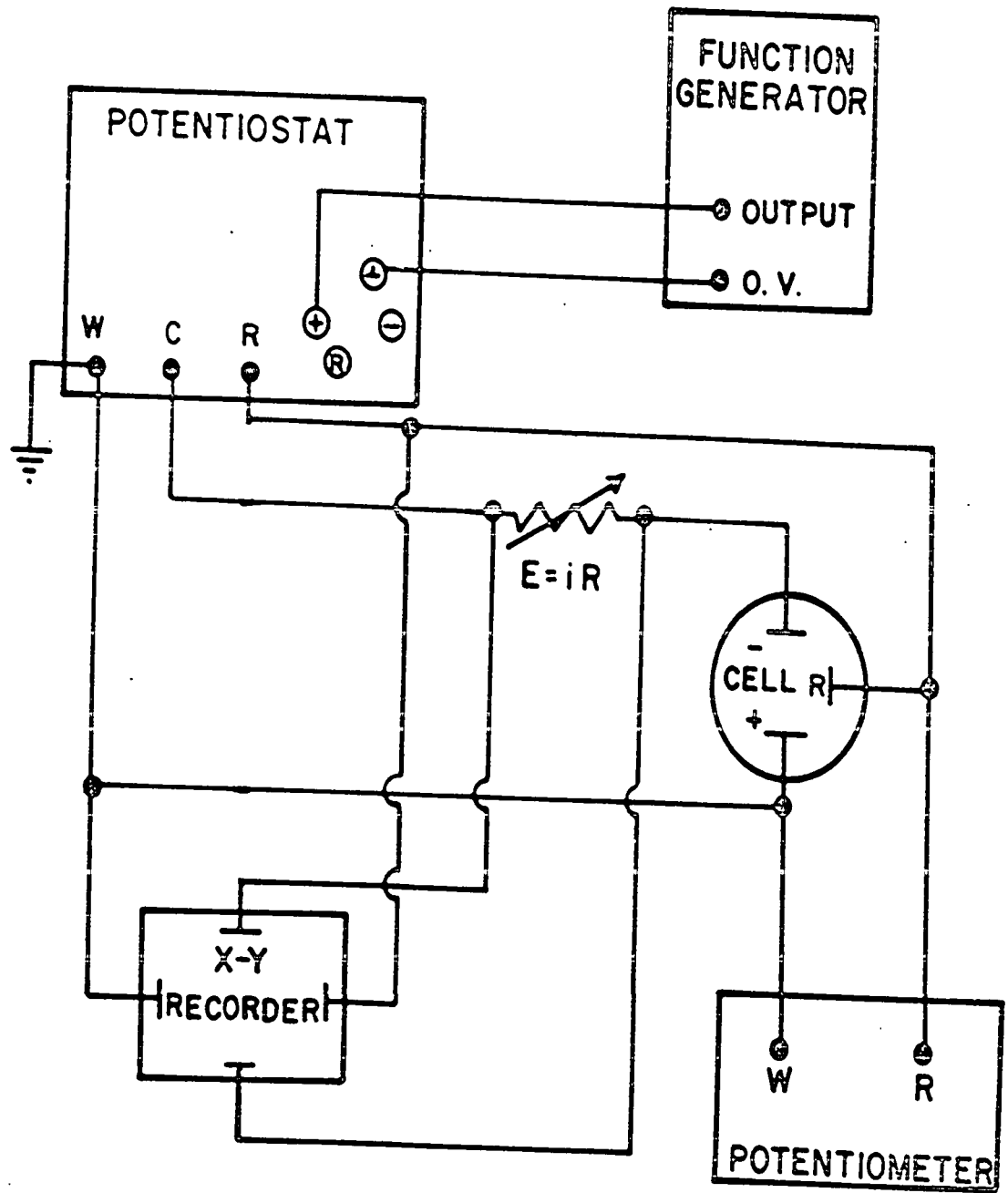


Fig. 5. Electrical circuit for potentiodynamic current-potential measurements.

Hewlett-Packard Model 2D-2AM X-Y recorder. The current-potential profile was precisely recorded by exact conversion of the time-dependent currents to corresponding potentials by passage through a calibrated decade resistance box in series with the cell. A cathode follower was employed to communicate the electrode potential to either an oscilloscope or an X-Y recorder. In the present work, a Tektronix storage oscilloscope was used extensively for the purpose of comparing and photographing a number of rapid sweep profiles (see Fig. 16).

8. Temperature

All experiments were performed at 25°C with thermostatic control being employed where necessary to maintain this temperature.

9. Experimental Procedures

(a) Steady-state measurements

Difficulties arise in obtaining steady-state polarization plots for formic acid oxidation at platinum because of the problem of defining conditions for any true steady-state for this reaction. In certain potential regions, not only does the variation of current with time continue after a period of 1 to 2 minutes but also the direction of variation of current may vary. In some of these cases, the current was found still to be decreasing or increasing to a significant extent after 10 minutes at a particular potential. Because of the

uncertainties associated with polarization for long periods of time (to achieve a reasonably steady current value), the polarization plots were taken with a standardized 90 sec. duration of current measurement at each controlled potential and both the initial and final current densities were recorded.

(b) Potentiodynamic sweep measurements

In all experiments where aqueous systems were studied, a potentiodynamic current-potential profile was initially recorded on the electrode in the absence of additives. In the case of platinum, the electrode was cycled between selected potential limits (e.g. 1.4 to 0.05 V, E_H) until the criteria of purity given above on p.48 were fulfilled. The electrode and solution purity were generally investigated by employing two sweep speeds (100 and 5 mV sec⁻¹) to ensure the absence of impurities which can behave selectively with respect to sweep speed. When a reproducible background i-V profile was obtained which fulfilled the criteria of solution purity, the electrode system was ready for the addition of the various organic and inorganic compounds and their subsequent experimental investigation.

Three procedures were employed for addition of the organic or inorganic compounds to the system. In the first case, the substance was added during a potentiodynamic sweep and the measurements were made after the i-V profile

had become reproducible. The number of sweeps required to achieve this state after addition of additive was always noted since it gave information on any slow transformation which the additive might undergo. The additives were completely deoxygenated before being injected as aliquots into the solution by means of a micro-syringe.

In the second case, addition was made during a potentiodynamic sweep, but at a certain predetermined potential. This, for example, was one of several methods employed to study the effects of acetonitrile on the oxidation of formic acid at platinum. Since it was of great importance for the deoxygenated additive to reach the electrode when the potential was at a certain desired value, rather slow sweep rates were used in this investigation (10 to 25 mV sec⁻¹).

A third method, used to investigate the adsorption behavior of various organic compounds at free and hydrogen-covered platinum surfaces, involved a somewhat modified procedure. After the current-potential profile was obtained for the clean platinum in aq. H₂SO₄, the electrode was held potentiostatically at various potentials and a "zero-current line" (with respect to time) was recorded as a basis of reference. The organic substance in deoxygenated solution was then added to the cell from the micro-syringe and the resulting current-time transient was recorded. This was followed by a further potentiodynamic i-V profile to determine the change of coverage by electrochemisorbed hydrogen due to adsorption of the organic additive on the platinum surface.

In this way, the charge associated with adsorption of the organic substance could be compared with the extent of blocking of the surface for adsorbed hydrogen caused by the organic additive. The organic compounds investigated in this way at platinum were acetonitrile, benzonitrile, 1,4-dicyanobenzene, benzene, cyclohexane, thiourea and dimethylsulfide; thiourea was also used at a nickel electrode to detect possible coverage by atomic hydrogen at potentials negative to that of the H_2 reversible potential. These additives were injected into the solution at concentrations which were high enough to give saturation limits of hydrogen blocking in a single i - V sweep as indicated from a study of the concentration dependence of the hydrogen blocking effects revealed in cyclic voltammetry experiments (Fig. 6).

(c) Evaluation of charge components for acetonitrile surface reactions at platinum

The experimental procedure used in determining the extent of reduction of acetonitrile at various potentials was somewhat complex and involved the use of several potentiodynamic programs. The reasons for choice of various programs will only be appreciated after the experimental results have been cited, i.e., the details of the experimental procedure developed in this case were governed by the progress of the work; consequently the rationale of the procedure will be outlined, as required, in Chapter III. The same applies

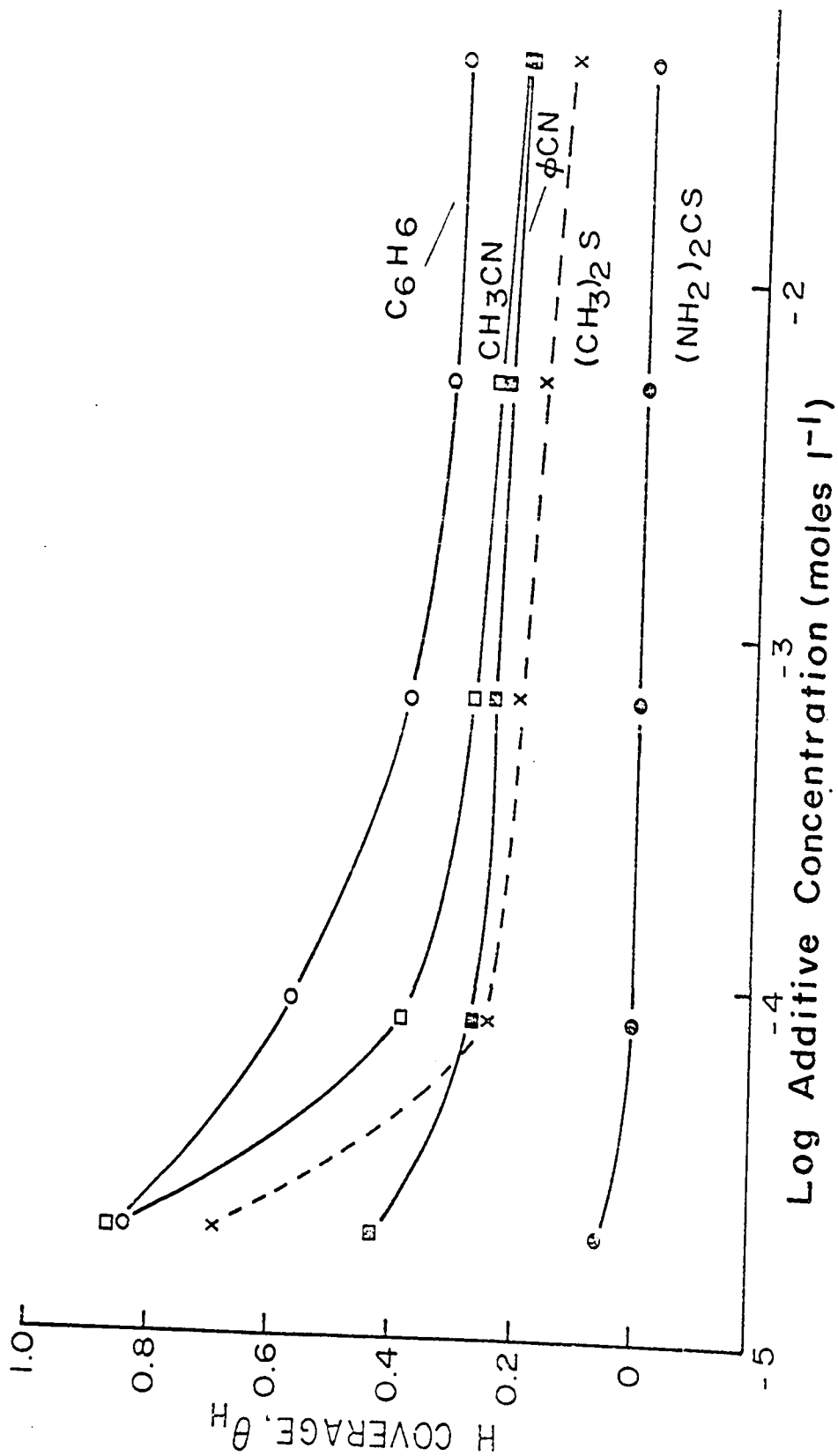


Fig. 6. Adsorption isotherm for thiourea (\bullet), dimethylsulphide (\times), acetonitrile (\square), benzonitrile (\circ), and benzene (\circ) at Pt at 25°C, 1N H_2SO_4 , represented in terms of their blocking effects on H electrochemisorption.

to the experimental procedure used in the kinetic relaxation technique to be discussed in Chapter III and with regard, for example, to the method of investigating the effect of the presence of adsorbed hydrogen on formic acid oxidation by (i) sweep reversal at various cathodic terminal potentials; (ii) progressive electrodeposition of mercury; (iii) adsorption of acetonitrile; and (iv) cycling for extensive periods of time in potential ranges which exclude the surface oxidation reaction and hence can give rise to impurity accumulation on the electrode surface. This approach will allow a more logical and less repetitive presentation of the work.

CHAPTER III

RESULTS AND DISCUSSION

The experimental results and the subsequent discussion will be presented together since the sequence of experiments and their interpretation were closely related. The presentation will be divided into four main sections (Parts I, II, III and IV) corresponding to the four principal areas of experimental work involving acetonitrile electrochemistry and electrocatalysis at Pt.

Part I

Electrochemisorption and Reactivity of Nitriles at Platinum Electrodes

I.1 Behavior of Acetonitrile at Platinum in Aqueous H₂SO₄ Solutions

(a) Introduction

The reactivity of low molecular weight organic molecules such as methanol, formaldehyde and formic acid at platinum anodes in anhydrous acetonitrile was the first subject to be experimentally investigated in the present work. The extent of platinum surface oxide formation could be controlled by addition of various amounts of water to the system as well as by the value of the anodic terminal potential in

the potentiodynamic sweep experiments. The results of these experiments, discussed in Part IV, led to an examination of the behavior of acetonitrile itself in more aqueous solutions in order to determine if acetonitrile is electrochemically reactive at platinum. Under completely anhydrous conditions there was no observed reactivity, except at extreme anodic and cathodic potentials, as indicated by the absence of significant currents during potentiodynamic cycling with sodium perchlorate as electrolyte. However, the possibility still existed that acetonitrile could be adsorbed on the platinum surface in pure, anhydrous systems and in that way influence the organic reactions which had been studied. Since interpretation of the results of experiments in non-aqueous acetonitrile is easier after the behavior of acetonitrile at platinum in aqueous media has been understood, the latter subject will be discussed first.

In aqueous acid media, the following new effects were observed in the investigation of the behavior of nitriles at platinum:

- (i) acetonitrile and a number of other nitriles undergo chemisorption at platinum electrodes and then set up a more or less reversible redox system in the "double-layer" region^{*} involving only adsorbed acetonitrile species;

^{*}The "double-layer" region refers to the range of potentials 0.35 to ca. 0.825 V, E_H , i.e., the potential range over which neither hydrogen nor oxygen species are significantly adsorbed on platinum (see p.6).

- (ii) the adsorbed nitriles block atomic hydrogen electrochemisorption at platinum substantially but not completely, even when the coverage with nitrile has reached its saturation value;
- (iii) if chemisorption of nitriles at platinum is allowed to occur in the "H region"^{*} near the reversible potential of the H_2/H^+ electrode in the same solution, adsorbed atomic hydrogen is electrochemically displaced and gives rise to an anodic electrochemical transient (117);
- (iv) the adsorbed nitrile is not only electroactive in the double-layer region but gives rise to a charge component in the H-region at Pt which can be distinguished from the contribution from H species by taking advantage of the different kinetic relaxation characteristics which the two species exhibit.

These effects form the basis for the study of the reactions of acetonitrile and other nitriles at platinum in aqueous media and will now be discussed in detail.

* The "H region" refers to the potential region in which adsorbed, atomic hydrogen exists on the platinum electrode surface, i.e., 0.35 to 0.05 V, E_H .

(b) General behavior of acetonitrile at platinum as determined by the potentiodynamic sweep method

Fig. 7 shows the overall potentiodynamic i-V profiles for platinum in the presence of acetonitrile at various concentrations in relation to that for platinum in 1N aq. H_2SO_4 . In the presence of acetonitrile, the following characteristics are to be noted:

- (i) the coverage with adsorbed hydrogen, θ_H , decreases with increasing acetonitrile concentration, $[CH_3CN]^*$, and resolution of the two main hydrogen peaks disappears;
- (ii) new reduction and oxidation current peaks appear in the double-layer regions of the cathodic and anodic-going sweeps, respectively;
- (iii) surface oxide formation is displaced to more positive potentials and the quantity of surface oxide which is reducible in the cathodic-going sweep decreases. There appears to be a reaction of acetonitrile in the surface oxide region as indicated by the increased current at potentials > ca. 1.1 V, E_H .

The decrease in coverage by both atomic hydrogen and surface oxide indicates that acetonitrile occupies platinum surface sites which were previously available for electro-sorption of hydrogen or oxygen species. The appearance of a

* The symbol $[CH_3CN]$ will refer to concentrations in moles l^{-1} .

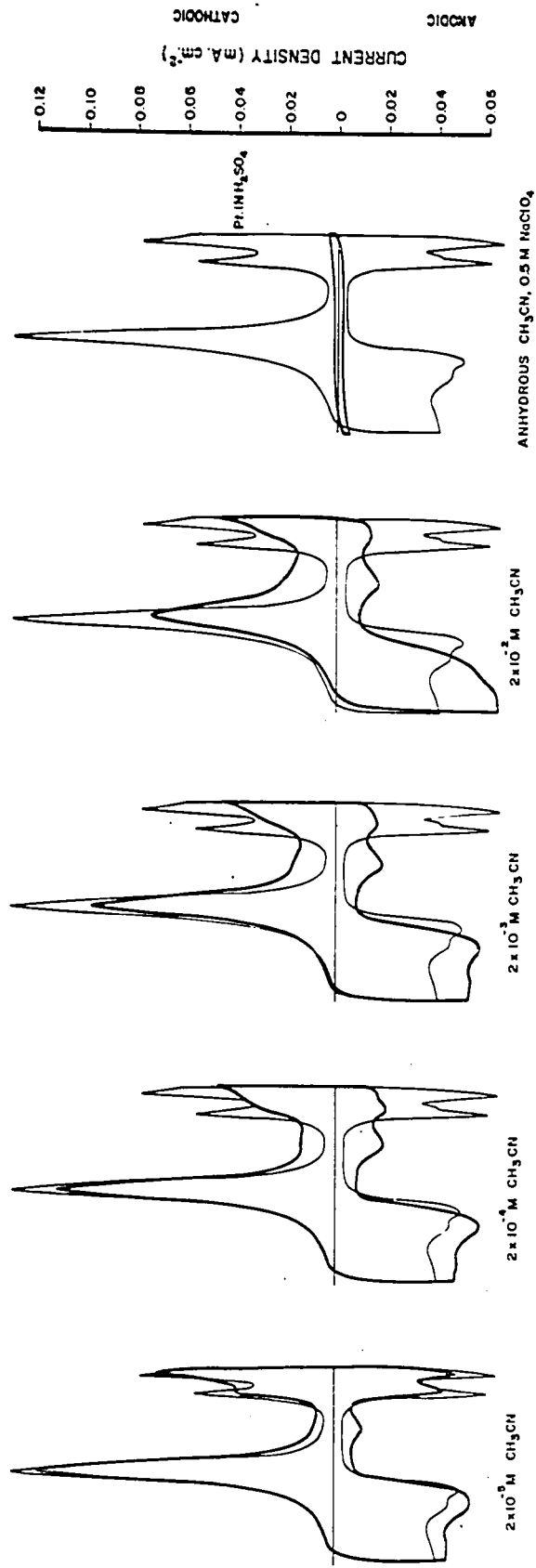


Fig. 7. Potentiodynamic i-V profiles for adsorbed acetonitrile at platinum as a function of [CH₃CN] in relation to background curves for hydrogen and oxygen electroreduction from 1N aq. H₂SO₄ at (dv/dt) = 50 mV sec⁻¹. Also shown is the i-V relation for anhydrous CH₃CN + NaClO₄ as electrolyte.

new reduction and oxidation peak in the double-layer region shows that the acetonitrile, or a species derived from it, not only partially blocks the ordinary surface reactions at platinum but also participates in a new electron transfer process itself which, as is shown below, involves only an adsorbed acetonitrile species. At gold electrodes, by contrast, no electroactivity of acetonitrile either as an adsorbed species or by reaction from solution is observed. Thus, adsorption at the platinum surface is essential for electroactivity of acetonitrile.

(c) Adsorption and reaction characteristics of acetonitrile in the double-layer region at platinum

Acetonitrile gives rise to a relatively reversible reduction-oxidation process in the double-layer region at platinum in aq. H_2SO_4 (Fig. 7). Fig. 8 shows the dependence of the double-layer acetonitrile oxidation peak current on the rate of potential scan, $dV/dt = S$, for various acetonitrile concentrations over the potential range 0.06 to 1.40 V, E_H . Reasonable linearity* of the peak current with sweep rate, S , was found for all concentrations except the lowest one employed, for which the peak current varies as $S^{1/2}$ (Fig. 8 and 9). This indicates that for $[\text{CH}_3\text{CN}] > \text{ca. } 2 \times 10^{-4} \text{ M}$,

* The small deviations from linearity observed at faster sweep rates are due to slowness in the prior reduction reaction in the cathodic-going sweep (see section I.2(e)).

Dependence of peak currents, i_p , for acetonitrile oxidation at platinum in the double-layer region on sweep rate, (dv/dt) , for various concentrations of acetonitrile. (∇) 2×10^{-5} M; (\square) 2×10^{-4} M; (\circ) 2×10^{-3} M; (\boxtimes) 2×10^{-2} M with 90 sec cathodic holding. Potential range 0.06 to 1.4 V, E_H .

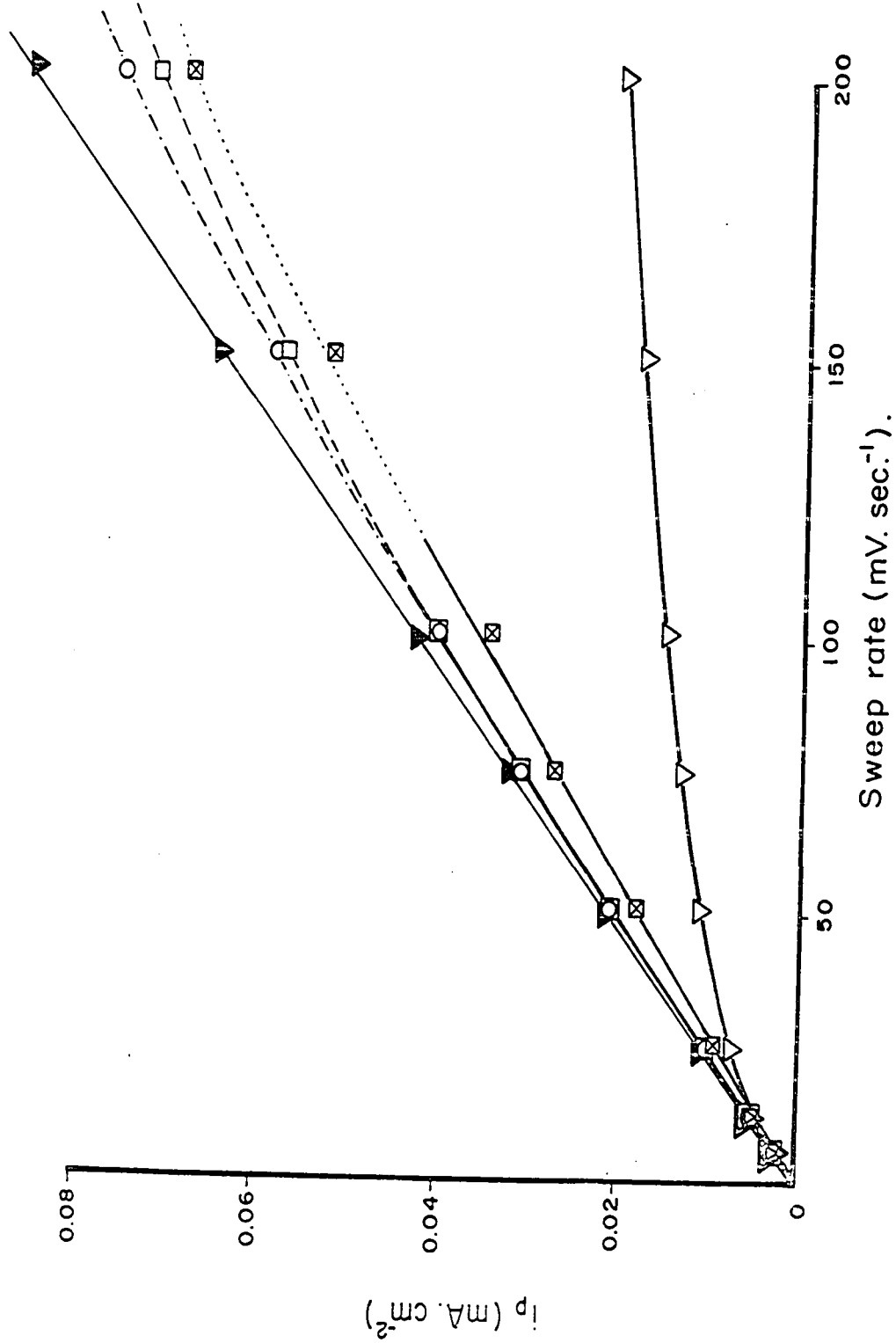


Fig. 8.

Dependence of peak currents, i_p , for acetonitrile oxidation at platinum in the double-layer region on sweep rate, (dv/dt) , for various concentrations of acetonitrile. (∇) 2×10^{-5} M; (\square) 2×10^{-4} M; (\circ) 2×10^{-3} M; (\boxtimes) 2×10^{-2} M with 90 sec cathodic holding. Potential range 0.06 to 1.4 V, E_H .

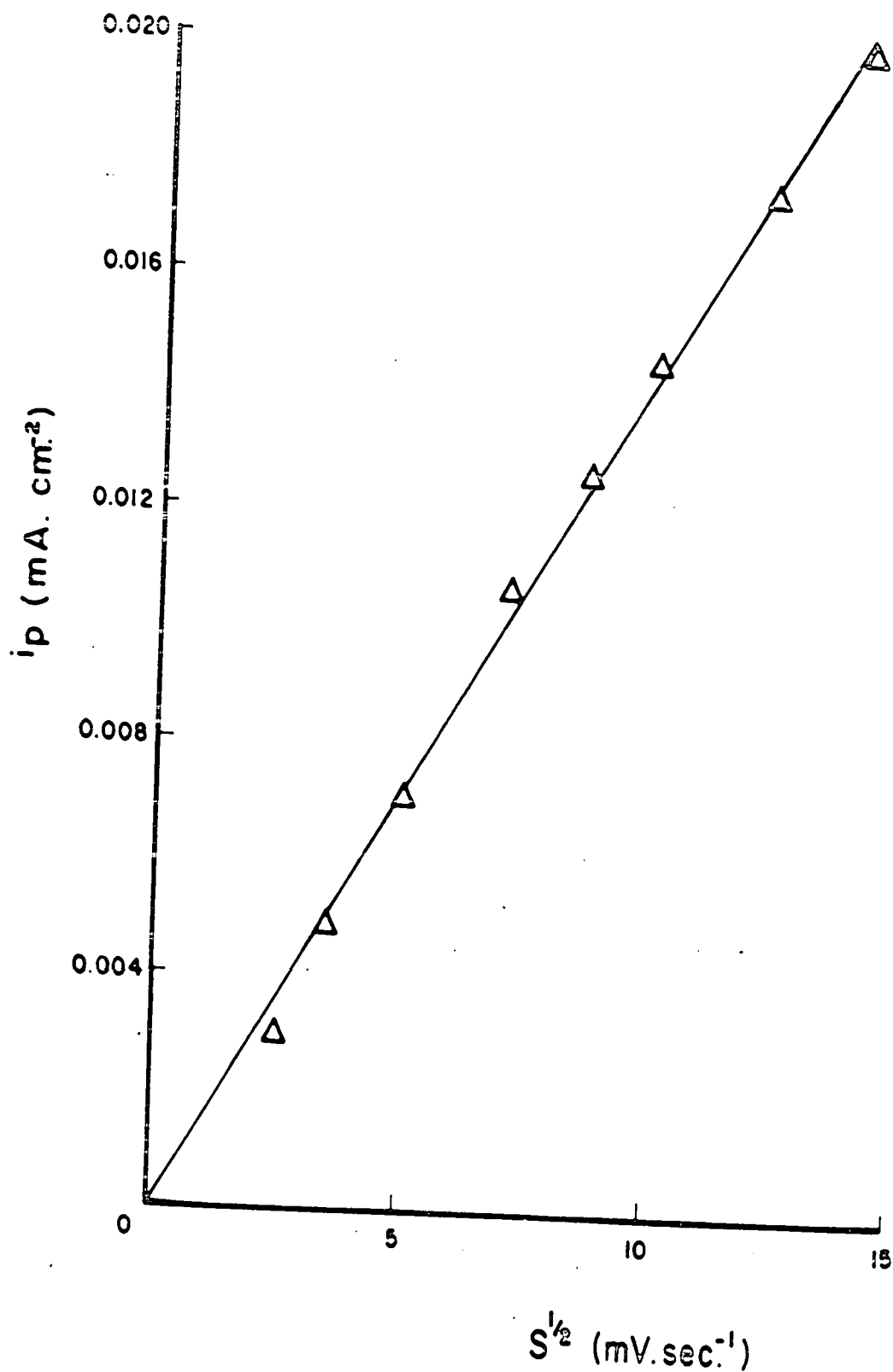


Fig. 9. Dependence of peak current, i_p , for acetonitrile oxidation at platinum in the double-layer region on square-root of sweep rate, $(dV/dt)^{1/2}$, with $[CH_3CN] = 2 \times 10^{-5}M$. Potential range 0.06 to 1.4 V, E_H .

the oxidation process in the double-layer region is associated with adsorbed acetonitrile, or a chemisorbed species derived from it, and not with acetonitrile diffusing from the solution.

Evaluation of the sweep rate dependence of the acetonitrile reduction peak in the double-layer region is not possible with anodic sweeps that terminate at potentials greater than $0.80 \text{ V}, E_H$ because of interference from the surface oxide reduction process (see Fig. 34 and section I.4(b)). However, the sweep rate dependence of the current at this peak was obtained by reversing the direction of the sweep after the acetonitrile oxidation process in the double-layer region had been completed but before any surface oxide could be formed (i.e. for $V < 0.80 \text{ V}, E_H$). The result is shown in Fig. 10 for a $5 \times 10^{-3} \text{ M}$ acetonitrile solution and the excellent linearity of the reduction peak current with S indicates that acetonitrile reduction in the double-layer region is also entirely a surface process at concentrations above ca. $3 \times 10^{-4} \text{ M}^*$. The reason for the discrepancy between the oxidation and reduction peak currents for acetonitrile in the double-layer region is discussed below. The absence of any dependence of acetonitrile peaks in the d.l. potential region on solution stirring when $[\text{CH}_3\text{CN}] > \text{ca. } 3 \times 10^{-4} \text{ M}$ gives further proof of the absence of diffusion controlled processes and hence the

* The importance of this observation will become evident after it has been shown (p.79) that the primary reaction of acetonitrile adsorbed on platinum is reduction. Oxidation processes (apart from those in the oxide region itself) involving acetonitrile species arise only after the species, initially adsorbed, has been reduced in a cathodic-going sweep or in an adsorption transient.

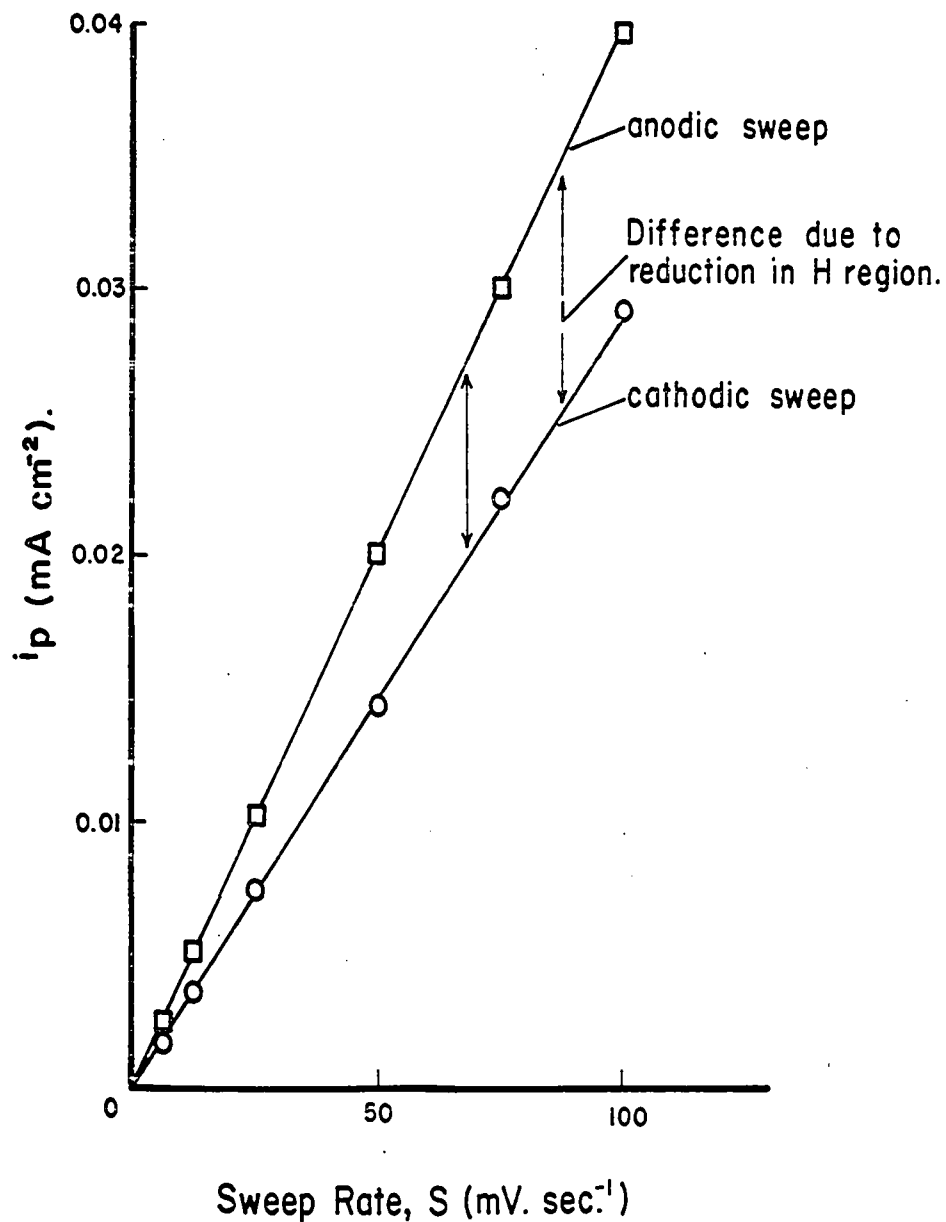
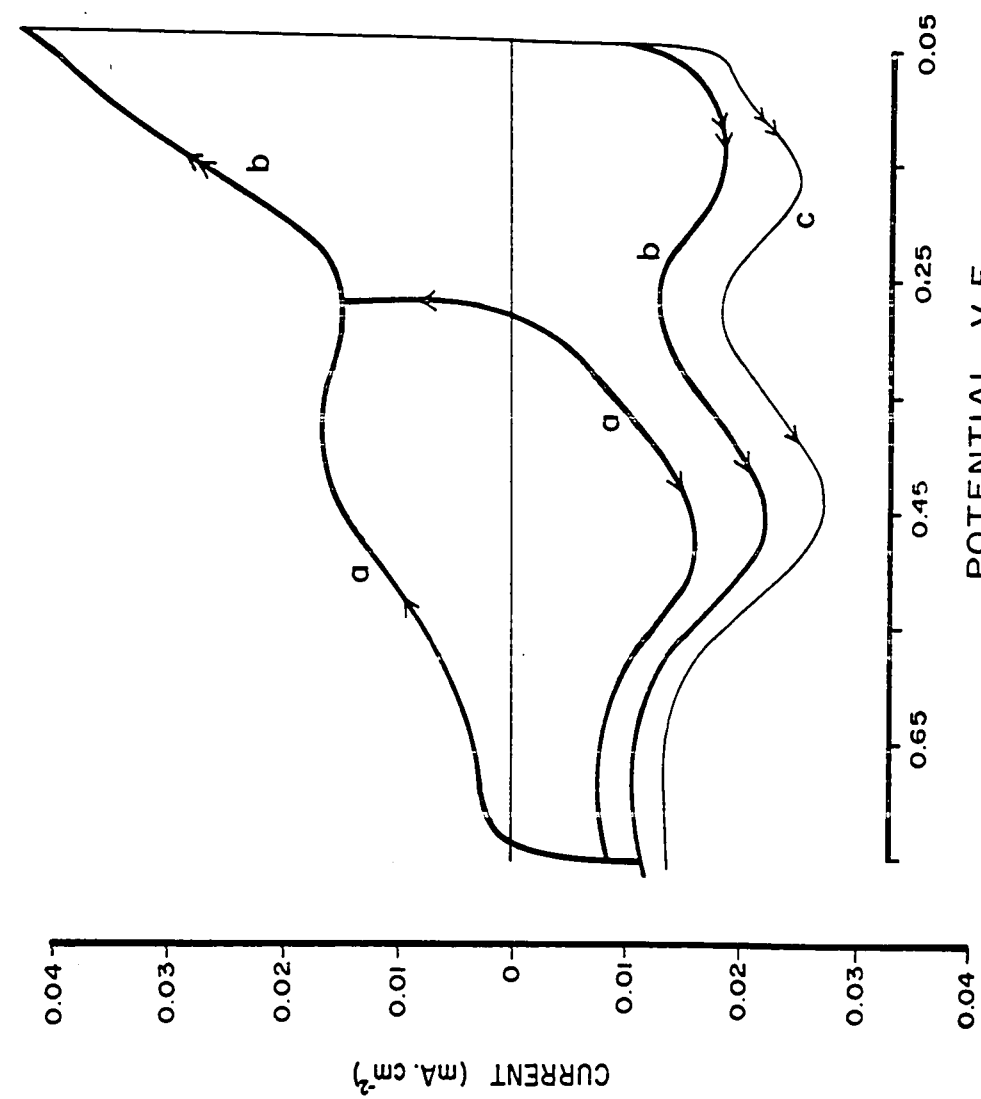


Fig. 10. Dependence of peak current, i_p , for acetonitrile reduction (○) and oxidation (◻) in the double-layer region at platinum on sweep rate, (dV/dt) , with $[CH_3CN] = 5 \times 10^{-3}$ M. Potential range 0.06 to 1.4 V, E_H for the oxidation peak and 0.8 to 0.06 V, E_H for the reduction peak.

lack of reaction of acetonitrile from solution once the initial electrochemisorption has occurred.

"Reversible" reduction-oxidation peaks of acetonitrile are observed in the double-layer region at platinum independently of whether or not the adsorbed hydrogen and/or surface oxide regions are traversed in the sweep since the cathodic and anodic current peaks still arise if only the double-layer potential region is scanned, i.e. between 0.35 and 0.70 V, E_H (Fig. 11). The presence of peaks in the double-layer potential region is therefore not associated with pre-history of the electrode or of acetonitrile in the oxide or hydrogen regions, although holding the potential at the H end of a cathodic sweep at 0.06 V, E_H , or simply cycling into the hydrogen adsorption region, does increase the charge for re-oxidation of the acetonitrile species in the double-layer region as may be observed in a subsequent anodic sweep (see below and Fig. 10). The dependence of the peak current on S was also investigated over this restricted potential range in the double-layer region and the results again showed linearity of i_p with S for the acetonitrile reduction and oxidation processes (Fig. 12). When cycling is restricted to the double-layer potential region, the charges associated with acetonitrile reduction and oxidation always balance to within 2% for $[CH_3CN] > ca. 3 \times 10^{-4} M$, thus providing another indication that it is an adsorbed acetonitrile species which undergoes reactions in the double-layer region at platinum in aq. H_2SO_4 .

0.04
0.03
0.02
0.01
0
0.01
0.02
0.03
0.04



POTENTIAL V, E_H.

Fig. 11. Anodic and cathodic peaks in potentiodynamic i-V profiles for adsorbed acetonitrile at platinum showing the effect of the H-region and cathodic holding at 0.06 V, E_H on the reactions in the double-layer region; curve (a) for the double-layer region; curve (b) for double-layer and H regions; curve (c) with holding of potential at 0.06 V, E_H for 90 sec. [CH₃CN] = 5 x 10⁻³M, dV/dt = 50 mV sec⁻¹.

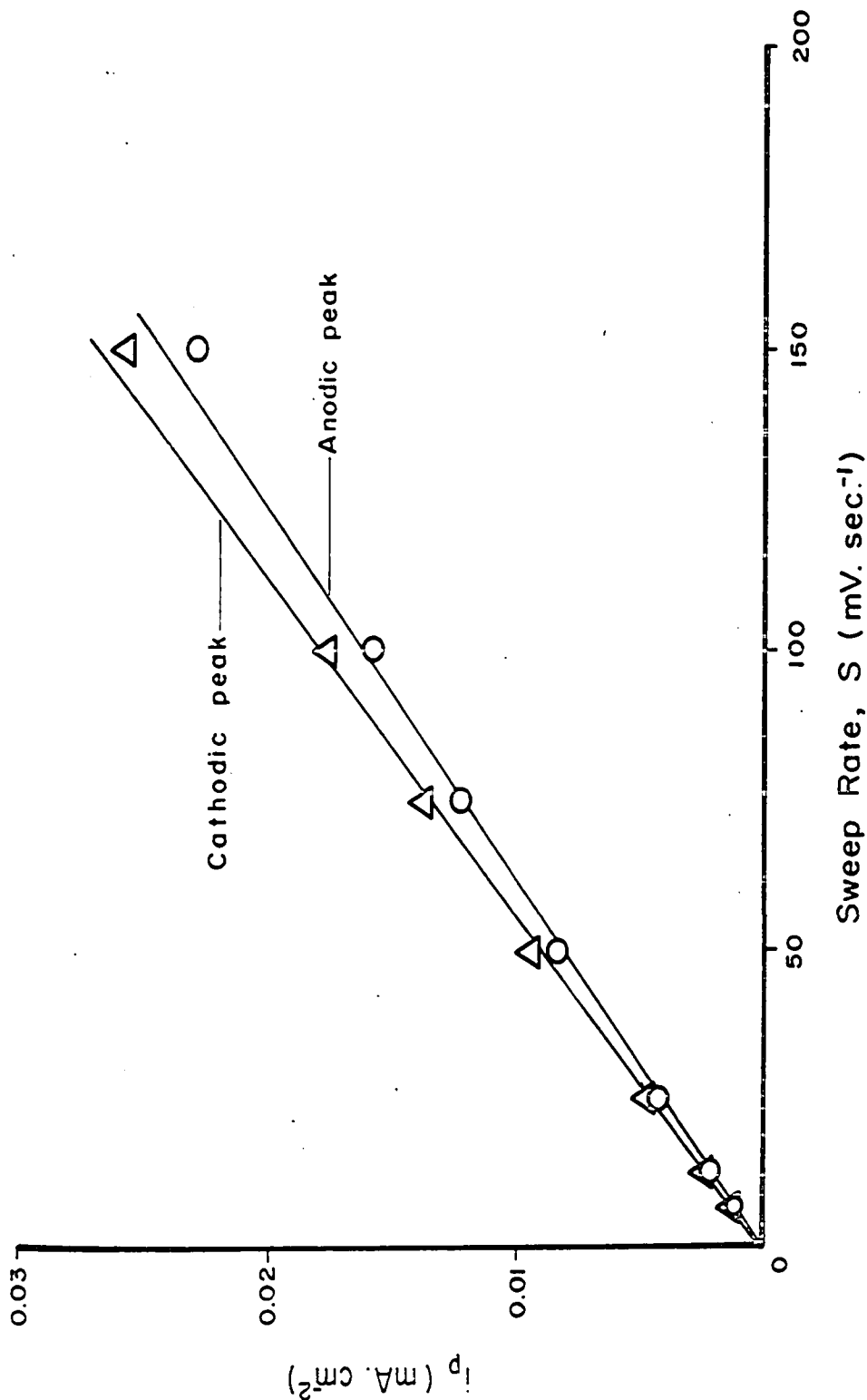


Fig. 12. Dependence of peak current, i_p , for acetonitrile reduction and oxidation in the double-layer region at platinum on sweep rate, (dv/dt) , for $[CH_3CN] = 5 \times 10^{-3}$ M with cycling restricted to the potential range 0.35 to 0.80 V, E_H.

The possibility that these effects could be due to an impurity in the acetonitrile was investigated by synthesizing the compound by a different route from that employed for manufacture of the commercially available material which is obtained, for example, as a co-product in the Sohio process for preparation of acrylonitrile (118). Dehydration of re-crystallized acetamide gave a very pure product after double-distillation; this material exhibited exactly the same electrochemical behavior as that of acetonitrile obtained by purification of the manufactured solvent. This result justified the special attention paid to the purification of the acetonitrile (84) used in the present work and flame-ionization vapor-phase chromatography showed impurity levels in that material of less than 5 ppm. Also, work with a series of 11 other nitriles (see below) of varying structures, which are synthesized by various routes, gave (i) a common type of redox behavior of an adsorbed species in the double-layer region and (ii) similar blocking of atomic hydrogen chemisorption at less positive potentials. The effects thus appear to be due to adsorption and reactivity of the CN-function itself.

In order to check if possible hydrolysis or reduction products derived from CH_3CN , viz. CH_3CONH_2 , CH_3COOH or $\text{C}_2\text{H}_5\text{NH}_2$, could be responsible for the observations with acetonitrile, potentiodynamic experiments were also conducted on these substances at a concentration of 5×10^{-3} M. None showed behavior similar or related to that of acetonitrile.

These results confirm that the behavior of acetonitrile discussed above is not associated with the most probable products of its side reactions.

(d) Electrode coverage by acetonitrile and blocking of hydrogen adsorption

The curves of Fig. 11 show that on the anodic sweep between the potential limits 0.80 to 0.05 V, E_H there are two principal regions where oxidation reactions on the surface occur, (i) the region which is usually associated with ionization of adsorbed atomic hydrogen; (ii) the double-layer region where oxidation of an adsorbed acetonitrile species occurs. The charge measured by integration of the peak in the region 0.05 to 0.30 V, E_H will be attributed for the moment (see below) to ionization of adsorbed hydrogen and designated as $q_{a,H}^*$. The charge measured between 0.3 and 0.8 V, E_H is associated with the reaction of an adsorbed acetonitrile species and will be called $q_{a,d.l.}$. In both cases, the non-faradaic double-layer charge has been subtracted to give real values of reaction charge. The difference between the hydrogen charge, $q_{a,H}$, in the presence of adsorbed acetonitrile and that for hydrogen adsorption, q_H^0 , in the background profiles (i.e. for absence of acetonitrile) of Fig. 7, gives the apparent** extent of blocking of the surface for H adsorption,

* For a complete tabulation of definitions of the symbols used in the present work, see Table I.

** It is shown below that the H-blocking effect must be corrected for the presence of some adsorbed acetonitrile species electroactive in the H region.

Table I

Definitions of Charge and Other Quantities

Discussed and Measured

q_t	total net charge passed in current transient following adsorption
$q_{a,d.l.}$ $q_{c,d.l.}$	charges, anodic (a) or cathodic (c) for oxidation or reduction, respectively, of chemisorbed CH_3CN species in the "double-layer" region
q_a, q_c	total charges for oxidation (a) or reduction (c) of CH_3CN species over the whole range of potentials including the H regions but corrected for H contributions
$q_{a,h}$	the value of q_a determined after 90 sec "holding" at a given potential
$q_{c,H}$ $q_{a,H}$	charges in cathodic-going (c) or anodic-going (a) sweeps measured in the H region (0.05 to 0.35 V) in multisweep experiments. (These are not necessarily the actual charges for H electrochemisorption - see text and definitions of $q_{H,+}$ and $q_{H,-}$ below)
$q_{a,H,h}$	charges in anodic-going sweep in the H region after "holding" (h) the potential V at various values for 90 sec
q_H^o	charge for electrochemisorption of H, in absence of CH_3CN measured at various potentials
$q_{H,+}$ $q_{H,-}$	actual charges for resolved H components in the H region in anodic (+) or cathodic (-) going sweeps
Δq_H	charge for displacement of H by chemisorbed species
q_r	derived charge component for CH_3CN reduction ($=q_t - \Delta q_H$)
V_a	potential for adsorption of CH_3CN and potential at which the potentiostatic adsorption transient is measured (V = a typical potential)
E_H	represents scale on which potentials are experimentally measured vs. the H_2/H^+ electrode at Pt in the same solution
S	sweep rate dV/dt , $V \text{ sec}^{-1}$

Δq_H . The variation of $q_{a,H}$ and $q_{a,d.l.}$ with acetonitrile concentration, is shown in Fig. 13, together with the corresponding quantities which arise if the potential of the electrode has been held at 0.06 V, E_H for 90 sec. before initiating the return anodic-going sweep.

The quantity of acetonitrile adsorbed, measured in terms of $q_{a,d.l.}$, is seen (Fig. 13a) to approach an almost limiting value at $[CH_3CN] = ca. 1.6 \times 10^{-4} M$. This plateau of $q_{a,d.l.}$ values could arise in two ways: (i) the acetonitrile coverage is really independent of concentration in this region; or (ii) the acetonitrile coverage is tending to increase with $[CH_3CN]$ but this tendency is opposed by competitive adsorption of another type of species. Since the coverage with adsorbed hydrogen, measured by $q_{a,H}$, continues (Fig. 13a) to decrease as the apparent coverage with acetonitrile remains constant, the surface coverage on a site basis with species other than hydrogen cannot really be constant. This fact gives support to explanation (ii) above, and it appears that a different type of adsorbed species, derived from acetonitrile, arises at higher concentrations. This species may, for example, be of a different geometry from that adsorbed and reactive on the surface at lower acetonitrile concentrations, thus occupying more Pt surface sites. Another possibility is that the second adsorbed species occupies Pt surface sites but is not reactive in the same manner as the adsorbed species formed at lower $[CH_3CN]$. It will be

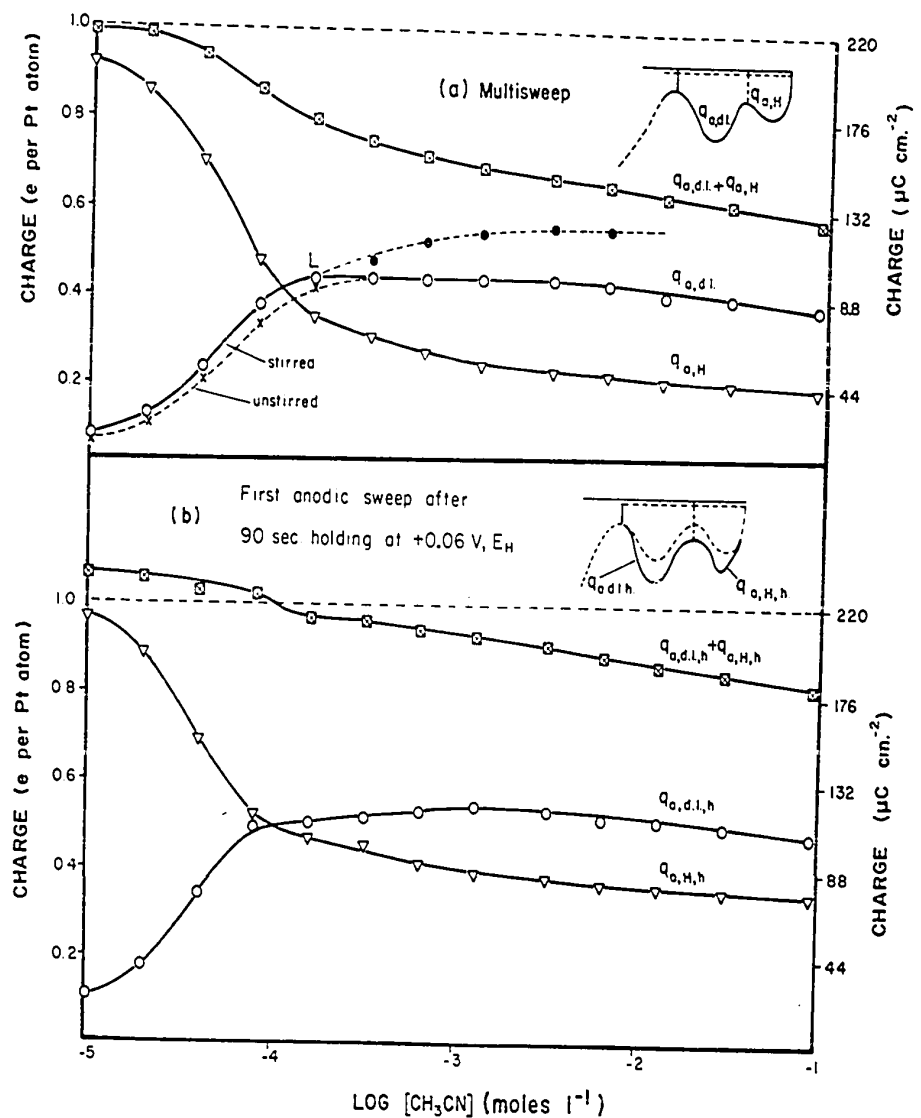


Fig. 13. Extent of adsorption of acetonitrile and corresponding apparent H blocking effects at platinum as a function of acetonitrile concentration; (a) in multisweep experiments; (b) after 90 sec cathodic holding at 0.06 V, E_H . The points, O, represent expected continuation of $q_{a,d,l}$ curve beyond L based on the assumption that $q_{a,H}$ should be constant if species "B" was not formed. (dV/dt) = 50 mV sec⁻¹.

convenient to refer to this species as "B" and its identity will be discussed in section I.4(b).

If the B species blocks hydrogen and acetonitrile adsorption in the same manner, it is possible to evaluate the way in which $q_{a,d.l.}$ would increase with $[CH_3CN]$ in the absence of B species. This is illustrated in Fig. 13a where it is assumed that the decrease in $q_{a,H}$ at $[CH_3CN] > 1.6 \times 10^{-4}$ M is due to the normal form of reactive adsorbed acetonitrile. The resulting plot of $q_{a,d.l.}$ shows no plateau and is similar to the $q_{a,d.l.,h}$ plot in Fig. 13b where the effects of holding the potential at the cathodic end of the sweep are shown. These effects will be discussed below in connection with the manner in which adsorbed hydrogen is involved in the acetonitrile reaction. The presence of the B species is further indicated by the fact that $q_{a,d.l.}$ decreases below its initial limiting value when $[CH_3CN] > 6 \times 10^{-3}$ M. The fact that the total charge for hydrogen adsorption and for reaction of acetonitrile, $q_{a,H} + q_{a,d.l.}$, decreases significantly with increasing $[CH_3CN]$ can be due to a difference in the charge equivalence per platinum atom between hydrogen and acetonitrile and/or the presence of the "B" species. The extent of hydrogen coverage, $q_{a,H}$, eventually falls to ca. 0.2 in 0.1M CH_3CN and only in 50% aq. CH_3CN does it approach zero. This indicates that a certain proportion of platinum surface sites remain unoccupied by CH_3CN , even at very high $[CH_3CN]$ (cf. results of section I.3(c)).

The dependence of $q_{a,H}$ on solution stirring is also shown in Fig. 13a, from which it is seen that the region of solution diffusion control extends only up to $[\text{CH}_3\text{CN}] = 3 \times 10^{-4} \text{ M}$. This is to be compared with the results of Fig. 14 which show the dependence of the peak current for acetonitrile oxidation in the double-layer region on $[\text{CH}_3\text{CN}]$, where similar behavior is indicated. The decrease in the peak current at $[\text{CH}_3\text{CN}] > 6 \times 10^{-3} \text{ M}$ is analogous to the corresponding decrease in $q_{a,d.l.}$ in Fig. 13, i.e. it is consistent with the presence of a "B" species at higher acetonitrile concentrations.

The value of Δq_H depends on the type of nitrile adsorbed as shown in Fig. 15 for 7 nitriles, 2 dinitriles, tetracyanoethylene and HCN, all adsorbed from $6.4 \times 10^{-4} \text{ M}$ solution*. As expected, the latter compounds exhibit the strongest H-blocking effects but $1-\theta_H$ still never becomes $> \text{ca. } 0.8$. Evidently there is room for some H-adsorption amongst chemisorbed $-\text{CN}$ groups (as will be shown in section I.3(a)) even when the coverage by such species has reached its own limiting value. This is not the case with small S-containing molecules which almost completely block H chemisorption at Pt electrodes (119).

* For all the nitriles examined, this concentration was sufficiently high that there were no elements of solution diffusion control but not so high that significant effects of the "B" species arose.

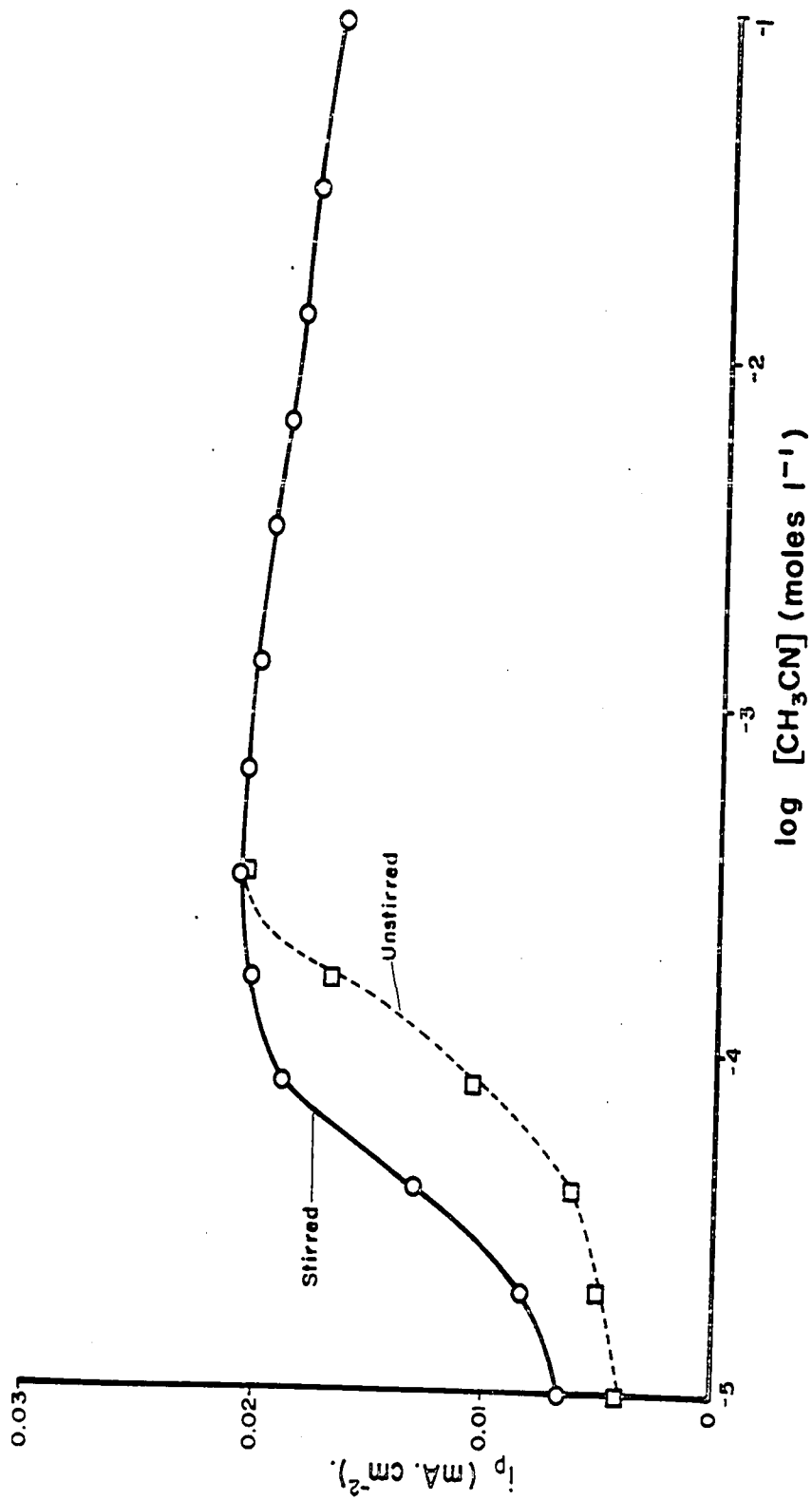


Fig. 14. Dependence of peak current, i_p , for acetonitrile oxidation at platinum in the double-layer region on acetonitrile concentration, with (o) and without (□) solution stirring. Potential range 0.06 to 1.4 V, E_H ; $(dV/dt) = 50$ mV sec⁻¹.

Journal of Electroanalytical Chemistry and Applied Electrochemistry, Vol. 10, pp. 1-10 (1964)

Blocking effects of RCN on H adsorption at Pt.

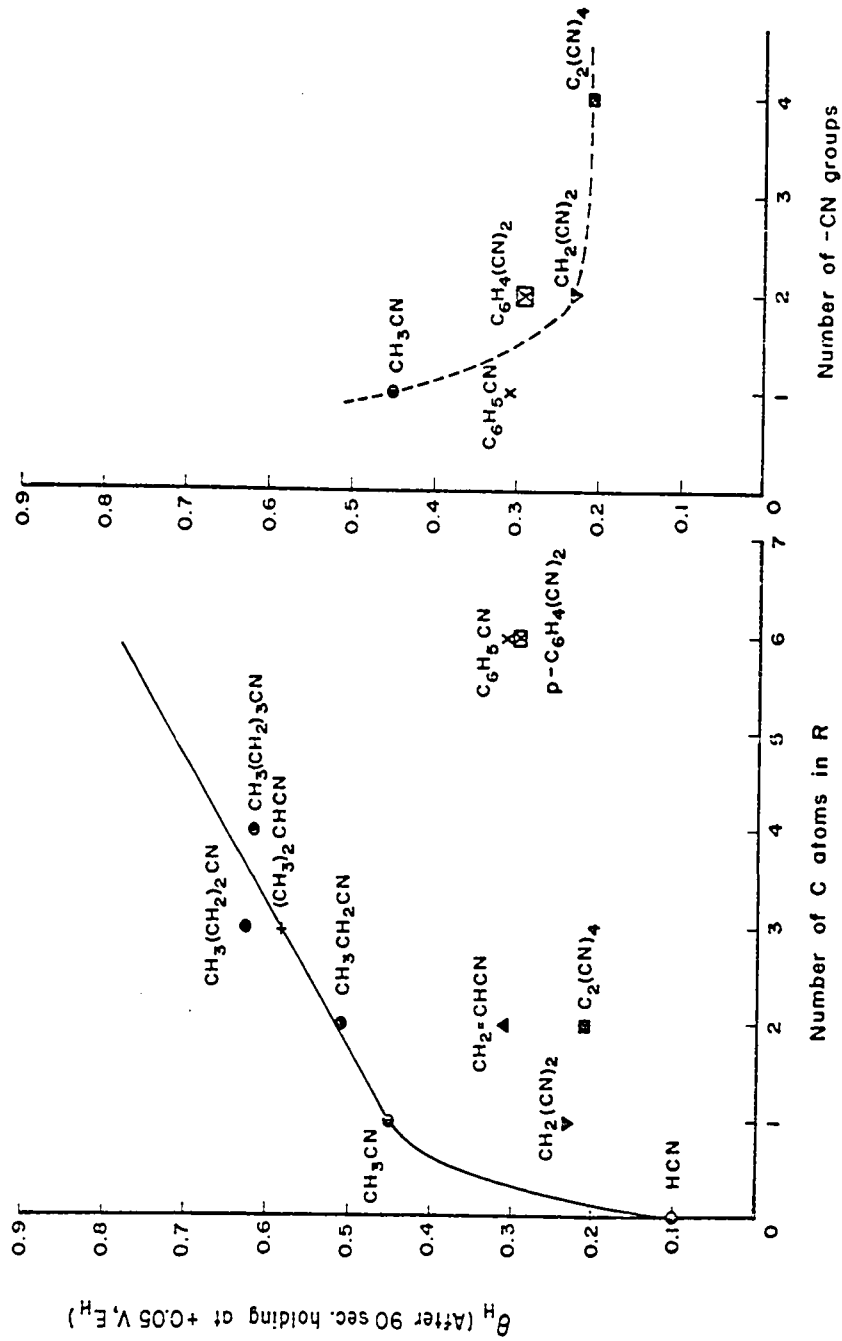


Fig. 15. Order of atomic hydrogen blocking at platinum by a series of nitriles at a concentration of 6.4×10^{-4} M in $1N$ H_2SO_4 after 90 sec cathodic holding at 0.05 V, E_H . Potential range 0.06 to 1.4 V, E_H ; $(dV/dt) = 50$ mV sec⁻¹.

(e) Reversibility of the acetonitrile reaction in the double-layer potential region

The processes of reduction and oxidation of acetonitrile at platinum in the double-layer region are fast (see Fig. 16)* surface reactions; however, these reactions of the adsorbed species are not as fast and reversible as the electrochemical adsorption or desorption reactions of atomic hydrogen at platinum which occur at less positive potentials. For $[\text{CH}_3\text{CN}] > 3 \times 10^{-4}$ M, and with cycling in potential ranges which either include or exclude the atomic hydrogen region, there is some inequality in the peak potentials, V_p , for the reduction and oxidation current peaks. In the case of cycling from 0.75 to 0.35 V, E_H , this inequality is 65 mV at a sweep rate of 50 mV sec^{-1} , while with cycling from 0.75 to 0.05 V, E_H , the inequality is 50 mV at $(\frac{dV}{dt}) = 50 \text{ mV sec}^{-1}$. The fact that the oxidation peak potential shifts to somewhat less positive potentials with cycling to 0.05 V, E_H is thermodynamically expected from the greater quantity of reduced acetonitrile (see below) which arises when the electrode is cycled to these more negative potentials.

* Fig. 16 shows the i - V profiles for acetonitrile at the platinum electrode at sweep rates of up to 50 V sec^{-1} . The fact that acetonitrile electroactivity persists even at such high sweep rates indicates that a very fast surface reaction is involved. As the sweep rate increases, the lower limit of $[\text{CH}_3\text{CN}]$ where diffusion effects become significant also increases, but this is as expected. The behavior of acetonitrile may be contrasted with that of formic acid and methanol at platinum where little or no reactivity results at such fast sweep rates even when the concentrations in solution are high, so that diffusion limitation is minimized.

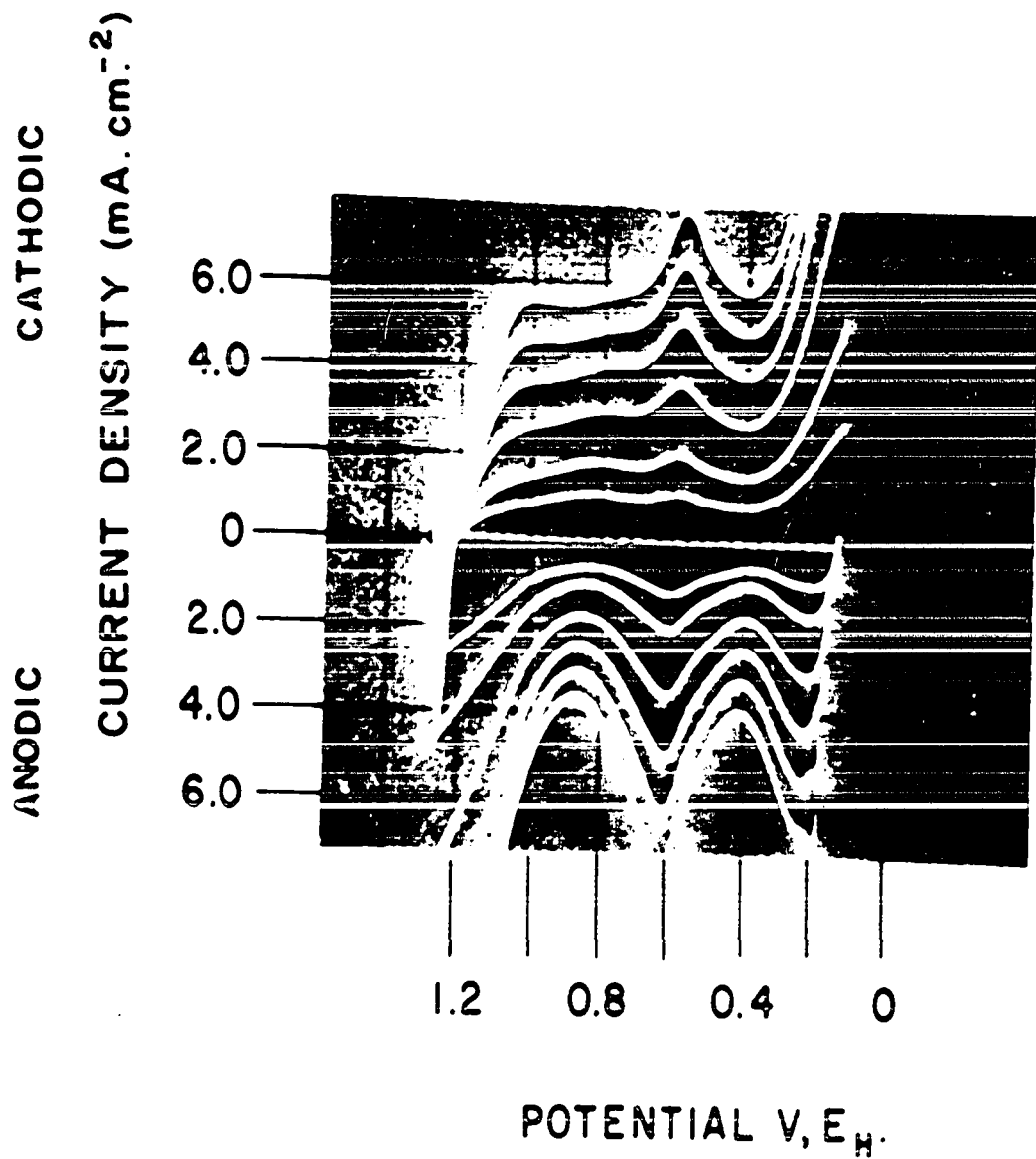


Fig. 16. *i*-V profiles taken on an oscilloscope at high sweep rates for 1M CH₃CN at Pt in 1M aq. H₂SO₄; (dV/dt) = 5,10,20,30,40 and 50 mV sec⁻¹. Potential range 0.05 to 1.25 V, E_H.

Fig. 17 shows i - V profiles for acetonitrile at platinum obtained in successive potentiodynamic experiments at 50 mV sec^{-1} over various potential ranges both in the anodic-going and cathodic-going directions of sweep. The potential ranges of cycling are varied by reversing the sweep at different potentials, the same sweep rate being always maintained. It is important to note that both the anodic and cathodic reactions have slow components (see below), otherwise reversal of sweep direction would immediately establish currents corresponding to potentials on a common i - V profile for all reversal potentials, as it does in the H adsorption region at platinum in pure aq. H_2SO_4 . The existence of these slow, irreversible components of the overall process is consistent with the small but significant deviation of the anodic peak current, i_p , from linearity in S (Fig. 8). However, after 90 sec holding of the potential at $0.06 \text{ V}, E_H$, the i_p is exactly linear in S (Fig. 8). The small deviation from linearity in S of i_p for acetonitrile reoxidation in the double-layer region in the multisweep experiment results from a slow cathodic current component which falls to zero upon holding at $0.06 \text{ V}, E_H$ for 90 sec.

The variation of peak potential with sweep rate for the reduction and oxidation reactions of adsorbed acetonitrile in the double-layer region was also studied. Since it was shown above (Fig. 8) that the reduction of acetonitrile on a cathodic-going sweep is a slow reaction requiring time at the

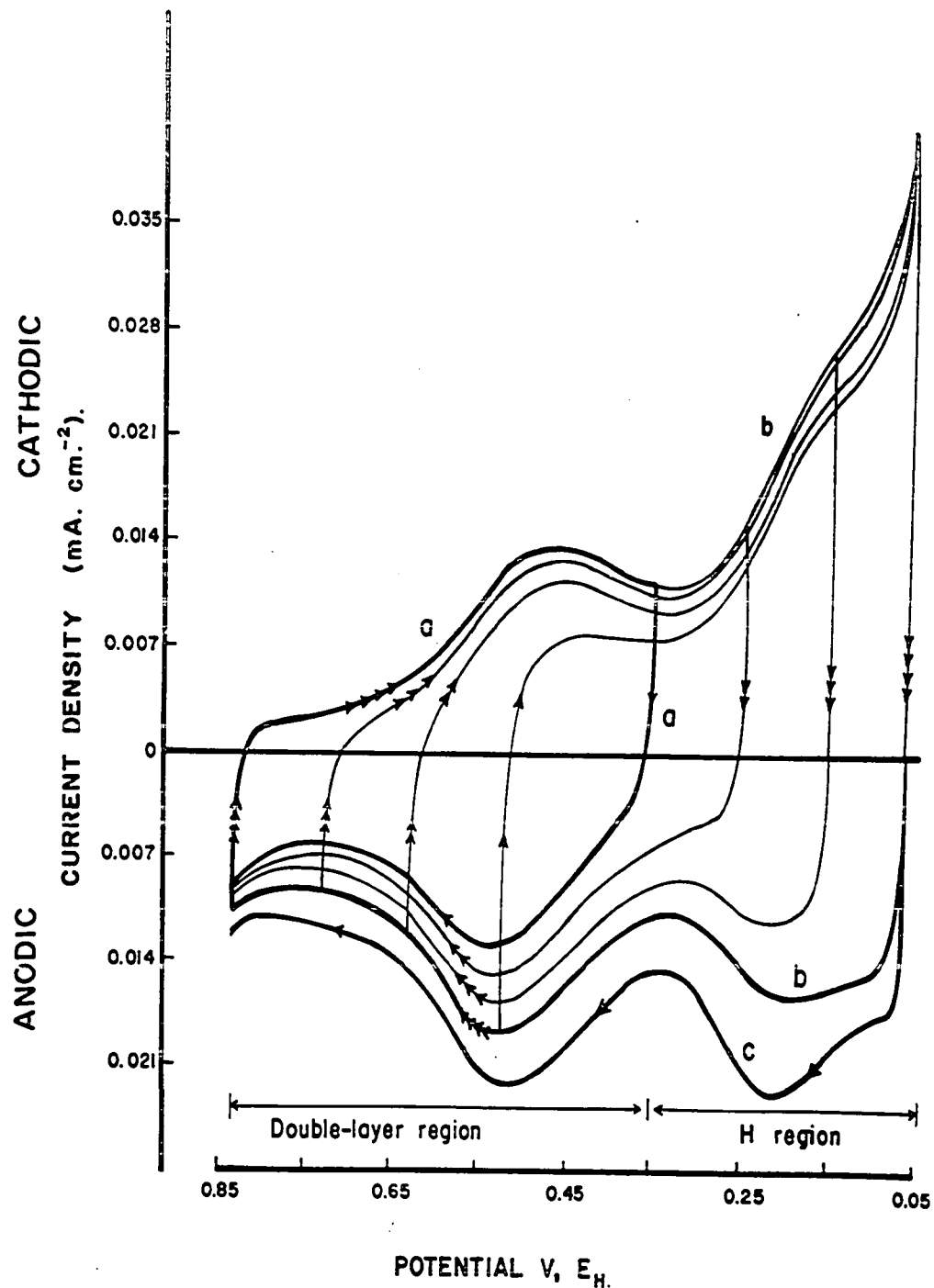


Fig. 17. Anodic and cathodic peaks in potentiodynamic i - V profiles for adsorbed acetonitrile over various potential ranges obtained by reversing the direction of the sweep at different potentials in both the anodic-going and cathodic-going sweep; curve (a) for the double-layer region; curve (b) for double-layer and H regions, curve (c) with holding of potential at $0.06 \text{ V, } E_H$ for 90 sec. $[\text{CH}_3\text{CN}] = 5 \times 10^{-3} \text{ M}$; $(dV/dt) = 50 \text{ mV sec}^{-1}$.

least positive potentials for its completion, the dependence of ΔV_p on S for the oxidation reaction was obtained at faster sweep rates ($>50 \text{ mV sec}^{-1}$) after a prior, slow (5 mV sec^{-1})* cathodic sweep. This procedure allowed the oxidation reaction to be studied independently of the reduction reaction. Fig. 18 shows that the limits of reversibility for the peaks occurs at a sweep rate of ca. 40 mV sec^{-1} and beyond this sweep rate Tafel polarization behavior obtains.

(f) Adsorption transients and the nature of acetonitrile chemisorption

The nature of the chemisorption of acetonitrile, indicated by the i - V profiles in Figs. 7 and 11, was investigated further by examining potentiostatic adsorption current transients** that arise in electrosorption of CH_3CN at Pt. Two adsorption mechanisms are possible:

(i) acetonitrile is electrosorbed like methanol (17) with dissociative adsorption at the CH_3 group; in this case, an anodic transient should arise upon electrochemisorption in the double-layer potential region, e.g. between 0.35 and 0.75 V, E_H , corresponding to the process:

* This cathodic-going sweep speed is found to be slow enough to give complete reduction of the adsorbed acetonitrile (see section I.2(b)).

** This method is described and discussed in detail in Part II with reference to a number of compounds.

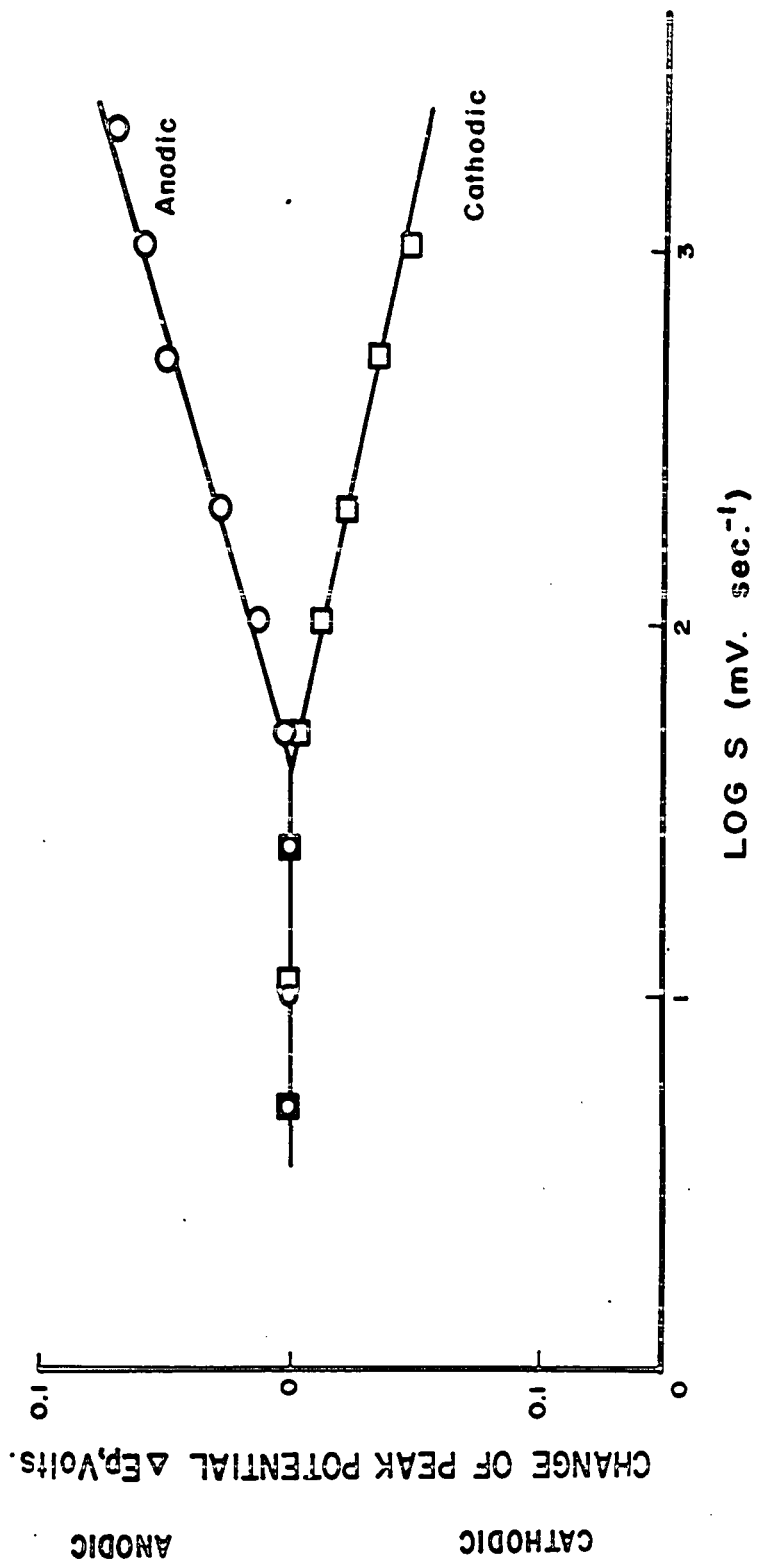
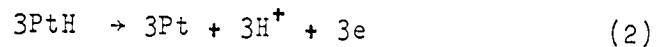
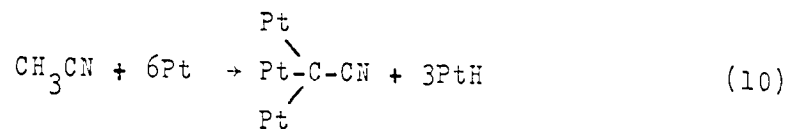


Fig. 18. Change of peak potential in cathodic and anodic sweeps in the double-layer region with log (sweep-rate) showing limit of reversibility of double-layer reduction/oxidation process.



It is evident from the i-V profiles of Fig. 7 that the nitrile residue ($\equiv\text{C}-\text{CN}$) is unlike the methanol residue ($\equiv\text{C}-\text{OH}$) arising from adsorption at platinum because of the lack of continuous faradaic currents* in the case of acetonitrile and absence of an anodic current on the cathodic-going sweep which is characteristic of methanol and formic acid oxidations (see section III(a)). In the region of significant H coverage, no transients will arise since H sites are already occupied (see section II(c)); or

(ii) acetonitrile is adsorbed at the CN-group; in this case, no anodic transient will arise in the double-layer potential region because the molecule will be inert towards oxidation of the methyl hydrogens. The possibility exists, however, that at less positive potentials electro-sorption can occur at the CN-group with uptake of protons and/or electrons to give a reduced chemisorbed species.

Fig. 19 shows the result of addition of deoxygenated CH_3CN solution to the 1N aq. H_2SO_4 electrolyte to give

* Potentiostatic polarization measurements on CH_3CN solutions at Pt electrodes in the potential range 0.1 to 1.4 V, E_{H} gave only residual steady currents which were $<10^{-8}$ A.cm⁻² and are associated with trace impurities in the system. In fact, the residual, steady currents due to trace impurities in the absence of acetonitrile decrease when CH_3CN at 5×10^{-3} M is added to the system.

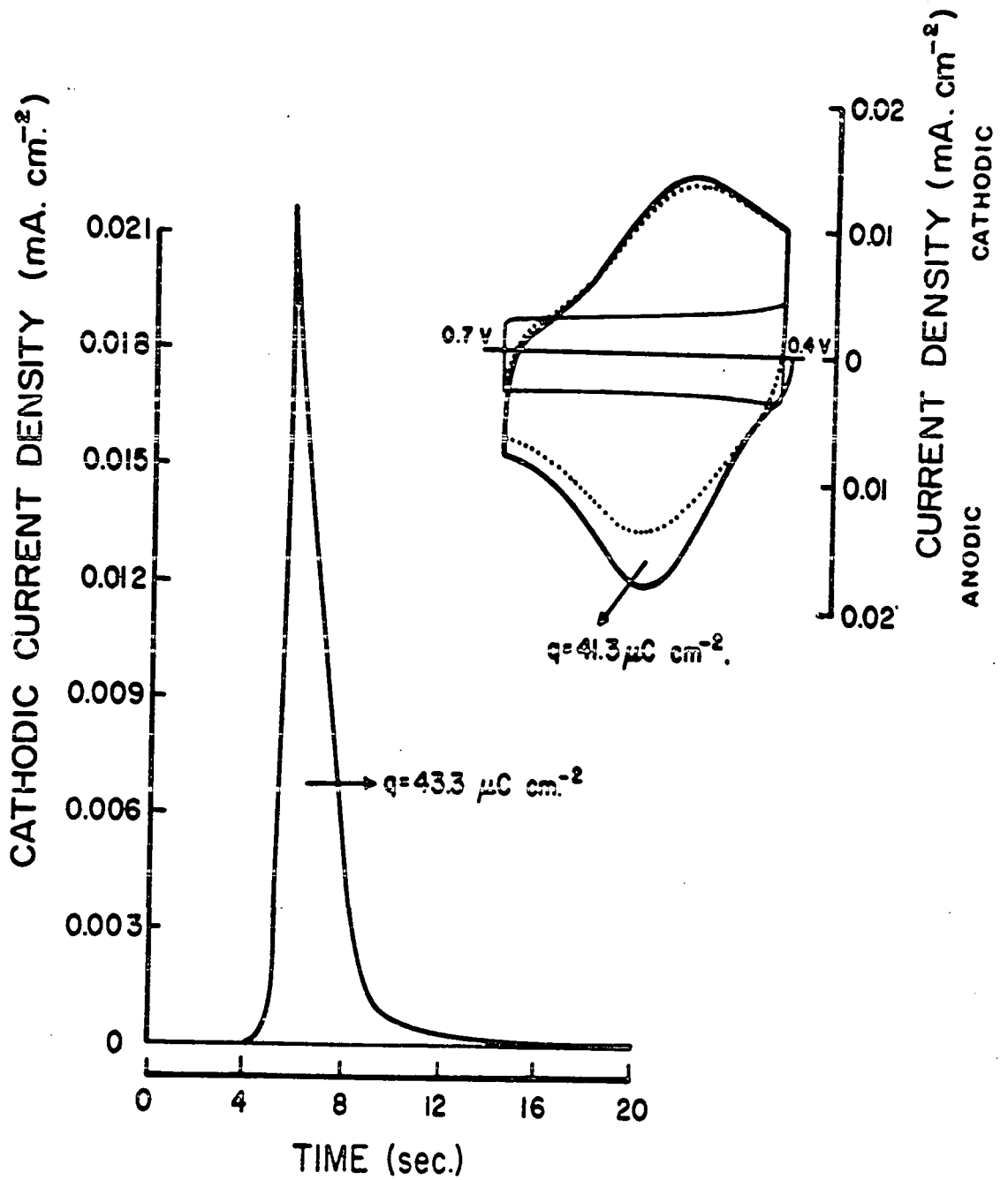


Fig. 19. Cathodic transient for acetonitrile adsorption at platinum at 0.40 V, E_H ; $[\text{CH}_3\text{CN}] = 5 \times 10^{-3}\text{M}$. Also shown are the first (-) and second (···) anodic and cathodic sweeps in the double-layer region after measurement of the transient.

$[\text{CH}_3\text{CN}] = 5 \times 10^{-3} \text{ M}$ while the electrode was held potentiostatically in the double-layer region at $0.40 \text{ V}, E_{\text{H}}$ (see section II(f)). The cathodic transient which is observed indicates process (ii) as the mechanism of electrosorption rather than a process of type (i) found with methanol (17). In fact, when acetonitrile is added to the $1\text{N aq. H}_2\text{SO}_4$ electrolyte in such a way that it reaches the electrode surface during the anodic-going sweep in the double-layer region, a cathodic reduction transient results before any oxidation in the double-layer region can occur (Fig. 20a). This indicates that the primary reaction of acetonitrile in the double-layer region, after its chemisorption, is reduction and not oxidation as is found with methanol. The methyl-H atoms in the acetonitrile molecule are evidently unreactive; hence the cathodic transient must be due to reduction of the CN-group.

The transient reduction charge resulting from acetonitrile adsorption at platinum, potentiostated in the double-layer potential region, can be compared with the subsequent oxidation charge on the first anodic sweep after addition of acetonitrile*. For these conditions, this charge is equivalent, within 2%, to the re-oxidation charge on the first anodic sweep after the transient, and this fact provides further proof that the acetonitrile is adsorbed on the

* For a complete description of this method see Part II.

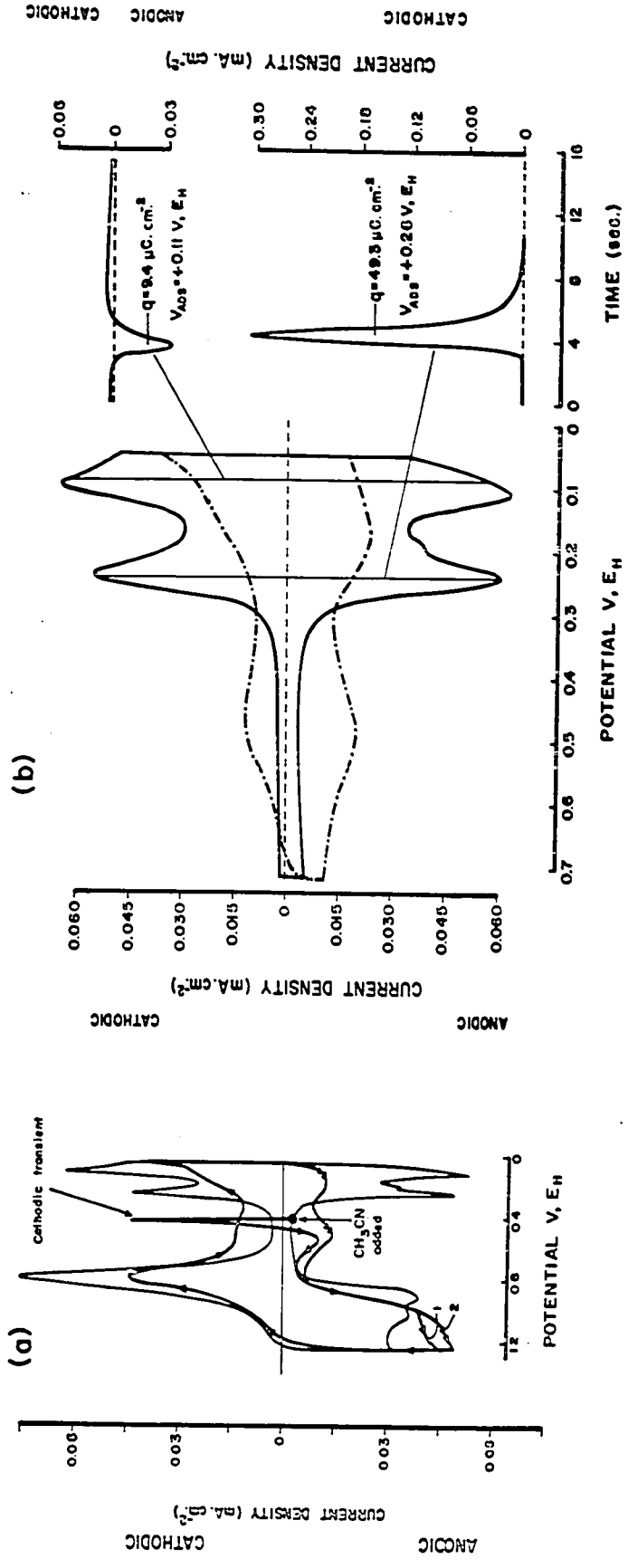


Fig. 20. (a) Cathodic transient for acetonitrile adsorption at platinum at ca. $0.45\text{ V}, E_H$ during an anodic-going potentiodynamic sweep; $[\text{CH}_3\text{CN}] = 5 \times 10^{-3}\text{ M}$, $(dV/dt) = 50\text{ mV sec}^{-1}$. First (1) and second (2) sweeps after adsorption of acetonitrile are shown in relation to the background sweep in the absence of acetonitrile.

(b) Potentiodynamic profile for $3 \times 10^{-3}\text{ M CH}_3\text{CN}$ (---) and background (—) at 50 mV sec^{-1} together with typical anodic and cathodic transients which arise on potentiostatic adsorption at 0.11 or $0.26\text{ V}, E_H$, with the anodic H displacement effect arising in the former case.

platinum surface and undergoes charge transfer processes in this adsorbed state.

If addition of acetonitrile is made at 0.70 V, E_H , or even more anodic potentials, adsorption occurs without passage of significant charge thus ruling out dissociative adsorption of the methyl hydrogens, as occurs with methanol. That adsorption does actually occur at this potential, even though no charge transfer occurs, is indicated (i) by blocking effects on surface oxide formation if a subsequent anodic sweep is taken from 0.7 to 1.4 V, E_H ; (ii) by a reduction peak linear in S (Fig. 10) which is observed in a sweep taken from 0.7 to 0.4 V, E_H ; (iii) by ellipsometry which shows (120) a decrease in the phase shift parameter Δ . Hence, the adsorption of acetonitrile on platinum in aq. H_2SO_4 can also occur (depending on potential) without charge transfer, which is consistent with mechanism (ii) above.

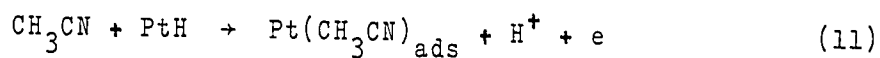
Potentiostatic current transients were also obtained for acetonitrile adsorption at a series of potentials less positive than 0.4 V, E_H (Fig. 19b), i.e. on a platinum surface where the coverage by atomic hydrogen was increasing. The cathodic transient currents described above diminish and eventually become anodic ones which increase as the potential of adsorption becomes less positive and approaches the reversible H_2 potential. This interesting and initially unexpected observation lead to the discovery of a new, general electrochemical effect, "anodic H displacement", to be

MANUSCRIPT DEPARTMENT OF CHEMISTRY



described fully in Part II. The effect consists of ionization of H^* , previously adsorbed on the electrode, when another adsorbate becomes chemisorbed on the surface. The effect thus tends to be larger at potentials where more H is present on the electrode, i.e. at the least positive potentials.

The observation with acetonitrile can only be accounted for in terms of the adsorption mechanism (ii) given above, since adsorption and the subsequent H displacement referred to above could not occur (117) via mechanism (i) at high coverages of atomic hydrogen (e.g. at 0.06 V, E_H). The anodic H displacement effect observed with acetonitrile must hence arise from competitive displacement of adsorbed H according to an anodic electrochemical mechanism of the form:



The effect provides useful information on the processes that occur when acetonitrile becomes adsorbed, in particular the connection between transient adsorption charge, H blocking (Δq_H) and H displacement.

The charge quantities associated with acetonitrile adsorption at various potentials are given in Table II and Fig. 21. The net adsorption current transient for acetonitrile between 0.4 V and 0.05 V, E_H corresponds to passage of

* A detailed analysis, given in section II(b), proves that the observed anodic transient charge at $V < 0.15$ V, E_H , resulting from acetonitrile addition, arises from anodic H displacement occurring when CH_3CN is adsorbed.

Table II
Charge quantities involved in CH₃CN and H adsorption and their surface reactions at Pt (25°C, 1 N aq. H₂SO₄)

Adsorption potential, V _a , volts	Charge for H adsorption on clean Pt surface q _H (μC.cm ⁻²)	Anodic and cathodic charges between +0.35 V and V _a in H region with CH ₃ CN adsorbed		q _{c, H} q _{a, H} (μC.cm ⁻²)	q _{c, H} q _{a, H} (μC.cm ⁻²)	Charge in adsorption transient q _t (μC.cm ⁻²)	Charge for H displacement Δq _H (μC.cm ⁻²)	q _t - Δq _H (μC.cm ⁻²)	Charge in d.l. and H region for CH ₃ CN oxidation in anodic sweep after transient** (μC.cm ⁻²)
		q _{a, H} (μC.cm ⁻²)	q _{c, H} (μC.cm ⁻²)						
0.06	220*	62.9	40.2	85.8	45.6	0 ± 1	157.1	-157.1 ± 1	150.0
0.11	164	42.1	21.7	51.8	30.1	0 ± 1	121.9	-121.9 ± 1	115.6
0.14	118.5	31.4	15.3	45.2	29.9	-13.65	87.1	-100.8	105.0
0.16	85.8	20.5	14.4	37.4	23.0	-25.0	65.3	-90.3	95.7
0.20	67.8	12.0	5.8	23.8	18.0	-32.8	55.8	-88.6	88.6
0.21	62.4	10.3	4.7	21.5	16.8	-30.8	52.1	-82.9	84.1
0.235	52.7	6.5	3.6	15.6	12.0	-36.2	46.2	-82.4	83.5
0.26	28.9	3.4	1.6	11.7	10.1	-49.3	25.5	-74.8	71.8
0.31	4.6(8)	0±1	0±1	3.9	3.9	-59.3	4.6±1	-63.9±1	61.3

* Based on assumed full coverage by H equivalent to 220 μC.cm⁻² (Ref. 12).

"h" = holding at each potential for period equal to total time involved in the measurement of the transient, viz. 90 sec.

"ms" = multiscan, i.e. as measured in repetitive cyclic voltammetry between +0.4 V and V_a.

** The time that this sweep was taken after the transient, corresponds to the holding time referred to above in the q_{a, H} column.

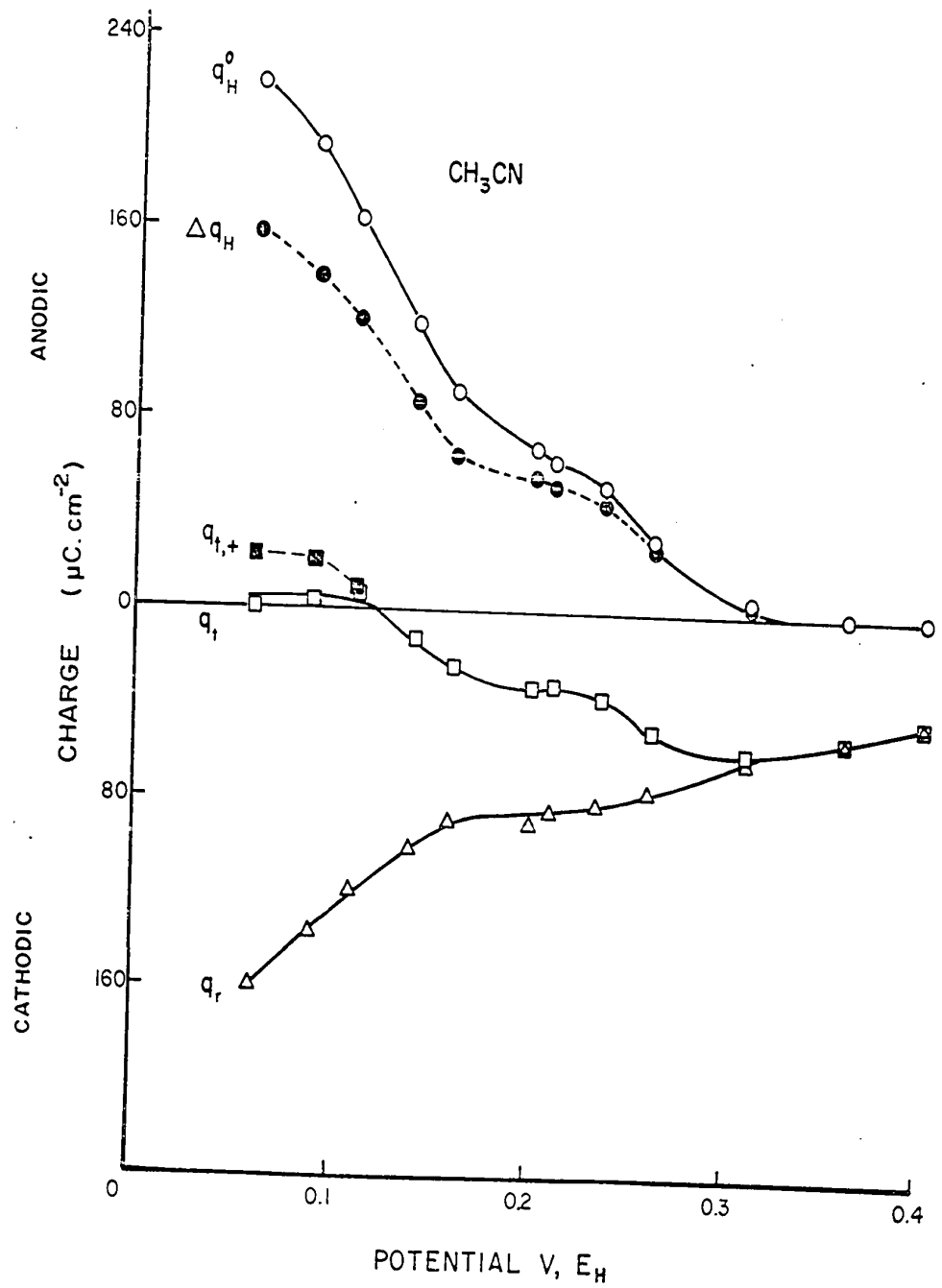


Fig. 21. Transient adsorption charges, q_t (\square), from current transients for acetonitrile adsorption at Pt in relation to H blocking, Δq_H (\circ), and total H coverage, q_H^0 (\circ), in absence of additive. The points \square represent q_t values before correction for slow reduction effects. q_r is as defined in the text. $[\text{CH}_3\text{CN}] = 3 \times 10^{-3} \text{ M}$.

charge, q_t , due to the following processes: (a) electron transfer to acetonitrile at vacant sites; (b) electron transfer to acetonitrile adsorbed at sites occupied initially by H at potentials $< 0.35 \text{ V, } E_H$; (c) anodic displacement of the H atoms at those sites; and (d) any reaction of neighbouring H atoms with the adsorbed acetonitrile that may leave a site vacant which could then become reoccupied by H in the normal cathodic process $\text{H}^+ + e + \text{Pt} \rightarrow \text{PtH}$. For these reasons, the values of q_t are all substantially less than the values of q_H^0 (the charge for H coverage at platinum in the absence of acetonitrile) at various potentials in the H-region and also less than the extent of blocking of H adsorption, Δq_H , as measured from the areas under the cyclic voltammetry curves after adsorption. The difference $q_t - \Delta q_H$ ($= q_r$ in Fig. 21) represents the cathodic charge component that is taken up as acetonitrile is adsorbed and electrochemical displacement of H occurs. Quantitative examination of the charges shows that q_r is almost equal, at all adsorption potentials, to the charge for anodic re-oxidation of the adsorbed CH_3CN species in the next anodic sweep taken up to $0.8 \text{ V, } E_H$ after measurement of the transient. This result is expected for an adsorption controlled, reduction-oxidation reaction. The significance of the measured charge quantities in relation to the reaction mechanism will be discussed in detail in section II(f).

(g) pH Dependence of the peak currents for acetonitrile reduction and oxidation

In order to determine whether acetonitrile reduction in the double-layer potential region occurs with the uptake of solution protons, the pH dependence of the cathodic process was investigated by evaluating the pH dependence of the peak potential, V_p . The same solution was employed in both the reference and working compartments so that no liquid junction was involved. The variation of V_p with pH over the pH range +1 to -1 was found to give a Nernst slope of 59 mV per unit pH change, i.e. the ratio of protons to electrons involved in the reaction is one. This indicates that acetonitrile reduction in the double-layer region is not a simple electron transfer process but involves protons from the solutions.

I.2 Involvement of the H Adsorption/Desorption Potential Region in the Acetonitrile Reactions at Platinum

(a) General observations

Figs. 11 and 17 showed the progressive increase of acetonitrile re-oxidation charge in the double-layer region ($q_{a,d.l.}$) as the cathodic-going sweep was taken to less positive reversal potentials. These sweeps were programmed to exclude or include (either partially or totally) the potential range for H adsorption at platinum (i.e. from 0.35 to 0.05 V, E_H). The results indicate that besides decreasing the coverage with atomic hydrogen, adsorbed acetonitrile

reacts in the H region of the cathodic-going sweep either with adsorbed hydrogen, or by electron and proton transfer to give an increased quantity of reduced adsorbed material which can be reoxidized in the double-layer region on the next anodic-going sweep*. The increase is not associated with further acetonitrile adsorption from solution since it is known that there are no elements of diffusion control when $[\text{CH}_3\text{CN}] > 3 \times 10^{-4}$ M.

(b) Resolution of component currents and charges in the anodic and cathodic H regions by means of kinetic relaxation studies

In order to determine accurately the manner in which the acetonitrile reoxidation charge in the double-layer potential region is influenced by reactions in the H region, it will be necessary to consider how any overlap of the acetonitrile reoxidation peak with that for atomic hydrogen ionization can be evaluated. Up to this point, the hydrogen charge has been considered to be that which would be obtained by integration of the i-V profile over the anodic hydrogen region taken from the reversible hydrogen potential (ca. 0.05 V, E_{H}) to a potential corresponding to the minimum

* At least one type of anodic electrochemical reaction is known, the surface oxidation of Pt (see p. 7), which gives rise to several distinguishable peaks over different potential regions in the anodic-going sweep, but the final adsorbed species gives only a single reduction peak in the cathodic-going sweep (this single oxide reduction peak can, however, be resolved into component peaks in very fast cathodic transients under certain conditions (121)).

in the i - V profile between the main acetonitrile and hydrogen peaks (see Fig. 7). The assumption was thus made that any overlap which existed between the two peaks was symmetrical, so that any errors in evaluation of the charges for acetonitrile reoxidation and H ionization were cancelled. It is obvious that such a simple procedure could not be employed for the cathodic-going sweep since $q_{c,H} > q_{a,H}$. This arises because the reduction of acetonitrile is occurring in the H region during the cathodic sweep and the charge adds to that for atomic hydrogen deposition. Cathodic holding effects produce substantial changes not only in the double-layer region on the next anodic sweep but also in the H region (Fig. 11). Such an observation is important with regard to possible rearrangements of acetonitrile on the surface during cathodic holding which could lead to an increased accommodation with atomic H. It is therefore important in this study, and also more generally, to be able to distinguish co-adsorbed H from other adsorbed organic species that may be reactive in the H region.

A special new experimental procedure was therefore developed to investigate this problem further by utilizing the principle that the kinetic relaxation rates in response to a fast changing potential signal (step or fast sweep) will be different for fast and slow reaction components at any given potential. The atomic hydrogen ionization reaction on platinum is a very fast, reversible process and it is likely

that any components of the acetonitrile oxidation reaction, which might occur over the hydrogen region, will be slower and less reversible than the atomic hydrogen deposition or ionization reactions (cf. Fig. 17). Separation of reaction components in the hydrogen region could thus be achieved by means of the potentiodynamic sweep program consisting of cycling the system in the normal potential range (0.05 to 1.3 V, E_H) at a standard (slow) sweep rate (e.g. 5 mV sec⁻¹) but interrupting this "guiding" sweep, while it is progressing in the anodic-going direction of the hydrogen adsorption region, by introduction of a much faster anodic-going potential pulse (fast linear sweep). Because of the type of function generator being used (Tacussel), the sweep rate alterations had to be made by factors of ten, e.g. from a normal sweep rate of 5 mV sec⁻¹ to 50 mV sec⁻¹ or 10 to 100 mV sec⁻¹. When this particular program was tested in a potential sweep at Pt over the H region in pure aq. H₂SO₄ solution, alteration of the sweep rate from slow to faster speeds resulted in the H ionization currents becoming re-adjusted immediately from their initial to their new values at the higher sweep rate as required for a fast relaxation process. Such behavior is illustrated in Fig. 22.

The important fact to be noted in relation to the method described here is that transient currents for atomic hydrogen ionization obtained after interruption of the sweep by changing from small to larger values of dV/dt were almost

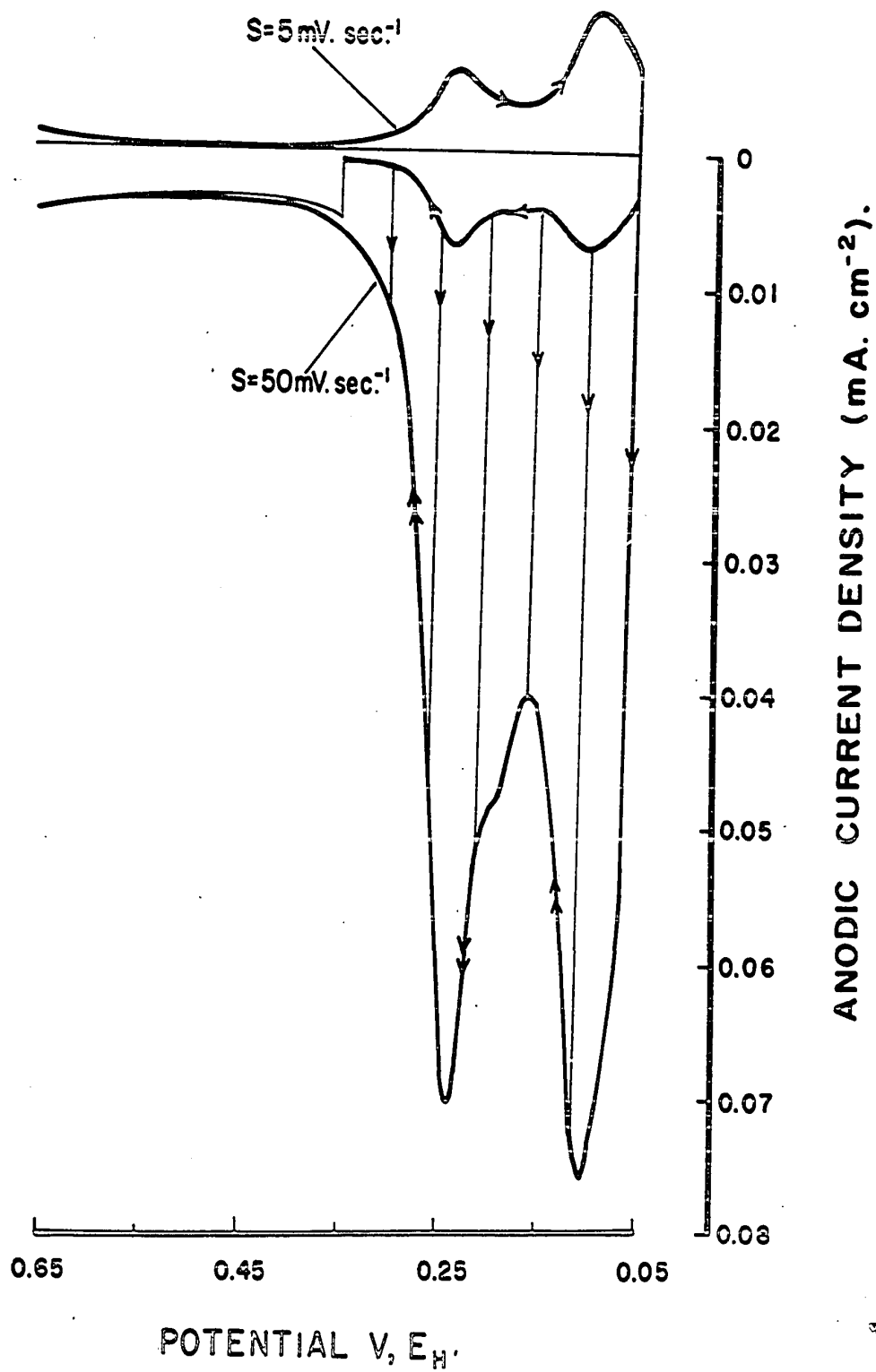


Fig. 22. Effect on the hydrogen region of changing from slow (5 mV sec^{-1}) to fast (50 mV sec^{-1}) sweep rates during an anodic-going sweep. Pt, $1N \text{ H}_2\text{SO}_4$.

identical to those obtained with multisweep cycling at the faster sweep rate (Fig. 22). The fact that there was no delay in attaining the new values after interruption is characteristic of the pseudo-capacitance behavior (50,96) of a fast, reversible electrochemical process and this characteristic will be used to distinguish the atomic hydrogen electrosorption reactions on platinum from slower processes involving organic species. Such slower, somewhat irreversible processes (cf. surface oxide formation on platinum) cannot immediately respond to the successively initiated fast sweeps and appear as a trailing of current after the initial fast H component has appeared (Fig. 23). Fig. 23b also shows the application of this method to the kinetic separation of reaction components which arise in the cathodic-going sweep. In this case, the fast, reversible reaction in the H region corresponds to deposition of atomic hydrogen.

Fig. 23b shows that the current associated with the reversible process of atomic hydrogen deposition or ionization is easily obtained since the cut-off point between the fast current rise and the delayed current rise is well-defined*. The fast component process in both the cathodic and anodic H regions falls to zero at ca. 0.3 V, E_H in the manner well known to be characteristic of adsorbed H. That the species associated with fast relaxation is H is also confirmed by the

* The slight overshoot of ca. 0.5 mm on an X-Y recorder, responding to a fast process, serves fortuitously to act as a marker for the termination of the fast process and commencement of the slow one.

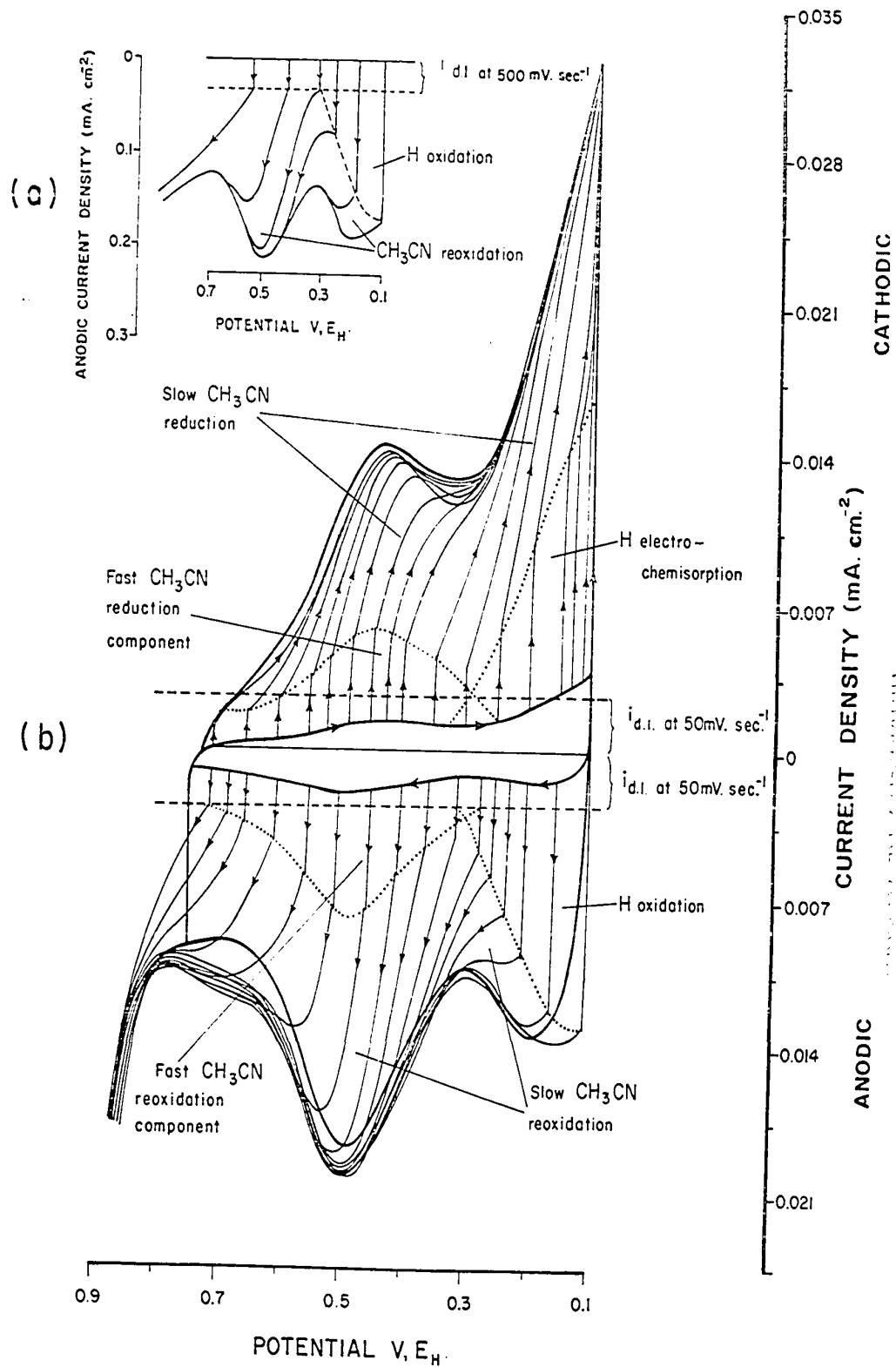


Fig. 23. (a) Resolution of the fast atomic hydrogen and acetonitrile processes obtained by initiating faster transients (50 mV sec^{-1}) on a slower anodic or cathodic-going one (5 mV sec^{-1}).

(b) Resolution of fast H ionization process with transients at 500 mV sec^{-1} taken on a slower anodic sweep of 5 mV sec^{-1} .

exact identity of its amount (charge) on the cathodic and anodic-going sweeps. Fig. 23b shows, however, that all the $q_{a,H}$ or $q_{c,H}$, i.e. the total charges passed in the cathodic or anodic H regions, is not identifiable uniquely with H. Qualitatively, this is already apparent from the experimental fact that $q_{c,H} > q_{a,H}$. In both anodic and cathodic sweeps, a substantial slower component process is indicated in the H region which must be associated with oxidation and reduction of adsorbed acetonitrile species rather than with electro-activity of H.

Since the experimental procedure discussed above involved slow sweeping (5 mV sec^{-1}) through at least part of the hydrogen region before the fast sweeps (50 mV sec^{-1}) were initiated, there was necessarily an effect equivalent to cathodic holding arising from the longer times, τ_H , spent in the cathodic region, ΔV_c , of the 5 mV sec^{-1} potentiodynamic sweeps ($\tau_H = \Delta V_c / S$). As was discussed above, cathodic holding effects give rise to significant changes in the charges for apparent H coverage and acetonitrile reaction on the electrode surface (Fig. 11). To eliminate these holding effects, the experimental procedure was modified by employing a potentiodynamic program in which the faster sweep was interrupted by switching to the slow sweep for a short time in the hydrogen region followed by switching to the faster sweep again. The procedure is thus similar to the one described above except that the slow "guiding" sweep through the cathodic and anodic

hydrogen regions is no longer employed. Instead, the current is allowed to fall to the value which it displayed on the slow (5 mV sec^{-1}) guiding sweep at the potential of interruption from the fast to slow sweep and the potential program is then switched back to the fast sweep rate.

The new procedure can be applied to any potential on the cathodic or anodic-going sweeps; hence the charge component associated with atomic hydrogen reactivity can be evaluated with only very small effects of cathodic holding. The true effect of holding at the cathodic reversal potential in the sweep can also be evaluated by using this modified procedure and will be discussed in section I.2(e) below.

(c) Kinetic heterogeneity in the double-layer potential region

Application of the kinetic relaxation method to the reactions of acetonitrile in the double-layer region (Fig. 23b) indicates that a fraction of the CH_3CN species is also associated with a relatively fast reduction or oxidation process. The fast component substantially diminishes with increasing sweep rate of the superimposed faster linear sweep, and at 500 mV sec^{-1} (at which sweep rate H is still reversible) the fast component has fallen to zero leaving only double-layer charging as a fast process above $0.3 \text{ V}, E_H$ (Fig. 23a). Initiation of the fast transient sweep at various rates in the double-layer region appears to reveal a spectrum of reversi-

bility or extents of the fast oxidation or reduction process, evidently depending on the rate constants of processes at various types of sites. That the same chemical species is involved (as that corresponding to the main peak) is indicated by the fact that the peak for the fast component appears at the same potential independently of the rise time of the sweep, and at the same potential as the overall peak observed in the slower sweeps (Fig. 23b).

(d) Dependence of acetonitrile oxidation charge on reversal potential in the cathodic-going sweep

Three potentiodynamic programs were employed in studying the influence of the reversal potential in the cathodic sweep on the charge recovered in reoxidation of reduced acetonitrile on the next anodic sweep. These experiments provide information on the extent of reduction of acetonitrile at various potentials in the H region in cathodic-going sweeps, since any reduction of acetonitrile in excess of that already achieved in the double-layer region results in an increased acetonitrile reoxidation charge on the next anodic sweep (Fig. 17). The potentials between which the reoxidation charge was integrated were chosen in relation the position of the peaks in the sweep profile, the anodic limit of integration being generally taken as $0.825 \text{ V}, E_H$.

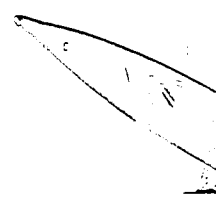
Justification for taking the anodic limit of integration as $0.825 \text{ V}, E_H$ comes from the fact that at this potential

UNIVERSITY LIBRARY



all reoxidation of acetonitrile in the double-layer region appears to be complete and at slightly higher anodic potentials the currents sharply increase because of surface oxide formation and/or reaction of acetonitrile in the oxide region (Fig. 7). It is to be noted that the region of acetonitrile reoxidation extends to $0.825 \text{ V, } E_H$ and includes a small shoulder observed at the higher anodic potentials. This current shoulder may or may not correspond to another stage of oxidation of reduced adsorbed acetonitrile but since it generally increases in the same manner as the main double-layer oxidation peak in the range 0.35 to $0.70 \text{ V, } E_H$, it was decided to include this charge as part of that evaluated for reoxidation of reduced acetonitrile. Choice of the cathodic limit of the integrand for acetonitrile reoxidation charge in the double-layer region depended on the reversal potential in the cathodic sweep and was initially taken as the potential for the current minimum (see e.g. Fig. 17 which shows the dividing line between the H and the double-layer region) in the i - V profile between the H desorption and acetonitrile oxidation regions. The acetonitrile reoxidation charge in the double-layer region thus obtained was corrected for charge contribution in the atomic hydrogen region by the method described above (section I.2(b)).

UNIVERSITY MICROFILMS



The first type of potentiodynamic program to be employed is shown in Fig. 24*. A multisweep was first established between standard potential limits, e.g. 1.3 to 0.06 V, E_H , and after several such sweeps had been registered, the sweep direction was reversed at certain selected potentials (differing from 0.06 V, E_H) on the cathodic-going sweep. These reversals of the sweep direction were achieved by appropriate settings of the function generator, the sweep rate after reversal being identical with that on the repetitive sweep. Between each such reversal of potential scan, a multisweep over the full potential range (i.e. 1.3 to 0.06 V, E_H) was again made to assure a reproducible condition of the electrode surface. By thus interrupting the cathodic sweep before the cathodic end potential of 0.06 V, E_H was reached, a series of anodic sweeps resulted for different amounts of reduced acetonitrile awaiting reoxidation. A plot of the corrected charge for acetonitrile reoxidation, q_a , versus cathodic end potential gives a very broad relationship with two linear regions (Fig. 24). The corrected hydrogen coverage, $q_{H,+}$, as determined from the resolved anodic sweep in the H region, was plotted with respect to the cathodic end potential but, unlike

* It should be noted that the separation of hydrogen and acetonitrile charge components in the H region by the kinetic relaxation procedure discussed above must be employed in such a way that it conforms with the potentiodynamic program given in Fig. 24. This simply means that the kinetic relaxation technique is employed separately for the various potential ranges that result from reversal of the cathodic-going sweep at different potentials in the H region.

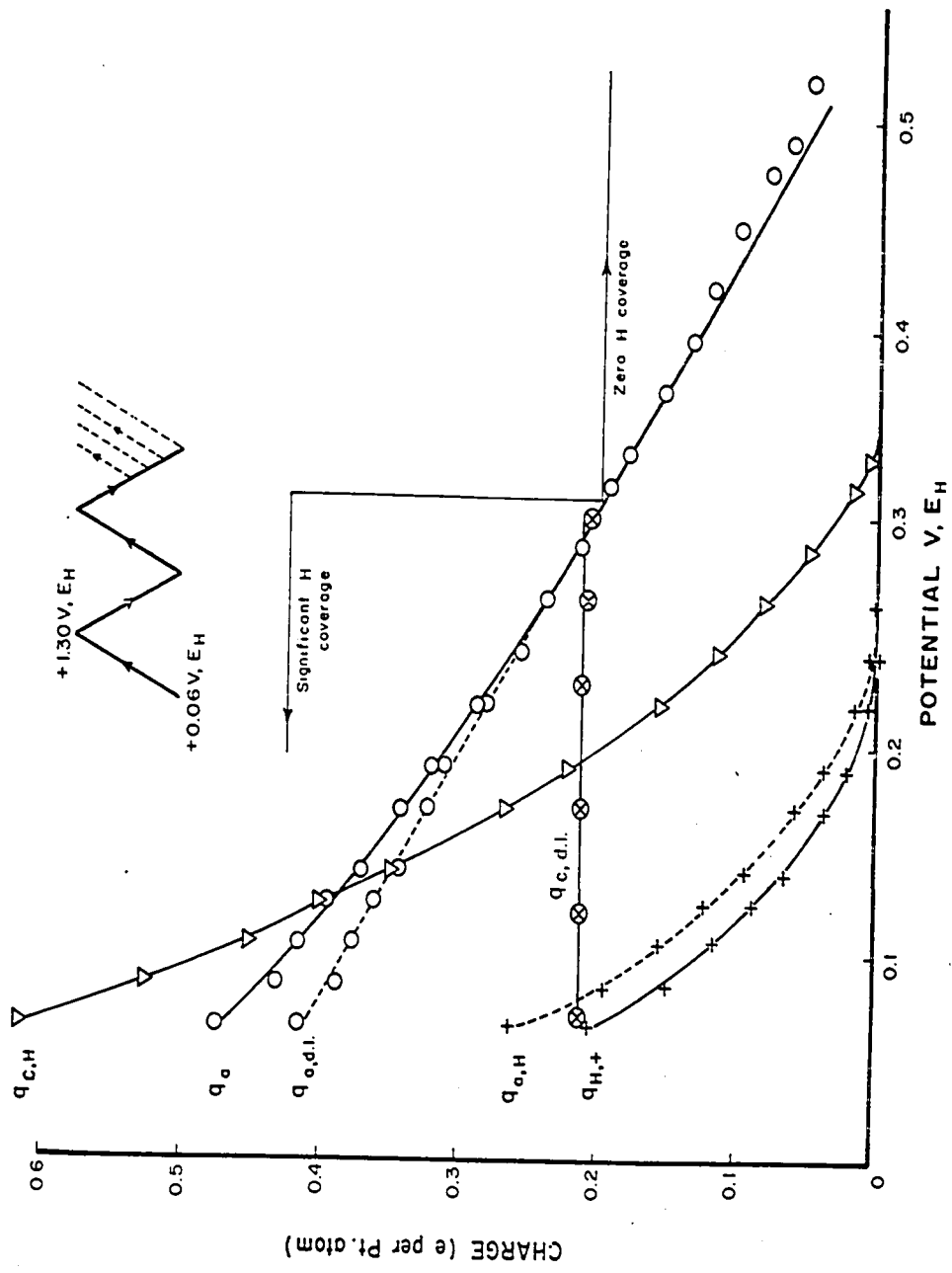


Fig. 24. Charges involved in reduction and oxidation of adsorbed acetonitrile determined in various potential ranges as a function of potential of sweep reversal in the cathodic-going sweep. Correction for acetonitrile reoxidation charge in the anodic H region was made and the true acetonitrile and hydrogen oxidation charges are shown (see Table 1 for definitions of charge quantities). $[CH_3CN] = 5 \times 10^{-3} M$, $(dV/dt) = 50 \text{ mV sec}^{-1}$.

the case for a sweep in the supporting acid electrolyte alone, (Fig. 21), no arrests are observed.

Another quantity which may be determined from the above experiment is the total charge in the cathodic hydrogen region at different cathodic end potentials. This quantity, $q_{c,H}$, is plotted in Fig. 24 but its interpretation in this case is complicated because of pre-history of the electrode in the surface oxide region. It will be shown in the section on oxide involvement (see p.117) that a process occurs in the surface oxide region which produces extra reducible material that reacts in the H region of the next cathodic-going sweep; however, this extra reduction process has no influence on the acetonitrile reoxidation peak on the next anodic-going sweep.

In addition to complicating the interpretation of charge measured in the cathodic hydrogen region, continuation of potential scan into the surface oxide region results (see section I.4(b), Fig. 34) in a charge component being added to the acetonitrile reduction peak in the double-layer region. These difficulties can be avoided by using a modified potentiodynamic program such as the one illustrated in Fig. 25. In this case, the sweep direction is reversed on the anodic-going cycle before the formation of surface oxide, i.e. at 0.825 V, E_H and this is followed by the same type of sweep reversal program discussed above involving various cathodic end potentials. Between cycles over the restricted range, the electrode can be driven into the oxide region so that the

UNIVERSITY LIBRARY



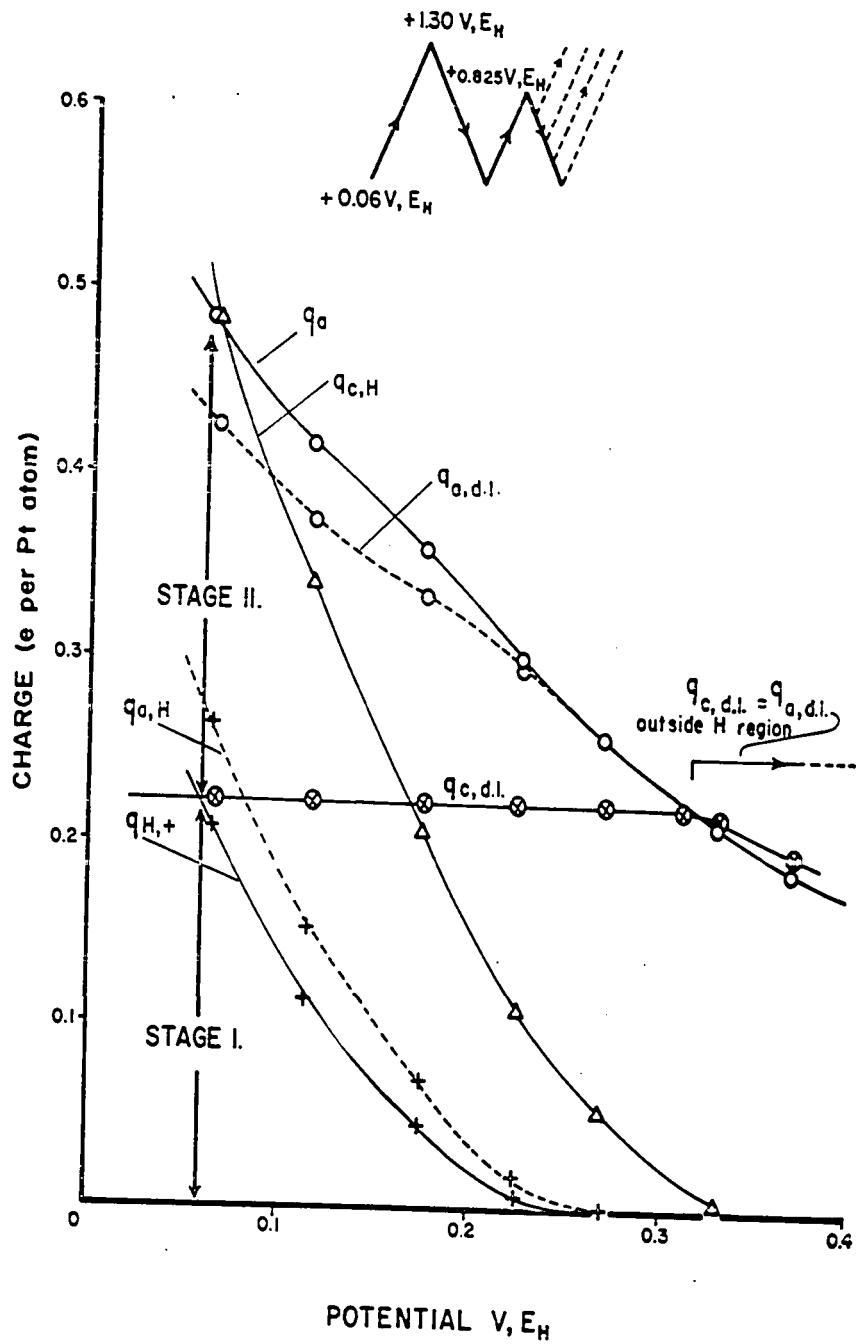
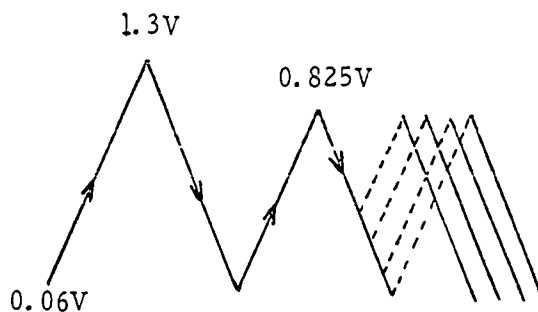


Fig. 25. As in Fig. 24 but with a modified potentiodynamic programme in which the surface oxide region is excluded.

usual anodic cleaning of adventitious impurities from the surface results.

A somewhat different potentiodynamic sweep program was used in determining the effect of cathodic end potential on the acetonitrile reduction charge in the double-layer region:



In this experiment, there is a "triple reversal" of the sweep, first at 0.825 V, E_H to avoid surface oxide formation thus enabling the true value of $q_{c,d.l.}$ to be obtained, followed by cutting at various cathodic end potentials and then finally another cutting at 0.825 V, E_H . Acetonitrile reduction on the cathodic-going sweep in the double-layer region is seen (Fig. 25) to be independent of the history of the electrode in the prior sweep which has covered the hydrogen region. However, if $q_{c,d.l.}$ is compared with $q_{a,d.l.}$ in sweeps which either include or exclude the H region, it is found that these charges are almost identical if the H region was excluded but $q_{a,d.l.} > q_{c,d.l.}$ for conditions where the H region is included in the cathodic-going sweep. There is a broad dependence of the

UNIVERSITY LIBRARY

charge for acetonitrile reoxidation on the range of potentials covered in the hydrogen region (Fig. 25) similar to the behavior shown in Fig. 24.

The charge in the hydrogen region in a cathodic-going sweep using the program shown in Fig. 25 is the sum of charges for each of the following surface reactions: (i) normal electrochemical hydrogen deposition on platinum; (ii) further reduction of acetonitrile beyond that which occurs in a cathodic-going sweep in the double-layer region. The true contribution from ionization of adsorbed hydrogen is given by $q_{H,+}$, determined by the kinetic relaxation method discussed above. The component of the charge $q_{c,H}$ which is associated with reduction of acetonitrile species in the hydrogen region can then be easily determined (see Fig. 23b).

(e) Evaluation of effects of holding the potential at the cathodic end of the sweep

The adsorption transient measurements discussed above for acetonitrile at the less positive potentials (Fig. 21) indicated a slow reduction process in the H region. Fig. 11 showed how both the charge $q_{a,d.l.}$ for reoxidation of adsorbed acetonitrile in the double-layer region and the apparent H coverage, measured in an anodic sweep, increased upon 90 sec holding at $0.06 \text{ V}, E_H$. In fact, 90% of the holding effect is already completed in 15 sec at $0.06 \text{ V}, E_H$ and no further effects are observed beyond 90 sec. However, the programs discussed

above (shown in Figs. 24 and 25) could not easily be used to investigate the effect of holding the potential at various values at the ends of cathodic sweeps because in these programs the cathodic-going sweep was simply reversed at the required potential and thus could not be held at the reversal value. This technique had the advantage of not requiring any instrument readjustment since the sweep rate for any potential range scanned remained the same. When effects of holding were investigated, the potential range for the prior multisweep (and hence the sweep rate itself) had to be adjusted each time the cathodic termination potential was changed. The potentiodynamic program used, together with the results obtained, are shown in Fig. 26.

Holding the potential for 90 sec at various termination potentials in a cathodic-going sweep indicates two important characteristics of the behavior of acetonitrile at Pt: (i) cathodic holding produces more of a material which is electrooxidized in the double-layer region in a subsequent anodic sweep (charge $q_{a,dl,h}$ of Fig. 26). The extra oxidizable material is evidently the same or similar to that produced with cycling into the H-region since the peak characteristics are unchanged by cathodic holding, except that the charge is increased (Fig. 11); (ii) a larger anodic charge passes in the H region (represented by $q_{a,H,h}$) as a result of cathodic holding (Fig. 11). It is important to note that holding effects also persist at more positive potentials,

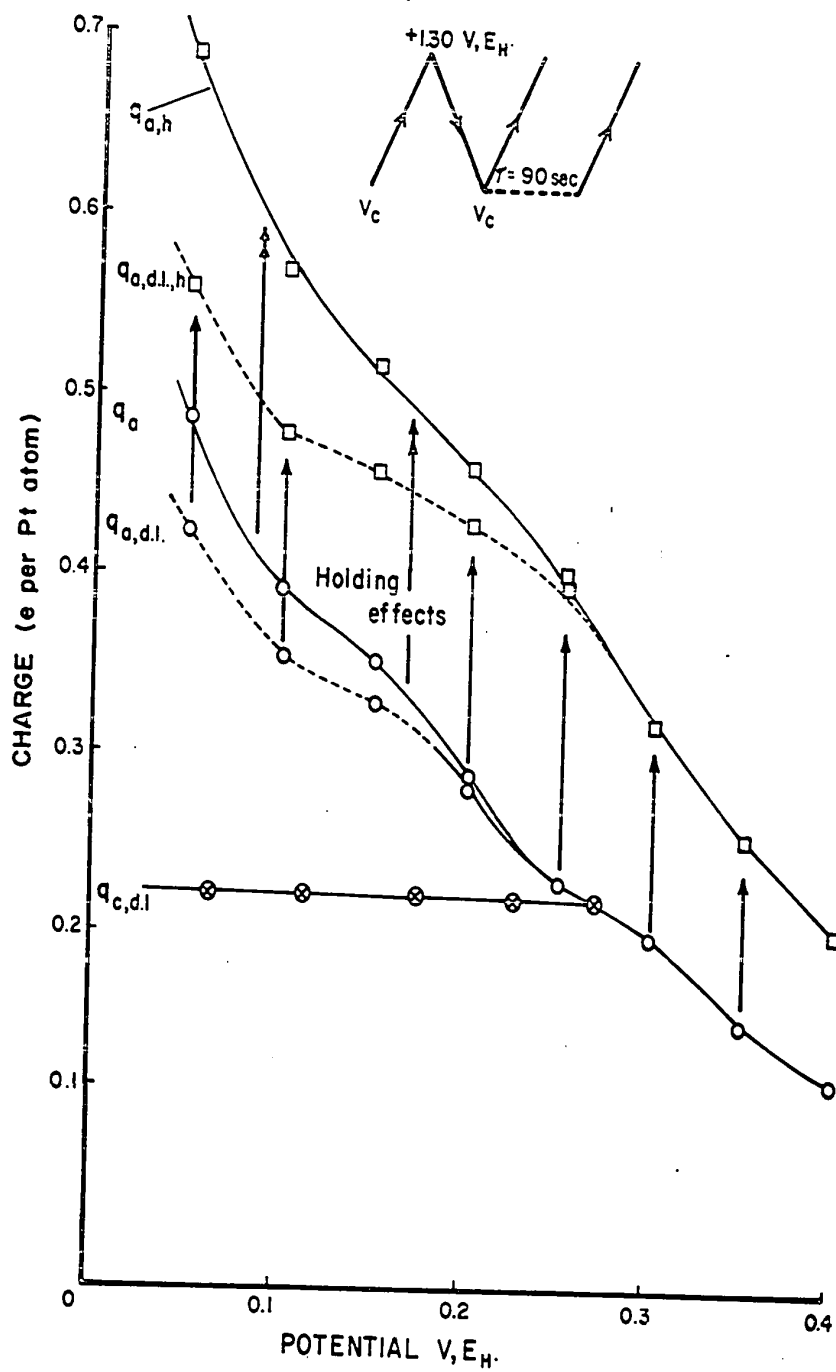


Fig. 26. Effect of cathodic holding at various potentials on charge recoverable in the following anodic sweep in d.l. region ($q_{a,d.l}$ and $q_{a,d.l,h}$). Holding effect, corrected for additional charge involved in reoxidation (in the H region) of reduced CH_3CN species, is represented by the solid lines marked q_a and $q_{a,h}$. The (constant) cathodic charge, $q_{c,d.l}$, for reduction in the double-layer region is also shown. $(dV/dt) = 50 \text{ mV sec}^{-1}$.

i.e. $>0.31 \text{ V}, E_{\text{H}}$ (Fig. 26), and are hence not dependent only on the presence of chemisorbed H. The holding effect is, however, larger at potentials where atomic hydrogen is present on the surface.

The kinetic relaxation method described above was used to determine $q_{\text{a,h}}$, i.e. the corrected acetonitrile re-oxidation charge measured on the next anodic-going sweep after cathodic holding, and it is compared with the corrected total value without cathodic holding, q_{a} , in Fig. 26. Also, the extent to which the increase of charge in the hydrogen region in the anodic-going sweep, resulting from cathodic holding, is due to an increase in reduced acetonitrile or to an increase in coverage of co-adsorbed H may be derived from these measurements. Fig. 27 shows the apparent and corrected hydrogen ionization charges with and without cathodic holding. Although a part of the total apparent charge increase in the anodic H region is evidently due to an increased amount of reoxidizable adsorbed acetonitrile species, the difference between the corrected hydrogen charges, $q_{\text{H,+}}$ and $q_{\text{H,+h}}$, appears to be quite substantial and would seem to indicate a rather large increase in the Pt surface available for atomic H adsorption resulting from long-term reduction of the adsorbed acetonitrile. However, when the value of $q_{\text{H,+h}}$ is compared with the resolved charge for atomic hydrogen deposition on the cathodic-going sweep, $q_{\text{H,-}}$ in Fig. 27, the difference is rather small (although such small differences ($<7\%$) could

UNIVERSITY MICROFILMS



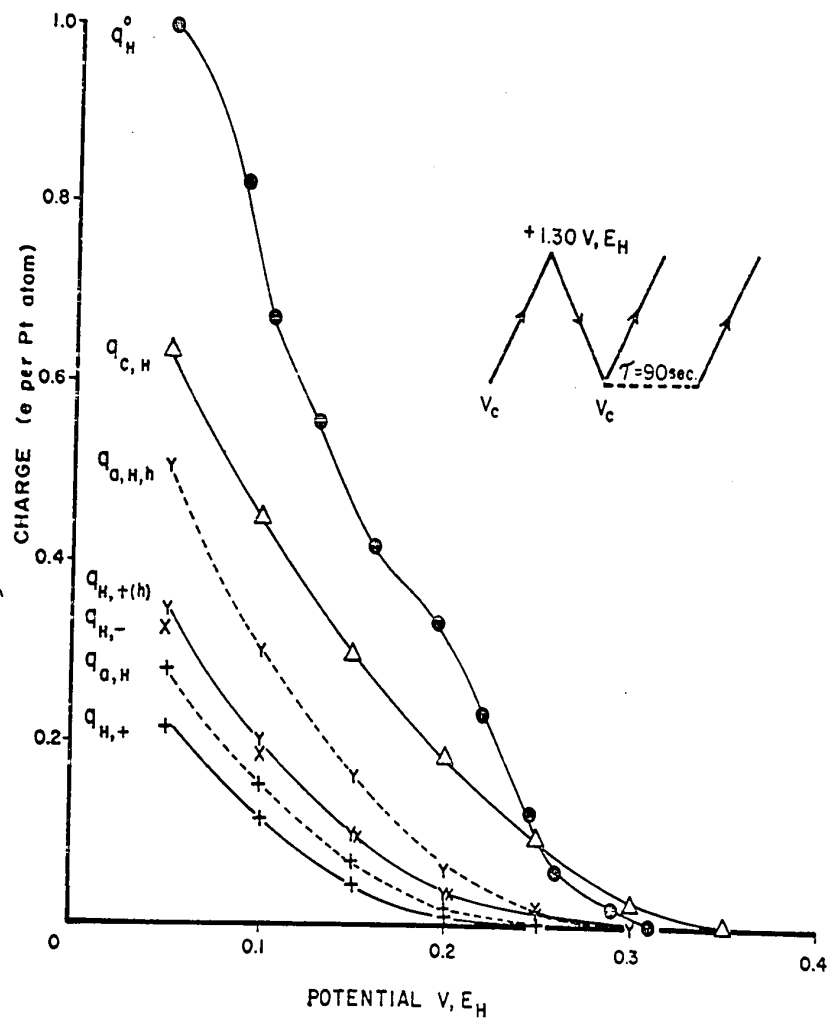
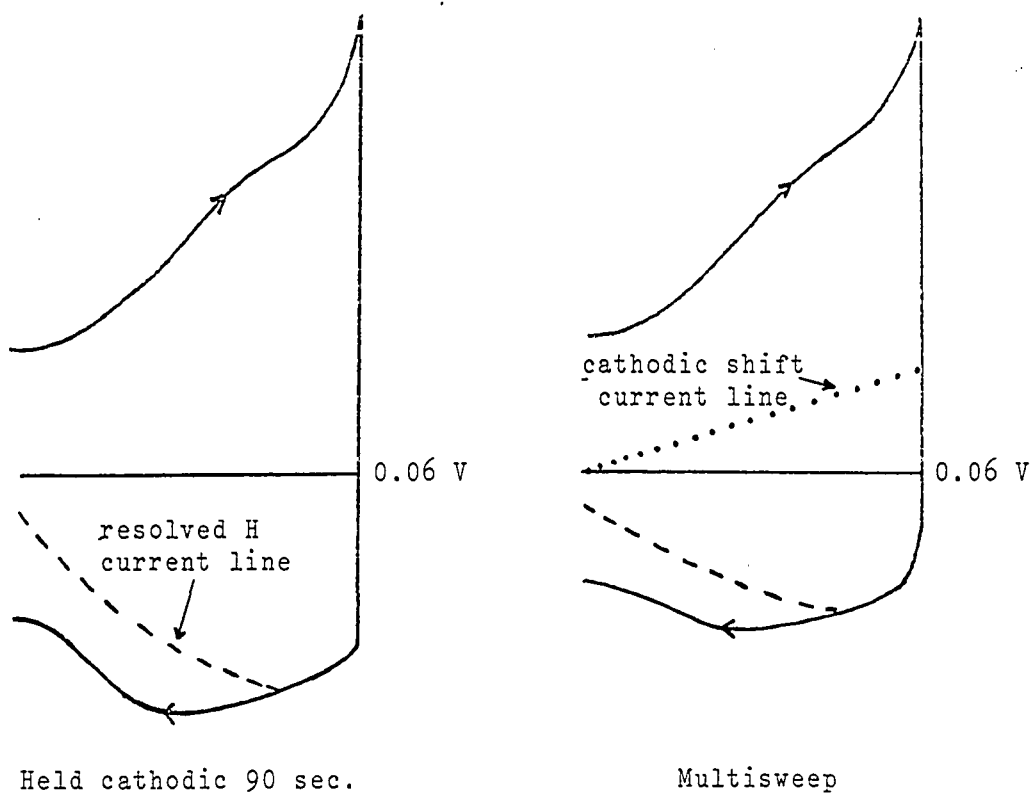


Fig. 27. Repetitive sweep charges $q_{c,H}$, $q_{a,H}$ in the H-region and the anodic charge $q_{a,H,h}$ recovered after 90 sec holding at various cathodic end potentials. $q_{H-(h)}$ and q_{H-} are the corresponding charges for the resolved, fast H desorption component, (with and without cathodic holding), giving the true extent of H adsorption in repetitive sweep and holding experiments. q_{H-} is the true charge for hydrogen deposition on the cathodic sweep; q_H^o is the H coverage in absence of acetonitrile as $f(V)$. $(dV/dt) = 50 \text{ mV sec}^{-1}$.

still be significant in the interpretation of the reaction mechanism). This fact indicates that there is no substantial change in the coverage with co-adsorbed H upon cathodic holding at a platinum surface covered by adsorbed acetonitrile.

The observed difference between $q_{H,+}$ and $q_{H,+h}$ originates because there is a cathodic shift of the i - V profile in the H region during a multisweep at a finite rate (e.g. at 50 mV sec^{-1}) shown schematically below:



This arises because the cathodic reaction during a sweep never reaches stages of completion corresponding to all potentials covered in the sweep, so that on the reverse, i.e. anodic, direction of the cycle (without holding) a

cathodic current component* remains and causes the whole i - V profile to be displaced towards the cathodic current side (cf. Fig. 17). Holding the potential at the cathodic end of a sweep evidently allows the slow cathodic process to be completed so that in the following anodic sweep, (i) the net anodic current no longer contains the potential-dependent cathodic component, and (ii) more of the reduced acetonitrile species is available for reoxidation causing $q_{a,h} > q_a$ (Fig. 26). In fact, support for the above conclusions is provided by the fact that the resolved hydrogen charges for both the cathodic- and anodic-going sweeps are identical so long as the potentiodynamic program makes use of a slow (e.g. 5 mV sec⁻¹) guiding sweep with switching to a faster sweep for resolution of the fast process. Use of the prior slow sweep in the H region has the effect of "equilibrating" the system, i.e. allowing a state of electrochemical adsorption, characteristic of a given potential, to be reached. Hence, the effect is similar to that achieved with cathodic holding**.

* For slow surface processes in cyclic voltammetry, this behavior is not unusual. For example, on reversal of an anodic sweep at the end of Pt surface oxide formation, an anodic current component remains initially for the first 100 mV of the following cathodic sweep while reversal of a cathodic sweep in the oxide reduction region gives initially a cathodic component on the following anodic sweep (121).

** It was also found that the peak current for the acetonitrile reoxidation peak in the double-layer region displayed much smaller deviations from linearity in S with slow (5 mV sec⁻¹) prior sweeping through the H region. The result is analogous to that shown in Fig. 8 for the anodic peak current as $f(S)$ after cathodic holding, where exact linearity arises.

These conclusions regarding completion of a slow cathodic reaction are consistent with the holding effects discussed in section I.1(c) and I.1(e) and illustrated in Figs. 8 and 17.

I.3 Mechanism of Acetonitrile Adsorption and Reaction at Platinum

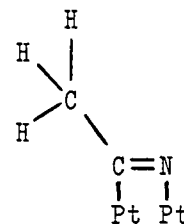
(a) Orientation, surface coverage and nature of the chemisorbed nitrile species

The evidence presented above in sections I.1(c) and I.1(f) led to the conclusion that acetonitrile (and other nitriles) must be adsorbed through the CN rather than the CH₃ group on Pt, as follows:



(i)

and/or associatively as



(ia)

Similar modes of bonding have been proposed for adsorption of gaseous acetonitrile on silica (86,92,93) and for the Pt...N bond in Pt(II) complexes of nitriles (87-89). Distinction between the orientations (i) and (ia) was investigated by examining the relative adsorption and H-blocking effects of benzonitrile and terephthalonitrile (the p-dinitrile).

These nitriles were added to the system while the electrode was held at a potential of 0.35 V, E_H , i.e. in the double-layer region, and the cathodic adsorption transient charge, q_t , was measured. Since q_t results from the reduction of the CN group, it should be directly related to the electrode coverage with adsorbed CN which becomes reduced at the adsorption potential employed. After measurement of q_t , a cathodic sweep was initiated from 0.35 to 0.05 V, E_H in order to obtain the atomic hydrogen displacement charge, Δq_H (see p.83). If orientation (ia) were the main configuration adopted by the adsorbed nitrile, the ratio $\Delta q_H:q_t$ should be different in the case of the dinitrile since the benzene group would be held to the surface by the two CN groups. This condition would give rise to a smaller ratio of $\Delta q_H:q_t$ for the mononitrile relative to that of the dinitrile if the benzene ring of benzonitrile in orientation (ia) could orient itself away from the surface or a larger relative ratio if this were not the case*. The fact that $\Delta q_H:q_t$ is 3.26 for the benzonitrile and 3.40 for the terephthalonitrile (i.e. only a 4.5% difference) indicates orientation (i) as the main mode of adsorption for acetonitrile**. Also, this orientation is

* Cf. section II(e) where it is stated that benzene itself effectively blocks 7 Pt atoms on the surface.

** The assumption is of course made that the CN group of acetonitrile behaves in a similar way to that of benzonitrile and p-terephthalonitrile; indeed, their behavior is quite similar as indicated by their i-V profiles at Pt and the ratio $\Delta q_H:q_t$ for acetonitrile itself is 2.80.

consistent with the direction of the double-layer field in relation to the electric dipole in the molecule. Formation of type (ia) species would also be expected to be somewhat irreversible, (cf. the behavior of ethylene on Pt (123)), while it is found in the present work that acetonitrile can be easily washed from the electrode surface. That the species in orientation (ia) may be the inhibitor B, referred to earlier on p.74, is discussed below.

The maximum reduction charge taken up by the adsorbed acetonitrile species is 0.68 e per Pt at 0.05 V, E_H with cathodic holding (Fig. 26) and the corresponding coverage by coadsorbed H is 0.35 e per Pt (Fig. 27). This acetonitrile reduction charge corresponds to a true maximum value since no further increase occurs upon polarization to 0.0 V, E_H . Models of the 111 platinum surface*, and space-filling models of acetonitrile and its reduced form, show that the maximum coverage by species (i) allowed sterically is 1 molecule per 3 Pt atoms (i.e. 33% of the surface) as shown in Fig. 28. Hence the coverage 0.68 e per Pt corresponds to 68/33, i.e. 2 e per CH_3CN molecule adsorbed at saturation. Fig. 28 also shows that at full coverage with acetonitrile, 2/3 of 50% of sites normally available for H electrosorption are still available, i.e. 33% or 0.33 e per Pt atom. This agrees very well with the observed, resolved maximum H coverage on the cathodic and anodic sweeps of 0.35 e per Pt. The geometry of adsorbed

* This particular crystal face was chosen because it is believed to be the predominant face in the case of drawn platinum wire, from which the electrodes were prepared. Also, calculations using the 100 face as a model of the surface gave expected results which were ca. 50% different from those observed.

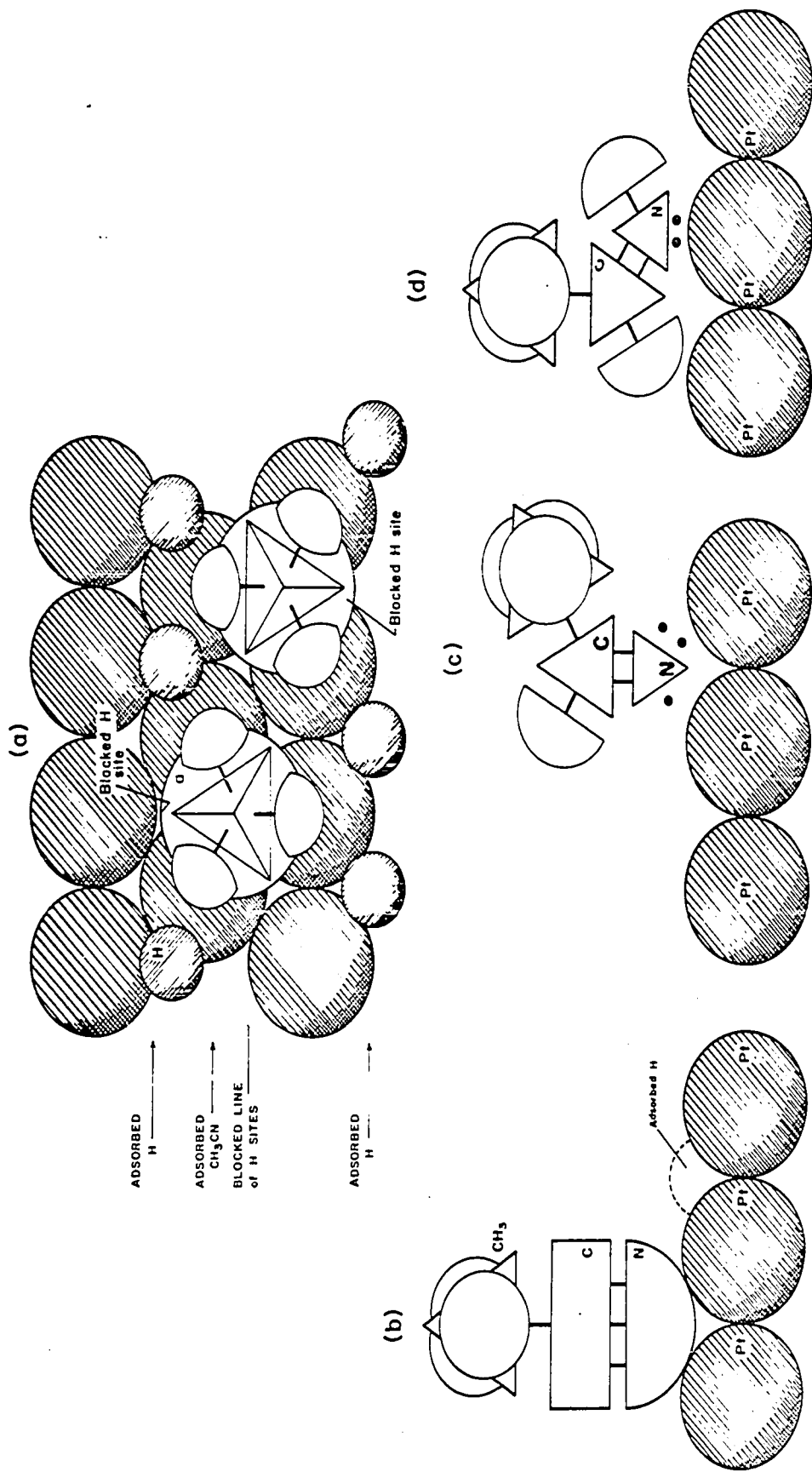


Fig. 28. a) Lattice of Pt atoms on the 111 face showing maximum accommodation of CH₃CN and coadsorbed H.
 b) Orientation of CH₃CN on Pt 111 surface lattice.
 c) Orientation and shape of CH₃CN reduced by 1e, 1H⁺ on Pt lattice.
 d) Orientation and shape of CH₃CN reduced by 2e, 2H⁺ on Pt lattice.

acetonitrile and its reduction products (Fig. 28) shows that somewhat more space on the Pt lattice is required for the reduced species owing to a change of shape of the molecule upon reduction.

(b) Characterization of the slow component in acetonitrile reduction

The reduction of acetonitrile adsorbed on Pt is characterized by a component of the reaction which is slower than any components of the reoxidation reaction. This conclusion comes from the increase of charge q_a for reoxidation of reduced material with time in the cathodic sweep or with cathodic holding (Fig. 26), in contrast to the absence of any increased reduction charge upon anodic holding (e.g. at 0.7 to 0.8 V, E_H). Although the effect of cathodic holding at various termination potentials for the cathodic-going sweep was discussed above with respect to Fig. 26, a somewhat different experiment was desirable in order to determine the true influence of the various potential regions for acetonitrile reduction on the slow process.

The following experimental procedure was adopted: during a cathodic sweep at 100 mV sec^{-1} , the sweep rate was lowered to 1 mV sec^{-1} for 50 sec, i.e. over various 50 mV potential ranges, between 0.6 and 0.1 V, E_H , the electrode was allowed to remain 100 times longer than if a continuous 100 mV sec^{-1} sweep had been applied; the same 100 mV sec^{-1} sweep was

continued in the following anodic sweep. Fig. 29b shows the resulting anodic i - V profiles (with the previous "slow" sweep regions on the cathodic sweep side indicated) and Fig. 29a gives the maximum currents in the double-layer and H regions together with the current corresponding to the minimum at 0.2 V, E_H . These currents are seen to depend on the potential range over which the cathodic sweep was slowed by 100 times.

When slow sweeping is conducted in the potential range 0.6 to 0.4 V, E_H , no time effects arise (Fig. 29a). This behavior is only observed when the overall sweep range includes the H region and is to be compared with the increase of reoxidizable adsorbed material upon cathodic holding at 0.4 V, E_H after fast cycling when only the double-layer region is included (Figs. 19 and 26). The extra reduced material formed during the slow sweep between 0.6 and 0.4 V, E_H would have been formed anyway during the fast sweep (100 mV sec^{-1}) in the H region. When the slow cathodic sweep is employed between 0.4 to 0.25 V, E_H (curve a, Fig. 29b), an increase in the anodic double-layer peak current is observed but at the same time a decrease of the current at the minimum of the i - V profile of Fig. 29b arises. This indicates that some of the material initially produced during the sweep in a fast cathodic reaction is transformed in a slow further stage of reduction into the final material which is then reoxidized in the following anodic sweep in the double-layer region. If the electrode is allowed to remain longer in the H region,

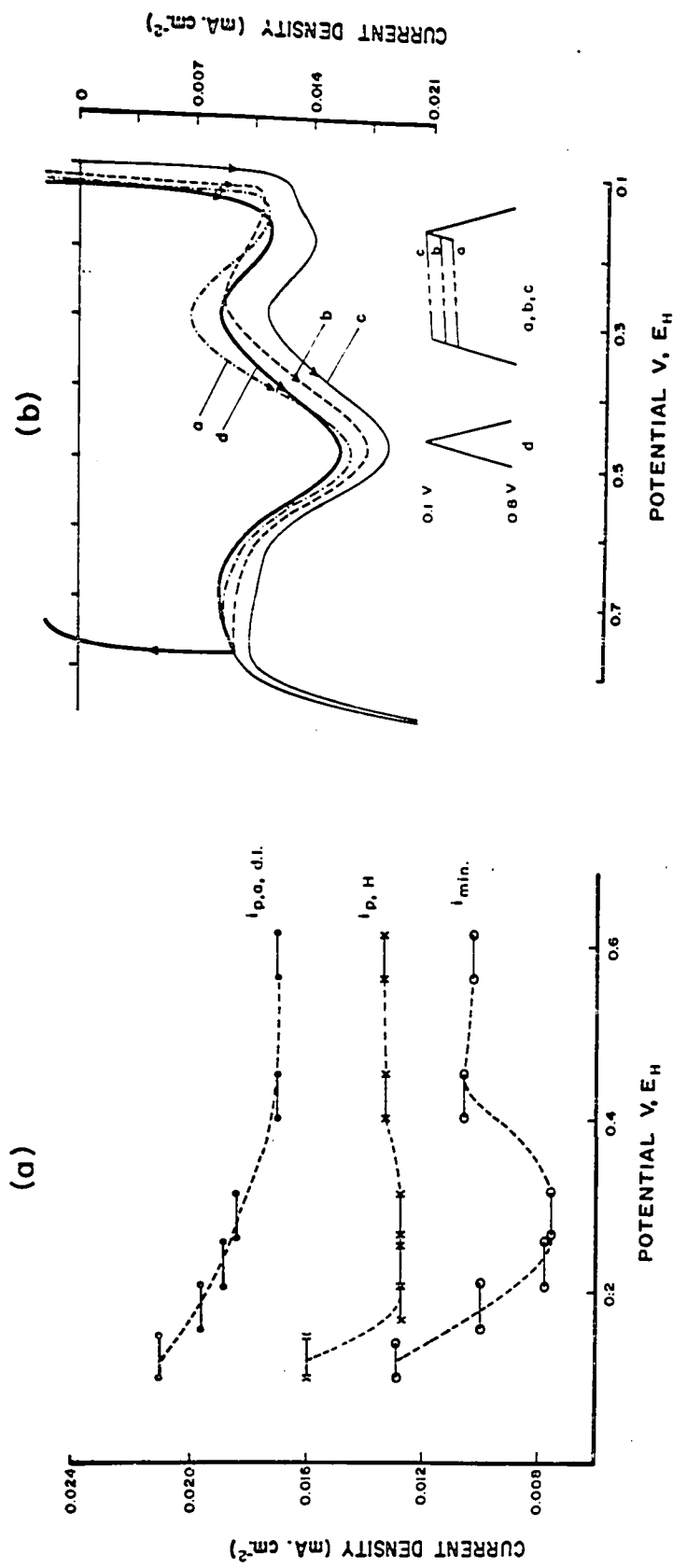


Fig. 29. a) Dependence of currents $i_{p,a,d.l.}$, $i_{p,H}$ and $i_{min.}$ from the anodic $i-V$ profile in Fig. 29(b), on the potential region where slow cathodic sweeping was introduced into 100 mV sec^{-1} over various potential ranges during a 100 mV, sec^{-1} cathodic-going sweep. Curve a: 0.33 to 0.38 V; curve b: 0.21 to 0.16 V; curve c: 0.15 to 0.10 V, E_H.
 b) Anodic-going potentiodynamic $i-V$ profiles at 100 mV sec^{-1} taken after 50 sec periods of slow sweeping at 1 mV sec^{-1} over various potential ranges during a 100 mV, sec^{-1} cathodic-going sweep. Curve a: 0.33 to 0.38 V; curve b: 0.21 to 0.16 V; curve c: 0.15 to 0.10 V, E_H.

an increase of current over the whole i - V profile results (curve c, Fig. 29b). These facts are consistent with the shape of the component i - V profiles for reoxidation of reduced acetonitrile (i.e. after correction for oxidation of co-adsorbed H; see Fig. 30). On a fast sweep (corresponding to curve d in Fig. 29b) the resolved i - V profile shows a second oxidation peak at the potential of the original minimum but this resolved peak diminishes (curve c in Fig. 29b) after the potential of the electrode has been held in the H region. The resulting increase of the whole i - V profile caused by the cathodic holding is principally due to an increase of the main reoxidation peak in the double-layer region.

The resolved i - V profile for adsorbed acetonitrile reduction, i.e. corrected for H deposition, shows (Fig. 30a) the peak for the fast process (0.7 to ca. 0.35 V, E_H) followed by a trailing current region (0.35 to 0.05 V, E_H) connected with the slow reduction process. Beyond the minimum following the reduction in the double-layer region (Figs. 11 and 30a), the cathodic current begins to increase again at the potential where H can be detected on the surface (ca. 0.3 V, E_H), and this increase follows that of H coverage, indicating participation of H in the reduction reaction in the potential range 0.3 to 0.05 V, E_H .

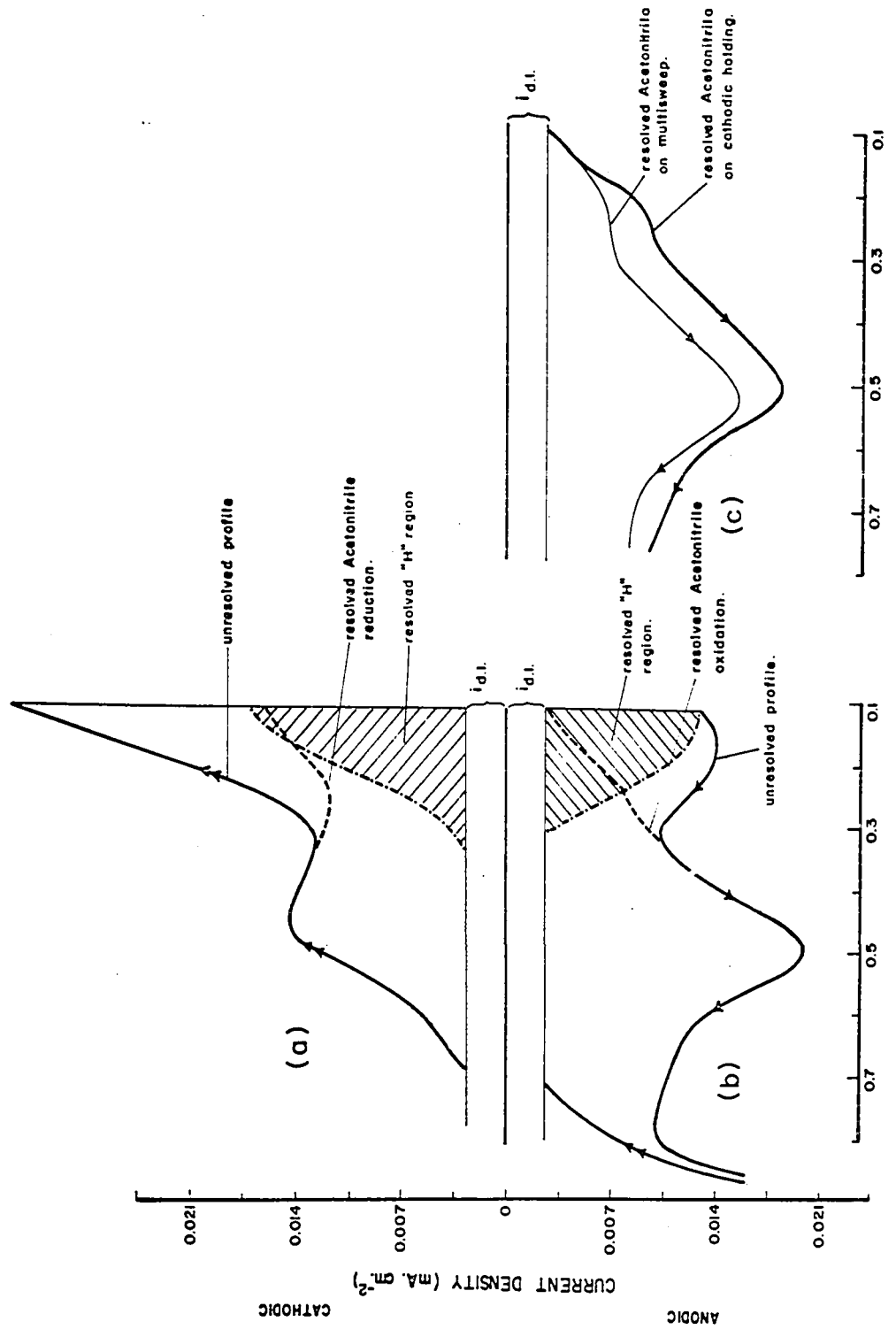
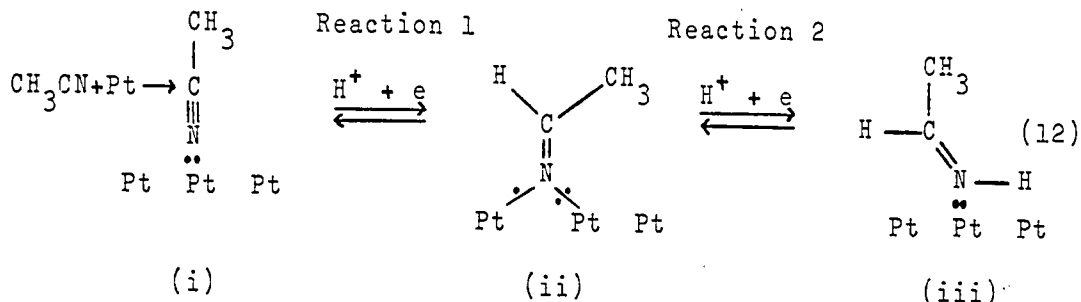


Fig. 30. a) Resolution of component currents in the cathodic-going sweep in the H region by the method illustrated in Fig. 23a. $[CH_3CN] = 5 \times 10^{-3} M$.
 b) As in (a) but for the anodic-going sweep.
 c) Resolved current-potential profile for reoxidation of adsorbed acetonitrile reduced in a cathodic-going repetitive sweep up to 0.10 V, E_H and after holding for 90 sec at this potential.

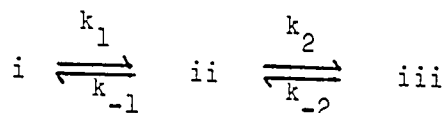
(c) Mechanism of the surface reactions of acetonitrile at platinum

In the light of the results described in the preceding section, a general mechanism for acetonitrile reduction at Pt can be written as:



This mechanism is consistent with (a) the observed pH dependence of the peak potential (59 mV) in the double-layer region; (b) adsorption of acetonitrile through orientation (i) as opposed to orientation (ia); and (c) the accommodation of the Pt surface for acetonitrile and the resulting maximum reduction charge. However, the following possibilities still exist regarding the reduction of the adsorbed acetonitrile over either the double-layer or H regions: (a) acetonitrile which was reduced in the double-layer region to (ii) is further reduced to (iii) in the H region; (b) acetonitrile which was not already completely reduced in the double-layer region can be reduced in the H region. From the resolved i-V profile for reduction (Fig. 30a), it indeed might be concluded that reaction 1 corresponds to reduction in the double-layer potential region while reaction 2 occurs in the H region. However, it is known that at least 95% of the fully reduced

acetonitrile gives rise to reoxidation in the double-layer potential region with a single anodic peak*. The reaction involving adsorbed acetonitrile, (i), can be written as follows:



and the observed single anodic peak could be explained with a small k_{-2} and a large k_{-1} so that (ii) oxidizes back to (i) as soon as it is formed from (iii) by oxidation. Such a mechanism would mean that the oxidation potential for the species (iii) is the same as that for the species (ii) since, as noted above (Fig. 11), there is no significant change in the anodic peak potential for acetonitrile reoxidation obtained when cycling either includes or excludes the H region. This important observation indicates that the acetonitrile species which undergoes reoxidation with cycling from 0.75 to 0.35 V, E_H is the same species which is produced with cycling into the H region, i.e. possibility (b) above.

There are three possible explanations why a certain fraction of adsorbed acetonitrile can undergo reduction in the double-layer potential region while the remainder requires the H region for reduction: (a) the acetonitrile is adsorbed on different kinds of Pt sites in the same way as atomic

* The small resolved peak at ca. 0.20 V, E_H , (Fig. 30b) represents less than 5% of the total acetonitrile reoxidation charge and cannot be the required second anodic peak.

VANPITER LIBRARY

hydrogen; (b) acetonitrile adsorbs on Pt to give at least two different species, each of which undergoes reduction in different potential regions but to the same reduced species; (c) it is the same adsorbed acetonitrile species which is reduced in the double-layer or H regions but difficulties arise in completion of its reduction after a certain fraction has been reduced. The first explanation is unlikely since oxidation of the reduced acetonitrile species on different Pt sites should give more than one peak (cf. the case of atomic hydrogen oxidation on Pt). The second explanation could involve the two species discussed above, i.e. (i) and (ia). The species (ia) would require reduction in the H region as is in fact the case with associatively adsorbed olefins (4,124, 125). However, it was shown above that orientation (ia) is unlikely because of the similarity in ratios $\Delta q_H : q_t$ for benzonitrile and terephthalonitrile. It was also found that the adsorbed acetonitrile could be easily washed from the surface with 1N H_2SO_4 , a situation which would be unlikely for an associatively adsorbed species at Pt (e.g. ethylene). This leaves the last explanation which is consistent with the experimental observations.

During reduction, the adsorbed acetonitrile must change its shape due to a transformation from the sp linear,

unreduced form to the bent sp^2 imine radical-type structure*. Space-filling models show that the accessibility of the N atom to protons from solution is poor due to the change of configuration from the initially linear sp one to the bent sp^2 structure, thus leading to slowness in reaction 2. The change of configuration with reduction (Fig. 28) of a surface fully covered with acetonitrile introduces steric hinderance in the reduction, especially in the second reaction, and this effect will increase with increasing extent of reduction of the adsorbed species.

When the electrode is brought from 0.8 V, E_H to less positive potentials in either a fast or slow sweep, the reaction initially occurs rapidly (cf. Fig. 16) corresponding to the cathodic d.l. peak which is associated with the $2e$ process (i) \rightarrow (iii) corresponding to Stage I in Fig. 24. With increasing extent of reduction of the ad-layer, however, further reduction by reaction 2 becomes hindered due to the steric limitations described above so that a fraction of the adsorbed acetonitrile molecules remain in state (ii) of reduction corresponding to reaction 1. This gives on reoxidation the (resolved) peak at 0.2 V, E_H in the anodic sweep as

* An imine species such as (iii) would normally be susceptible to hydrolysis. The reduced species is, however, quite stable as indicated by the reversibility and the holding effects discussed above, and the surface nature of the reactions. This stability of the imine probably arises from the fact that (a) it is adsorbed and (b) the double bond is conjugated with the delocalized metal electron system in the surface (cf. the relative stability of aromatic imines in relation to that of aliphatic ones).

shown in Fig. 30b. Time is required to complete the reduction reaction 2, transforming the species of Fig. 28c into that of Fig. 28d; this explains the important observation that the resolved peak at $0.2 \text{ V}, E_{\text{H}}$ on the reoxidation sweep (Fig. 30b) diminishes with time (in the cathodic sweep) allowing the charge for the main d.l. peak to increase, i.e. for $2e$ reoxidation of completely reduced species. Bearing in mind this kinetic limitation, it is reasonable to suppose that the increase of cathodic current which occurs at potentials more negative than $0.3 \text{ V}, E_{\text{H}}^*$, beyond the minimum, is due to preferred reaction with adsorbed H that then appears on the surface with increasing coverage as the potential becomes less positive. As was shown above (p.104), the reoxidation of reduced adsorbed acetonitrile is a much faster process, which is consistent with the above mechanism.

I.4 Involvement of Surface Oxide in Acetonitrile Reactions at Platinum

(a) Introduction

Fig. 7 showed that adsorbed acetonitrile displaces the potential for surface oxide formation at platinum to more positive values and decreases the charge for reduction of the

* As mentioned above, the fact that the increase in current on a cathodic-going sweep begins at $0.3 \text{ V}, E_{\text{H}}$, after a previous trend of decreasing current indicates a reaction with atomic hydrogen in reaction 2 in this region rather than with solution protons, since the coverage with H becomes substantial as the potential becomes $<0.3 \text{ V}, E_{\text{H}}$.

UNIVERSITY LIBRARY

oxide on a following cathodic-going sweep. The oxidation currents observed at potentials more anodic than ca. 1.0 V, E_H , are, however, larger in the presence of added acetonitrile than in the pure, aq. H_2SO_4 electrolyte and this indicates that a reaction of acetonitrile or a species derived therefrom occurs over this potential region at platinum. It was noted above that the inclusion of the surface oxide region in the potentiodynamic programs complicates the interpretation of $q_{c,d.l.}$ and $q_{c,H}$ and this led to the use of programs where the surface oxide region was excluded in measurements of charge (Fig. 25). One interesting aspect of cycling into the surface oxide region in the presence of acetonitrile is that the subsequent anodic-going sweep on the next cycle taken from 0.05 V, E_H remains unchanged, in comparison to that observed in the absence of surface oxide, even at very high concentrations of acetonitrile (>1M) where the effect of the B species (see p. 74) normally becomes significant in the double-layer and H regions. This is to be contrasted (see below) with the great importance of the cathodic region (i.e. for potentials more negative than ca. 0.5 V, E_H) on maintenance of the activity of the platinum electrode at such high $[CH_3CN]$.

(b) Reaction of acetonitrile in the surface oxide region

As mentioned above, acetonitrile gives rise to an anodic reaction in the surface oxide region at Pt, the charge in the anodic-going sweep, q'_{OX} , being larger than

UNIVERSITY LIBRARY

that* for oxide reduction, q'_{red} , as shown in Fig. 31 as a function of $[\text{CH}_3\text{CN}]$. Also shown is the charge, q_{bl} , representing the extent by which surface oxidation would be blocked if the initial displacement of the surface oxide formation potential (in the anodic-going sweep) were the only factor to influence the charge recoverable on reduction in a following cathodic sweep. The fact that q_{bl} corresponds quite closely to $q_{\text{red}}^{\text{O}} - q'_{\text{red}}$ (where $q_{\text{red}}^{\text{O}}$ is the charge for surface oxide reduction in the absence of acetonitrile) indicates, in fact, that most of the oxide charge not recoverable on the cathodic sweep can be accounted for by the q_{bl} charge. This is not unreasonable since it is evident that the complete oxidative desorption of CH_3CN (to form $\text{CO}_2 + \text{H}_2\text{O} + \text{N}_2$) from the surface would require 11e per molecule. Hence the overall reaction charge, $q'_{\text{ox}} - q'_{\text{red}}$, observed in the surface oxide region may correspond to oxidation of a relatively small fraction of the adsorbed acetonitrile from the surface.

The charge for oxidation of adsorbed acetonitrile in the surface oxide region, q_{react} , is shown in Fig. 32 for various $[\text{CH}_3\text{CN}]$. This charge depends on $[\text{CH}_3\text{CN}]$ in a way similar to that for $q_{\text{a,d.l.}}$ (Fig. 13) up to $[\text{CH}_3\text{CN}] = 2 \times 10^{-3}$ M. Only the initial increase in reaction charge, q_{react} , at low $[\text{CH}_3\text{CN}]$ is due to diffusion control (cf. Fig. 14) while at

* Corresponding quantities q_{ox}^{O} and $q_{\text{red}}^{\text{O}}$ refer to the surface oxide formation and reduction charges in the absence of acetonitrile (see p. 4).

Journal of Electroanalytical Chemistry and Applied Electrochemistry

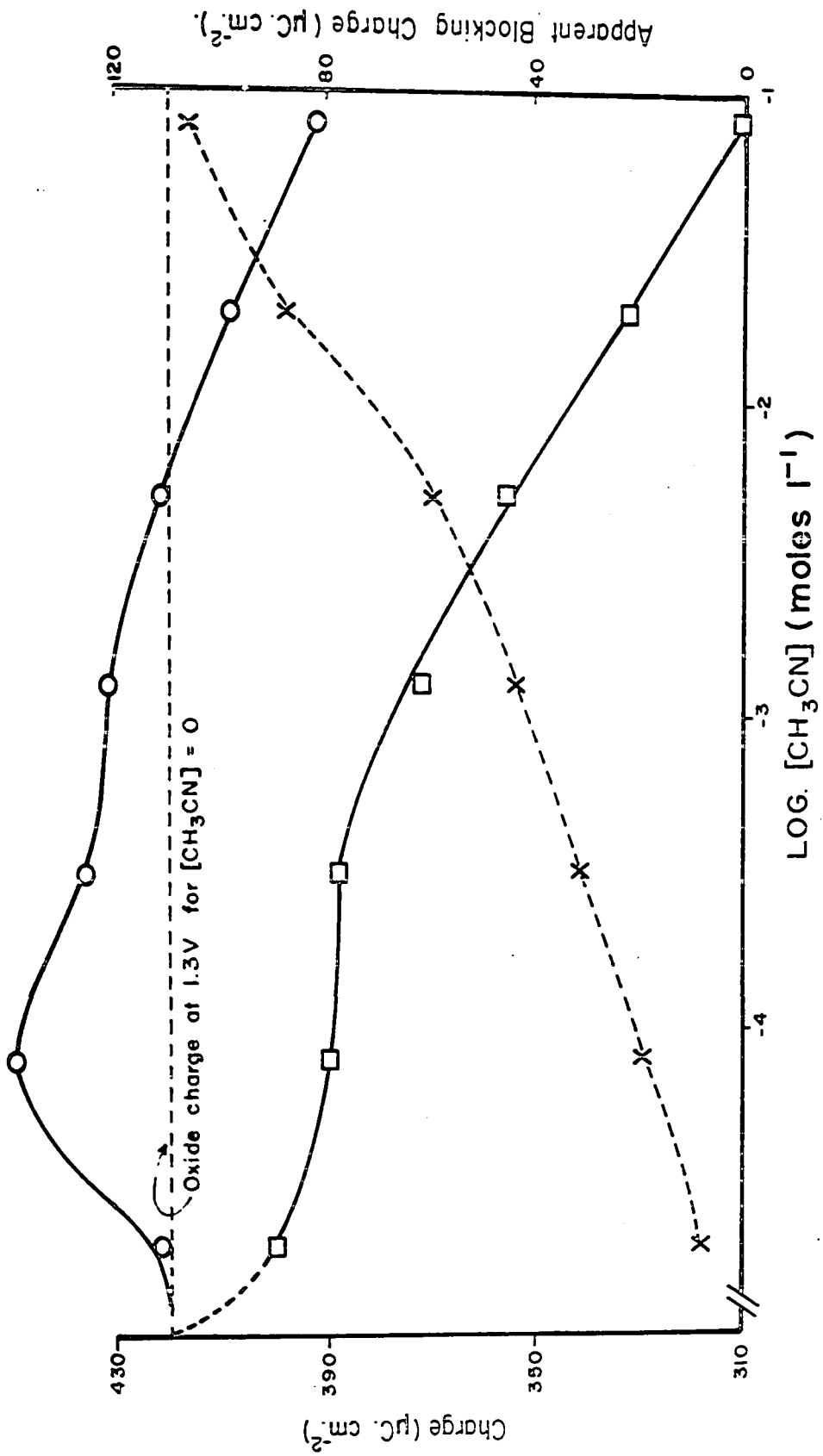


Fig. 31. Anodic (o) and cathodic (□) charges in the surface oxide region at Pt as a function of CH_3CN concentration, together with the apparent charge (X) for blocking of oxide formation. Difference between (o) and (□) points give q_{react} . of Fig. 32. $(dV/dt) = 50 \text{ mV sec}^{-1}$; potential range 0.05 to 1.3 V, E_H.

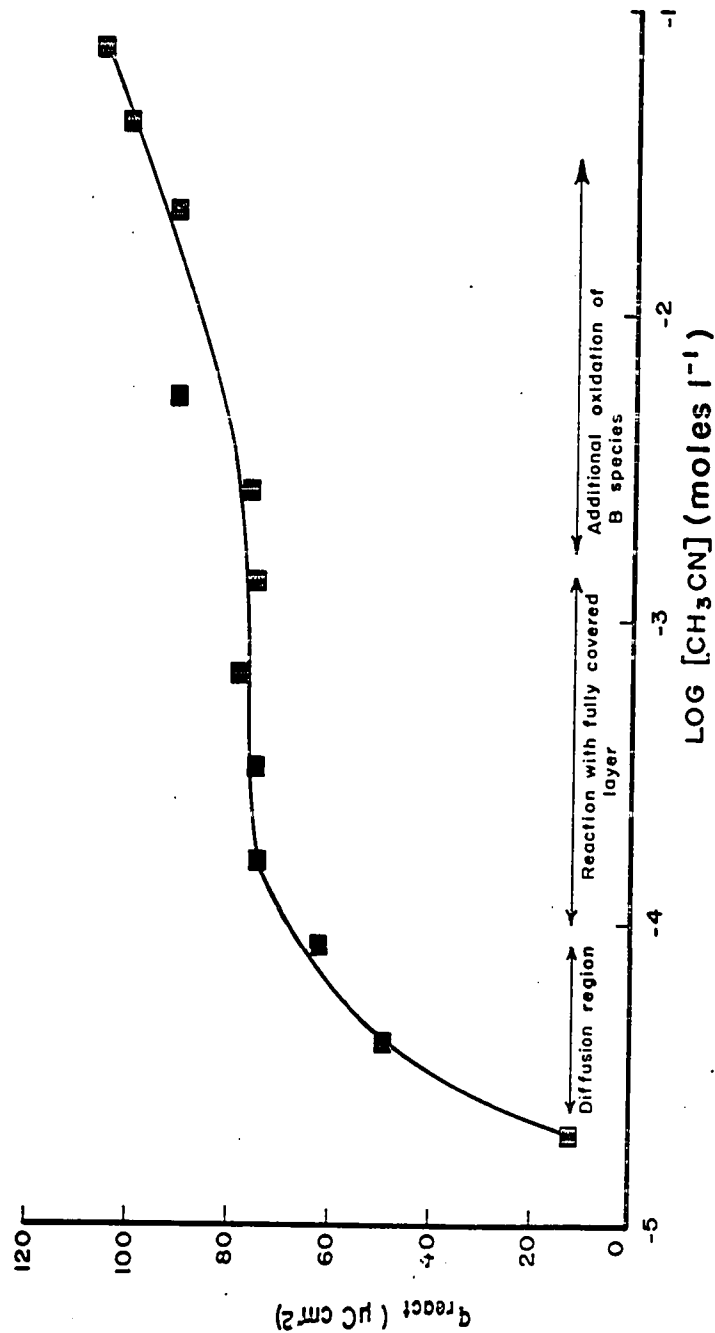


Fig. 32. Reaction charges q_{react} for oxidation of adsorbed CH_3CN species over the surface oxide region at Pt determined from the difference of anodic and cathodic oxide charges measured in this region (from Fig. 31) for various CH_3CN concentrations. $(dV/dt) = 50 \text{ mV sec}^{-1}$, potential range 0.05 to 1.3 V, E_H .

$[\text{CH}_3\text{CN}]$ above 3×10^{-4} M the reaction becomes a true surface process, independent of solution concentration and stirring. When $[\text{CH}_3\text{CN}] > 2 \times 10^{-3}$ M, the effects of the B species become significant as was indicated in Fig. 13 by the decrease of the reoxidation charge in the double-layer with increasing $[\text{CH}_3\text{CN}]$; Fig. 32 thus shows that the B species reacts in the Pt surface oxide region since q_{react} increases when $[\text{CH}_3\text{CN}] > 2 \times 10^{-3}$ M. This result can be seen in a qualitative way in Fig. 7 which shows the potentiodynamic i - V profiles at various acetonitrile concentrations. With increasing $[\text{CH}_3\text{CN}]$ up to ca. 2×10^{-3} M, an oxidation peak is observed in the potential region of initial oxide formation, i.e. ca. 1.0 V, E_{H} . At higher acetonitrile concentrations, this reaction peak diminishes but another develops and increases at higher anodic potentials, >ca. 1.25 V, E_{H} and it may be concluded that this latter peak is associated with a reaction of the B species.

A charge imbalance between the anodic and cathodic multisweeps only arises when the termination potential in the anodic sweep is >1.1 V, E_{H} . When $[\text{CH}_3\text{CN}] = 3 \times 10^{-3}$ M, the imbalance is approximately 5% of the total charge* at 1.2 V, E_{H} and 15% of the total charge at 1.5 V, E_{H} . Thus only a small quantity of acetonitrile is oxidatively desorbed from the surface in the anodic sweep, this being in agreement with the reaction charges cited above and the requirement of 11e for

* Note that the total charge referred to here is the sum of all charges (except that for d.l. charging) passed between 0.05 V, E_{H} and the anodic termination potentials.

the complete oxidation of CH_3CN . The desorbed acetonitrile must be replaced on the next cathodic sweep since the coverage with acetonitrile, as measured in the d.l. region, is not altered by extending the range of the potential sweep into the oxide region (see p.117). Any readsorption which occurs is a very rapid process since the reduction peak for acetonitrile in the double-layer region is not controlled by diffusion when $[\text{CH}_3\text{CN}] > \text{ca. } 3 \times 10^{-4} \text{ M}$. At intermediate acetonitrile concentrations, e.g. $3 \times 10^{-3} \text{ M}$, oxidation of the platinum surface to potentials as high as $1.8 \text{ V, } E_{\text{H}}$ still leaves a significant coverage of acetonitrile on the surface as indicated by the decrease of the charge for oxide reduction by about 20% of the q_{red}° value in a following cathodic sweep. This means that acetonitrile behaves differently from hydrocarbons (e.g. C_2H_4 , C_2H_6) examined, e.g. by Gilman (126), where oxidation of the electrode to high anodic potentials (e.g. $1.7 \text{ V, } E_{\text{H}}$) resulted in coincidence of the anodic current profiles and identity of the cathodic surface oxide reduction i - V profiles with and without the presence of hydrocarbon. Although a fraction of the adsorbed acetonitrile may be oxidized from the surface at high anodic potentials, a situation cannot be reached where all the acetonitrile is oxidatively desorbed from the electrode surface. At $[\text{CH}_3\text{CN}] = 1\text{M}$, the potential can be taken to $2.6 \text{ V, } E_{\text{H}}$, since the adsorbed acetonitrile inhibits the oxygen evolution reaction at this concentration, with desorption of only a small fraction of the acetonitrile from the surface.

The following evidence indicates that the reaction of acetonitrile in the oxide region is not simply another stage of oxidation of adsorbed acetonitrile, previously reduced in a cathodic-going sweep: (a) addition of acetonitrile at $V_{\text{ads}} = 0.75 \text{ V, } E_{\text{H}}$, (i.e. at a potential where adsorption is not followed by reduction) still results in a net oxidation reaction when the potential is subsequently swept through the oxide region, and (b) the acetonitrile reduction and reoxidation charges between 0.825 and 0.06 $\text{V, } E_{\text{H}}$ balance to within 5%. It is very unlikely that the reaction in the oxide region is associated with oxidation of molecular CH_3CN arriving from the solution since the reaction charge is independent of solution stirring at $[\text{CH}_3\text{CN}] > \text{ca. } 3 \times 10^{-4} \text{ M}$. Also, when acetonitrile was added to the electrolyte solution with the Pt electrode potentiostated to 1.4 $\text{V, } E_{\text{H}}$ in pure, aq. H_2SO_4 , no transient reaction current was observed, indicating that acetonitrile in the solution does not react on a Pt surface covered by a layer of oxide. It can be further concluded that acetonitrile does not adsorb at 1.4 $\text{V, } E_{\text{H}}$ since the following cathodic sweep gave $q'_{\text{red}} = q^0_{\text{red}}$; hence, the absence of reaction on the fully oxidized Pt surface probably arises because acetonitrile is unable to adsorb under these conditions.

The reaction of adsorbed acetonitrile in the region of Pt surface oxidation between 0.95 and 1.3 $\text{V, } E_{\text{H}}$ is slow and the reaction charge is found to increase at slower sweep rates (Fig. 33). However, as was demonstrated above, this slowness

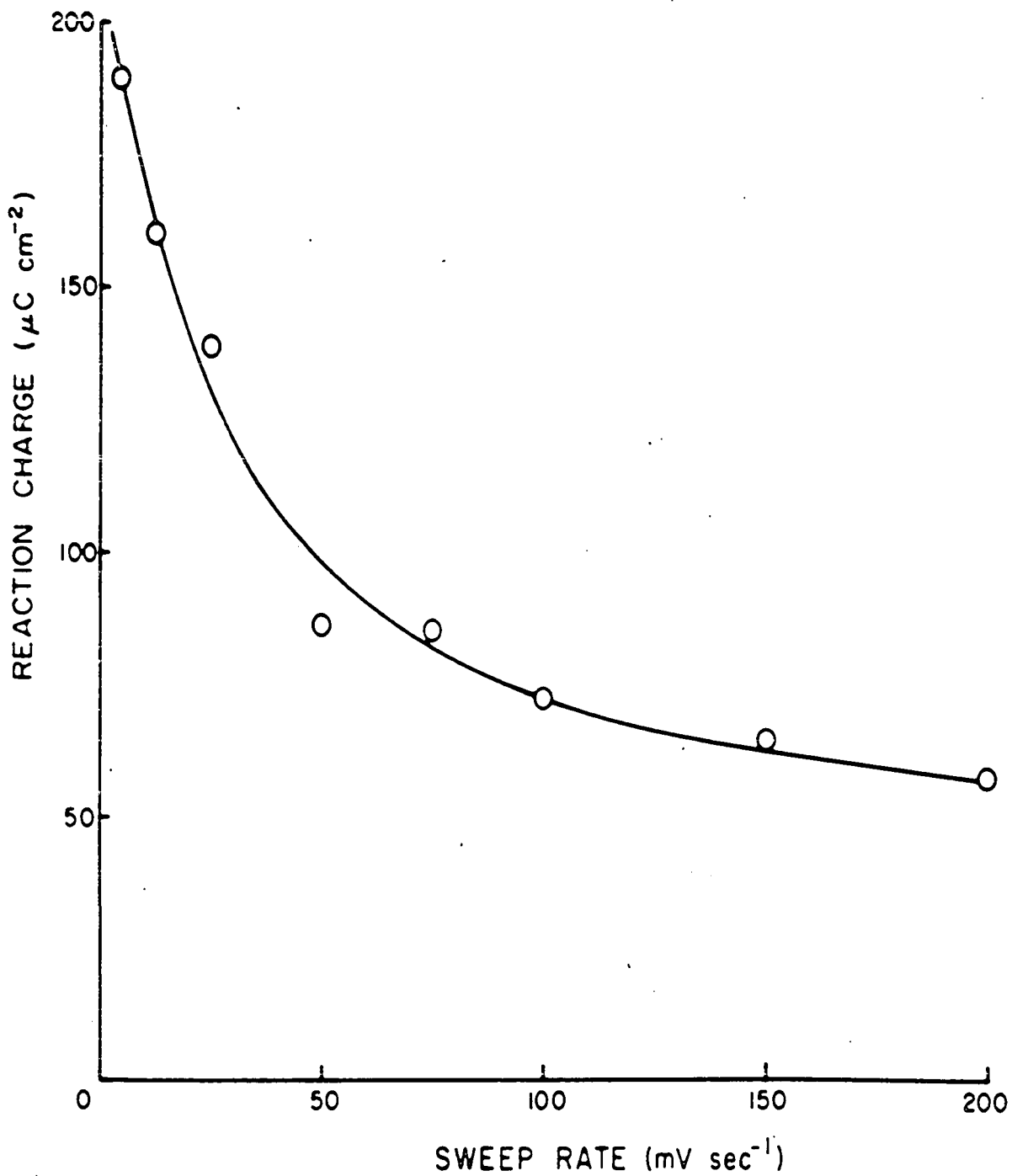


Fig. 33. Dependence of acetonitrile reaction charge in oxide region, q_{react} , on sweep rate. $[\text{CH}_3\text{CN}] = 5 \times 10^{-3}\text{M}$, potential range 0.05 to 1.3 V, E_{H} .

in the oxidation reaction is not due to diffusion control. At very fast sweep rates ($>10 \text{ V sec}^{-1}$) and correspondingly higher $[\text{CH}_3\text{CN}]$ to avoid diffusion effects, the charge for oxide reduction decreases significantly with increasing sweep rate (cf. the normal behavior where q_{red}° is more or less independent of sweep rate). This effect is directly opposite to that which would have been expected had diffusion of acetonitrile from solution been the controlling factor. The formation of platinum surface oxide at high concentrations of acetonitrile is thus a slower process than is observed in the pure, aq. H_2SO_4 alone because the oxidation reaction creating free surface sites is quite slow. Although this effect of decreasing q'_{red} with increasing sweep rate is observed both with and without inclusion of the H region in the potentiodynamic sweep, it is much more pronounced under the latter conditions (see below, p.120).

In addition to some oxidative desorption of acetonitrile species at potentials $>1.1 \text{ V}, E_{\text{H}}$, the potential region of Pt surface oxide formation also gives rise to an oxidation of adsorbed acetonitrile to produce a species which remains on the surface, and becomes reduced over both the d.l. and H regions of the following cathodic sweep (Fig. 34). However, the next sweep in the anodic direction is identical with that observed if only the potential range 0.75 to $0.05 \text{ V}, E_{\text{H}}$ had been traversed. This means that the oxidation and reduction processes which adsorbed acetonitrile undergoes on traversal

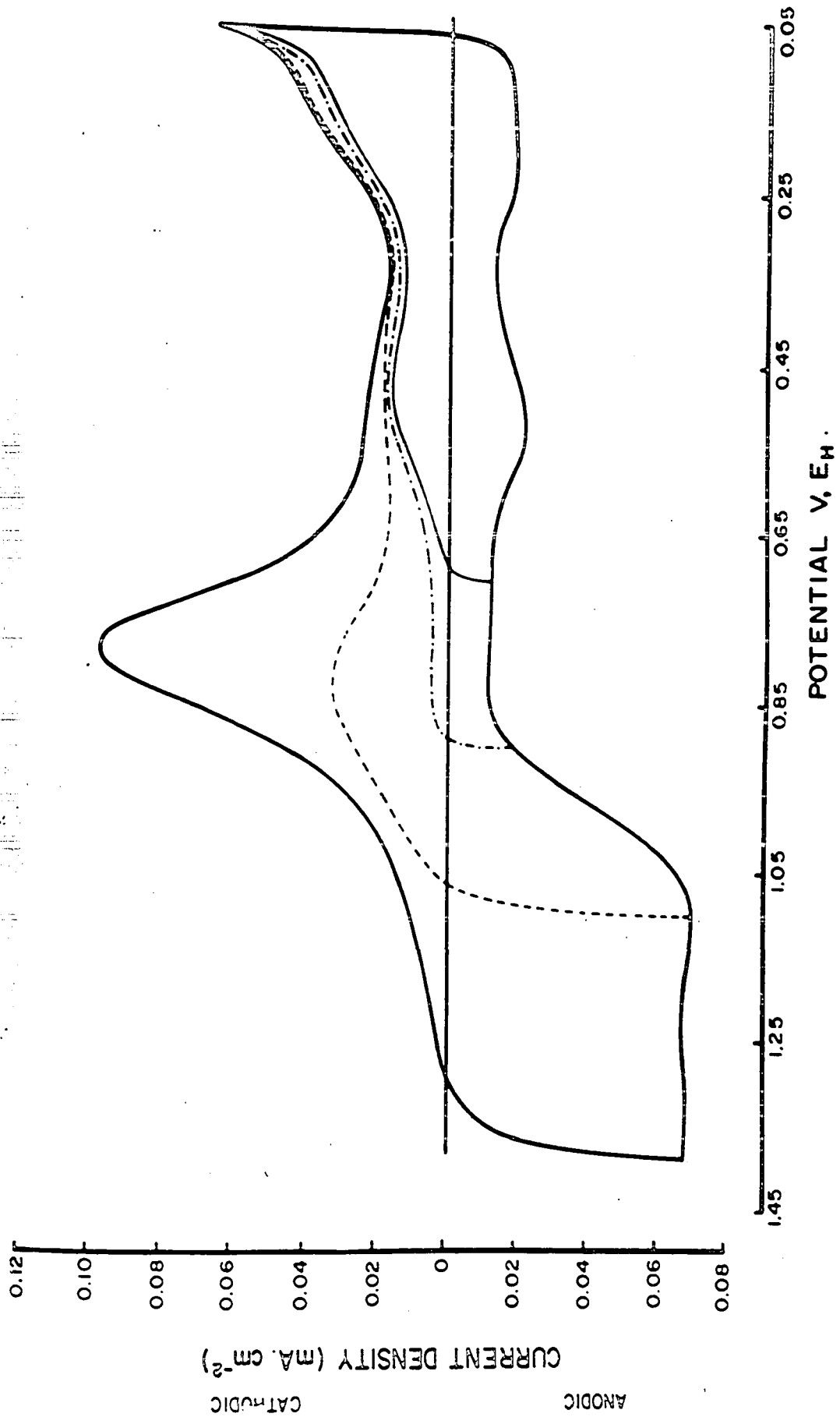


Fig. 34. Effect of different anodic termination potentials on the cathodic and anodic going i-V profile for acetonitrile at Pt in 1N H₂SO₄. [CH₃CN] = 5 x 10⁻³M, $dv/dt = 50 \text{ mV sec}^{-1}$.

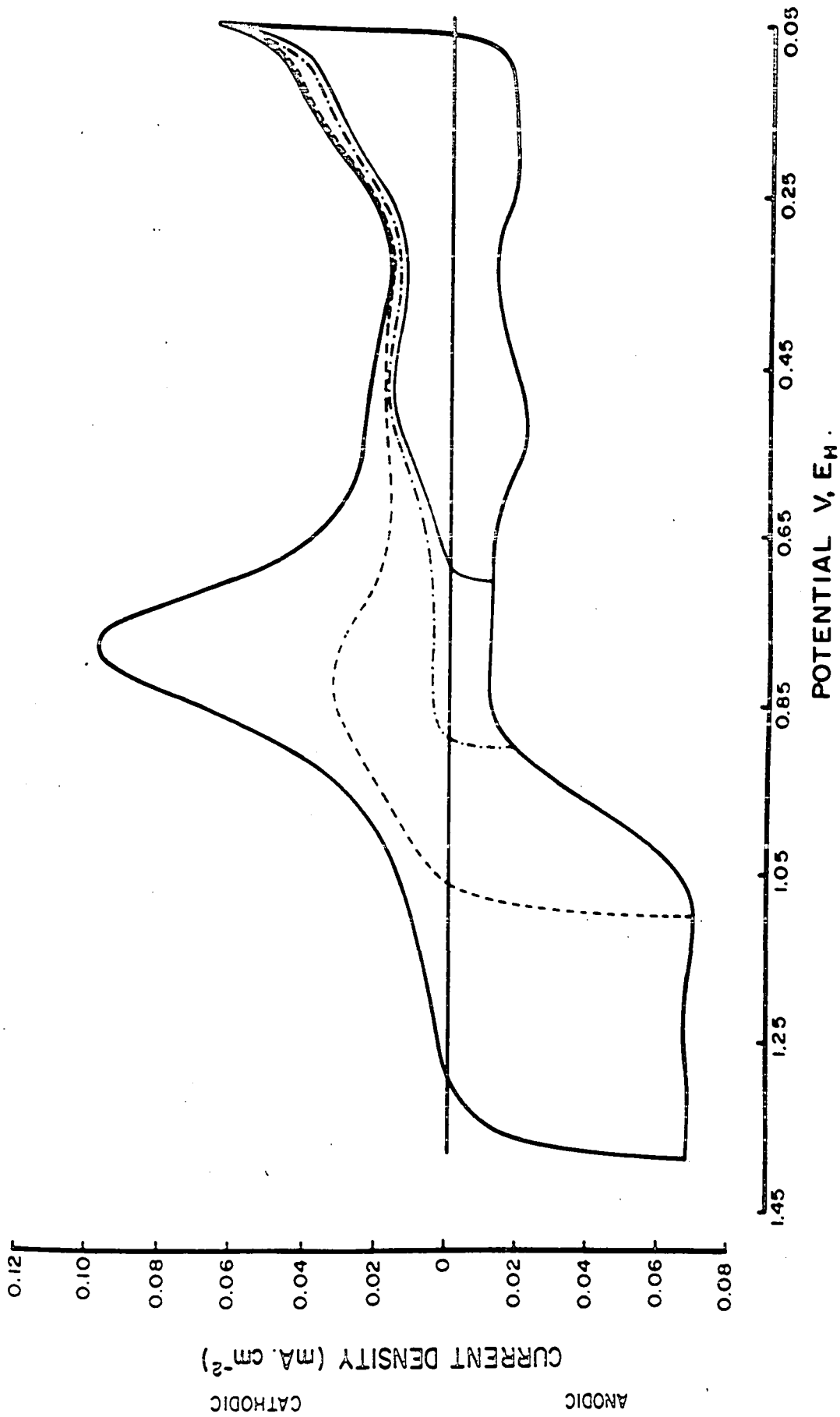


Fig. 34. Effect of different anodic termination potentials on the cathodic and anodic going i-V profile for acetonitrile at Pt in 1N H₂SO₄. [CH₃CN] = 5 x 10⁻³M, dV/dt = 50 mV sec⁻¹.

of the oxide potential region at Pt involves a center in the molecule that is not irreversibly changed by these processes. It was this oxidation reaction followed by the reduction on the subsequent cathodic-going sweep that prompted the use of the potentiodynamic program of Fig. 25 for obtaining values of $q_{c,d.l.}$ and $q_{c,H}$. An important aspect of this acetonitrile oxidation in the oxide region is that the resulting additional reduction charge which passes when the potential is returned to the cathodic H region (i.e. in the region where $q_{c,H}$ is measured) reaches its maximum value when the potential is reversed at 1.15 V, E_H in the anodic-going sweep. As seen in Fig. 34, there are no further changes in $q_{c,H}$ even after an anodic termination potential of 1.40 V, E_H . This could mean that either this oxidation reaction* in the oxide region is not, in fact, associated with surface oxide formation (an unlikely possibility) or that the reaction only occurs with the initially formed surface oxide. If the second possibility is correct, the acetonitrile species resulting from the oxidation reaction could be an adsorbed nitrilium oxide $CH_3CN^+ \rightarrow \bar{O}$ which would be both stable and susceptible to reduction back to adsorbed CH_3CN .

* It should be noted that the oxidation referred to here is not that observed at higher anodic potentials (>ca. 1.1 V, E_H) which gives rise to the charge imbalance.

(c) Relation between the behavior of adsorbed CH_3CN
in the surface oxide region and that in the H region

With increasing sweep rate and/or concentration of acetonitrile, the effects of the B species discussed above (p. 74) become more prominent and cathodic holding at 0.05 V, E_H results in a substantial increase of the surface oxide reduction peak (Fig. 35). In addition, the charge associated with reduction of adsorbed acetonitrile in the double-layer region, $q_{c,d.l.}$, also increases with cathodic holding (Fig. 35). This last observation, along with the absence of any such activation effect with cathodic holding at 0.05 V, E_H at low concentrations of acetonitrile ($< 5 \times 10^{-3}$ M) and slow speeds (e.g. 50 mV sec^{-1}), indicates that the activation effect in Fig. 35 resulting from cathodic holding is due to a transformation of the B species rather than to ordinary reactive adsorbed acetonitrile. This transformation is probably brought about by reduction of the B species into a form which can be oxidized from the surface in the next anodic sweep. The fraction of the surface which was previously occupied by B species is thus made available for oxygen electroadsorption and reactive acetonitrile species, until the B species is formed again on the surface (see below).

The observation of a cathodic holding effect at 0.05 V, E_H on q'_{red} for fast sweep rates, together with the sweep rate dependence of q'_{red} discussed above, shows that an important factor in the activity of the Pt surface in acetonitrile solutions towards ordinary oxidation at fast sweep

VANUFR LPPPPPP

rates is the time spent in the H region of the sweep. The behavior of the Pt surface with respect to this factor was next investigated under conditions where the H region was excluded in the sweep. Fig. 35 shows the rather surprising result that in 1M CH₃CN the surface is completely inactive, even with regard to the normal acetonitrile reactions, when the H region is excluded in a sweep at 10 V sec⁻¹. One possibility is that this deactivation effect results from the accumulation of surface oxide which requires potentials more cathodic than 0.4 V, E_H for its reduction at such rapid sweep rates in acetonitrile solutions. Fig. 36b shows that this is not really the case since anodic holding at 1.3 V, E_H reactivates the surface for the ordinary reactions by oxidation of the poisoning species, as indicated by the significant increase in q'_{red} on the following cathodic sweep. Since a reactivation effect can also be achieved by cathodic holding at 0.4 V, E_H (Fig. 36a), the presence of adsorbed H atoms* on the surface is not essential for the cathodic holding effect to manifest itself. This may indicate that the cathodic reaction of reduction of B species is a slow, potential dependent reaction which is not influenced by hydrogen coverage. It can, however, be similar to the situation described above (p.98) for reduction of adsorbed (reactive) acetonitrile where, although the reaction can proceed without

* Compare this result with that shown in Fig. 26 and discussed on p.98.

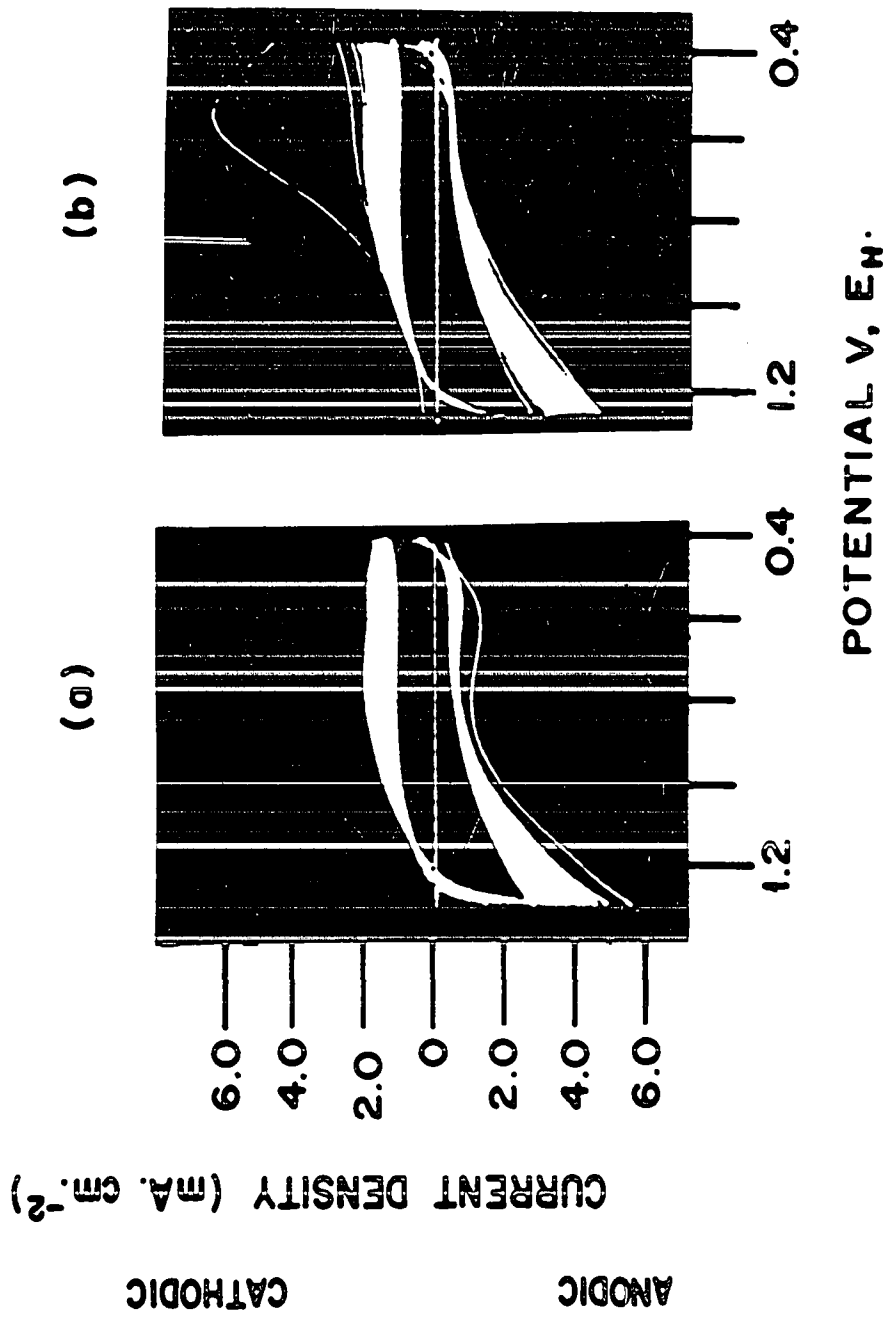


Fig. 36. (a) Effect of cathodic holding for 90 sec at 0.4 V, E_H on the i-V profile of 1M CH₃CN at Pt in 1N H₂SO₄ at dV/dt = 10 V sec⁻¹. Potential range 0.4 to 1.3 V, E_H.

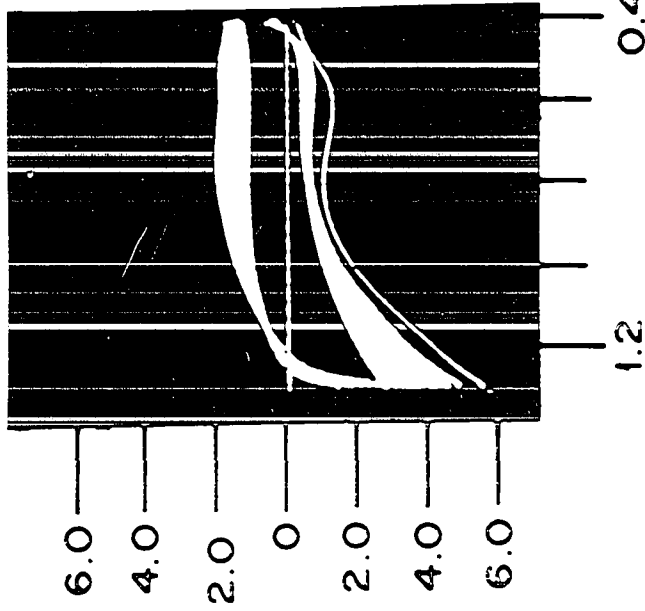
(b) As in (a) but with 90 sec anodic holding at 1.3 V, E_H.

CURRENT DENSITY (mA. cm.⁻²)

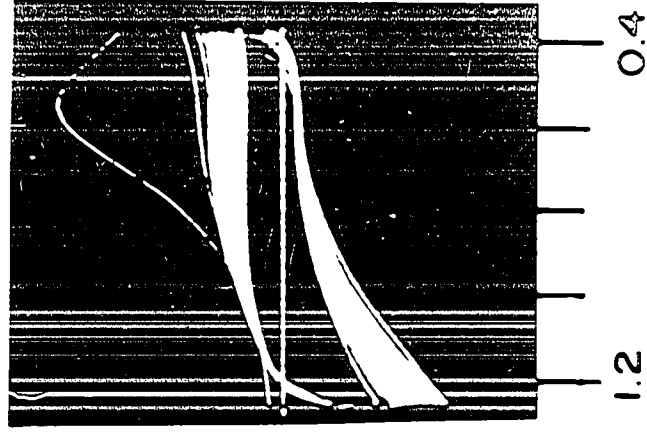
CATHODIC

ANODIC

(a)



(b)



POTENTIAL V, E_H

the participation of adsorbed H, the reaction is greatly facilitated by the presence of H on the surface (reaction 12).

It is seen from both the anodic and cathodic holding effects (Fig. 36) that a rather long period of time (in terms of number of cycles) is required for re-establishment of the multisweep conditions after holding, i.e. a significant time is required for the poisoning species, B, to become formed again on the electrode surface. In the light of this observation, the above experiment was also performed without solution stirring and the time required for complete surface deactivation was almost identical with that observed with solution stirring. Indeed, when the i-V profiles at slower sweep speeds (e.g. 50 mV sec⁻¹) in concentrated acetonitrile solutions (>1M) are analyzed with and without solution stirring, no differences are observed. These facts indicate that the reaction giving rise to formation of the B species is not limited by solution diffusion and is probably a slow (perhaps chemical) reaction at the electrode surface.

The independence of the current peaks in the anodic-going sweep between 0.05 and 0.75 V, E_H upon extension of the sweep into the surface oxide region was discussed above for low acetonitrile concentrations and slow sweep rates. The same results are obtained when $[CH_3CN] = 1M$ and $(dV/dt) = 10 V sec^{-1}$, i.e. in this case also the anodic peaks are independent of cycling into the oxide region. This is to be

VA007R 11P000V

contrasted with the results in Fig. 35 showing the effect of cycling with and without the H region included in the i - V profile. It becomes immediately evident that whereas the H region plays a very important role in the reactions of acetonitrile at platinum, the surface oxide region plays no equivalent role except with regard to removal of ordinary impurities which may somewhat affect the activity of the electrode.*

The behavior of the peak current for Pt surface oxide reduction in the presence and absence of the H region, i.e. in the potential ranges 0.05 to 1.3 V, E_H and 0.4 to 1.3 V, E_H , respectively, for various $[CH_3CN]$ is shown in Fig. 37. Also shown are the effects of 90 sec holding at the cathodic termination potential on the oxide reduction peak current. Although this experiment was performed at a slower sweep rate (50 mV sec^{-1}) than those employed above ($>10 \text{ V sec}^{-1}$), the same observations and hence conclusions result. It is seen that the oxide reduction peak current decreases with increasing $[CH_3CN]$ at a more rapid rate if the H region is excluded in the sweep. Whereas cathodic holding increases i_p for oxide reduction for both sweep ranges (i.e. with the H region included or excluded), the effect is much more pronounced at higher $[CH_3CN]$ if the sweep range is 0.4 to 1.3 V, E_H because of exclusion of the H-region. It is to be noted that although

* Ordinary accumulation of impurities affects the anodic current peak after 10 min of cycling in the absence of formation of Pt surface oxide up to potentials $>1.1 \text{ V}$.

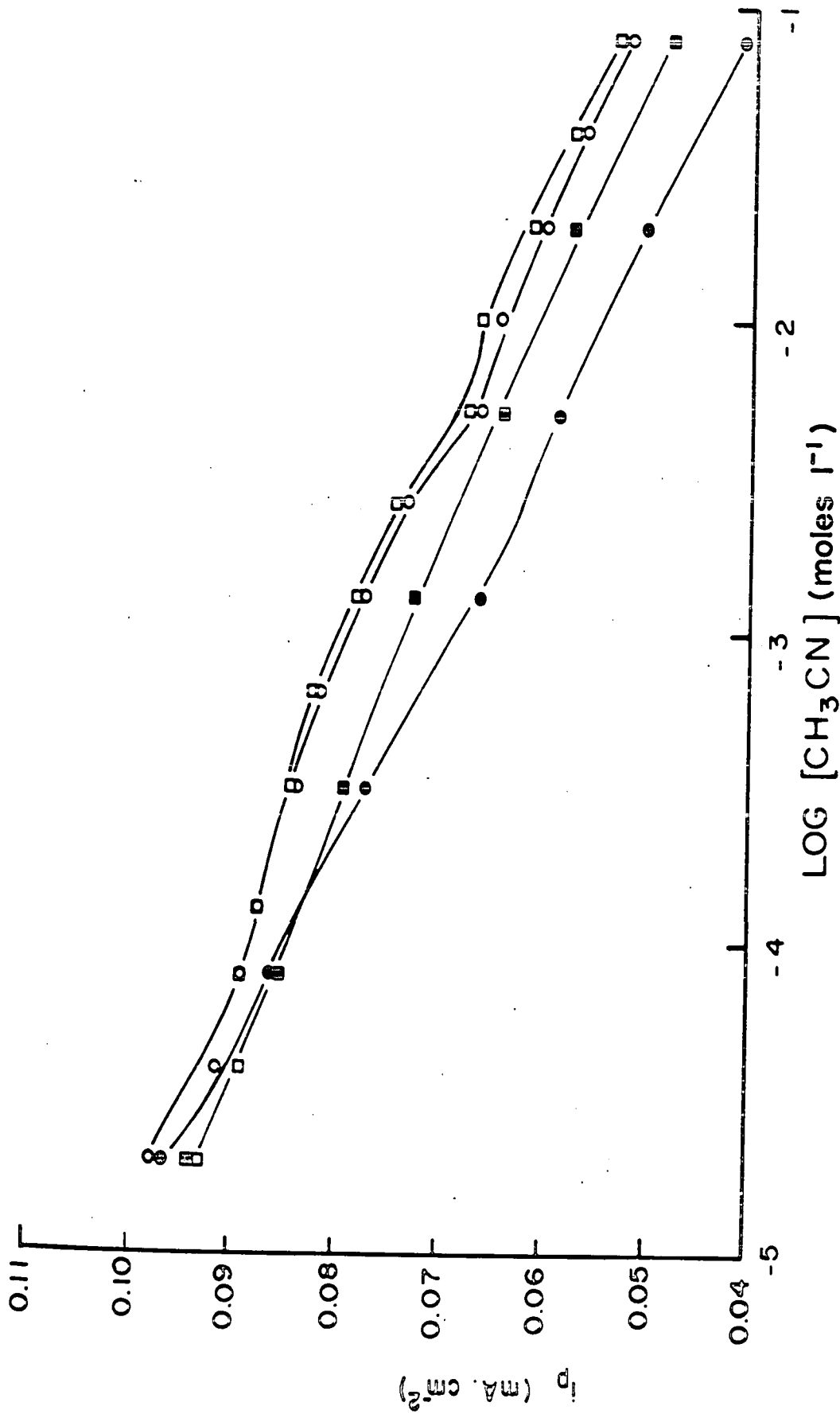


Fig. 37. Dependence of peak current for oxide reduction on $[\text{CH}_3\text{CN}]$ for potential range 0.05 to 1.3 V, E_H with (□) and without (O) 90 sec cathodic holding and for potential range 0.4 to 1.3 V, E_H with (■) and without (●) cathodic holding. ($dv/dt = 50 \text{ mV sec}^{-1}$).

cathodic holding at $0.4 \text{ V}, E_{\text{H}}$ results in an increase of (i_{p}) for oxide reduction, the peak current is not as large as that attained by cycling to $0.05 \text{ V}, E_{\text{H}}$. This fact again illustrates the special significance of the potential region of hydrogen adsorption on the activation of the Pt surface when acetonitrile is present at higher concentrations.

(d) Identity and characteristics of the B species

The results in Figs. 13, 14, 35, 36 and 37 showed that both platinum surface oxidation and the ordinary reactions of adsorbed acetonitrile (Figs. 7, 11 and 17) become inhibited at higher concentrations of acetonitrile. This effect was ascribed to a second type of surface species, referred to as B, different from the reactive adsorbed acetonitrile which predominates at lower $[\text{CH}_3\text{CN}]$ (Fig. 7).

The effect of the B species increased with increasing $[\text{CH}_3\text{CN}]$ (Figs. 13 and 14) and resulted in a steady decrease of $q_{\text{a,d.l.}}$ at $[\text{CH}_3\text{CN}] > \text{ca. } 6 \times 10^{-3} \text{ M}$. At high $[\text{CH}_3\text{CN}]$ and rapid sweep rates, the effect of the B species becomes more pronounced, especially when the potential range is restricted so as to exclude the atomic hydrogen region (Figs. 35 and 36). The B species can be removed from the surface only by a very slow oxidation reaction at potentials $> \text{ca. } 1.1 \text{ V}, E_{\text{H}}$ (Fig. 36b) or it can be first reduced in the potential region ca. 0.4 to $0.05 \text{ V}, E_{\text{H}}$ and then burned more readily from the surface in the oxide region (Fig. 36a). Desorption of the B species

results mainly from reactions in the H region, the oxide region having little effect on the coverage by B species except after long periods of holding at high anodic potential. After oxidative desorption from the surface, the B species requires time for its reappearance on the surface; however, the reaction is not controlled in any way by solution diffusion.

Two of the experimental facts mentioned above appear to contradict each other, i.e. the amount of B species on the surface, as determined by its effect on $q_{a,d.l.}$, increases with increasing $[CH_3CN]$, however, the reaction is not influenced by diffusion from the solution. Actually, $q_{a,d.l.}$ decreases very slowly with increasing $[CH_3CN]$ (Fig. 13) and it is unlikely that solution stirring at a particular $[CH_3CN]$ can achieve the same effect as significantly increasing the $[CH_3CN]$, e.g. by a factor of 10.

A number of possibilities exist for the identity of the B species:

- (i) that B results from polymerization of adsorbed acetonitrile. It is known (127) that the dimerization of acetonitrile is catalyzed by the presence of an electron acceptor, such as a Lewis acid, and the platinum electrode could act in the same way at positive potentials. The dimeric product would be β -amino crotonitrile (128) and when this substance is added to a 5×10^{-3} M CH_3CN system, the currents for

MANIP. 11/2/64

acetonitrile reaction in the double-layer region do diminish; however, this decrease in current is dependent on solution stirring, i.e. the inhibiting reaction is diffusion controlled. There are no elements of diffusion control in the pure acetonitrile system even at $[\text{CH}_3\text{CN}] = 5 \text{ M}$ and this fact negates the possibility of a dimer in solution. However, there is still the possibility that the dimer is formed on the surface but is not desorbed as such into the solution. Trimer formation gives rise to a pyrimidine ring structure (127) but the conditions required for this reaction are elevated temperatures ($>250^\circ\text{C}$) at high pressures (30 atm) in the presence of catalysts (e.g. $\text{TiCl}_4 + \text{ZnCl}_2$). A major argument against any polymerization of the acetonitrile is the fact that the potentiodynamic i-V profile for Pt in strong CH_3CN solutions is reproducible within one complete cycle, e.g. ca. 45 sec at 50 mV sec^{-1} over a normal potential range. This is to be contrasted with the case of HCN addition where polymerization results in the i-V profile continuously changing even after 30 min of cycling.

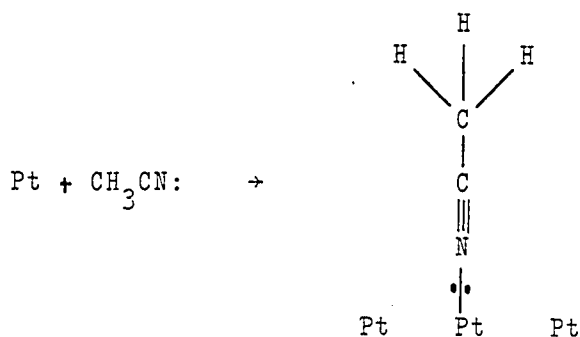
- (ii) that B is a product of a side reaction of acetonitrile and may be acetamide, acetic acid or ethylamine. However, (see p. 71), all of these compounds were examined and none gave behavior similar to that of

the B species. Hence, the B species is not a simple product of hydrolysis or reduction of acetonitrile.

- (iii) that B is associatively adsorbed acetonitrile, i.e. (ia) (see p.101). If this species behaved in a manner similar to that of associatively adsorbed ethylene, it could be reduced with adsorbed H, and this would explain the activating effect associated with the H region at high $[\text{CH}_3\text{CN}]$. Cathodic holding could convert (ia) into reduced acetonitrile, i.e. (ii) or (iii), and in this way the surface would become activated.

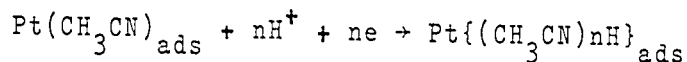
(e) Summary of the behavior of acetonitrile at platinum in aq. H_2SO_4

- (i) In the potential range 0.8 to 0.05 V, E_{H} , acetonitrile adsorbs on Pt from aq. H_2SO_4 solution without charge transfer as follows:



- (ii) This adsorption may be followed by reduction of the CN group if the electrode potential is less positive than ca. 0.60 V, E_{H} , the extent of reduction depending on potential.

- (iii) Reduction is the primary reaction of adsorbed acetonitrile and it occurs with the uptake of solution protons:

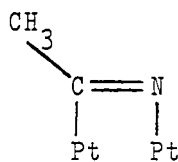


Oxidation below ca. 1.1 V, E_{H} can only occur if the adsorbed acetonitrile is in a reduced state.

- (iv) The resulting reduction-oxidation reactions are surface processes (above $[\text{CH}_3\text{CN}] = 3 \times 10^{-4}$ M) which are relatively reversible, especially at slower sweep rates where time effects are not so important.
- (v) The reduction of adsorbed acetonitrile extends, however, into the H region at platinum because of the changing geometry of acetonitrile upon reduction. This leads to substantial time effects for the acetonitrile reduction reaction. At low extents of reduction of adsorbed acetonitrile, i.e. in the double-layer potential region, reduction of the CN group to the corresponding imine occurs, while at higher extent of reduction of the acetonitrile, completion of the reduction is more difficult to achieve. The fact that completion of the reduction tends to occur in the H region may indicate the participation of adsorbed H in that reaction.
- (vi) Although reoxidation of reduced acetonitrile on the anodic-going sweep occurs mainly in the double-layer

region, an oxidation component also arises in the H region and necessitates the use of different potentiodynamic programs to separate the H and acetonitrile oxidation charges. The kinetic relaxation technique developed enabled the true acetonitrile reaction components to be determined.

- (vii) Adsorbed acetonitrile oxidizes slowly over the Pt surface oxide region but cannot be completely oxidized from the surface, even at 1.8 V, E_H . Acetonitrile from the solution does not react on a surface fully covered with oxide since the nitrile group cannot adsorb.
- (viii) At higher concentrations of acetonitrile, another species is formed on the electrode surface and decreases the extent of coverage by reactive adsorbed acetonitrile. This species is called B and its presence and subsequent inhibiting effects are strongly dependent on treatment of the electrode in the H region. For very rapid sweep rates and high $[CH_3CN]$, exclusion of the H region in a potentiodynamic sweep can result in complete deactivation of the platinum surface. The most probable identity of the B species is associatively adsorbed acetonitrile, i.e.



(ix) Although inclusion of the H region in a sweep has a very important influence on both the extent of reduction of adsorbed acetonitrile and the B species, the surface oxide region has no effect on q_a and $q_{a,H}$, even at high $[CH_3CN]$ and very fast sweep rates.

PART II

Anodic Displacement of Adsorbed Hydrogen in Electrochemi-
sorption of Organic Molecules at Platinum

(a) Introduction

In the double-layer potential region at platinum, potentiostatic adsorption of acetonitrile gives rise to a cathodic electrosorption transient (see p. 79 and Fig. 19). The charge, q_t , for this process can be evaluated by integration of the current-time transient and can give the coverage with reduced acetonitrile at the potential of adsorption. In the H region at less positive potentials, adsorption of acetonitrile gave rise to the new electrochemical H displacement effect (see p. 81 and refs. 117,119) in the form of an anodic transient (Fig. 20b). This effect is observed with a number of other organic molecules (e.g. benzonitrile, benzene, thiourea, dimethylsulfide) when adsorption occurs at a platinum electrode surface which is either partially or fully covered by adsorbed atomic hydrogen, i.e. when the platinum electrode is maintained at a potential more cathodic than $0.35 \text{ V}, E_H$ in aqueous solution.

The anodic transient is associated with the electrochemical displacement of previously adsorbed atomic hydrogen and the transient charge, q_t , can be correlated with the amount of hydrogen displaced by the organic substance. This latter quantity is obtained by initiating an anodic-going

RESEARCH LIBRARY

A

sweep through the hydrogen region and measuring the quantity of hydrogen which remains on the surface after the adsorption process is complete. The origin of the anodic H displacement effect and its relation to the dissociative chemisorption of organic molecules will now be discussed.

(b) Chemisorption of sulfur compounds with anodic hydrogen displacement

Sulfur compounds provided the most clear-cut example of the new effect because of the absence of any side reactions of these substances at the platinum electrode. Addition of thiourea to a solution in which a platinum electrode is held potentiostatically in the hydrogen adsorption region produces an anodic current-time transient as shown in Fig. 38. All additives were injected into the solution to give final concentrations of 3×10^{-3} M, because at this concentration their effect in blocking hydrogen adsorption had reached saturation limits in a single sweep (Fig. 6). Although several cyclic potential sweeps were required for adsorption saturation to be reached in the case of dimethylsulphide, this was associated with slow electrochemical adsorption rather than diffusion and hence solution concentration.

The displacement effect is seen to increase as the potential at which the additive is injected into the solution is made progressively less positive (Fig. 39), i.e. as the

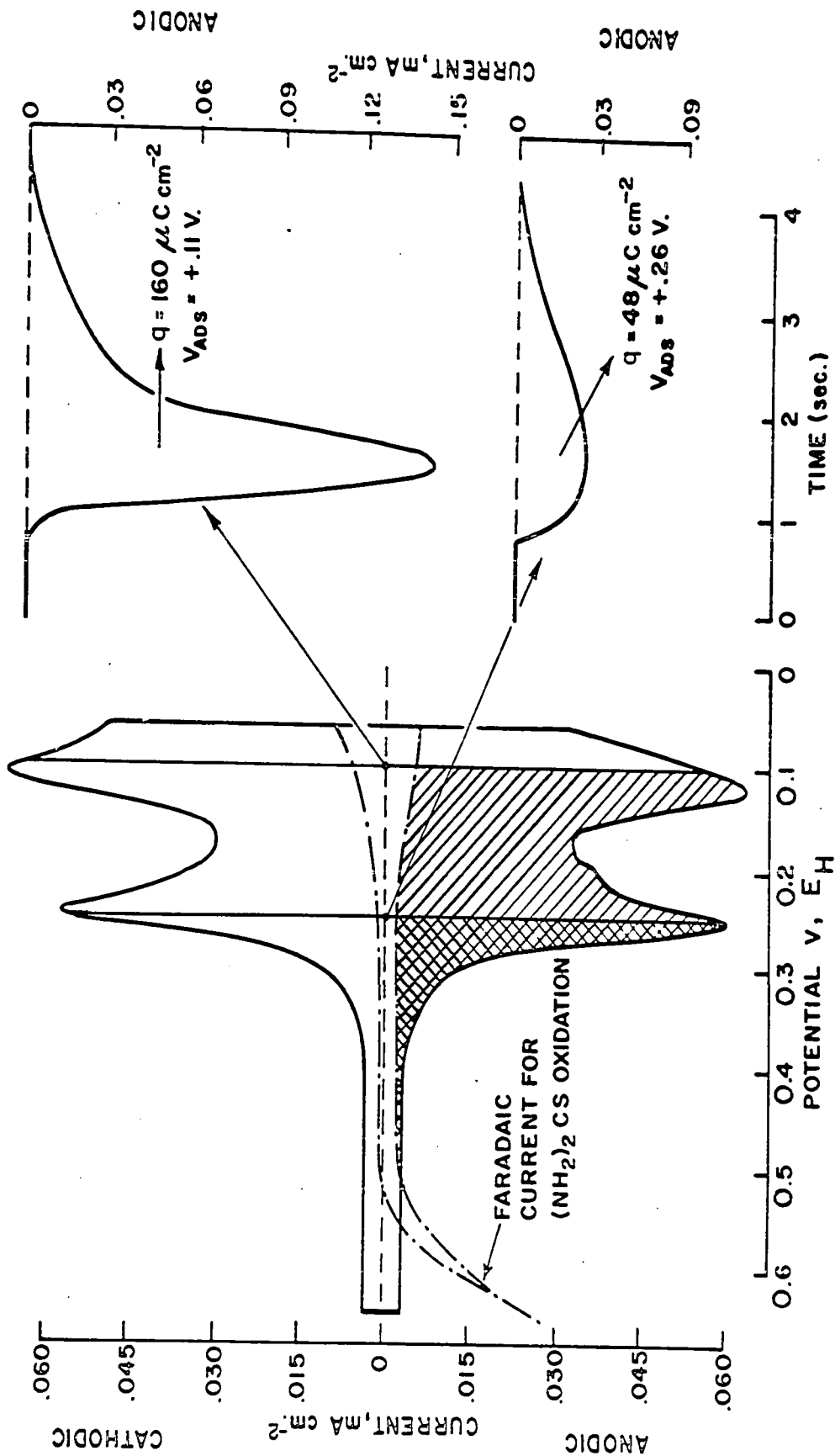


Fig. 38. Potentiodynamic current-potential profiles for Pt in the H and double-layer regions showing background current (—) for 1N H₂SO₄ and corresponding curve (- - -) for addition of thiourea 3 x 10⁻³ M. Curves at r.h.s. are two (anodic) transients which arise when thiourea is added at 0.11 or 0.26 V, E_H. Hatched area corresponds to quantity of H displaced by thiourea adsorbed at 0.11 V, E_H; X - hatched area to that for thiourea adsorption at 0.26 V, E_H. (dV/dt) = 50 mV sec⁻¹.

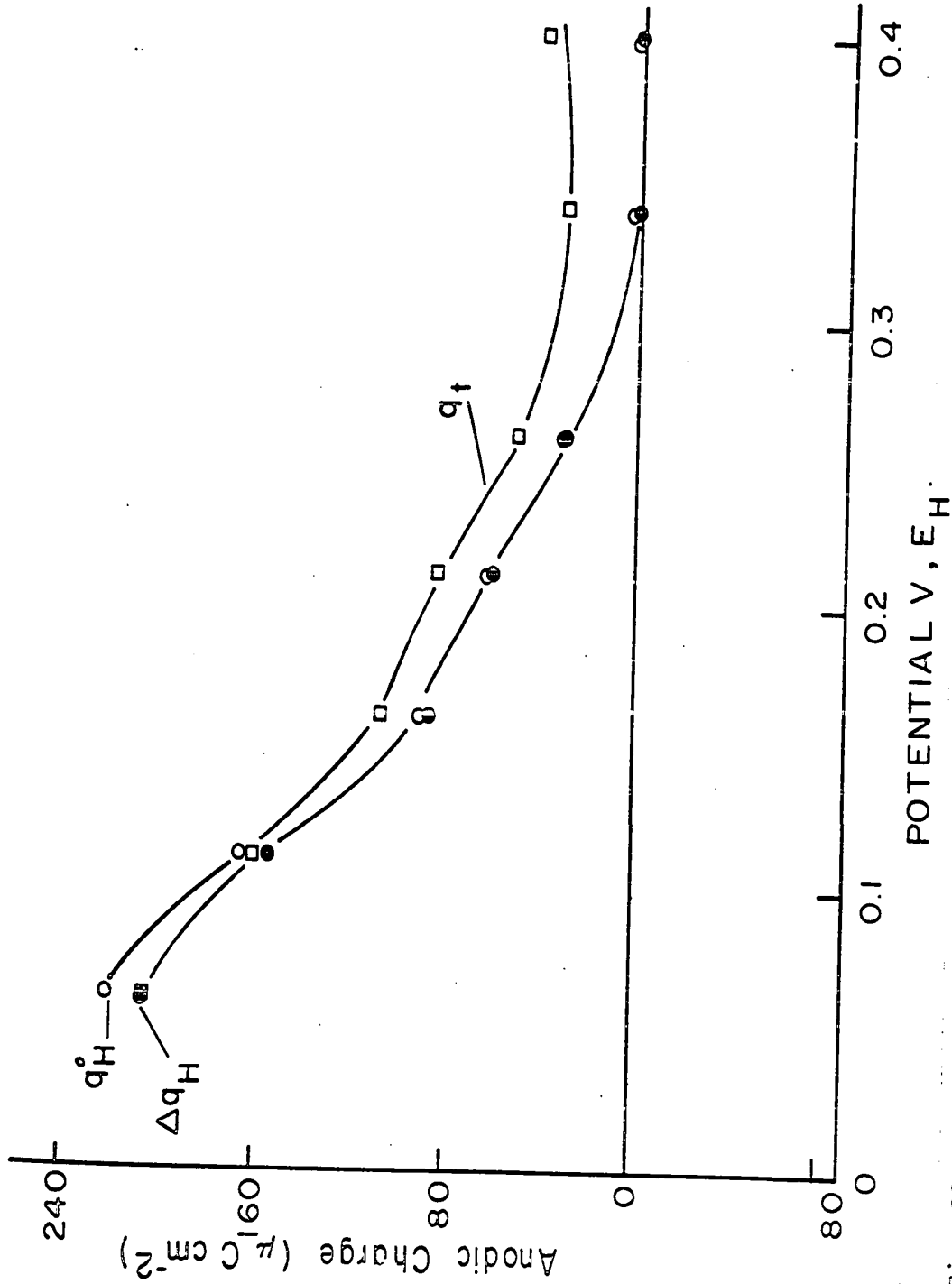


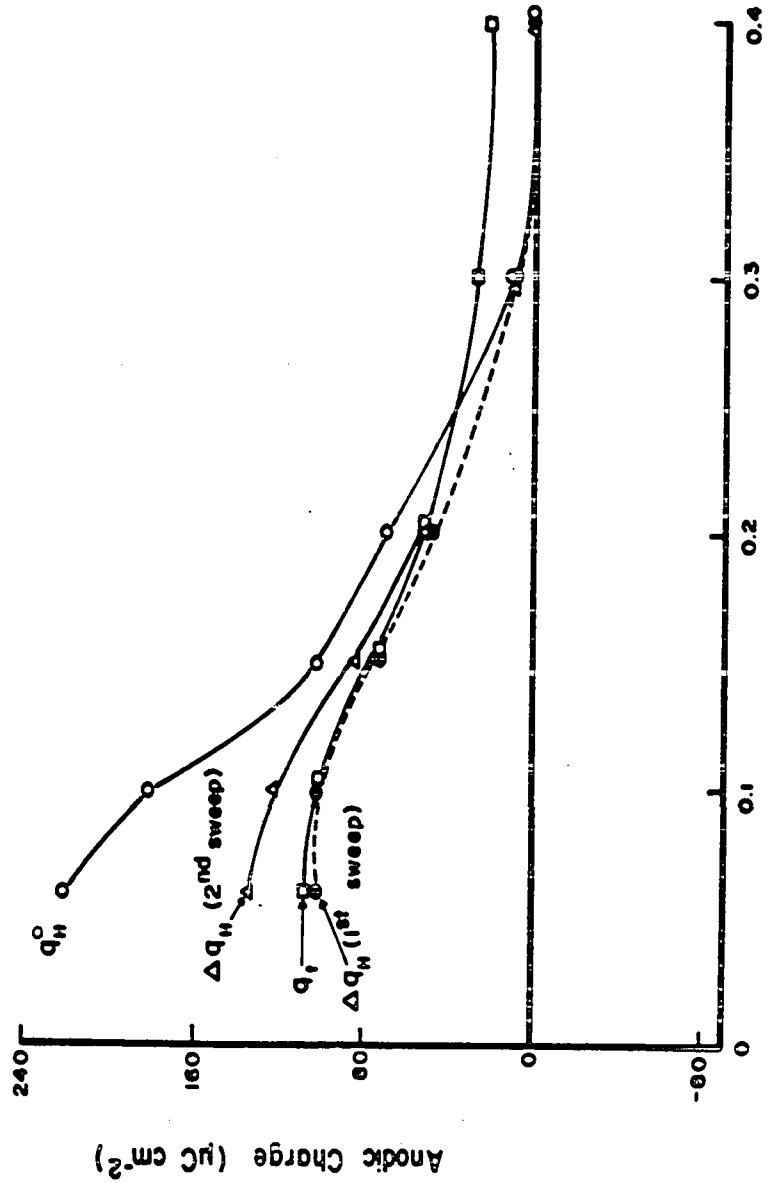
Fig. 39. Anodic H desorption charges, q_t (\square), from current transients for thiourea adsorption at Pt in relation to H blocking, Δq_H (\bullet), and total H coverage, q_H^0 (\circ), in the absence of additive.

coverage with atomic hydrogen increases. The anodic transient charge, $q_t = \int i dt$ (i.e. the area under the current transient curve), thus follows the initial coverage by chemisorbed hydrogen on the surface. The anodic current transient must therefore be associated with ionization of the atomic hydrogen previously on the surface which becomes displaced by adsorption of the sulfur compound. If the anodic charge were in any way connected with oxidation of the thiourea itself, it should decrease rather than increase as the potential is taken to more cathodic values.

The quantity of chemisorbed hydrogen (q_H^0) initially held on the electrode surface can be obtained by a simple integration of the area of the $i-V(t)$ profile over the hydrogen region from $0.35 \text{ V}, E_H$ down to the potential of interest, i.e. $\int_{0.35}^{V_a} \frac{i}{S} dV$, where V_a is the experimental adsorption potential. The integration is always performed on the hydrogen peaks in the anodic-going sweep in order to avoid any complications associated with components of hydrogen evolution in the cathodic peaks when the potential is near $0.10 \text{ V}, E_H$. The quantity of hydrogen still on the surface after addition of the organic substance at a particular potential, i.e. any atomic hydrogen not displaced by the organic additive, is determined from the area under the first anodic sweep after addition of the adsorbate under potentiostatic conditions. The quantity of hydrogen displaced by adsorption of the organic substance, Δq_H , can thus be compared with the anodic H displacement charge,

q_t . In the case of thiourea (Fig. 39) the correspondence between Δq_H and q_t is excellent except at the more positive adsorption potentials, e.g. $>0.30 \text{ V, } E_H$. The deviations at these potentials are due to a component current arising from faradaic oxidation of thiourea at the more positive potentials in the double-layer region, as seen from the potentiodynamic sweep (Fig. 38) for the electrode in thiourea solution. The close correspondence between Δq_H and q_t at the more negative potentials, combined with the fact that q_t becomes larger as the initial hydrogen coverage (q_H^0) increases, indicates that the transient anodic charge observed with thiourea injection corresponds quantitatively with displacement of atomic hydrogen by electrochemical ionization from the electrode surface.

Dimethylsulfide adsorption and coupled displacement of hydrogen occurs in a similar manner (Fig. 40); however, the adsorption and resultant hydrogen blocking was slower than with thiourea as indicated by the fact that the change of H coverage as measured by the charge Δq_H becomes larger on the second anodic sweep after addition of the substance. This is due to slower adsorption of dimethylsulfide in comparison with that of thiourea. The anodic displacement charge, q_t , for dimethylsulfide corresponds more closely to Δq_H over a wider range of potentials than was the case with thiourea. This arises, as is seen from the cyclic voltammogram for dimethylsulfide, because there is no faradaic oxidation process in the double-layer potential region. The



POTENTIAL V. E_H

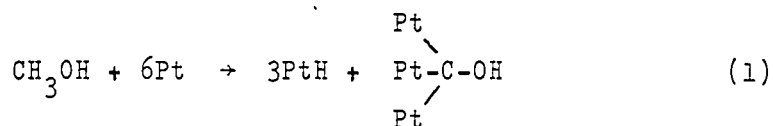
Fig. 40. Anodic H desorption charges, q_t (\square), from current transients for dimethylsulfide adsorption at Pt in relation to H blocking, Δq_H (\circ), on both first and second anodic sweeps after adsorption, and total hydrogen coverage, q_H^0 (\circ), in the absence of additive.

smaller stability of thiourea in comparison with that of dimethylsulfide is probably due to the greater facility of anodic oxidation of the unsaturated thiocarbonyl group of the former compounds than of the S in the latter compound. However, both q_t and Δq_H for dimethylsulfide adsorption are appreciably less than the charge for the total quantity of H on the surface, so that amongst the chemisorbed $(CH_3)_2S$ molecules, some adsorbed H atoms can remain.

(c) Anodic H displacement in relation to dissociative chemisorption

The relation of the anodic transients discussed above to those observed in dissociative chemisorption of organic molecules (e.g. CH_3OH , C_2H_6 , C_3H_7 at Pt electrodes) was investigated.

Methanol provides an excellent example of an organic compound which undergoes dissociative chemisorption at Pt in the double-layer region and coupled oxidation of the resulting adsorbed hydrogen atoms. The mechanism for methanol oxidation involves adsorption on a free platinum surface (17) and is as follows:

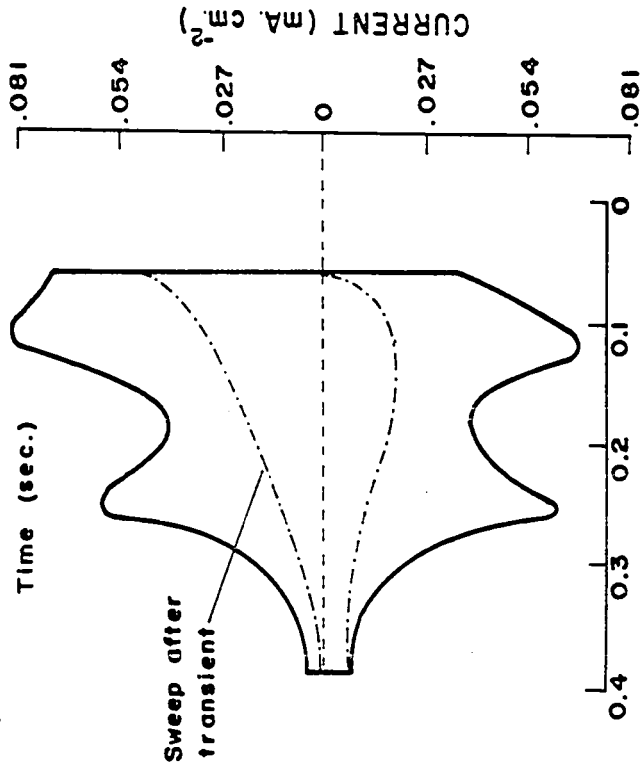
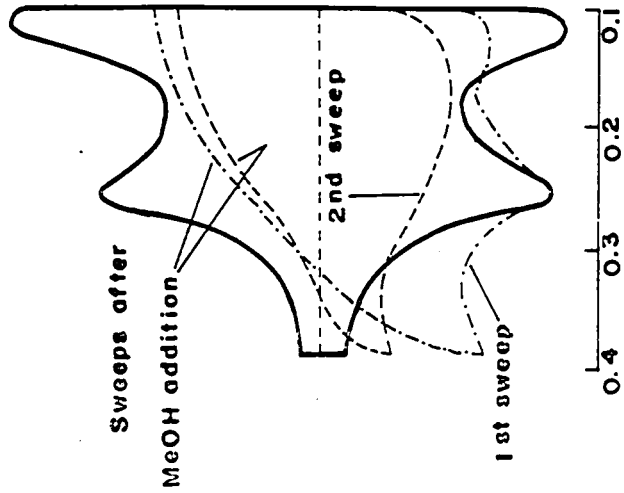
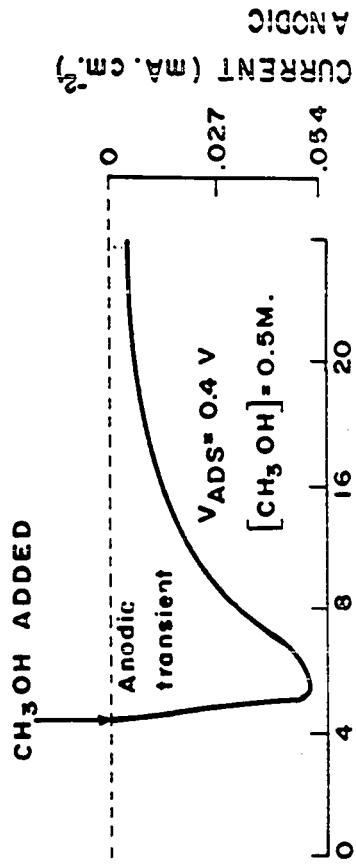
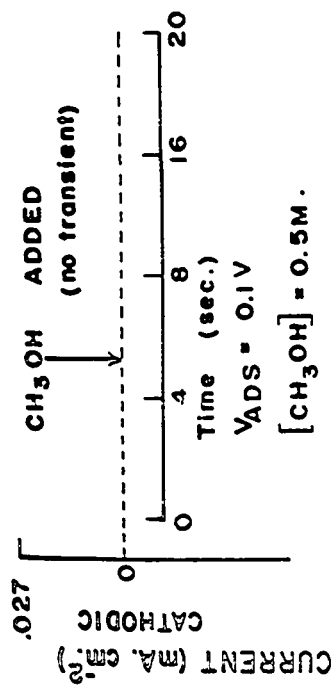


with rapid electrochemical oxidation of the atoms of hydrogen. The driving force for the reaction is provided by the adsorption and bond formation on the platinum surface. This type

of reaction is therefore quite different from that discussed above for adsorption of sulfur compounds since in the latter case no dissociative chemisorption occurs.

With methanol, the anodic transient arises from electrochemical ionization of H that originates from the adsorbed molecule itself and is only transiently adsorbed on the surface in the dissociative chemisorption step. However, in the case of adsorption of the sulfur compounds, the H which is ionized is already present on the electrode at an initial coverage determined by the electrode potential. The displacement results in a new, lower coverage of H as the S-compound becomes adsorbed, a quantity q_t of H being ionized at the potential V_a that would not normally be ionized from the surface at this potential, e.g. in a potential sweep originating from $0.06 \text{ V}, E_H$. This indicates that the energy gained from the sulfur compound adsorption more than compensates for the energy required to oxidize the adsorbed hydrogen. The question then arises whether methyl alcohol will chemisorb at a surface covered with atomic hydrogen.

Fig. 41 shows the result of experiments where methanol was injected into the system at two adsorption potentials, with and without adsorbed hydrogen present. Addition of methanol to an electrode that is covered with adsorbed hydrogen, i.e. at $0.10 \text{ V}, E_H$, does not result in any anodic transient and there is no change of H adsorption as indicated by zero value of Δq_H measured from the first anodic



POTENTIAL V, EH

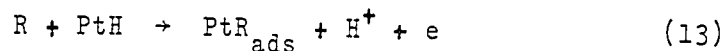
POTENTIAL V, EH

Fig. 41. Anodic electrochemisorption transient for 0.5 M CH₃OH adsorption in the double-layer region (cf. ref. 17) and absence of transient in the H region. Note relative lack of adsorption of CH₃OH in 1st sweep after addition at 0.1 V, E_H in comparison with behavior in 2nd sweep. Potentiodynamic i-V profile at r.h.s. shows effect of methanol on the H region after dissociative adsorption at 0.4 V, E_H .

sweep after addition of the methanol. The fact that subsequent sweeps show blocking of H adsorption indicates that some methyl alcohol has become adsorbed as the potential was being swept into the beginning of the double-layer region, i.e. around 0.4 V, E_H . Addition of methanol at 0.4 V, E_H results in passage of the characteristic anodic transient charge, the mechanism of which was explained above. The fact that methanol adsorption does not occur at a platinum surface in the hydrogen region indicates that the energy gained from the Pt-C bond formation is not great enough to compensate for the energy required to ionize the hydrogen atoms already adsorbed at this potential together with those that must arise from the CH_3 group. In related terms, the tendency for C-H dissociative adsorption is negligible if the surface is already substantially covered by H.

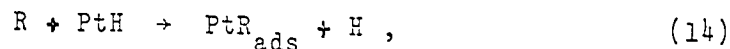
(d) Mechanism of sulfur compound adsorption

The anodic displacement reaction observed with the organic sulfur compounds may be represented as follows in a general way for an organic adsorbate, R:



The adsorbate R may chemisorb with occupation of one or more Pt sites per molecule depending on the nature of R (see below) but the general anodic displacement reaction (13) of 1H per Pt site will still apply. The observed anodic H

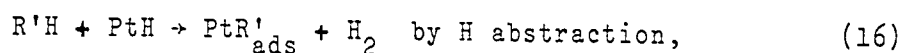
displacement is of importance since it means that a non-electrochemical displacement of the type



coupled with



or



is evidently not favored. This is presumably because processes (15) and (16) are not possible under the experimental conditions employed since they involve evolution of molecular H_2 and all potentials were positive to the reversible hydrogen potential. In fact, it is known that at Pt electrodes, H_2 cannot evolve by H recombination from the surface at potentials more positive than the reversible hydrogen potential, even when the coverage by hydrogen is quite large, e.g. at 0.1 V, E_H . The pathway (13) for H displacement is hence the preferred one for thermodynamic reasons.

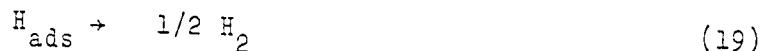
Preferential anodic desorption by process (13) is also indicated by consideration of the energetics of (13) with respect to (14) and (15). The difference of energy of processes (13) and (14) will be equal to the difference between the energies of the elementary reactions:



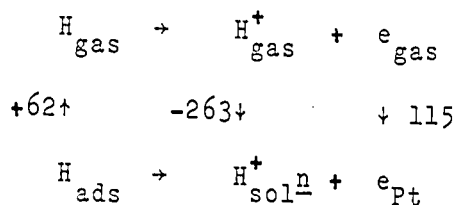
and



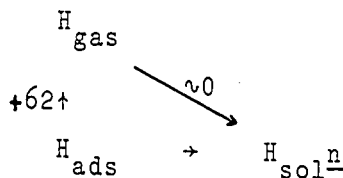
or



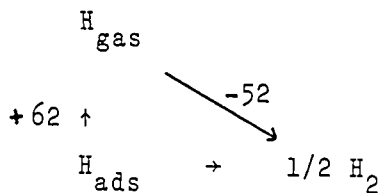
for a given adsorbed additive. The Born-Haber cycle for process (17) is as follows:



while that for (18) is:



A knowledge of the hydration energy of H^+ (130) and the work function of Pt shows that the energy difference between processes (17) and (18) is -64 ± 7 kcal mole⁻¹ in favor of (17). For process (19) the Born-Haber cycle is:



and in this case the energy difference between (17) and (19) is ca. 13 kcal mole⁻¹ in favor of the ionization process, (17).

The anodic hydrogen displacement effect has been discussed above for adsorption of sulfur compounds at platinum over the hydrogen adsorption region. A series of other organic compounds which were also examined show a more complex

behavior due to other reactions, e.g. hydrogenation, which are coupled with or occur after the hydrogen displacement.

(e) Adsorption of benzene in the hydrogen region
at platinum

The anodic hydrogen displacement effect described above was used to investigate the electrochemisorption of benzene at a platinum surface which was either partially or fully covered by adsorbed hydrogen. This case is more complicated than that involving sulfur compounds because benzene can undergo electrochemical hydrogenation at the cathodic potentials corresponding to the hydrogen region. This is shown in Fig. 42 for benzene injection at two potentials, .06 V and .11 V, E_H ; cathodic faradaic currents are observed in both cases after addition of the benzene. It is interesting to note that at $V_{ads} = -0.05$ V, E_H a significant anodic hydrogen displacement charge is still observed even though there is some cathodic H_2 evolution at this potential in the absence of additive. This would suggest that those hydrogen atoms displaced upon chemisorption of benzene are different from those which participate in the hydrogen evolution reaction. This result provides further support for mechanism (13) shown above for the anodic hydrogen displacement process since, even when the hydrogen evolution reaction can occur, an anodic hydrogen displacement charge is observed.

The measurement of the anodic hydrogen displacement charge is somewhat complicated at 0.06 V, E_H because of the

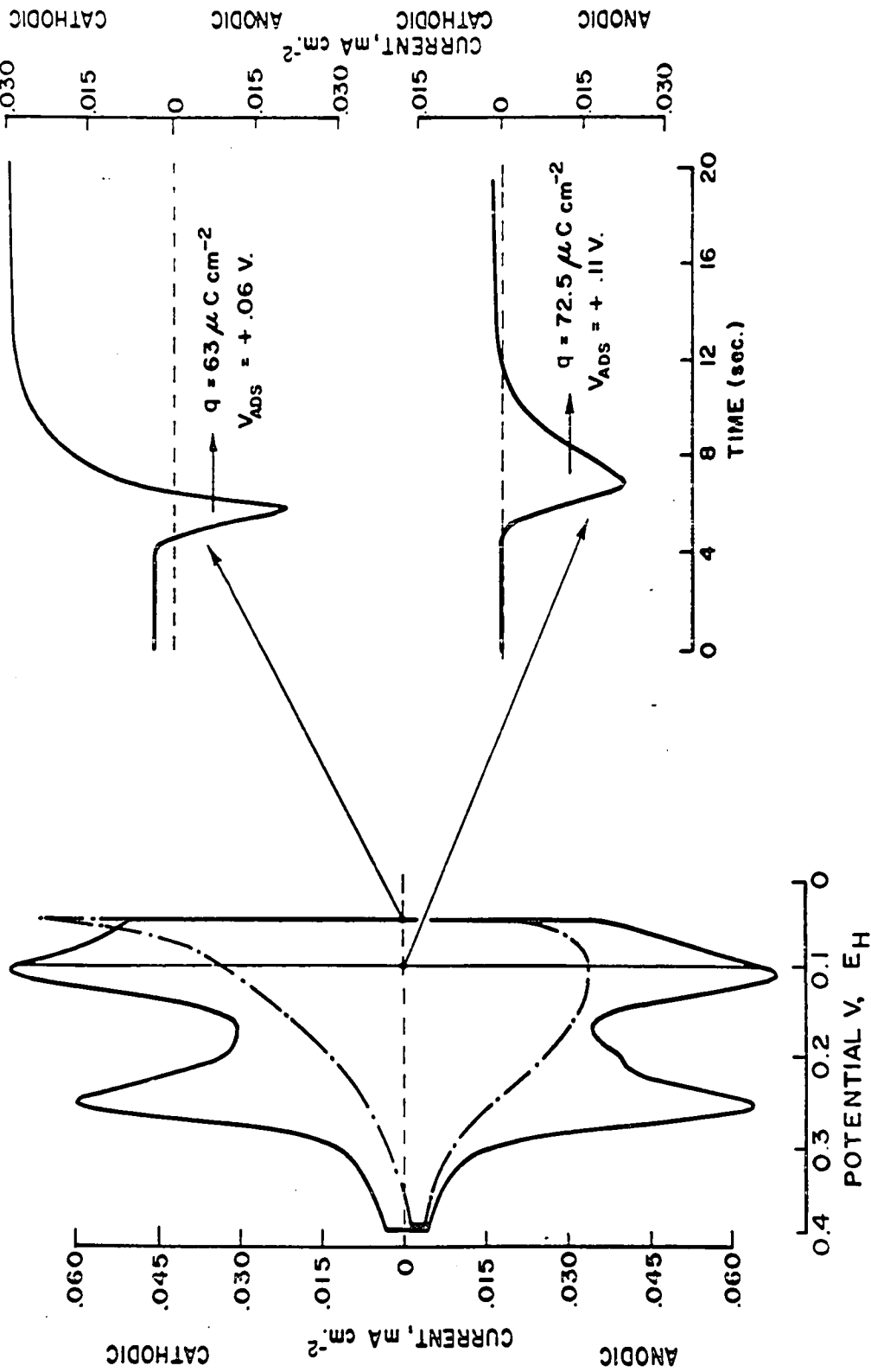


Fig. 42. Potentiodynamic profile, as in Fig. 38, for background (—) and for addition of benzene ($3 \times 10^{-3} \text{ M}$, - - -) together with typical anodic transients which arise from benzene adsorption at 0.11 and 0.06 V, EH. In the latter case, note increased steady-state cathodic current in the transient corresponding to benzene reduction.

added component of benzene electroreduction. At more anodic potentials, there is, of course, less complication due to this extra reaction of benzene reduction in the displacement transients; however, Fig. 43 shows that a small faradaic reduction component exists up to 0.25 V, E_H giving $q_t < \Delta q_H$. Unlike thiourea, benzene is seen to be inert with respect to anodic oxidation up to 0.35 V, E_H (Fig. 42) as found in other work (30). The potentiodynamic sweep, after benzene addition, shows that benzene is significantly oxidized at platinum only at potentials above ca. 0.80 V, E_H at room temperature.

Fig. 43 also shows a plot of $q_t - \Delta q_H$, i.e. there is a finite difference between the anodic transient charge and the actual amount of hydrogen displaced. As mentioned above, this difference arises because the benzene can undergo electrochemical hydrogenation upon adsorption, this cathodic current adding to the anodic H displacement current with the result that the measured q_t is lower than Δq_H . The maximum coverage by benzene at 0.06 V, E_H is approximately 55% of the total Pt sites available for atomic hydrogen adsorption, as may be derived from the Δq_H and q_H^0 values. The geometry of the molecule in relation to the (111) close-packed plane of a platinum surface shows that the whole molecule can occupy an area equivalent to 7 Pt atom sites (see also 61,131). However, for steric reasons, a certain proportion of the surface will remain unavailable to benzene adsorption and hence provide sites for H adsorption. This explains why

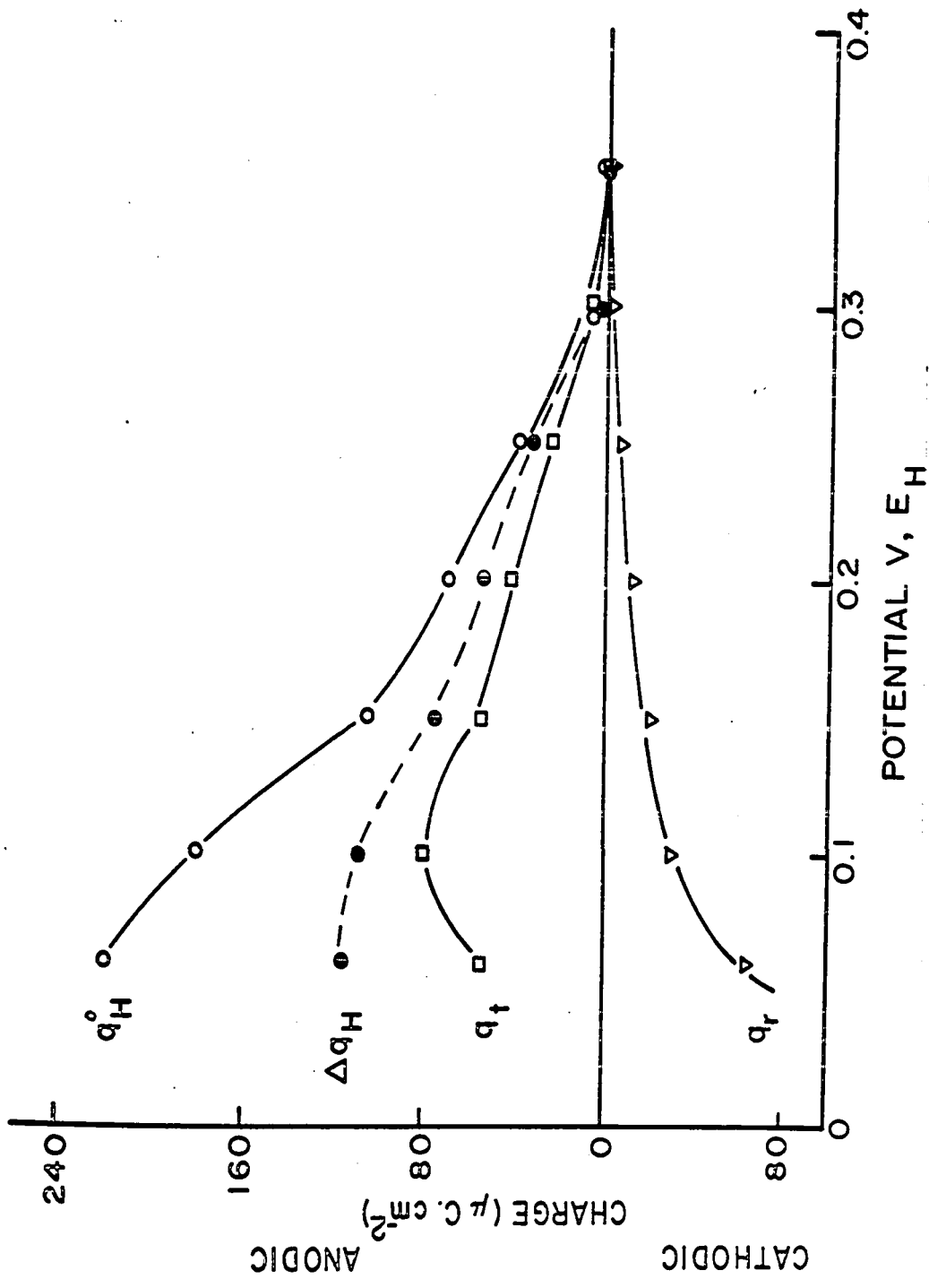


Fig. 43. Anodic H desorption charges, q_t (\square), from current transients for benzene adsorption at Pt in relation to H blocking, Δq_H (\bullet), and total hydrogen coverage, q_H° (\circ), in the absence of additive. Lower curve (q_r) represent difference of q_t and Δq_H due to electrochemical hydrogenation effects which increase as the potential becomes less positive.

benzene, being a relatively large molecule, does not block the surface for hydrogen as effectively as does thiourea. Six of the platinum atom sites blocked by benzene are those at which associative adsorption of the three double bonds can occur (132), 2H atoms per double bond being displaced. The blocking of the 7th site arises simply on account of the physical size of the molecule in relation to the surface lattice spacing.

The electrochemical adsorption behavior of cyclohexane was also investigated by the above methods but, as expected, there was no anodic hydrogen displacement current upon injection of this additive into the solution; correspondingly, Δq_H on the subsequent anodic sweep was zero. This lack of adsorption activity is consistent with the electrochemical inactivity of paraffins at platinum at ambient temperatures and with the fact that product adsorption after chemical catalyzed hydrogenation of benzene at platinum (in water) does not inhibit the reaction.

(f) Adsorption of nitriles in the hydrogen region at platinum

The general effects of acetonitrile on the usual surface processes at a platinum electrode in aq. solution between 0.05 and 1.5 V, E_H were previously described (e.g. Section I.1(b)). The hydrogen displacement effect upon adsorption of acetonitrile in relation to surface coverage

by atomic hydrogen was briefly discussed (p. 81). It was shown that when acetonitrile is adsorbed potentiostatically in the double-layer potential region a cathodic current transient results (Fig. 18), especially at potentials between 0.55 and 0.3 V, E_H . This cathodic current transient was associated with reduction of adsorbed acetonitrile and from the charge, the acetonitrile coverage can be derived at various potentials, provided a satisfactory assumption can be made concerning the number of electrons transferred per platinum site in the surface. The adsorption and reaction characteristics of acetonitrile were thus quite different from those of methanol (Figs. 19 and 41) where dissociative chemisorption results (17) in large anodic current transients in the double-layer potential region.

The adsorption characteristics of both acetonitrile and benzonitrile in the hydrogen region were investigated in detail. Fig. 20b shows the type of transient obtained when acetonitrile adsorption occurs in the hydrogen region; also shown is the potentiodynamic sweep profile before and after nitrile addition which enables the change of H coverage Δq_H to be evaluated. The fact that the adsorption transient is cathodic at 0.26 V, E_H or higher potentials up to ca. 0.6 V, E_H , but becomes anodic at a less positive potential, indicates a more complicated behavior than was observed with the sulfur compounds; at the same time, this result confirms that the anodic transient must arise from oxidation of adsorbed H.

Fig. 21 shows the charge quantities obtained when acetonitrile is adsorbed at various potentials. The charge q_t for the adsorption transient is seen to pass from anodic to cathodic values at approximately $0.12 \text{ V}, E_H$. This behavior is associated with the fact that the transient charge, q_t , is made up of two components: (a) an anodic component due to ionization of adsorbed H; and (b) a cathodic component from the reduction of adsorbed acetonitrile. For adsorption potentials less positive than $0.12 \text{ V}, E_H$, the charge for displacement of atomic hydrogen, Δq_H^* , becomes greater than the acetonitrile reduction charge because coverage by adsorbed hydrogen becomes higher at these potentials. At more positive potentials, there is a smaller hydrogen coverage and thus more free surface is available for adsorption to occur; the acetonitrile reduction charge then becomes greater than the H displacement component. The cathodic adsorption transient charge decreases at potentials anodic to $0.33 \text{ V}, E_H$ because of incomplete reduction of the acetonitrile on the surface, the reduction peak potential in the sweep being at ca. $0.45 \text{ V}, E_H$ (see p.106). A similar treatment applies to the results obtained with benzonitrile

* The charge, Δq_H , for displacement of atomic hydrogen is given by $\Delta q_H = q_H^0 - q_H^1$, where q_H^1 is the quantity of adsorbed atomic hydrogen remaining on the surface after acetonitrile adsorption as determined from the next anodic-going sweep, following the adsorption transient. This charge has been corrected by the kinetic relaxation method discussed on p.86 for the charge component due to acetonitrile electroactivity in the hydrogen region. Thus, the Δq_H values given in Fig. 21 are the true adsorbed H displacement charges and are larger than the apparent values which would be obtained by simple integration over the (unresolved) hydrogen adsorption region.

(Fig. 44); Fig. 45 shows that for benzonitrile* the transition from anodic to cathodic charge transients occurs at 0.18 V, E_H .

A closer examination of the adsorption transients for acetonitrile and benzonitrile in the potential region where anodic charges are observed reveals a slow cathodic current component after the anodic one has been completed. The corresponding cathodic charge, $q_{t,-}$, represents a continuing element of the acetonitrile reduction process that is slower than the initial reduction and, when added to the $q_{t,+}$ charge, gives the correct net transient charge q_t . As the potential for adsorption becomes more positive, this long-time reduction effect diminishes. For both acetonitrile and benzonitrile, the difference between q_t , the net adsorption transient charge, and Δq_H , is due to reduction of the nitrile as it adsorbs and displaces adsorbed H. The differences between Δq_H and the corrected q_t values for acetonitrile are given in Fig. 21 as q_r . The maximum value of q_r for acetonitrile is $160 \mu\text{C cm}^{-2}$ at 0.06 V, E_H , and this represents a fractional acetonitrile coverage corresponding to 0.72 electrons per Pt site. This coverage value is in excellent agreement with that, 0.68 e per Pt, obtained from the anodic-going potential sweep by integration of the acetonitrile reoxidation charge up to 0.825 V, E_H after 90 sec cathodic holding at 0.05 V, E_H (see p.97 and the $q_{a,h}$ values in

* The Δq_H values for benzonitrile adsorption were also corrected for the charge component associated with benzonitrile activity in the hydrogen region, by the same procedure as that described for acetonitrile.

6.0 5.0 4.0 3.0 2.0 1.0 0.0 1.0 2.0 3.0 4.0 5.0 6.0

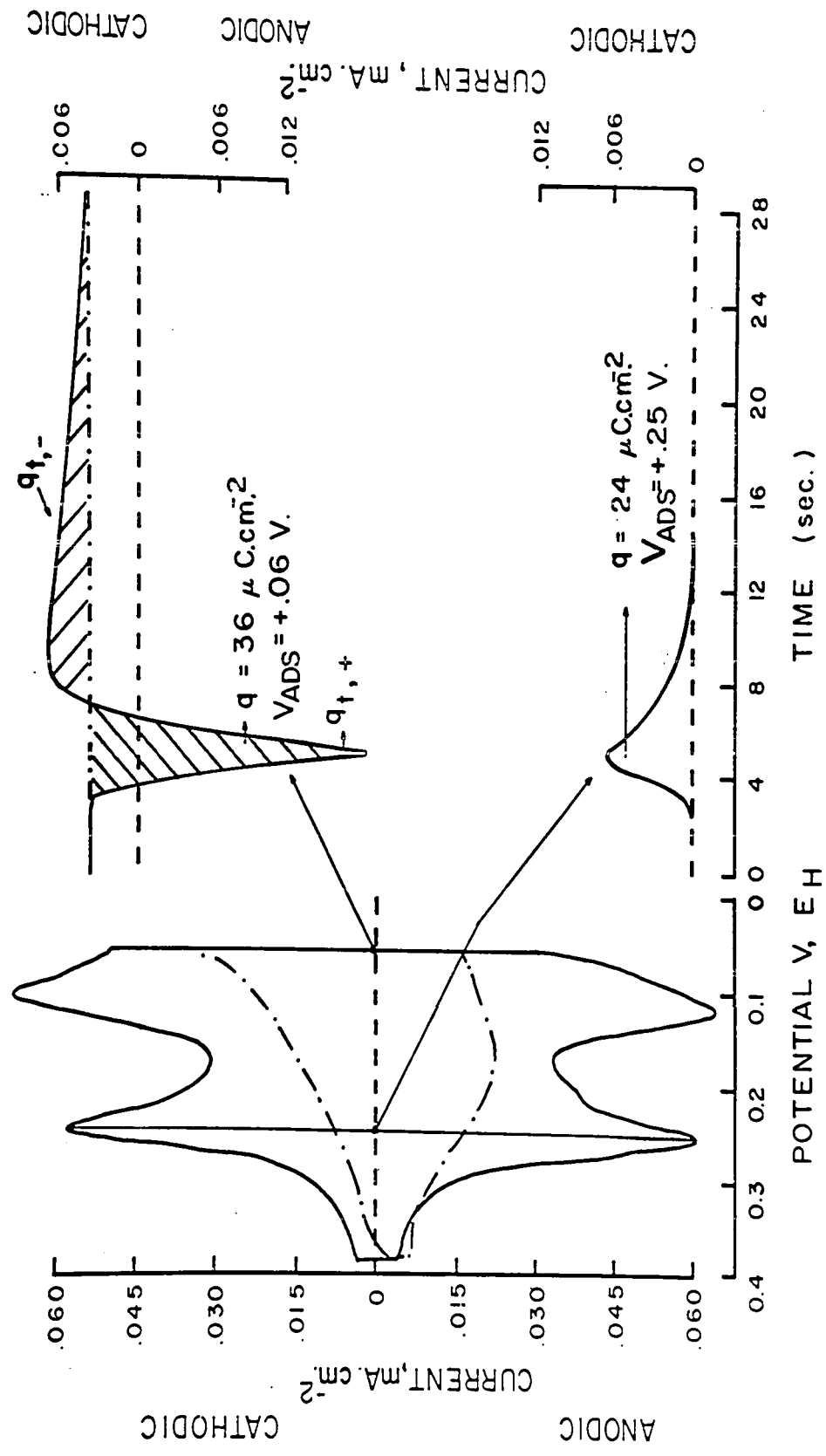


Fig. 44. Potentiodynamic profile, as in Fig. 38, for background and for addition of benzonitrile ($3 \times 10^{-3} \text{ M}$, $-\cdot-\cdot-$) together with typical anodic and cathodic transients for benzonitrile adsorption at 0.06 and 0.26 V, EH , respectively. Note long-term cathodic reduction involving charge $q_t, -$ at $V_{\text{ads}} = 0.6 \text{ V, EH}$ after initial H displacement.

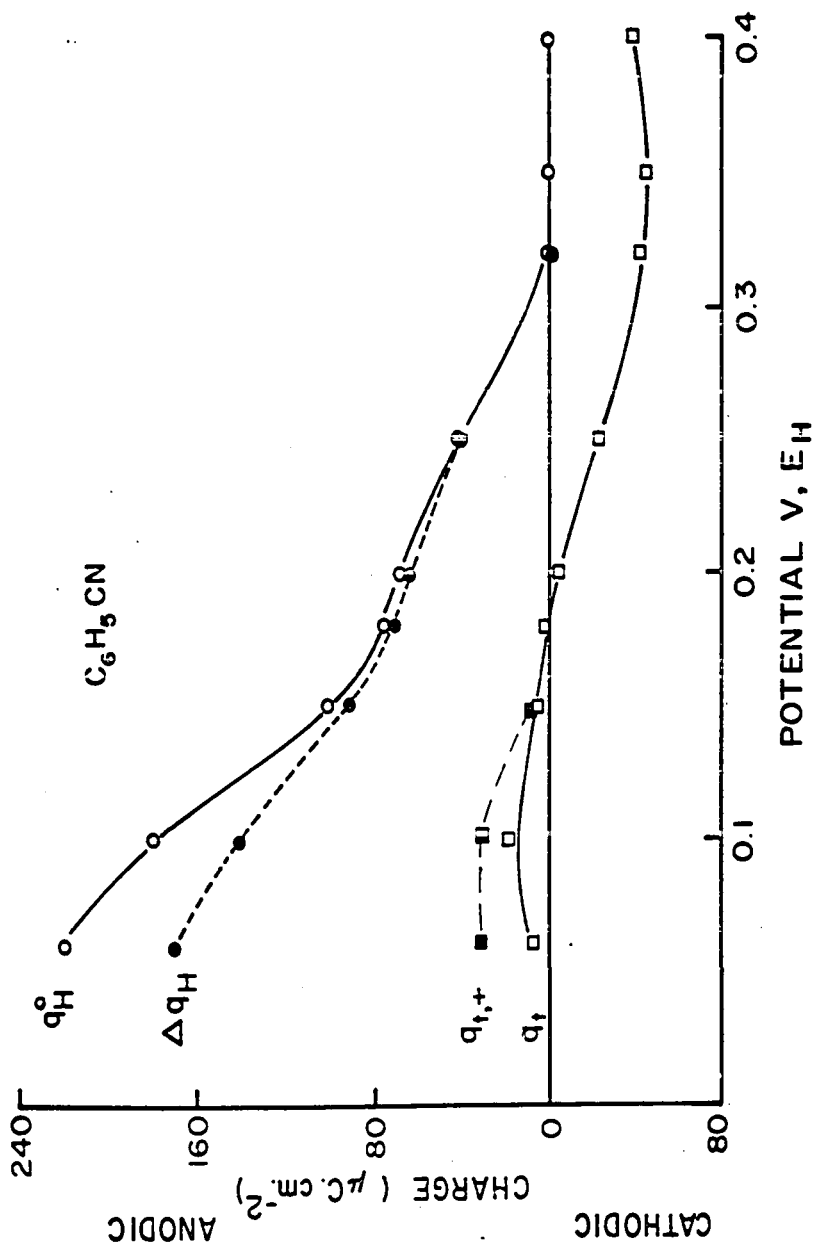


Fig. 45. Transient adsorption charges, q_t (\square), from current transients for benzotrinitrile adsorption at Pt in relation to H blocking, Δq_H (\bullet), and total H coverage, q_H^0 (\circ), in the absence of additive. The points (\square) represent the q_t values before correction for long-term reduction effects associated with charge $q_{t,-}$ in Fig. 44.

Fig. 26). For acetonitrile, a detailed analysis of the charge quantities involved in H displacement and electrochemical adsorption is given in Table II as a function of adsorption potential, V_a .

From Table II it is seen that $\Delta q_H - q_t$ is almost equal, at all V_a , to the charge for anodic oxidation of adsorbed acetonitrile species in the double-layer region, corrected by the kinetic relaxation procedure for the charge component which arises in the H region on the next anodic sweep taken after the measurement of the transient. This follows from the fact that the adsorption transient charge, q_t , is equal to the algebraic sum of the cathodic transient charge component, q_r , passed in initial reduction of the nitrile group and the H displacement charge, Δq_H ; i.e. $q_t = \Delta q_H - q_r$. Therefore $q_t - \Delta q_H$ is equal to q_r , corresponding to the charge taken up by the chemisorbed species which becomes reoxidized on the next anodic sweep.

The behavior of benzonitrile is similar, as shown in Fig. 45, where q_H^0 , Δq_H and q_t are compared. The adsorption transient in this case (Fig. 44) shows the usual anodic component when θ_H is appreciable but a cathodic component at longer times as in the case of acetonitrile. The significance of this component, $q_{t,-}$, in the case of benzonitrile adsorption at the least positive V_a values is similar to that in the case of acetonitrile reduction.

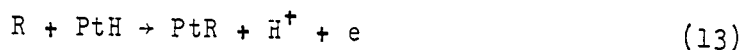
The electrochemical reduction of acetonitrile and benzonitrile (together with benzene) is evidently a process which initially requires anodic displacement of adsorbed H. This is of general interest with regard to the mechanism of electrochemical hydrogenation, since the reducible molecule must evidently become chemisorbed on sites previously occupied by H and then become reduced rather than being physically adsorbed on the H layer and then reacting with the adsorbed H (Rideal type mechanism).

(g) Behavior of thiourea at nickel electrodes

The observation of anodic H displacement transients at platinum led to an investigation of the possible use of this method at nickel electrodes. In the case of nickel, potentiodynamic and current pulse methods cannot be readily applied to the determination of H coverage since the corrosion currents which arise at these metals in any aqueous acidic medium complicate the application of transient methods. In an experiment in which nickel was potentiostated at -0.05 and -0.15 V, E_H in 0.1 N H_2SO_4 , no anodic adsorption transient was observed upon addition of thiourea (3×10^{-3} M) although the residual corrosion current was diminished by a factor of ca. 10 times, as expected. This result is of interest in that it means nickel electrodes support negligible ($<10 \mu C \text{ cm}^{-2}$) H coverage near the reversible H_2 potential (cf. 133), unlike the case of platinum.

(h) Summary of the anodic hydrogen displacement effect

- (i) Adsorption of an organic molecule at a platinum site occupied by atomic hydrogen, i.e. PtH, proceeds with coupled ionization of the atomic hydrogen:



This effect is best illustrated with sulfur-containing compounds, such as dimethylsulfide, where the charge associated with adsorption at potentials more negative than 0.3 V, E_H , arises from ionization of adsorbed H and is exactly equivalent to the extent of subsequent blocking of the surface for H adsorption, Δq_H . The effect is quite different from that observed with dissociative adsorption of organic molecules like methanol in the double-layer potential region.

- (ii) The transient charge, q_t , resulting from adsorption of nitriles in the H region is the sum of a charge component due to reduction of the adsorbed nitrile, q_r , and with coupled ionization of adsorbed H. Because of the magnitude of q_r , the anodic H displacement effect is observed with nitriles only at quite negative adsorption potentials, i.e. at high θ_H .
- (iii) From the measured quantities q_t and Δq_H the real reduction charge resulting from adsorption of the nitrile can be calculated since $q_r = q_t - \Delta q_H$. This same reasoning can be used to determine the reduction

charge associated with benzene adsorption in the \bar{H} region.

- (iv) An anodic transient charge is observed when the adsorption of benzene occurs at potentials where a net faradaic current due to hydrogen evolution is observed. This suggests that the H atoms participating in the rate controlling step of H_2 evolution are not in the same state as those that are displaced in the chemisorption of organic substances.

PART III

Effects of Acetonitrile on the Oxidation of Formic Acid
and Methanol in Aqueous Media

(a) Introduction

The oxidation of formic acid and methanol at platinum in aqueous media was discussed briefly in Chapter I. During an anodic sweep, formic acid exhibits oxidation currents in three distinct potential regions (Fig. 2): i) the double-layer region; ii) the region where surface oxidation begins, i.e. 0.80 to 0.95 V, E_H ; and iii) a region of higher anodic potentials, i.e. ca. 1.2 to 1.5 V, E_H . Regions of decreasing currents with increasing anodic potential also arise and correspond to passivation of the reaction by surface oxide formation (24,27). In the cathodic-going potential sweep, a large anodic current peak arises in the potential region where surface oxide reduction occurs. Similar electro-oxidation behavior at platinum has been observed with methanol (102), although in this case there is no double-layer peak in the anodic-going potential sweep (Fig. 2).

After confirming the above behavior in aqueous solution, the oxidation of formic acid and methanol was also studied at platinum under anhydrous conditions with acetonitrile as solvent (see section IV(b)). The complete lack of activity of methanol and the relatively small degree of activity of formic acid under these conditions even with

added water lead to an examination of (i) the effect of acetonitrile itself on the normal surface reactions at platinum (described already in Part I), and (ii) the effect of small quantities of acetonitrile on the oxidation of organic molecules at platinum electrodes in aqueous media. With regard to (i), it has been shown in section I.1(b) that acetonitrile is electroactive at platinum in aqueous media and this information is used in interpreting the results of (ii) given below. The effect of other additives, including mercury, on the oxidation of formic acid at platinum was also investigated in relation to the behavior of the reaction in the presence of acetonitrile.

(b) Formic acid and methanol oxidation at platinum
in the presence of acetonitrile

The oxidation of methanol at platinum gives rise to three anodic current peaks upon cycling from 0.05 to 1.5 V, E_H ; two of these appear on the anodic sweep and one on the cathodic sweep (Fig. 2). The presence of acetonitrile, even in trace quantities ($<10^{-4}$ M), results in a decrease of the oxidation currents for all three peaks (Fig. 46). The peak current for methanol oxidation at ca. 0.9 V, E_H has decreased by a factor of ten at $[CH_3CN] = 2 \times 10^{-1}$ M (Fig. 47); indeed, the major fraction of the peak current at this concentration of acetonitrile is probably due to reoxidation of acetonitrile itself, which has been previously reduced (see section I.1(f)).

Accepted for publication, J. Electroanal. Chem., 1967, 18, 1-10.

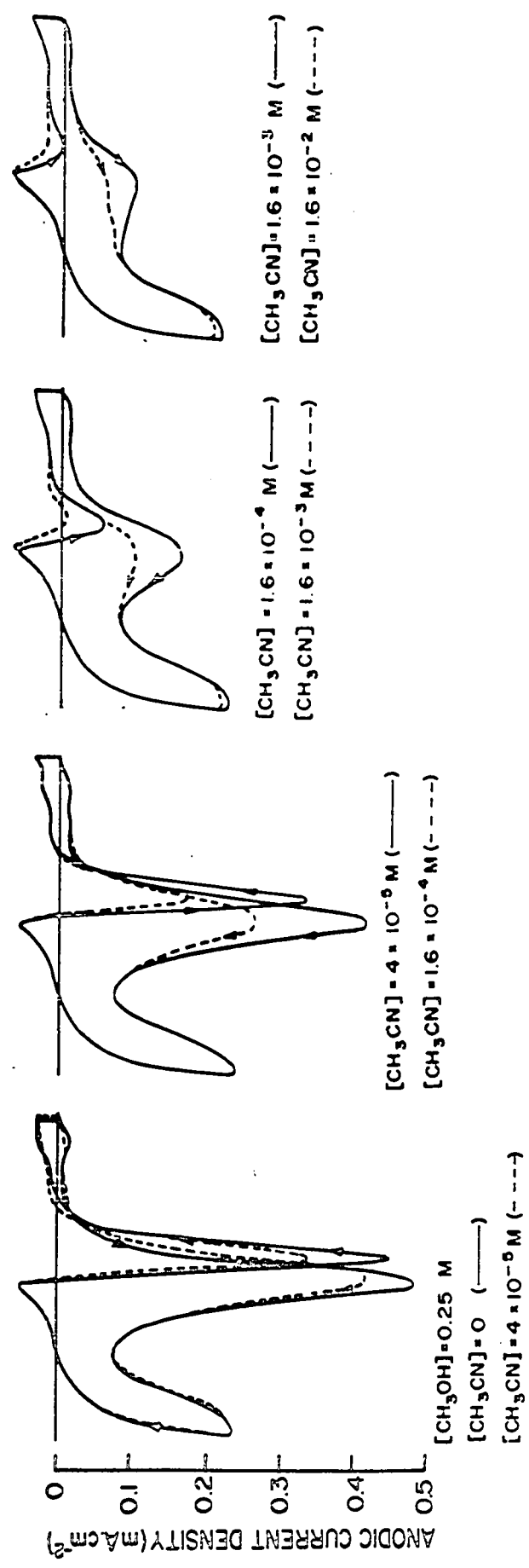


Fig. 46. Potentiodynamic i-V profiles for 0.25M CH₃OH at platinum with various concentrations of acetonitrile. (dV/dt) = 50 mV sec⁻¹, potential range 0.05 to 1.5 V, E_H.

\square $(i_p)_{FA_1}$
 \circ (i_p) for CH_3OH at $+0.9$ V, E_H .

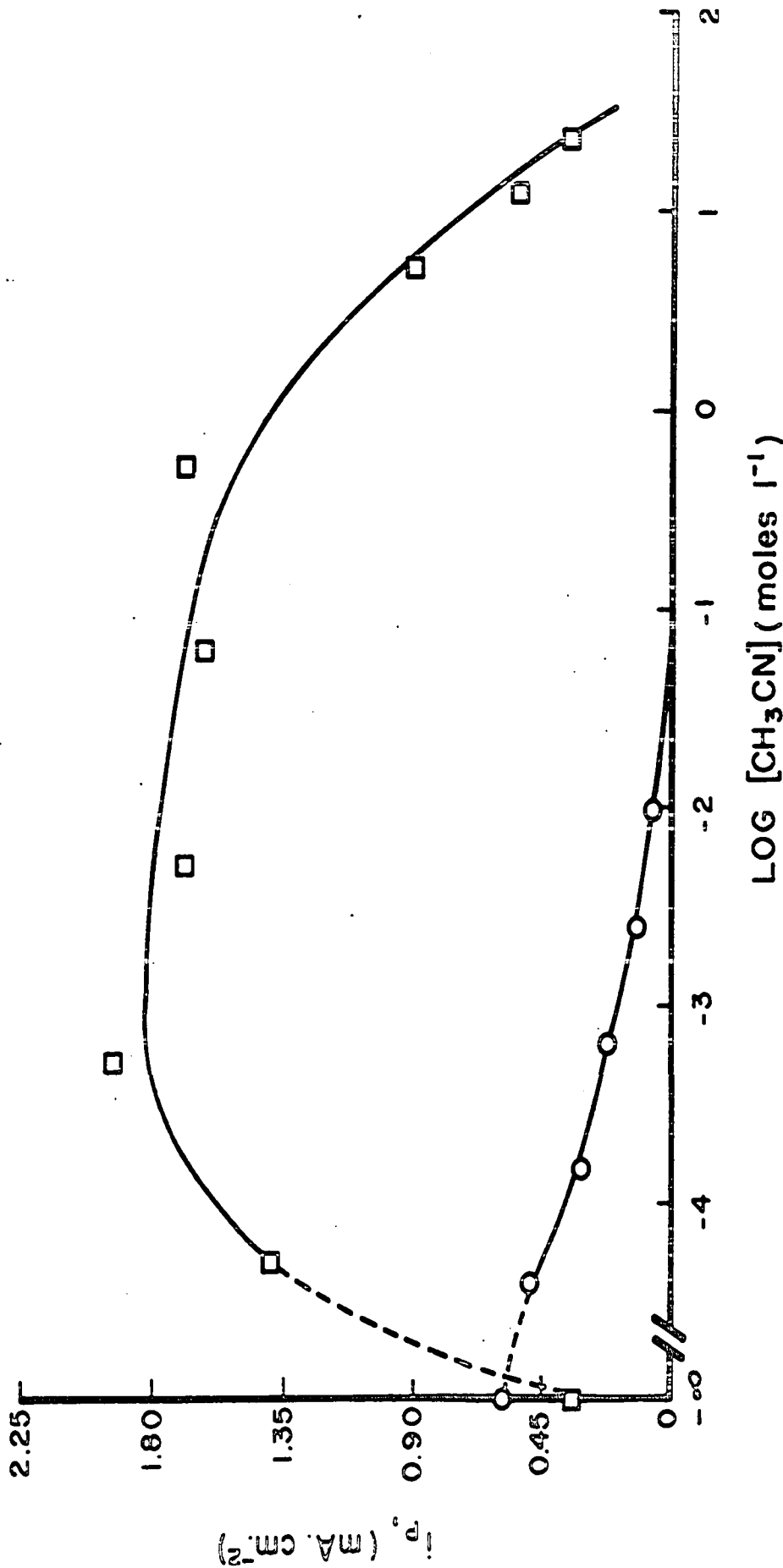


Fig. 47. Dependence of peak current for the FA_1 process, i.e. formic acid oxidation in the double-layer region (\square) and methanol oxidation at ca. 0.9 V, E_H (\circ) on $[CH_3CN]$. The peak currents were determined from the potentiodynamic i-v profiles in Figs. 46 and 48. $[HCOOH]$ and $[CH_3OH] = 0.25M$, $(dv/dt) = 50$ mV sec⁻¹.

Peak currents for the oxidation of methanol on the cathodic sweep are seen to be reduced to zero by an acetonitrile concentration of only $1.6 \times 10^{-3} \text{ M}$ (Fig. 46). These observations are consistent with the facts that (i) methanol electro-sorption requires three geometrically adjacent sites (17), and (ii) ca. 70% of the surface is covered by acetonitrile species at $[\text{CH}_3\text{CN}] > 3 \times 10^{-4} \text{ M}$; therefore, the site requirements for the electro-sorption of methanol cannot be fulfilled. Acetonitrile also gives rise to a decrease in the peak current for methanol oxidation at high anodic potentials, ca. 1.3 V, E_{H} , and this effect can be correlated with the fact that acetonitrile remains adsorbed on the electrode surface even at potentials in the oxygen evolution region on platinum (cf. the example at 1.8 V, E_{H} in section I.4(b)).

In contrast to the general inhibition effect which adsorbed acetonitrile has on the electro-sorption and subsequent oxidation of methanol at platinum, acetonitrile has an activating effect on the formic acid oxidation peak (FA_1^*) in the double-layer potential region at platinum (Fig. 48). Fig. 47 shows the dependence of the peak current $(i_p)_{\text{FA}_1}$ for this process on acetonitrile concentration, the increase of $(i_p)_{\text{FA}_1}$ in a potentiodynamic cycling experiment conducted over the full potential range (i.e. 1.4 to 0.05 V, E_{H}) being of the

* The symbol FA_1 will be used to refer to the formic acid oxidation reaction in the double-layer region at platinum in an anodic-going sweep. Correspondingly, FC will be used to denote the formic acid oxidation peak in the cathodic-going sweep.

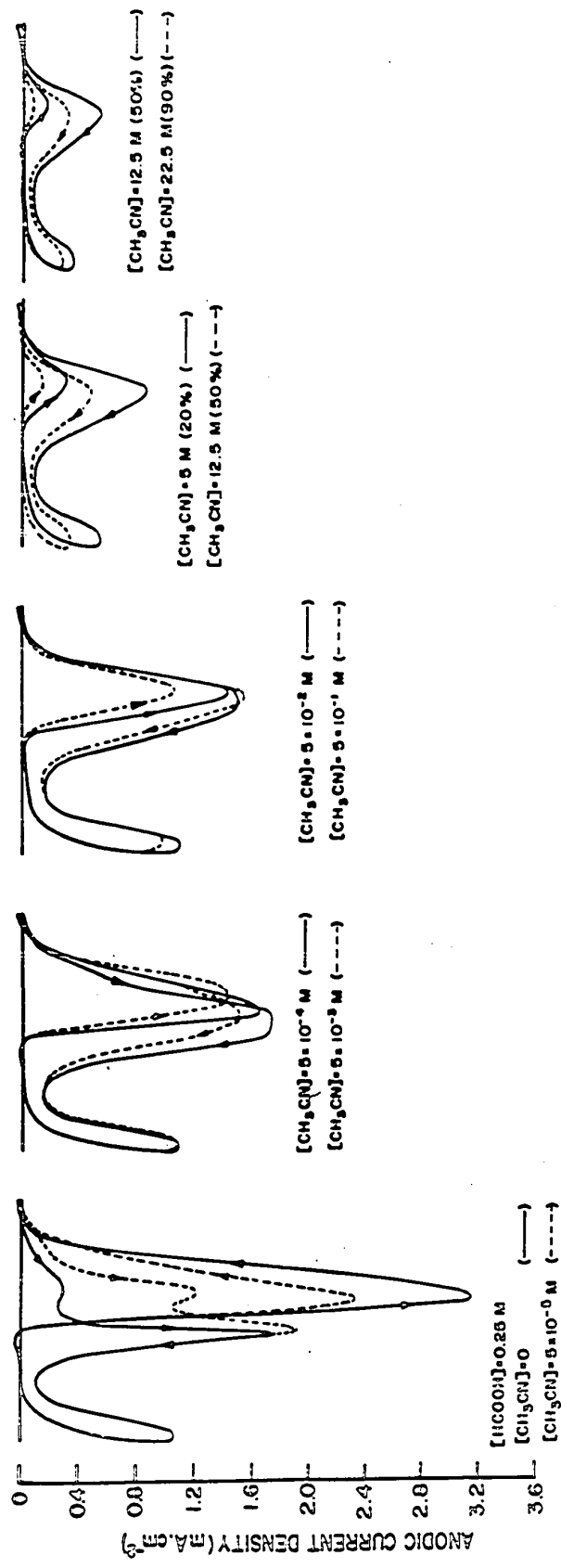
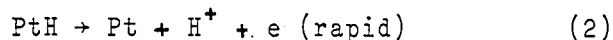
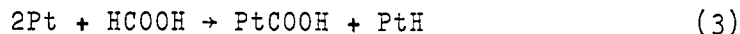


Fig. 48. Potentiodynamic i-V profiles for 0.25M HCOOH at platinum with various concentrations of acetonitrile. (dV/dt) = 50 mV sec⁻¹, potential range 0.05 to 1.5 V, E_H.

order of 600% for acetonitrile concentrations of up to 5×10^{-2} M. At higher concentrations of acetonitrile, $(i_p)_{FA_1}$ begins to decrease; however, even at 2M acetonitrile, $(i_p)_{FA_1}$ is still greater than its value measured in the absence of acetonitrile, i.e. in 1N H_2SO_4 , 0.25M $HCOOH$.

The dependence on acetonitrile concentration of the peak current for formic acid oxidation observed on the cathodic-going sweep, $(i_p)_{FC}$, can be seen in Fig. 48. In this case, there is a current decrease which follows, in a general way, the dependence of acetonitrile coverage at platinum on its concentration (see Fig. 13). The decrease of $(i_p)_{FC}$ is quite rapid at low acetonitrile concentrations but varies less sensitively with concentration in the range where acetonitrile coverage only changes slightly with further increases in $[CH_3CN]$. The rate of decrease of the formic acid current peak on the cathodic sweep can be compared with that for methanol on the cathodic sweep where the current has decreased to zero at $[CH_3CN] = 1.6 \times 10^{-3}$ M (Fig. 46). The less sensitive dependence of the currents for formic acid oxidation on $[CH_3CN]$ can be correlated with the requirement of only one free platinum site for the dissociative chemisorption:



It is to be noted that while two sites are required for the initial adsorption of the formic acid molecule, the site on

which atomic hydrogen is adsorbed immediately becomes vacant (because of the rapid coupled anodic reaction of H ionization at appropriate potentials) so that further formic acid adsorption can occur. Also, it will be shown below that although one formic acid molecule probably gives rise to only one chemisorption bond with platinum, the molecule effectively shields three platinum atoms. The implications of this fact with regard to the reaction mechanism are discussed on p.194.

The formic acid oxidation peak on the anodic-going sweep at 1.3 V, E_H is almost independent of acetonitrile concentration up to $[CH_3CN] = 5 \times 10^{-2}$ M (Fig. 48). There is a slight increase in peak current initially with increasing acetonitrile concentration which can be due to a contribution from the oxidation of acetonitrile which is observed in this potential region (section I.4(b)). That the increase is not due to an activation effect of the type observed for formic acid oxidation in the double-layer region will become evident following the explanation for the latter effect to be given below. The peak current for methanol oxidation on the anodic sweep at 1.3 V, E_H continuously decreases with increasing $[CH_3CN]$ (Fig. 46); however, it is not possible to separate this peak from that for acetonitrile oxidation itself since, at higher $[CH_3CN]$, the observed peak current for methanol at 1.3 V, E_H is the same order of magnitude as that for acetonitrile oxidation in this potential region.

The peak current for formic acid oxidation at ca.

0.9 V, E_H , i.e. in the potential region corresponding to the initial stages of surface oxidation of platinum, decreases with increasing $[CH_3CN]$. However, the dependence of i_p for this reaction on $[CH_3CN]$ could be determined only up to $[CH_3CN] = 1 \times 10^{-4}$ M because at higher concentrations of acetonitrile, e.g. 5×10^{-4} M, this peak at ca. 0.9 V, E_H begins to merge with the double-layer peak, FA_1 , as shown in Fig. 48, and eventually only one peak can be distinguished. The resulting peak may contain a component of formic acid oxidation originally observed at ca. 0.9 V, E_H but it is completely obscured by the broad and large FA_1 peak which has increased substantially with increasing $[CH_3CN]$. It is assumed that the anodic current peak at 0.9 V, E_H arises from reaction of formic acid with the initial surface oxide on platinum (see reaction 5), the decrease of the peak with $[CH_3CN]$ is consistent with the experimental fact, demonstrated in section I.4(b), that acetonitrile decreases the extent of surface oxidation at a given potential at platinum.

The major effect of interest is the activating effect which acetonitrile has on the FA_1 reaction of formic acid at platinum. Similar activating effects by what would normally be regarded as catalyst poisons have also been observed by Binder et al (134) who found that partial coverage of the electrode by sulfur from sulfide enhanced the electro-catalytic activity of the surface for formic acid oxidation. Satisfactory explanations for these effects have not yet been

provided; consequently, the main purpose of the work to be described in this section will be to determine the reason(s) for the activation effect described above by working under different conditions of the electrode surface with various catalyst poisons.

(c) Role of acetonitrile in formic acid oxidation

In general, there are two possible explanations for the observed effect of acetonitrile on the FA_1 reaction:

(i) it is a true activation effect with the adsorbed acetonitrile having a direct influence on the rate of oxidation of formic acid either by altering the catalytic efficiency of the platinum electrode or by serving as an activating intermediate in the overall reaction; (ii) it is an indirect effect, i.e. the acetonitrile influences some species which is an inhibitor for the reaction in such a way that the species no longer inhibits the formic acid reaction. To distinguish between these two possibilities, the FA_1 reaction itself was first investigated in the absence of acetonitrile.

It has been shown above (p.65) that acetonitrile adsorbs on the platinum surface and decreases the coverage of adsorbed hydrogen. To determine if acetonitrile increases $(i_p)_{FA_1}$ by decreasing the hydrogen coverage, the formic acid reaction at platinum was studied by the potentiodynamic sweep method with different cathodic termination potentials in the cathodic sweep and hence with different amounts of

adsorbed hydrogen. An activation effect, similar to that found in the presence of acetonitrile, resulted when the sweep range was adjusted so as to exclude the hydrogen adsorption region (Fig. 49a). The dependence of $(i_p)_{FA_1}$ on the termination potential in the cathodic-going sweep is shown in Fig. 49b. The peak current is very sensitive to the reversal potential in the cathodic sweep, the increase of $(i_p)_{FA_1}$ with more positive reversal potentials indicating that a reaction in the cathodic potential region diminishes the rate of the FA_1 reaction.

In order to investigate the inhibiting effects described above in a formic acid solution which had not been subjected to extensive periods of cycling, an experiment was performed by adding deoxygenated formic acid to the electrolyte from a syringe at such a moment during a slow sweep that it would reach the electrode surface either before ($0.30 \text{ V}, E_H$ on the cathodic sweep) or after ($0.30 \text{ V}, E_H$ on the anodic sweep) the potential had passed through the range corresponding to the hydrogen adsorption/desorption region. The results are shown in Fig. 50. When formic acid is added during the cathodic-going sweep at $0.30 \text{ V}, E_H$, a small, transient oxidation current is observed as the formic acid reaches the electrode surface. On the next anodic sweep, the usual formic acid oxidation peaks result, the currents being of the same magnitude as they are in the multisweep experiment (i.e. after a number of repetitive cathodic and anodic sweeps

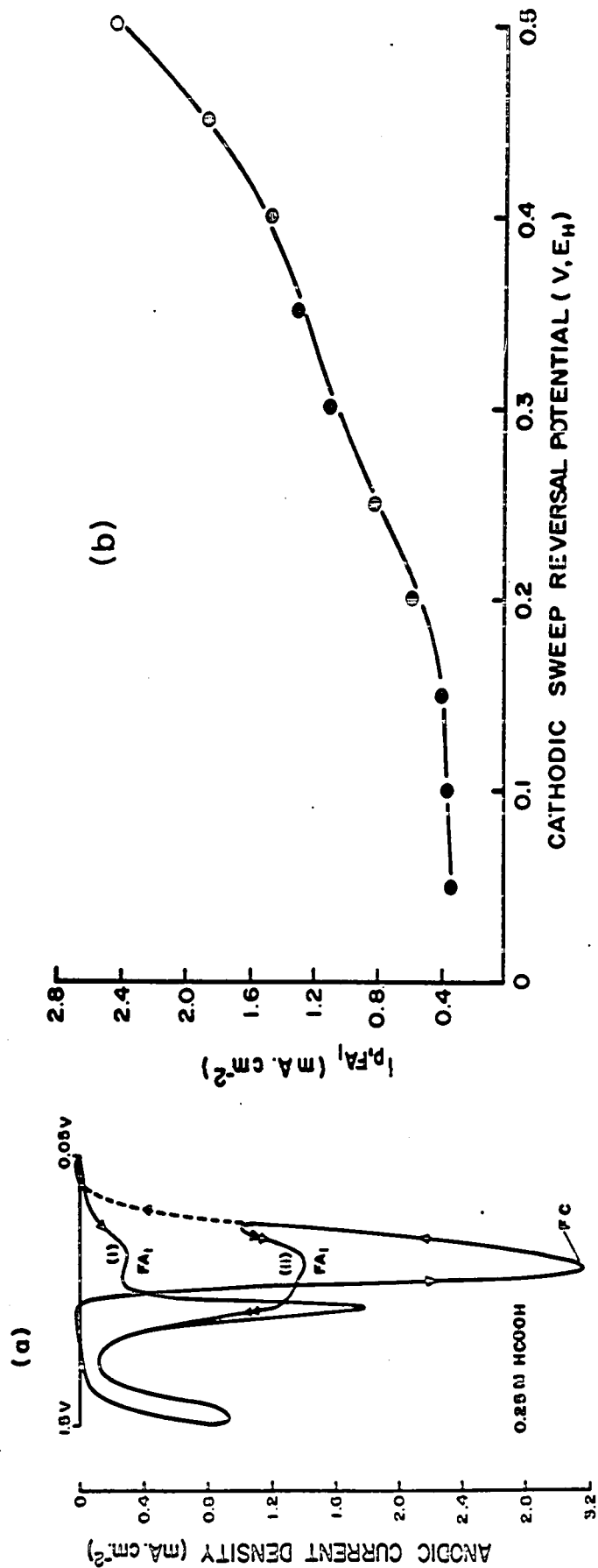


Fig. 49. (a) Effect of cycling in a restricted potential range, in this case without the H region, on the i-V profile for 0.25M HCOOH at Pt. (dv/dt) = 50 mV sec⁻¹, potential ranges: (i) 0.05 to 1.5 V,E_H; (ii) 0.05 to 1.5 V,E_H; (iii) 0.4 to 1.5 V,E_H.
 (b) Dependence of (i_p)_{FA₁} on termination potential in the cathodic sweep for the same conditions as described in (a).

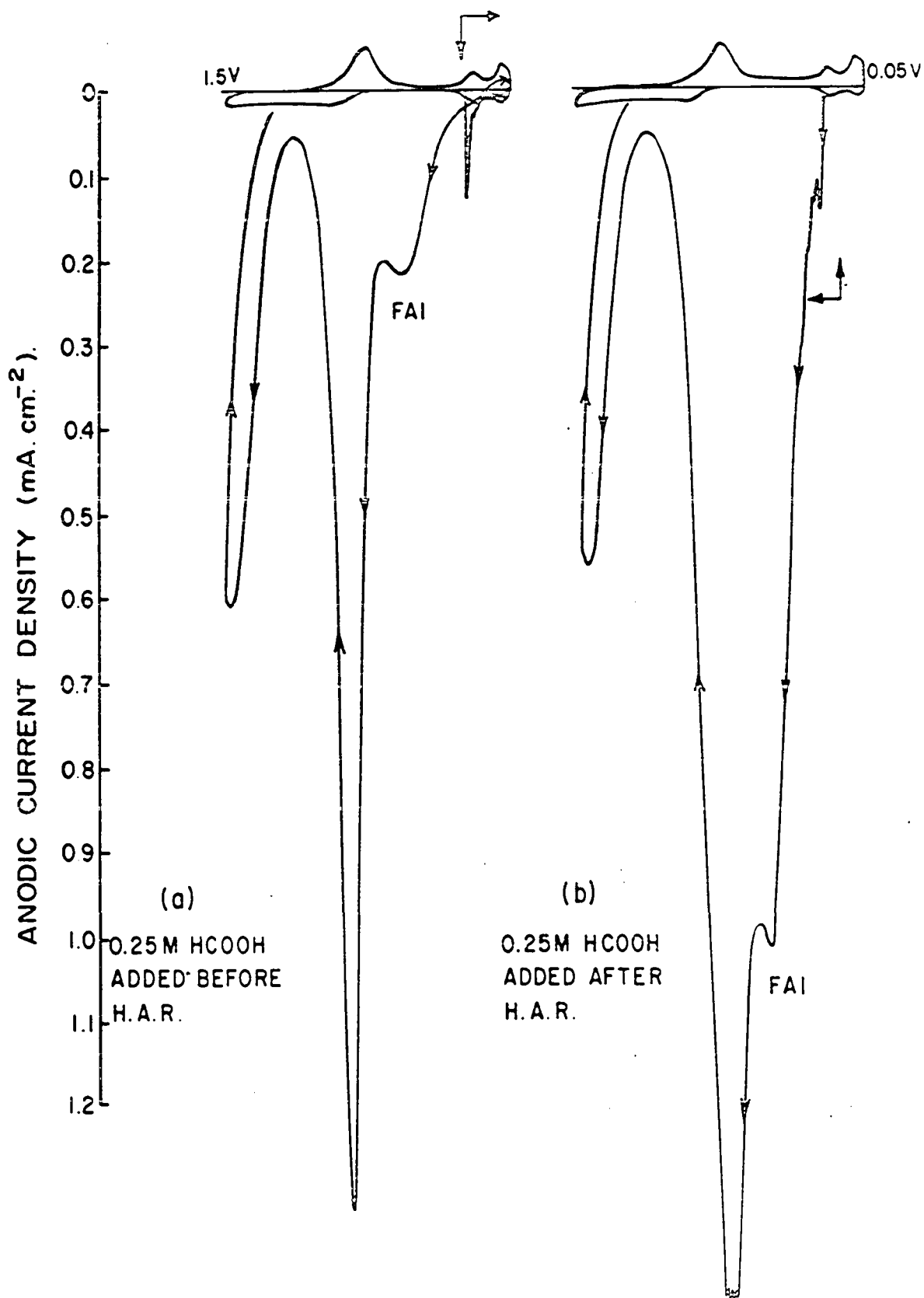


Fig. 50. Anodic-going potentiodynamic i - V profiles resulting from HCOOH addition at $0.3 \text{ V}, E_H$ on the cathodic-going sweep (a) and at $0.3 \text{ V}, E_H$ on the anodic-going sweep (b). $(dV/dt) = 25 \text{ mV sec}^{-1}$, potential range 0.05 to $1.5 \text{ V}, E_H$.

had been observed, with no further changes occurring). If the formic acid is added, however, during the anodic-going sweep at 0.30 V, E_H , i.e. after most of the hydrogen region has been traversed so that coverage by H is negligible when the formic acid reaches the surface, the FA_1 peak is much higher than on a multisweep; the peak at ca. 0.9 V, E_H is also higher but to a much smaller extent. It is evident that the increase in current for the FA_1 reaction in this experiment is associated with the absence of some reaction in the hydrogen region; these inhibiting reactions can occur even on an electrode surface which was fully covered with adsorbed hydrogen, as indicated by a decreased FA_1 peak after addition of formic acid at the cathodic end potential in a sweep, i.e. 0.05 V, E_H relative to that for addition of formic acid at 0.3 V in the anodic sweep.

The influence of acetonitrile on $(i_p)_{FA_1}$ when cycling is restricted to the potential range 1.5 to 0.4 V, E_H , i.e. in the absence of the hydrogen region, is shown in Fig. 51. Although the current does increase by ca. 30% in the presence of acetonitrile, this is insignificant in comparison with the 600% increase in $(i_p)_{FA_1}$ which results from addition of acetonitrile to the system with cycling in the range 1.5 to 0.05 V, E_H (Fig. 47). These observations suggest that acetonitrile increases $(i_p)_{FA_1}$ through an effect which is similar to that brought about by cycling over a restricted potential range, excluding the H region. The acetonitrile

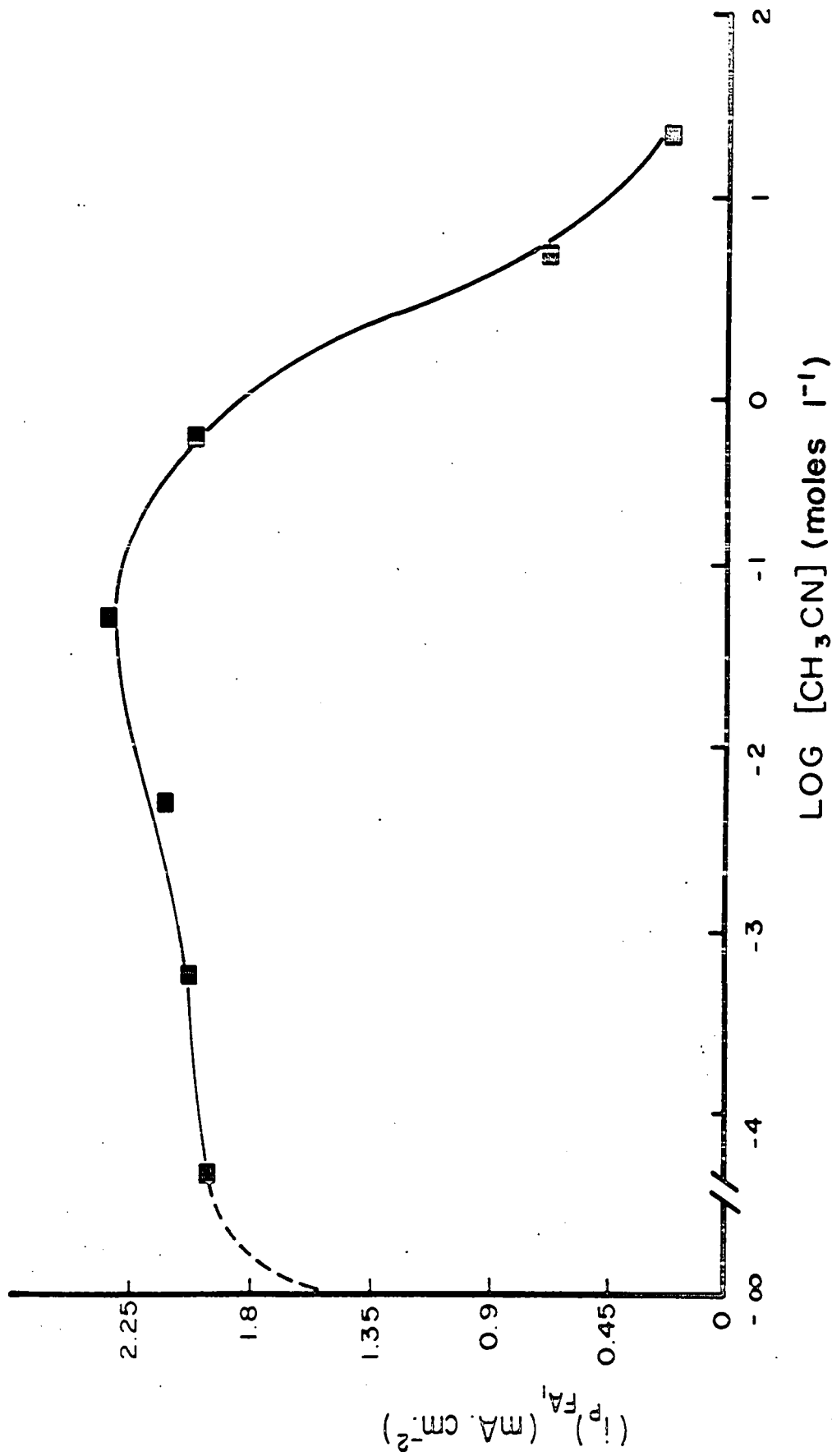


Fig. 51. Dependence of $(i_p)_{FA1}$ for 0.25M HCOOH at Pt on $[\text{CH}_3\text{CN}]$ when cycling is restricted to the range 0.4 to 1.5 V, E_H , i.e. in the absence of the H region.

allows the peak current for FA_1 to attain a value which is closer to that which would arise in the absence of poison, i.e. the acetonitrile diminishes the extent of formation of the poison species. Hence, acetonitrile increases $(i_p)_{FA_1}$ in an indirect fashion, in agreement with possibility (ii) above. Although it would initially appear that acetonitrile increases $(i_p)_{FA_1}$ by decreasing the hydrogen coverage, it will be shown below that the indirect role of acetonitrile in the formic acid reaction is quite different from this proposal.

The effect of CH_3CN is not due to some non-steady state effect, i.e. because the i - V profile was measured under potentiodynamic conditions, as is shown by the results in Fig. 52 where the steady-state point-by-point i - V profile (90 sec per point) is shown in relation to the 50 mV sec^{-1} profile. Slow time effects in the point-by-point curve are also indicated by the direction of change from the (X) to the (O) points during the 90 second observation time and a probable explanation for this behavior is given below. It is clear that the activating effects of CH_3CN are even larger on the steady-state curve than on the dynamical one and all the features of the results of Fig. 48 are retained in the steady-state behavior.

In order to investigate the role of acetonitrile in the formic acid oxidation reaction in the double-layer potential region, an experiment was performed with acetonitrile which was identical in design to that described above

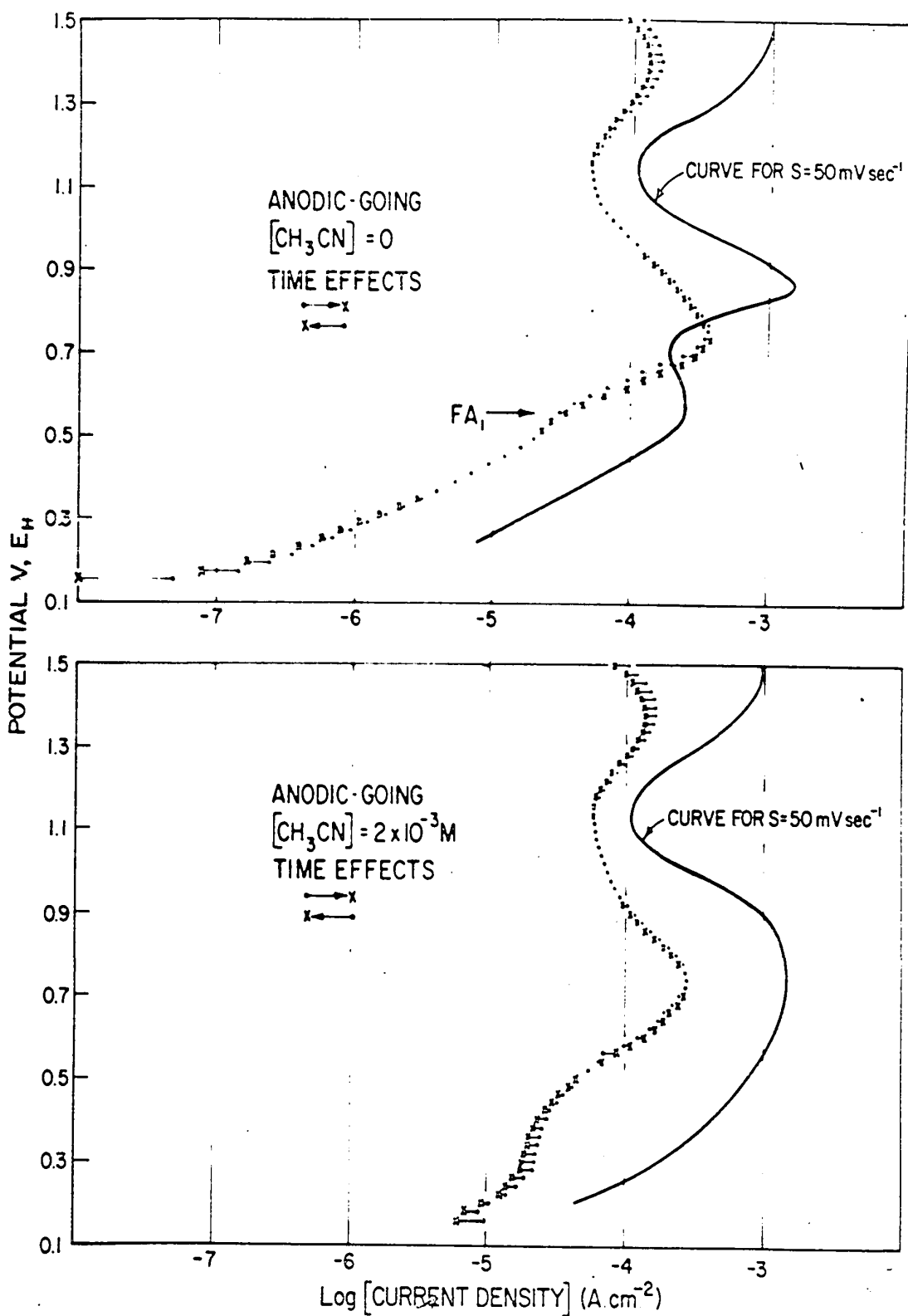


Fig. 52. Relation between steady-state point-by-point i - V curves for 0.25M formic acid oxidation in the presence and absence of CH_3CN ($2 \times 10^{-3} \text{ M}$ in 1N aq. H_2SO_4) and the corresponding potentiodynamic i - V profiles taken at 50 mV sec^{-1} over the same potential range in anodic-going direction.

for formic acid, i.e. additions of CH_3CN (5×10^{-4} M) were made to the 1N aq. H_2SO_4 already containing 0.25 M HCOOH before and after cycling through the atomic hydrogen region. Fig. 53 shows that the acetonitrile is effective in increasing the FA_1 peak current on the next anodic sweep only when it has been added before the electrode potential has been driven into the range where atomic hydrogen electro-sorption occurs. When, however, the addition is performed after the hydrogen region has been traversed, i.e. at 0.30 V, E_{H} on the anodic-going sweep, no increase in the FA_1 peak current is observed during that sweep; however, there is understandably an increase in current on the succeeding anodic sweep because the acetonitrile will have been present in the system during that sweep through the atomic hydrogen region.

Under conditions when acetonitrile is added before the potential in the cycle has reached that for H electro-sorption, the FA_1 peak is higher after the second cycle through the hydrogen region. This difference may originate because the potential range over which the poisoning effects determining the FA_1 peak current are observed is not necessarily restricted to the hydrogen region but extends to more anodic potentials, * e.g. where the maximum current in the FC peak arises (see section III(e) below). It will only be on the second cathodic cycle after addition of acetonitrile that this region will be

* This observation is one of several used in section III(e) to prove that acetonitrile does not increase $(i_p)_{\text{FA}_1}$ by diminishing the hydrogen coverage.

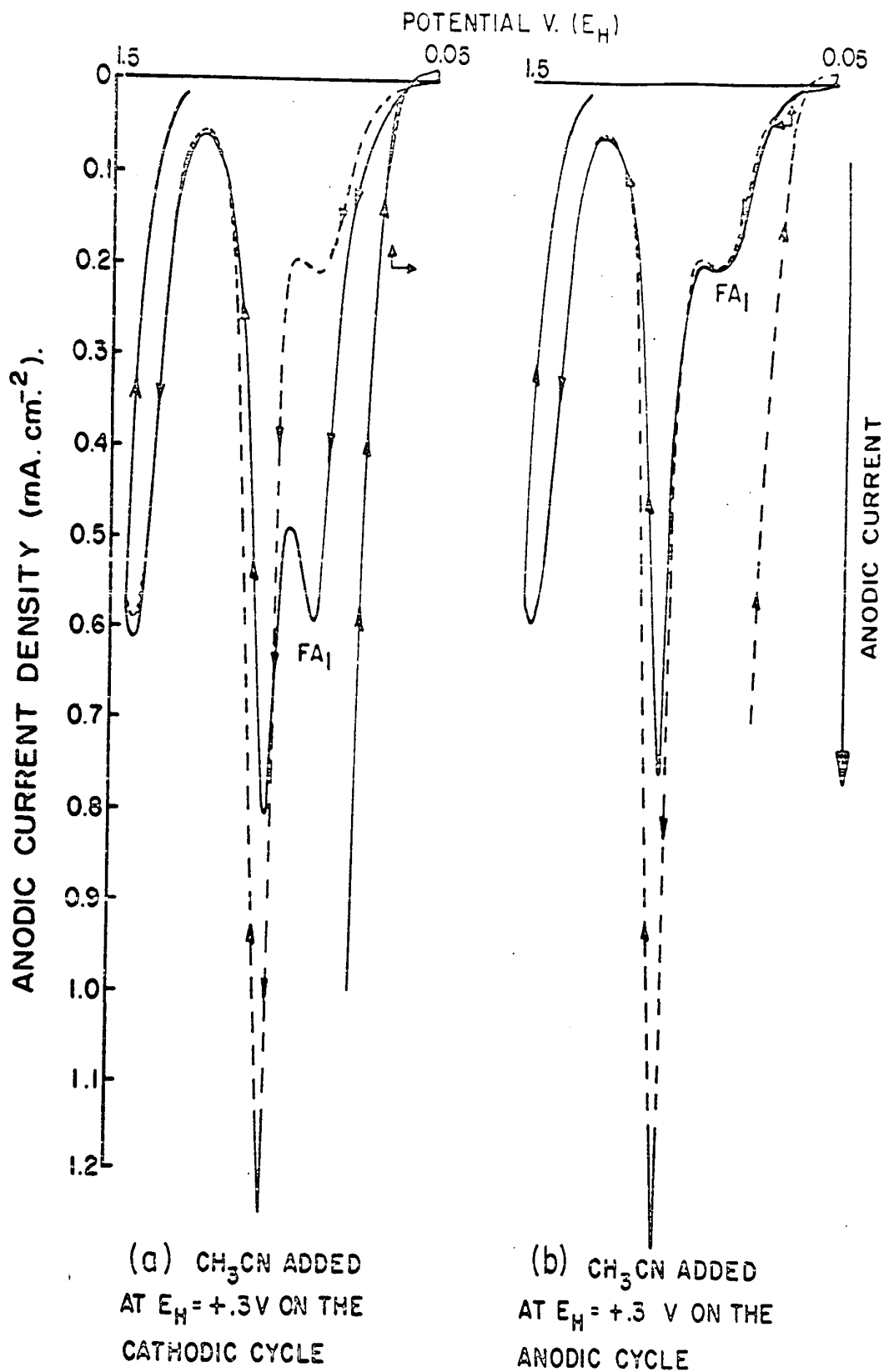


Fig. 53. Anodic-going potentiodynamic i - V profiles for 0.25M HCOOH resulting from addition of $5 \times 10^{-4}\text{M}$ CH_3CN at 0.3 V, E_H on the cathodic-going sweep (curve a) and 0.3 V, E_H on the anodic-going sweep (curve b). $(dV/dt) = 25 \text{ mV sec}^{-1}$, potential range 0.05 to 1.5 V, E_H .

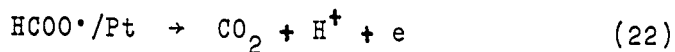
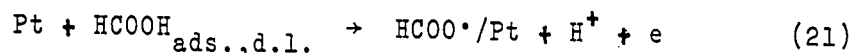
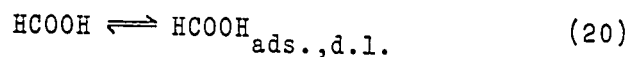
affected by the additive when the addition has been made at 0.3 V, E_H on the cathodic sweep. Slower sweep speeds (25 mV sec⁻¹) were employed in these experiments to ensure that the time of diffusion of the additive to the surface was not responsible for the observed differences; the similarity of these results to those obtained at faster sweep rates (50 mV sec⁻¹) shows that diffusion was not a significant factor. In fact, the differences on the first and second anodic sweeps mentioned above are consistent with the results of Fig. 51 which shows that acetonitrile has an effect on the FA_1 peak current even when the cycling is restricted to a potential range in which H electro sorption is excluded.

In general, the results described above can be best interpreted by supposing that acetonitrile increases the FA_1 peak current by blocking sites on the surface where a reaction producing an inhibiting species, p, can occur. When the acetonitrile is added at 0.3 V, E_H on the cathodic sweep, it subsequently adsorbs on the surface and blocks sites for the production of poison. However, when the acetonitrile is added at 0.3 V, E_H on the anodic sweep, p has already formed and it would seem that acetonitrile cannot displace it from the surface. The implications of the results with regard to reaction mechanisms are examined below.

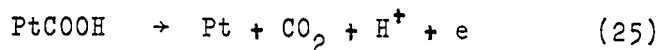
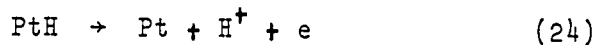
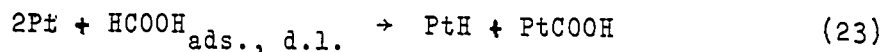
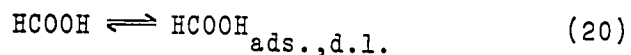
(d) Relation to mechanism of formic acid oxidation

The effects of acetonitrile described above must be examined in relation to the mechanism of oxidation of formic acid itself, particularly with regard to the behavior of the HCOOH molecule at the bare platinum surface and at the surface on which coadsorbed hydrogen is present.

Two main pathways for HCOOH oxidation have been proposed, one involving oxidative electrosorption at the carboxylic acid group (135):



and the other involving dissociative chemisorption with coupled electrochemical oxidation steps (28):



Both pathways involve physically and electrostatically adsorbed HCOOH molecules in the double-layer prior to chemisorption.

One of the main features of interest in the kinetics of formic acid oxidation is that the kinetics of the reaction, i.e., the current density at various potentials, does not increase in relation to the coverage of chemisorbed species on the electrode as deduced from oxidative and reductive (H accommodation) transients. In fact, under some conditions the oxidation current falls as the coverage by adsorbed species increases (23,26,136,137), a conclusion which was interpreted by Brummer (23) in terms of formation of a blocking species which is produced in a step in parallel with the main reaction sequences shown above. Such a species cannot therefore be $\text{HCOO}\cdot$ or $\cdot\text{COOH}$, either of which are involved in the main reaction. The blocking species is also responsible for long-time effects in which the activity of an initially cleaned electrode for HCOOH oxidation decreases after exposure to HCOOH solution.

Various possible inhibiting species, such as CO , "reduced CO_2 ", HCOO^- anion, and $\begin{array}{c} \text{CHO} \\ | \\ \text{COOH} \end{array}$ (glyoxalic acid) formed by dehydration of two HCOOH molecules, have been discussed (23). CO , "reduced CO_2 " and HCOO^- anion have, however, been discounted as the inhibiting species on the basis of various arguments given by Brummer and Makrides (23); it is also unlikely that the HCOOH molecule itself (24) can be the inhibiting agent unless some dissociatively chemisorbed condition of the molecule is established.

In the present work, the results obtained with acetonitrile suggest that an adsorbed species plays a

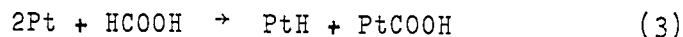
significant role in the formation of p. Two possible proposals may be offered for the reaction which forms the inhibitor and leads to the effect of acetonitrile:

i) the inhibitor is formed in a reaction between adsorbed H and the adsorbed species derived from formic acid oriented on the surface in the proper geometry. Once the poison is formed, the acetonitrile cannot displace it and hence has little effect (Fig. 53). In the case where acetonitrile addition is made before the poison has been formed in the H region, adsorption of H is blocked by the adsorbed acetonitrile (as discussed earlier in this Chapter) so that poison cannot be formed;

ii) the poison is formed in a potential-dependent reaction, without the participation of adsorbed hydrogen and, in this case, when the poison is formed it cannot be displaced with acetonitrile. Acetonitrile could, however, displace whatever formic acid species is the reactant in the poisoning reaction; hence, addition of the nitrile before the poison is formed could give rise to an increase in the FA_1 peak current.

With regard to (i), the fact that the activating effect of acetonitrile is also, but in a much diminished way, experienced outside the normal hydrogen adsorption region on platinum (Fig. 51) seems to indicate that presence of adsorbed hydrogen is not an essential requirement for the reaction which produces inhibiting species giving rise to the decrease in the FA_1 peak current. However, in the course of formic acid

oxidation there is always a transitory but low coverage with atomic hydrogen even at potentials anodic to 0.35 V, E_H due to the reaction



A decision between the two proposals given above can be made after discussing the kinetics of formation of p in the next section.

(e) Time effects in the hydrogen region

The results presented above indicated that acetonitrile influences $(i_p)_{FA_1}$ because of its effect on formation of the poisoning species p. The sweep rate and thus time spent in the adsorbed hydrogen region, t_H , plays a very important role in the reaction which produces the p species. In order to study the dependence of $(i_p)_{FA_1}$ on time, t_H , without complications from its own dependence on sweep rate, (dV/dt) was carefully varied in only the adsorbed hydrogen region, a standard sweep rate of 50 mV sec^{-1} being always employed over the potential range of the FA_1 process. The result is shown in Fig. 54 where $(i_p)_{FA_1}$ is plotted as a function of t_H . At a relatively fast sweep rate (200 mV sec^{-1}) and correspondingly short time (3 sec) in the hydrogen region, the FA_1 peak current (observed still at 50 mV sec^{-1}) increases by 500% over the value observed after a slow sweep (12.5 mV sec^{-1} , $t_H = 56 \text{ sec}$) through the hydrogen region.

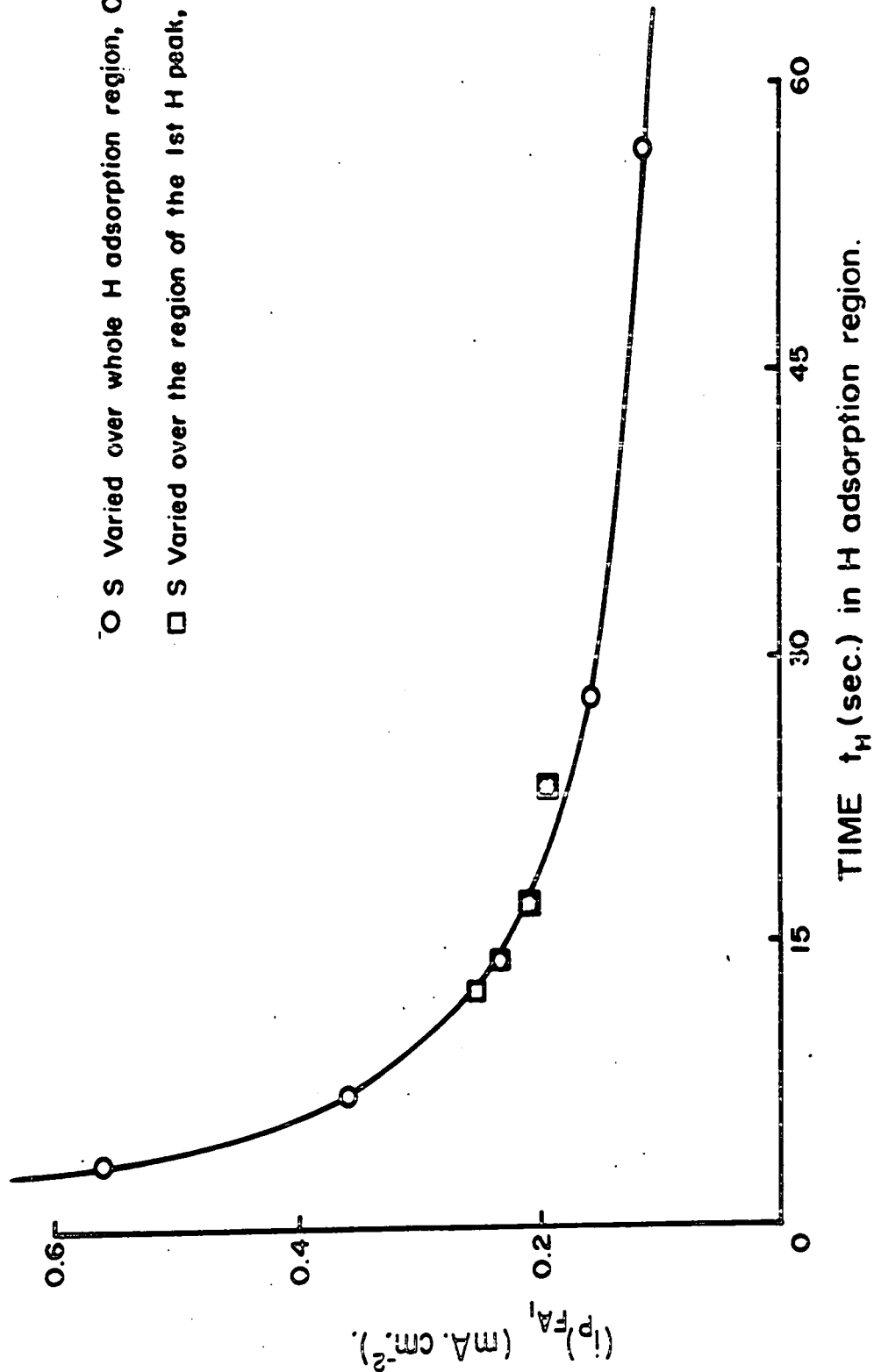


Fig. 54. Peak current for FA_1 process as a function of time t_H spent in the H region in potentiodynamic sweeps. $[HCOOH] = 0.25M$, (dV/dt) in FA_1 region = 50 mV sec^{-1} , potential range 0.05 to 1.5 V, E_H .

It is to be noted that the percentage change in $(i_p)_{FA_1}$ between various sweep rates decreased quite sharply upon going to slower sweep rates. Evidently, under the latter conditions, the time spent in the H adsorption region is sufficient to allow the production of poison to be more or less complete (Fig. 54). At faster sweep rates, even small changes in t_H give significant changes in $(i_p)_{FA_1}$, because t_H was short in comparison with the time required for the production of p to be complete.

It was noted above that the cathodic end potential in the potentiodynamic sweep for formic acid oxidation at platinum has a profound effect on the oxidation peak current for the FA_1 process as shown in Fig. 49b. The major increase in $(i_p)_{FA_1}$ occurs at potentials where θ_H for Pt in aq. H_2SO_4 , in the absence of CH_3CN or $HCOOH$, would have decreased to <0.3 , i.e., at potentials more positive than $0.20 V, E_H$. Again, a problem exists in that the hydrogen coverage during the $HCOOH$ reaction may be finite (though small) even at potentials anodic to $0.3 V, E_H$; this is coupled with the indications (138) that the $HCOOH$ reaction occurs only on 10% of the available platinum surface, the remaining 90% being occupied either by p or H at low anodic potentials. Hence, even quite small coverages by H could have significant kinetic effects for that 10% of the platinum surface on which formic oxidation actually occurs.

Although the increase of FA_1 peak current as the cathodic termination potential of the sweep is made more

positive can be explained in terms of the production of less poison due to lower θ_H , the same, or an even higher degree of poisoning of the FA_1 reaction can be achieved by holding the potential for various periods of time at more anodic values in the H region, i.e., potentials at which θ_H is smaller. Fig. 55 shows the results of this kind of experiment with respect to $(i_p)_{FA_1}$ values and the effects of various holding times t_h at the different end cathodic potentials are easily seen. It is to be noted that the maximum decrease of FA_1 peak current occurs at a cathodic end potential of 0.20 V, E_H ; in fact, 5 sec of cathodic holding at this potential gives a value of $(i_p)_{FA_1}$ equivalent to that observed after 40 sec of cathodic holding at 0.1 V, E_H .

These results (Figs. 54 and 55) indicate that the formation of p is a slow reaction, the maximum rate occurring at ca. 0.2 V, E_H and decreasing at either more cathodic or more anodic potentials. Actually, significant quantities of p can still be formed at 0.5 V, E_H with sufficiently long holding times, t_h . At this potential, the adsorbed hydrogen resulting from dissociation of formic acid will be immediately ionized from the surface. Since the formation of p is slow and would hence require the adsorbed reactants to be present on the surface for some time, atomic hydrogen is evidently not necessary for p formation. This leaves proposal (ii) on p.163 as an explanation of formation of p and the effects of acetonitrile on the reaction.

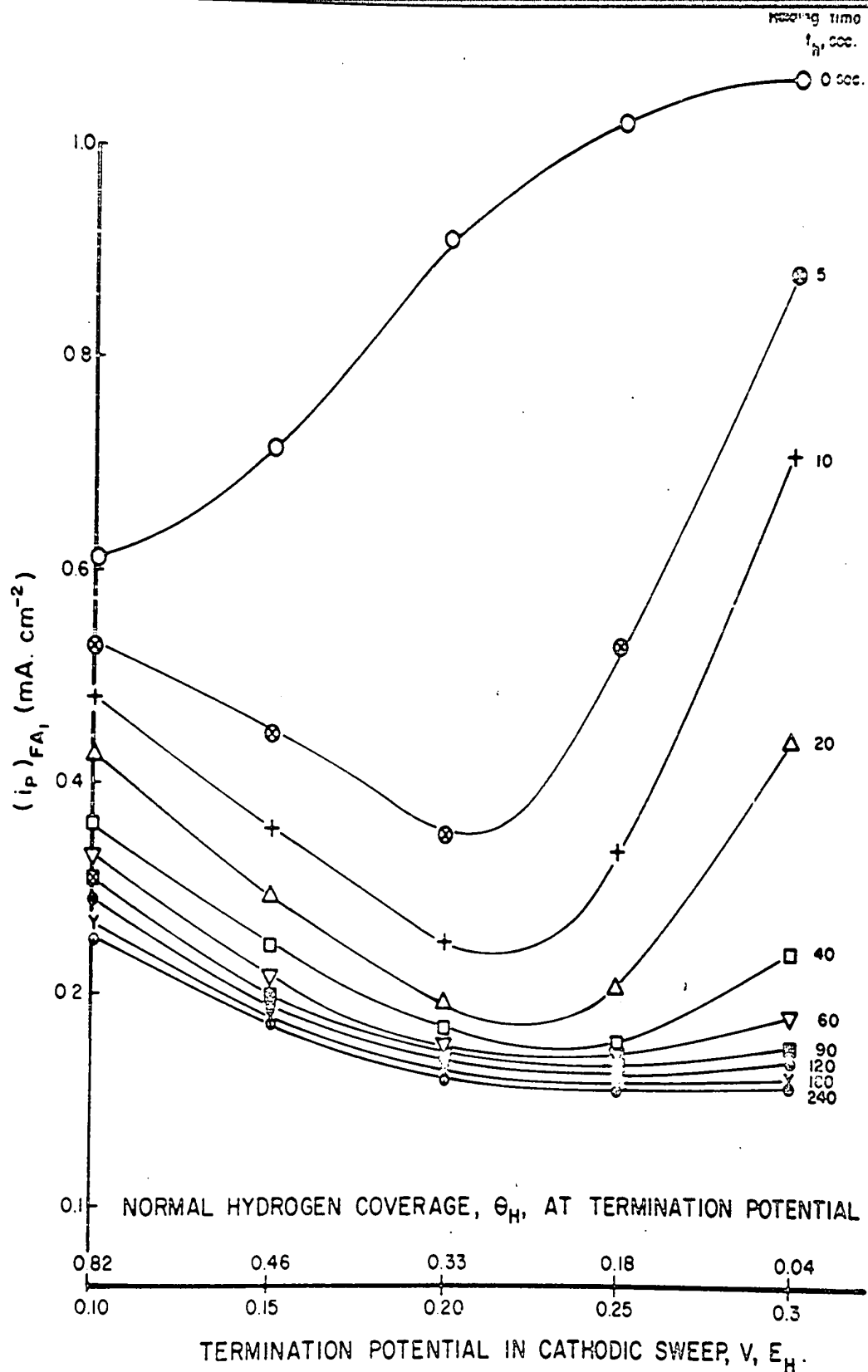
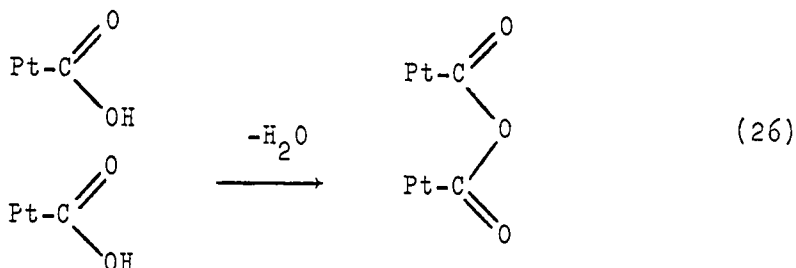


Fig. 55. Dependence of $(i_p)_{FA_1}$ on termination potential in the cathodic sweep for various holding times, t_h , at that potential. Also shown on non-linear scale are the corresponding H coverages in 1M H_2SO_4 at the different cathodic termination potentials. $[HCOOH] = 0.25M$, $(dV/dt) = 100 \text{ mV sec}^{-1}$ to minimize t_h effects in comparison with t_h in the H region, potential range to 1.5 V, E_H .

There are evidently three factors which are important in the production of the poison: i) the time spent at a given potential; ii) the electrode potential itself; iii) the free space available for the adsorption of HCOOH which can then form the poison. It is difficult to distinguish (ii) from (iii) because of the dependence of coverage with adsorbed species on potential; however, the contribution of (i) to the reaction of p formation can be separated. Reversing the cathodic-going sweep at more positive potentials results in a shorter period of time being spent in the overall hydrogen region as well as the obvious exclusion of a certain potential region in the sweep. The FA_1 peak current was found to increase 67% when the cathodic end potential was changed from 0.10 to 0.25 V, E_H (Fig. 55) while the increase was only 42% when the sweep rate was adjusted so that the hydrogen region is traversed 3 sec faster with the same (dV/dt) through the FA_1 peak (Fig. 54). This means that when the cathodic end potential is cut from 0.1 to 0.25 V, E_H , ca. 42% of the increase in $(i_p)_{FA_1}$ is associated with a time effect while ca. 25% is due to coverage and/or potential dependence of the reaction which forms the poison.

From the above evidence, it appears that p is formed in a slow reaction, involving adsorbed formic acid species, which is parallel to the oxidation reaction. Formation of p is very dependent on the coverage by formic acid species, the maximum formation rate being at 0.2 V, E_H where coverage with formic acid species is at a maximum (24,28).

The reaction of formation of poison must be a type of "dimerization" on the electrode surface between adsorbed formic acid species which thereby lowers the coverage with the electrochemically reactive species, i.e. -COOH. It cannot be a poison arising independently of the adsorbed formic acid species, e.g. a poison such as chloride ion (138), since there is no reason why displacement of such a poison by acetonitrile should increase $(i_p)_{FA_1}$. Indeed, one poison has simply been replaced by another in such a case. A possible reaction between two adsorbed formic acid molecules adjacent to each other on the electrode surface is dehydration; thus:

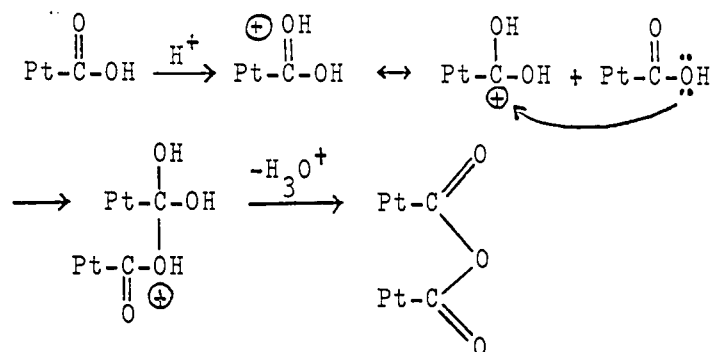


The poison p in this case is formic anhydride formed by dehydration of two adjacent adsorbed formic acid species.* This reaction diminishes the surface available for reactive formic acid species, transforming it instead into the anhydride species which is unreactive except at higher anodic potentials (>ca. 0.9 V, E_H). Acetonitrile adsorbs on the surface and acts as a third body, decreasing the coverage with adsorbed formic acid so that there is less chance that two reactive species

* A geometric requirement for the above reaction may exist that would limit the reaction of anhydride formation to those adjacent formic acid species on the surface which have the proper geometry.

will be adjacent to one another and thus undergo dehydration.

The mechanism of reaction (26) may be written as follows:



Although the formation of formic anhydride has not been observed in solution, it is proposed that the above reaction is possible since the formic acid is in an adsorbed state on the platinum surface. The identity of the p species as formic anhydride formed by the above reaction mechanism is supported by the observed potential dependence of the rate of formation of p. Significant p formation only occurs in the cathodic potential region, i.e. when the electrode is acting as a source of electrons. This is in agreement with the reaction mechanism since electron donation by the platinum will tend to increase the rate of protonation of the adsorbed formic acid species with stabilization of the resulting protonated species and will also increase the nucleophilicity of those adsorbed species which are not protonated, i.e. the attacking species. At more positive potentials the rate of reaction (26) should decrease since the platinum is then acting as an electron withdrawing agent.

(f) Effect of higher concentrations of acetonitrile

As the concentration of acetonitrile increases in the formic acid system, the effects of the "B" species, discussed on p. 74, become evident. The manner in which $(i_p)_{FA_1}$ varies with $[CH_3CN]$ in the potential ranges 0.05 to 1.5 V, E_H and 0.4 to 1.5 V, E_H was shown in Figs. 47 and 51. For acetonitrile concentrations up to 5×10^{-1} M, the $(i_p)_{FA_1}$ increases if the potential of the cathodic end of the sweep is cut to the more positive value of 0.4 V, E_H ; this would indicate that up to this $[CH_3CN]$, the major influence of the cathodic end potential is in the production of the poison p for the FA_1 reaction. For $[CH_3CN] > 5M$, sweep reversal at 0.4 V, E_H results in a decrease in FA_1 peak current in comparison with cycling to 0.05 V, E_H . At these high concentrations of acetonitrile, the H adsorption region is necessary for the maximum extent of reduction of adsorbed CH_3CN since reduction of the acetonitrile has the effect of creating free surface sites for other reactions (cf. Figs. 35 and 37 and p.122).

As the concentration of acetonitrile increases, its reduction becomes more important in so far as liberation of free surface sites is concerned. At a concentration of CH_3CN as high as 5M, the necessity for reducing the acetonitrile is a more important factor than the value of the cathodic end potential in producing the poison p for the FA_1 reaction. This idea is supported by the fact that at $[CH_3CN] > 1 \times 10^{-4}$ M and with a cathodic end potential of 0.05 V, E_H , the peak current for FC is less than the peak current for FA_1 . This indicates

that unreduced acetonitrile on the platinum surface poisons the oxidation of formic acid while reduction of the acetonitrile at more cathodic potentials in the H region decreases the acetonitrile poisoning effect. The same effect is also observed when the cathodic end potential is $0.4 \text{ V, } E_H$; hence, the potential does not have to be taken to high cathodic values for acetonitrile reduction to result. This corresponds with the conclusion reached in section I.1(f) where it was noted that acetonitrile is reduced already at $0.4 \text{ V, } E_H$ on platinum in aqueous H_2SO_4 , but the extent of reduction is smaller than that arising at more cathodic potentials down to $0.05 \text{ V, } E_H$.

Another point in support of the above view is the fact that cathodic holding at $0.4 \text{ V, } E_H$ gives a decrease in the peak current for the FA_1 reaction for $[\text{CH}_3\text{CN}] < \text{ca. } 5\text{M}$ at which point cathodic holding at $0.4 \text{ V, } E_H$ gives an increase in the peak current for the FA_1 reaction. All of these facts indicate that at high acetonitrile concentrations, $> \text{ca. } 5\text{M}$, the effect of the inhibitor produced from HCOOH in the cathodic potential region becomes secondary to the poisoning effects of unreduced acetonitrile in the form of the B species. However, even at $[\text{CH}_3\text{CN}] > 5\text{M}$, cathodic holding at $0.05 \text{ V, } E_H$ still results in a decrease in the peak current for reaction FA_1 . This decrease must be associated with the formation of the formic acid poison and also indicates that most of the acetonitrile reduction has occurred during the multisweep up to $0.05 \text{ V, } E_H$ at $(dV/dt) = 50 \text{ mV sec}^{-1}$. Further holding at $0.05 \text{ V, } E_H$ allows production of the formic acid poison and

hence decreases the peak current for reaction FA_1 in the manner described above. The decrease of $(i_p)_{FA_1}$ with cathodic holding at $0.05 V, E_H$ is still evident with 90% acetonitrile in the system. At such high concentrations of acetonitrile, there would only be a very small proportion of surface available with adsorbed, adjacent formic acid molecules; however, since the oxidation reaction occurs on only 10% of the surface, quite small amounts of adsorbed poison would be sufficient to noticeably decrease the FA_1 reaction current.

(g) Effects of mercury on the oxidation of formic acid at platinum

It was considered desirable to provide a further way of blocking H adsorption in formic acid oxidation experiments without introduction of another electroactive organic molecule such as acetonitrile. It was found that mercury met this requirement very well and it could be conveniently and controllably electro-deposited in sub-monolayer quantities at the platinum surface in aqueous H_2SO_4 using mercuric sulfate. This deposition of mercury was achieved under repetitive sweep conditions with the anodic reversal potential $<1.0 V, E_H$; the cathodically deposited mercury is not then oxidized off from the surface so that the mercury coverage on successive sweeps progressively increases as indicated by corresponding decreases of hydrogen coverage (Fig. 56). The rate of change of coverage by mercury depended on its concentration in solution, the rate of solution stirring and the anodic termination potential in

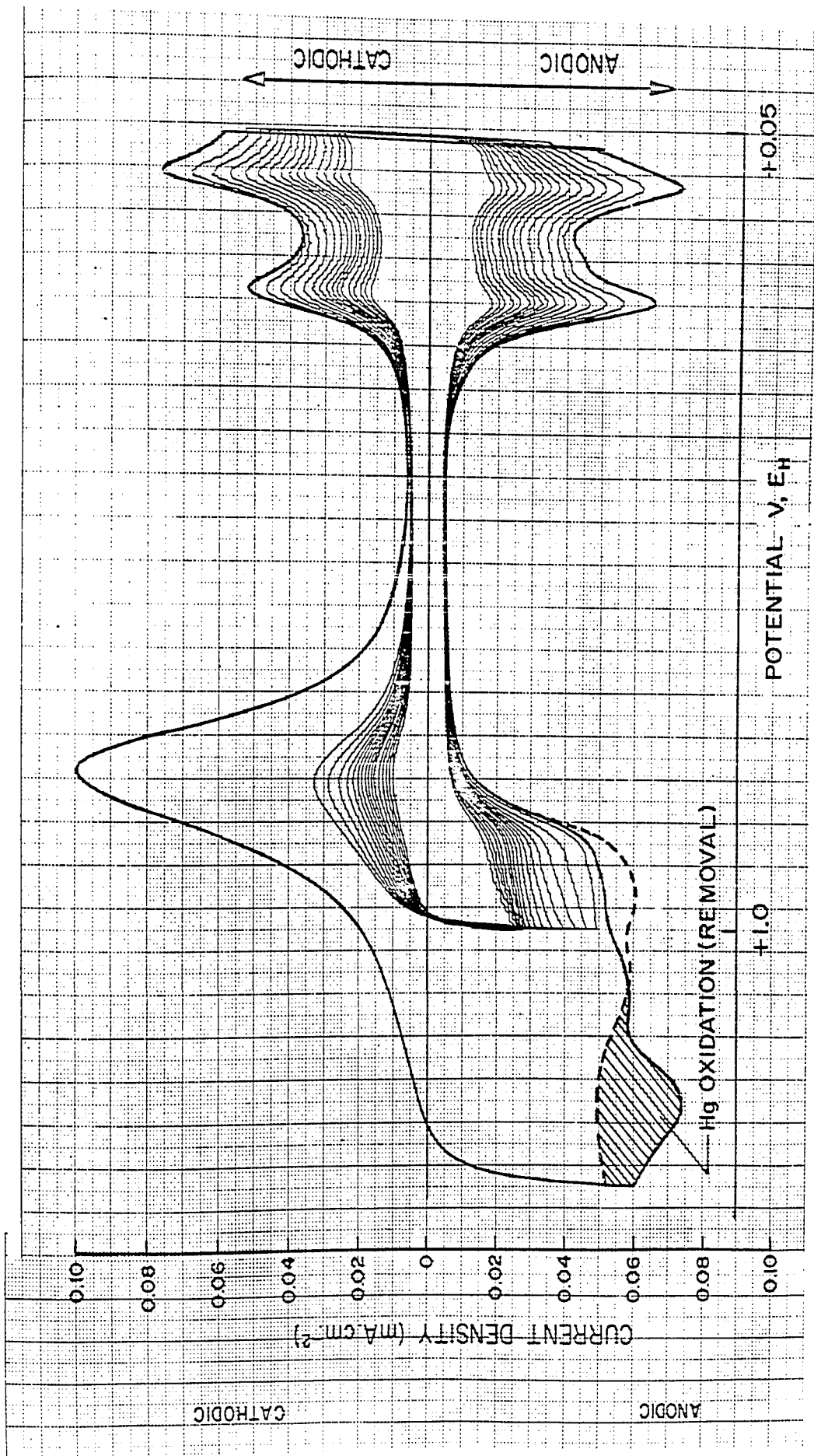


Fig. 56. Progressive blocking of H adsorption peaks at Pt (but with maintenance of their resolution) upon electrodeposition of Hg from $3 \times 10^{-6}M$ aq. $HgSO_4$ during successive cathodic sweep in potential range 0.05 to 1.0 V, E_H. Quantitative oxidation of deposited Hg is measured in an anodic sweep taken to 1.4 V, E_H.

the sweep. The electrodeposited mercury could be quantitatively oxidized from the surface by sweeping to 1.4 V, E_H , mercury oxidation giving rise to the new peak shown in Fig. 56.

By means of this method, the coverage with adsorbed hydrogen at platinum could be controlled over a wide range of values with only one concentration of mercury in the solution. For progressively increasing Hg deposition, it is of interest to note that the two main H peaks still remain completely resolved down to a high level of blocking by mercury. This indicates that mercury blocks the H adsorption on an individual site by site basis* rather than changing the state of H adsorption. This situation is of particular value for the studies with HCOOH where a large range of H coverages and corresponding values of free surface area were of interest.

Fig. 57 shows the variation of the FA_1 peak current with θ_H controlled by Hg deposition in the presence of formic acid. It is necessary to make the assumption (see below) that the hydrogen coverages observed in the absence of formic acid when the surface is progressively blocked by electrodeposited Hg (Fig. 56) change in proportion to those observed when formic acid is present. Thus, full hydrogen coverage, $\theta_H = 1$ in Fig. 57b, is to be regarded as the relative hydrogen coverage

* The possibility that the electrodeposited Hg simply forms 2-dimensional islands of Hg with otherwise free Pt sites is ruled out because the FA_1 peak current is increased by Hg (Fig. 57). If Hg had the effect of simply cutting the available surface area, all currents would be uniformly decreased.

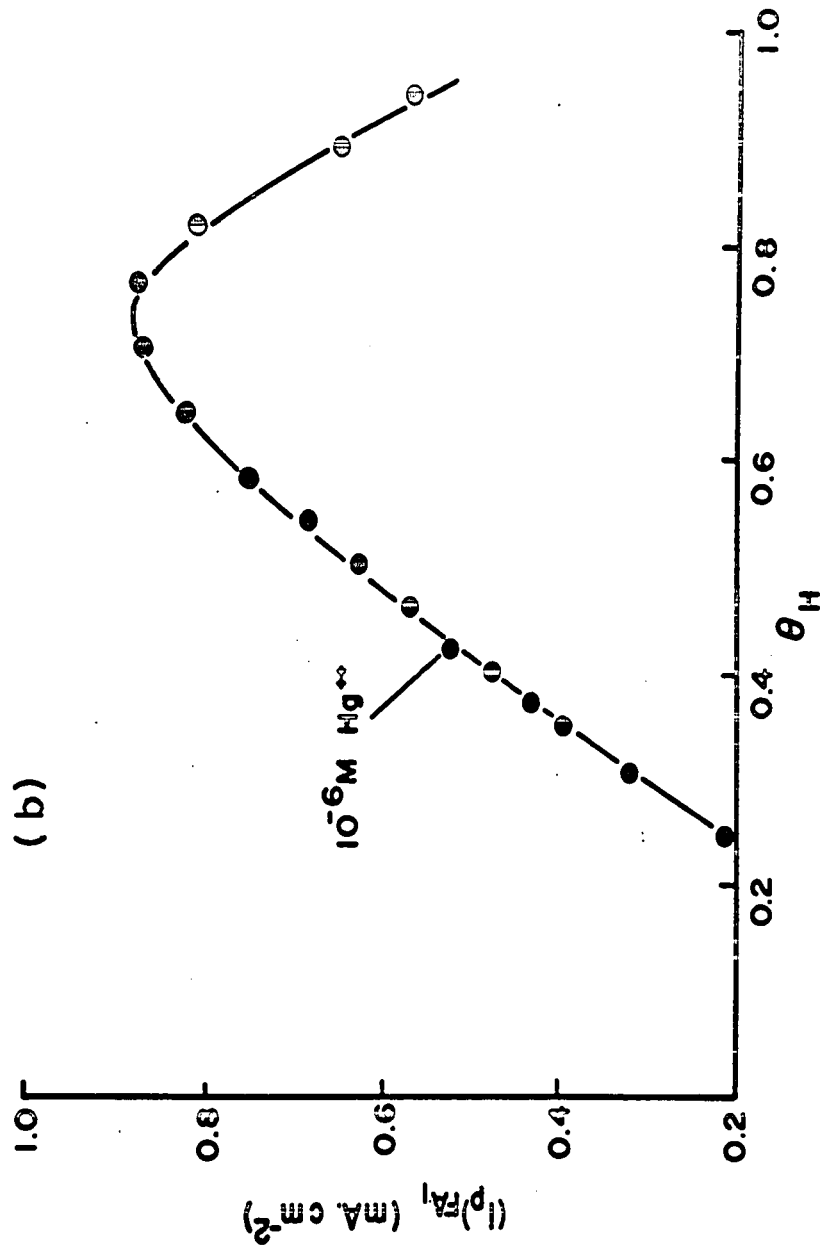
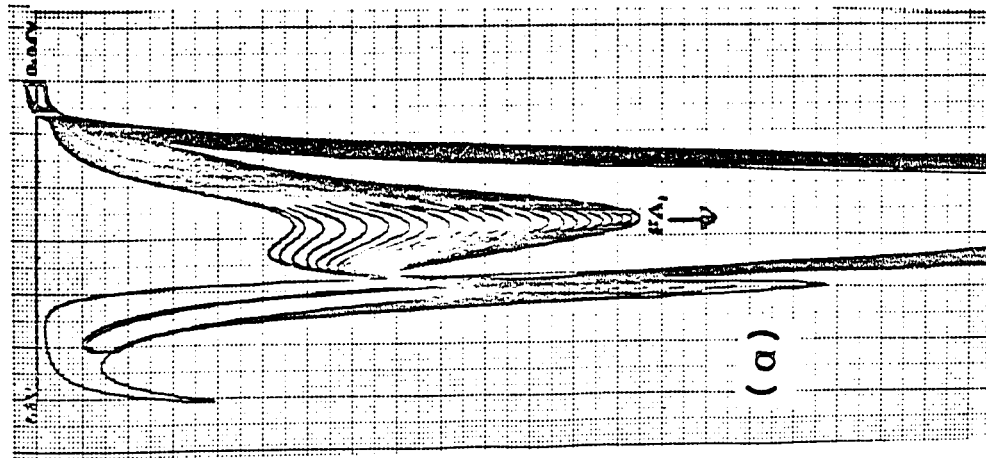


Fig. 57. (a) Variation of potentiodynamic i-V profile for 0.25M HCOOH at Pt with Hg electrodeposition, as in Fig. 56. $[HgSO_4] = 10^{-6}M$, $(dv/dt) = 50$ mV sec⁻¹, potential ranges 0.05 to 1.3 V, E_H and 0.05 to 1.05 V, E_H.
 (b) Variation of $(i_p)_{FA1}$ with H coverage, θ_H , at platinum controlled by Hg electrodeposition ($[HCOOH] = 0.25M$, $(dv/dt) = 50$ mV sec⁻¹).

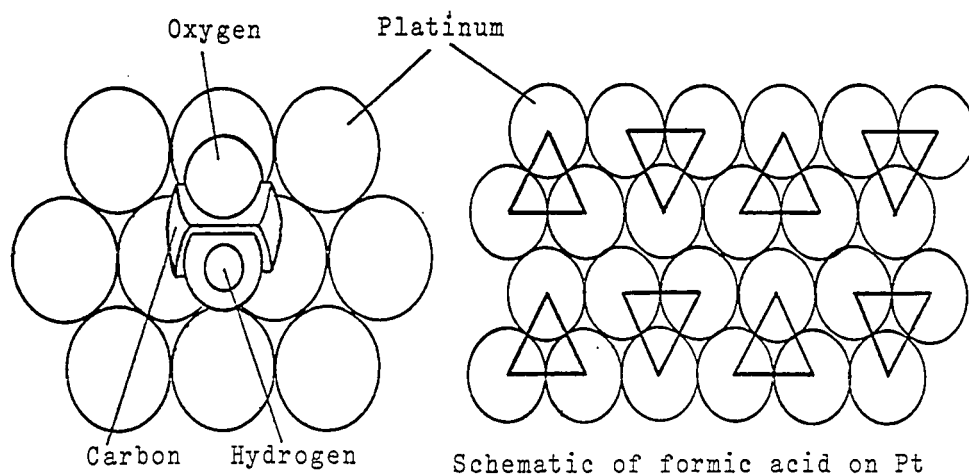
when formic acid, but not mercury, is present. The initial increase in the peak current for reaction FA_1 , as mercury begins to decrease the coverage by atomic hydrogen and/or the available free space for $HCOOH$ adsorption, continues until approximately 25% of the platinum sites at which H is electrochemisorbed has been blocked by mercury. Since the percentage of sites blocked at the inflection point is important when considering the reaction of formation of p , the 25% figure was checked by a procedure which did not involve the above assumption*. In this case, known coverages of mercury were first electrodeposited on the surface and the formic acid was added and the height of the FA_1 peak registered. This procedure was repeated in separate experiments for a series of θ_H values and the 25% figure was confirmed.

It is concluded that mercury acts in the same way as acetonitrile with regard to the FA_1 reaction, i.e. it behaves as a third body whose presence on the electrode surface decreases the formation of poison p (reaction (26)). The situation giving rise to the maximum $(i_p)_{FA_1}$ should correspond to the highest coverage by formic acid which can be attained without the presence of adjacent, adsorbed formic acid species close enough to one another to give rise to dehydration (i.e. reaction (26)). The maximum $(i_p)_{FA_1}$ exists when the platinum surface is ca. 25% covered with mercury and the subsequent decrease of $(i_p)_{FA_1}$ at higher mercury coverages (Fig. 57) is probably simply caused by mercury adsorption on platinum sites

*The assumption, simply stated, is that the mercury deposition occurs to the same extent in the presence or absence of formic acid.

on which the normal, main FA_1 reaction itself is occurring. It is seen, however, that even when mercury has blocked 75% of the surface, $(i_p)_{FA_1}$, after passing through its maximum value (Fig. 57), has the same value it had in the initial formic acid solution in the absence of mercury. This is consistent with the experimental findings of Brummer et al (138) who concluded that the formic acid oxidation reaction occurs on only 10% of the available platinum surface.

An approximate value of the mercury coverage which should give rise to a maximum $(i_p)_{FA_1}$ can be obtained with reference to a schematic representation of adsorbed formic acid on the 111 face of platinum. This representation is given below where the geometry of a formic acid molecule adsorbed on the 111 face is shown in relation to a schematic view of space occupied by two rows of adsorbed formic acid molecules* on the 111 face of platinum.



* The adsorbed formic acid molecules are drawn as triangles (shielding three platinum atoms) for convenience of representation. The formic anhydride molecule, not shown, can be seen from space-filling model to shield 5 platinum atoms.

It is to be noted that while one molecule of formic acid can form a chemisorption bond to one platinum atom site, the whole molecule effectively shields three platinum atom sites. This observation is discussed below (p.194) with regard to reaction mechanism.

The important conclusion from the above schematic model is that formic acid can occupy 30% of the sites on one line (or row) and none on the next line (or row), i.e. it occupies 1/3 of the available sites on each line. One-half of these occupied sites becomes blocked by mercury when its coverage is ca. 17%. The difference between this value and that of 25% which is experimentally observed is probably associated with the assumption in the above calculation that the adsorbed mercury only displaces those formic acid molecules which give rise to the reaction of p formation. There will probably be a certain amount of mercury which displaces otherwise reactive formic acid molecules and hence does not contribute to the increase in $(i_p)_{FA_1}$. In this way, it is reasonable that the experimentally determined mercury coverage corresponding to maximum $(i_p)_{FA_1}$ is found to be somewhat higher than that determined from models of the surface.

(h) Relation between the effects of mercury and acetonitrile

It is important to note that when $(i_p)_{FA_1}$ in Fig. 47 is plotted with respect to the hydrogen coverage, θ_H ,

corresponding to the various acetonitrile concentrations in aq. H_2SO_4 (Fig. 13), the reversal of direction of the increase in $(i_p)_{FA_1}$ occurs at 70% surface coverage by nitrile (Fig. 58). As was the case with mercury deposition (see above), the same results were obtained when θ_H was controlled with a particular $[CH_3CN]$ in the absence of formic acid followed by formic acid addition to the system.

The difference between the results with mercury and acetonitrile is probably associated with the ability of formic acid to displace, to some extent, acetonitrile from the surface. Therefore, the free space available for formic acid adsorption, which may be measured by θ_H determined in the presence of the added acetonitrile, can be substantially different from the space actually occupied by formic acid molecules when the latter are present on the surface together with acetonitrile. Formic acid coverage can hence be higher with reactant formation of p. In fact, it was noted on p.103 that acetonitrile can be rather easily washed from the platinum surface and would therefore be susceptible to displacement by formic acid. Electrodeposited mercury is much more difficult to clean from a platinum electrode and requires polarization at high anodic potentials for its complete removal; hence, the results with mercury (Fig. 57) should not be complicated by the possibility of displacement of mercury by formic acid and subsequent variation of θ_H . These conclusions are consistent with the above calculation of the θ_H value which would

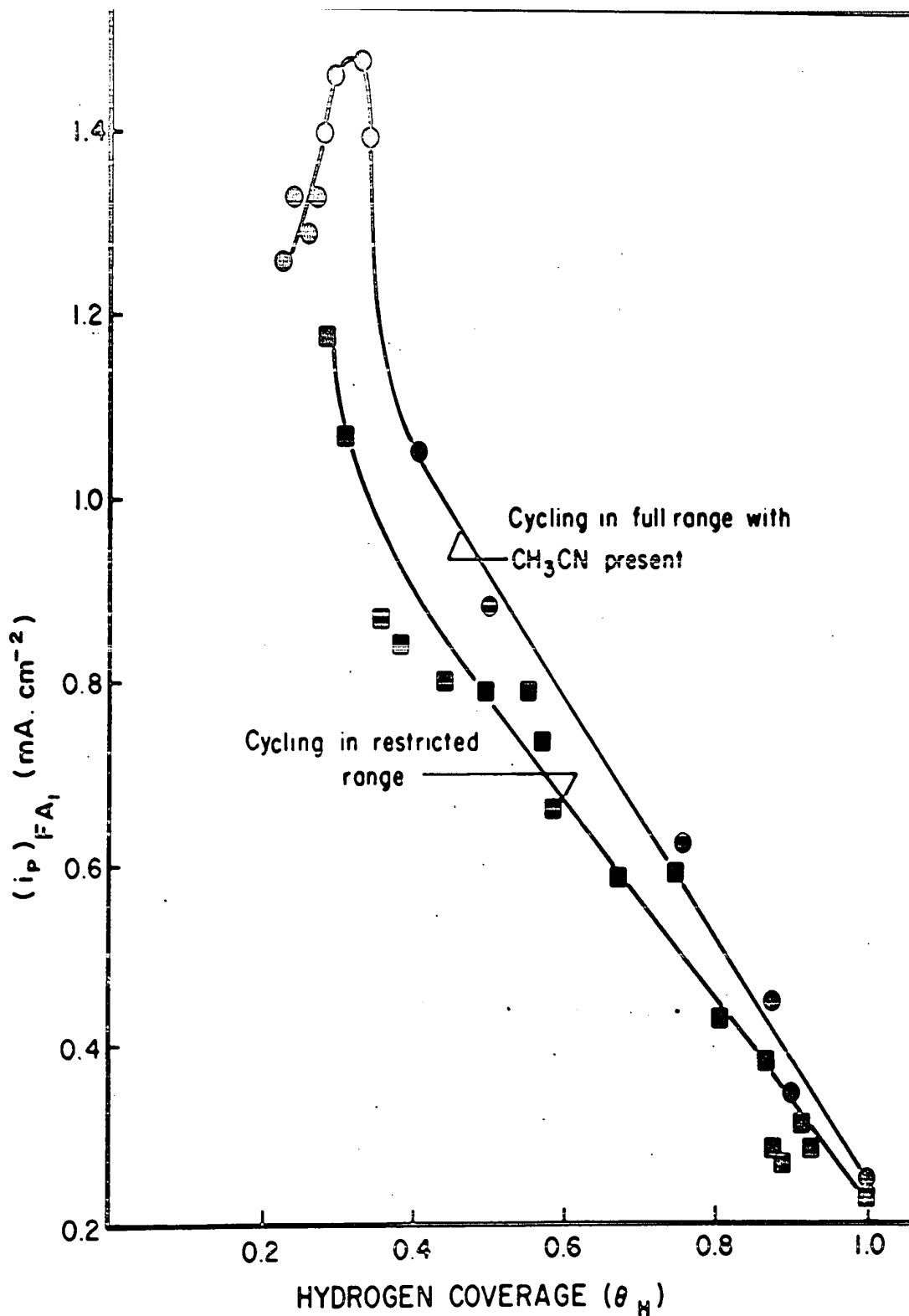


Fig. 58. Dependence of $(i_p)_{FA_1}$ on the apparent hydrogen coverage, θ_H , obtained with addition of various concentrations of acetonitrile (-o-, see text); potential range 0.05 to 1.5 V, E_H . Also shown is the increase of $(i_p)_{FA_1}$ as a function of apparent θ_H (see text) due to accumulation of adsorbed impurities during long-period cycling in a restricted potential range excluding surface oxidation (-□-), i.e. 0.05 to 0.9 V, E_H . For both cases, $[\text{HCOOH}] = 0.25\text{M}$, $(dV/dt) = 50 \text{ mV sec}^{-1}$.

correspond to a maximum $(i_p)_{FA_1}$, i.e. ca. 83% which is close to the value that was observed with mercury (ca. 75%).

(i) Effect of solution impurity adsorption on the formic acid reaction

Long-period cycling of a platinum electrode in aqueous H_2SO_4 in a restricted range of potentials (0.90 V to 0.05 V, E_H) without the participation of surface oxide which normally leads to repetitive cleaning of the surface causes a progressive decrease in the extent to which the electrode can be covered with atomic hydrogen. Depending on the length of time the restricted-range cycling is performed, θ_H and hence that part of the surface free from impurities can vary from 1.0 down to ca. 0.35. It is interesting to note that adsorption of adventitious impurities from solution affects the structure of the H adsorption region in much the same way as does mercury, i.e. there is a uniform and progressive decrease of both the peaks with time.

The effect of the varying θ_H caused by impurity adsorption upon the FA_1 reaction current was investigated by adding formic acid at 0.30 V, E_H on the cathodic sweep and registering the peak current for FA_1 on the first anodic sweep. The hydrogen coverage in this case is the actual one to which the formic acid is exposed and corresponds to the modified procedure described for mercury adsorption. A separate experiment is required for each θ_H value and hence each point obtained in Fig. 58 for impurity accumulation.

The reversal of direction of the increase in $(i_p)_{FA_1}$ for the acetonitrile system at ca. 70% apparent surface coverage with nitrile was due (as in the mercury case at coverages >ca. 25%) to blocking of those sites on which the FA_1 reaction itself is occurring. No such reversal was observed in the case of cycling in a restricted potential range, but this is no doubt associated with the ability of the formic acid to displace the accumulated impurities from the surface and thus considerably alter the true value of θ_H from the apparent value which is plotted in Fig. 58.

The ability of adsorbed impurities from solution to substantially alter $(i_p)_{FA_1}$ provides an explanation for the time-effects noted in the steady-state polarization curves for formic acid (Fig. 52). Between 0.54 and 0.7 V, E_H , the value of $(i_p)_{FA_1}$ was larger after the 90 sec polarization compared with the initial value. This may be due to slow decomposition of the poison p at these potentials, followed by some impurity accumulation because of the long periods of time at the potential of polarization without the electrode being subjected to surface oxidation. The adsorbed impurities evidently give rise to a "third body" effect, in the same way as did acetonitrile or mercury, with a consequent increase in $(i_p)_{FA_1}$.

The peak current for reaction FA_1 also increases with cycling in the restricted potential range (0.9 to 0.05 V, E_H) when formic acid is already in the electrolyte solution.

In this way, the value of $(i_p)_{FA_1}$ can be varied, depending on the end anodic potential of the sweep, i.e. depending on the extent of surface oxide formation on the platinum which results in various degrees of cleaning of the surface and hence increases the free surface available for adsorption of formic acid. It is obvious that after an increase in $(i_p)_{FA_1}$ is obtained by cycling in the restricted range, the extent of surface cleaning resulting from polarization to different end anodic potentials can be followed by the decrease in $(i_p)_{FA_1}$. This is shown in Fig. 59 for results obtained in a 0.25M HCOOH solution where impurity accumulation had occurred after sweeping over a restricted potential range. The end anodic potential was increased from the initial restricted range value of 0.9 V, E_H in increments of 0.05 V and the respective values of $(i_p)_{FA_1}$ were recorded after a reproducible multisweep was obtained. It is to be noted that the critical anodic potential for oxidation of impurities from the electrode surface is 1.1 V, E_H in the 0.25M HCOOH system. Up to this potential there is an increase in $(i_p)_{FA_1}$ which must be associated with the fact that the critical coverage with adsorbed formic acid species and subsequent formation of poison on a large part of the surface is only attained at 1.1 V, E_H . In the case of cycling in the absence of formic acid, it is found that an anodic potential of 1.1 V, E_H represents monolayer coverage of the surface with "OH" species (1 OH per Pt atom). However, with formic acid present in the

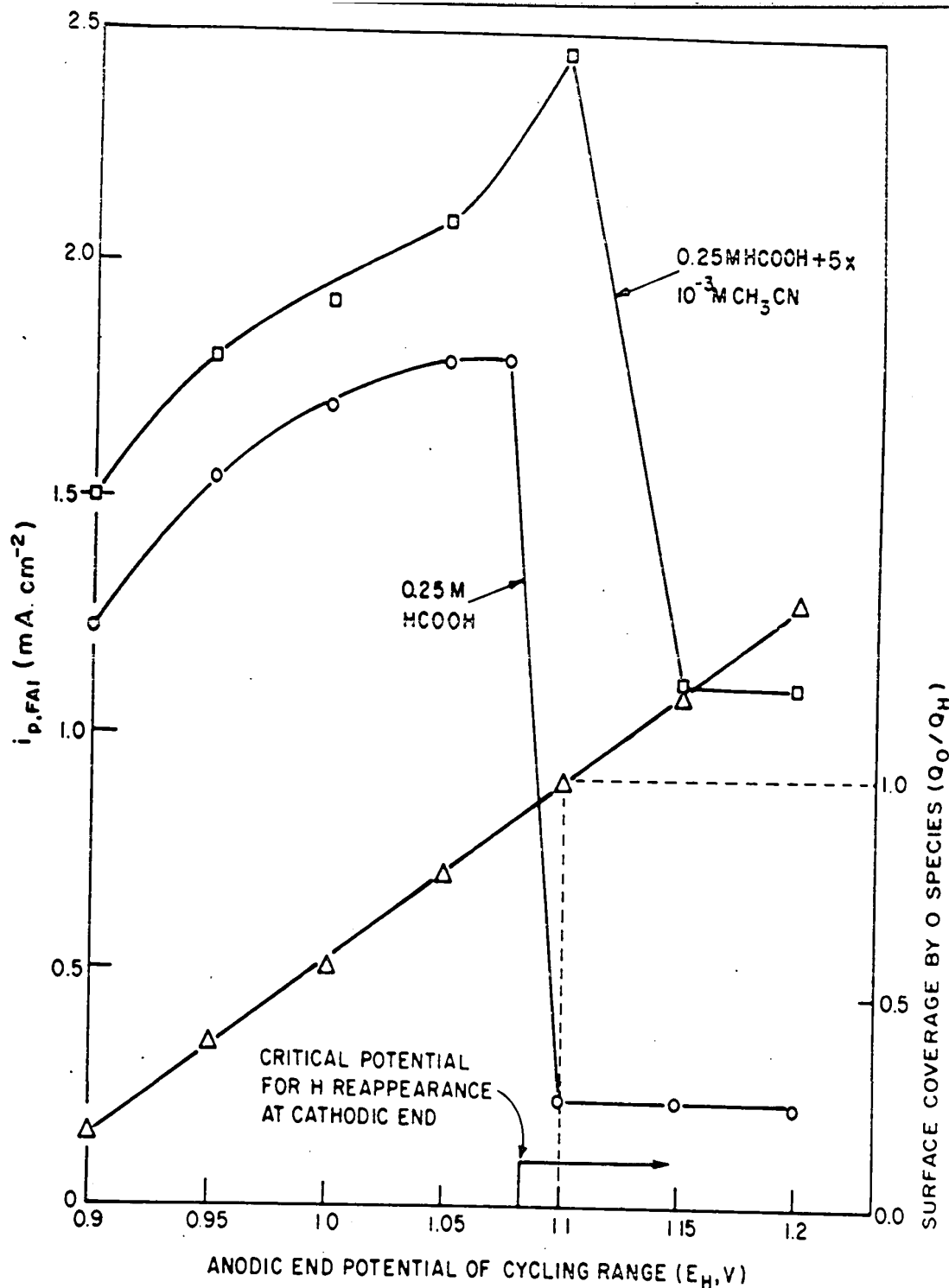


Fig. 59. Variation of $(i_p)_{FA1}$ with progressively increasing reversal potential in the anodic sweep in the region of Pt surface oxidation. Initial condition of $(i_p)_{FA1}$ at 0.9 V, E_H was achieved by extensive cycling in this restricted potential range with 0.25M HCOOH in the system. Critical surface cleaning effect arises at ca. 1.1 V, E_H leading to increase in coverage by adsorbed formic acid species. Also shown are the results of the same type of experiment but with $5 \times 10^{-3}M$ CH₃CN also present. $(dV/dt) = 50 \text{ mV sec}^{-1}$. The relative charge, Q_0/Q_H , for platinum surface oxidation is also given (Δ).

system, the potential at which monolayer coverage of surface oxide is reached will be shifted to somewhat more anodic values because of consumption of the surface oxide through reaction with the formic acid.

Fig. 59 also shows the results obtained with increasing anodic end potentials after previous cycling over the restricted potential range when 5×10^{-3} M CH_3CN was present in the solution together with the 0.25 M HCOOH . In this case, the decrease in $(i_p)_{\text{FA}_1}$ when the electrode surface is cleaned by means of anodic formation of surface oxide is not as large as that observed in the system in the absence of formic acid because the presence of acetonitrile decreases the extent to which free sites for formic acid electrochemisorption are made available by surface cleaning in the oxide region. The critical anodic end potential for cleaning impurities from the electrode surface which have arisen from the solution is higher with acetonitrile in the system; this is consistent with the observation that acetonitrile displaces the potential for formation of surface oxide at platinum to higher anodic values (as shown earlier in Fig. 31). The fact that there is an increase in $(i_p)_{\text{FA}_1}$ with cycling in the restricted potential range when acetonitrile is present indicates that there is still a substantial coverage with adjacent formic acid species at $[\text{CH}_3\text{CN}] = 5 \times 10^{-3}$ M. This arises because the formic acid can displace some of the adsorbed acetonitrile from certain surface sites whereas it cannot so effectively displace the impurities adsorbed from solution.

(j) Summary of the effects of acetonitrile on the oxidation of formic acid and methanol at platinum

- (i) Adsorbed acetonitrile decreases the currents for oxidation of methanol at platinum during potentiodynamic cycling in the potential region 0.05 to 1.5 V, E_H . In the case of formic acid, the anodic currents are also decreased by the presence of acetonitrile but with the important exception of the FA_1 reaction current, i.e. for formic acid oxidation in the double-layer region, on an anodic-going sweep which is increased.
- (ii) The increase of $(i_p)_{FA_1}$ during a potentiodynamic sweep in the presence of adsorbed acetonitrile can be as much as 600%, and this increase is also observed in the steady-state polarization curves for formic acid with acetonitrile present.
- (iii) A similar increase in $(i_p)_{FA_1}$ can be achieved by cycling in a potential range where the H region is excluded. Thus, acetonitrile does not give rise to a true activation effect but instead increases $(i_p)_{FA_1}$ by preventing formation of an inhibiting species p which is otherwise formed in the H region.
- (iv) The formation of p does not involve H itself since poison formation still occurs at 0.5 V, E_H . This fact, combined with the effect of acetonitrile, points to a sort of "dimerization" of adsorbed formic acid, perhaps in the form of a dehydration reaction to give adsorbed

formic anhydride as the poison. Adsorbed acetonitrile decreases the probability that two adsorbed formic acid species will be adjacent to one another; hence the extent of formation of p is decreased.

- (v) Electrodeposition of mercury also increases $(i_p)_{FA_1}$ up to a mercury coverage of 0.25, beyond which $(i_p)_{FA_1}$ begins to decrease because of mercury deposition on platinum sites at which the main FA_1 reaction occurs.
- (vi) A similar increase in $(i_p)_{FA_1}$ results from cycling in a restricted potential region, without the surface oxide reaction, because of accumulation of impurities on the electrode surface. After such treatment, an anodic potential of ca. 1.1 V, E_H is required for oxidizing the adsorbed impurities from the electrode surface and hence substantially decreasing $(i_p)_{FA_1}$ to its original value prior to impurity accumulation.

PART IV

Studies under Non-Aqueous Conditions

(a) Introduction

It is well known that the platinum electrode surface can act as a catalyst in numerous organic oxidation reactions (1). In aqueous systems, an increase in the electrode potential in the anodic direction not only results in stronger electron accepting properties but also gives rise to the formation of surface oxides on platinum. Mechanistic studies of oxidation reactions are complicated by the various stages of oxidation (see p. 6) of the platinum surface; indeed, as the potential of the platinum electrode changes, the organic reaction mechanism may also change since the type and coverage with surface oxide species can change. Consequently it is difficult to obtain information regarding the effect of electrode potential or corresponding electron charge density in the metal surface on catalytic activity from studies performed under aqueous conditions. The effects referred to here are concerned with catalytic activity per se, e.g. in dissociative chemisorption of organic molecules, and not with the direct electron accepting properties of the anode in an electrochemical charge transfer reaction.

Non-aqueous acetonitrile solutions were employed to study the effect of potential on some organic oxidations at platinum surfaces free from oxides. By comparison with the

behavior of water-containing solutions, these studies may provide information on the role of surface oxides in organic oxidation reactions at platinum. In non-aqueous acetonitrile systems, the platinum electrode can be potentiostated to high anodic potentials (up to 3.0 V, E_H) with no surface oxide formation (79,80). Amounts of surface oxide can then be independently controlled by water content of the solution and by anodic "end" potentials in a controlled potential program. However, as was shown above, acetonitrile can adsorb onto a platinum electrode surface without charge transfer from an aqueous solution, e.g. at 0.75 V, E_H , and therefore may also adsorb from the pure liquid. This means that although the platinum surface is free from oxide under 100% non-aqueous conditions in acetonitrile, it may not be free of adsorbed species derived directly from the acetonitrile without prior reduction or oxidation. These factors were taken into account in considering the results obtained with formic acid, methanol, formaldehyde and hydrogen oxidation reactions at platinum in anhydrous and water-containing acetonitrile, to be discussed below.

(b) Reference current-potential profiles in anhydrous acetonitrile in the absence of oxidizable substances

Comparison between the potentiodynamic sweep behavior at platinum in 1N H_2SO_4 and that in anhydrous acetonitrile containing 0.5 M $NaClO_4$ was given in Fig. 7. In the

anhydrous acetonitrile system, there is, as expected, no evidence of hydrogen or oxygen reactions at the platinum surface, only what appears to be the double-layer charging current. The latter is smaller in anhydrous acetonitrile because of the different dielectric properties of the solvent and solution of the ions of the electrolyte. Absence of residual currents in the potential range from 0.4 to 2.6 V, E_H in pure acetonitrile as solvent was best achieved with NaClO_4 as supporting electrolyte (see Fig. 62 below).

(c) Effects of additions of small quantities of water to the anhydrous system

The effect of addition of water on the potentiodynamic sweep for platinum in initially anhydrous acetonitrile in the potential range 0.15 to 1.4 V, E_H is shown in Fig. 60. The behavior of the system is not affected to a significant extent by added water until a concentration of 1M is reached, i.e. 2.0% H_2O . At this concentration of water, a small oxidation current is observed at the end of the anodic sweep but little effect arises on the cathodic sweep. Ninety seconds holding of the potential at 1.4 V, E_H in acetonitrile/1M H_2O gave the profile shown in Fig. 60d; the lack of any normal oxide reduction peak is to be noted. However, the anodic holding did result in an increase of the cathodic charge associated with reduction of a species produced in some prior oxidation reaction which occurred during the anodic holding.

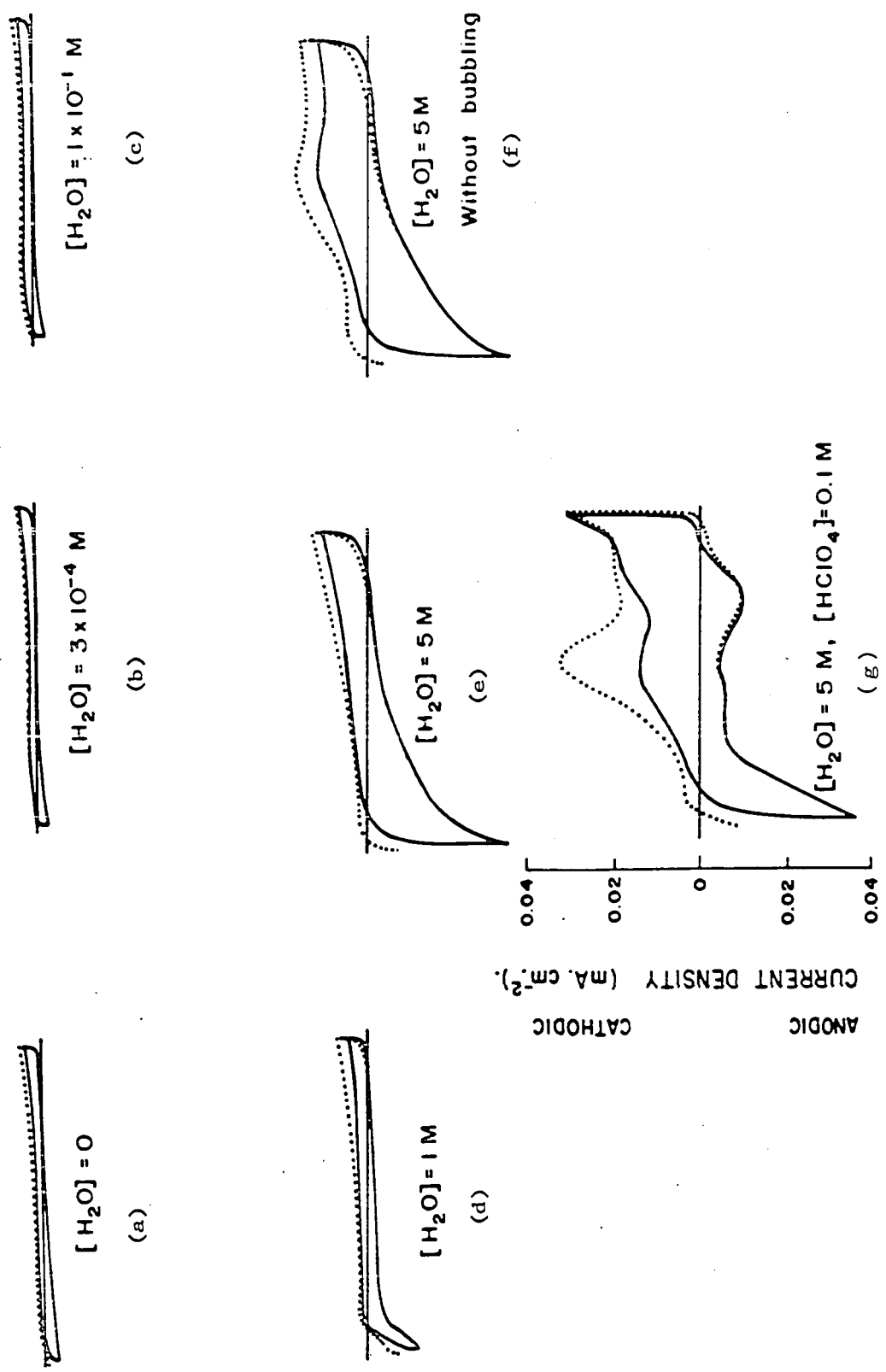


Fig. 60. Potentiodynamic *i*-V profiles for Pt in acetonitrile with 0.5 M NaClO₄ in the potential range 0.15 to 1.4 V, E_H showing the effects of various amounts of added water. Sweep profiles are shown in the case of multisweeps (---) and after 90 sec holding at the anodic termination potential (...). (dV/dt) = 50 mV sec⁻¹.

When the water content is increased to 5M, the i - V profile in Fig. 60e results; but even at this high water concentration, no observable oxide reduction peak results, even with 90 sec anodic holding at 1.4 V, E_H . When, however, the multi-sweep and anodic holding experiments are performed in the 5M H_2O system without nitrogen bubbling to stir the solution, a well defined oxide reduction peak immediately results (Fig. 60f). This reduction peak at 0.65 V, E_H again disappears when nitrogen bubbling is resumed.

There are two possible explanations for these results:

(i) nitrogen bubbling transports a species to the electrode which consumes the oxide and does not allow further oxidation of the platinum surface; (ii) nitrogen bubbling transports protons formed during the oxidation reaction ($Pt + H_2O \rightarrow PtOH + H^+ + e$) away from the electrode interface into the solution where they cannot easily be recovered for the reduction of surface oxide. The fact that the anodic potentiodynamic sweep in the oxide formation region is similar with or without nitrogen bubbling tends to refute the first argument, unless a chemical reaction were involved. Firm support for the second argument comes from Fig. 60g which shows that the oxide reduction peak for the 5M H_2O/CH_3CN system is very distinctive, even with nitrogen bubbling, when the system is made 0.1 M in perchloric acid. The amount by which this addition of perchloric acid increases the water content is insignificant, ($<10^{-2}$ M); however, it does provide a large increase in

proton concentration. In those cases where nitrogen bubbling was employed without added protons, oxide reduction was a slow, diffusion controlled process occurring over a large range of cathodic potentials, i.e., without exhibiting the sharp peak characteristic of surface oxide reduction in water.

In the H_2O/CH_3CN system with added perchloric acid, two other peaks are observed and correspond to acetonitrile reduction and oxidation in the double-layer region discussed in section I.1(c) above.

(d) Oxidation of molecular hydrogen in acetonitrile

The oxidation of molecular hydrogen at platinum is normally blocked by the formation of surface oxide (Fig. 61a). However, in anhydrous acetonitrile, oxidation of molecular hydrogen occurs at platinum over a broad range of potentials both in cathodic and anodic-going potentiodynamic sweeps (Fig. 62). In the presence of 1% water, the maximum currents for molecular hydrogen oxidation are enhanced but the range of potentials over which appreciable oxidation rates arise is diminished (Fig. 63). The significant decrease in the potential range for hydrogen reactivity in the cathodic sweep is due to oxide formation on the prior anodic sweep and the characteristic hysteresis between oxide formation and reduction is enhanced in acetonitrile systems because the potential for surface oxide formation is displaced to more anodic potentials (see p.67). Fig. 63 also shows a potentiodynamic sweep with an anodic termination potential of 1.6 V, E_H .

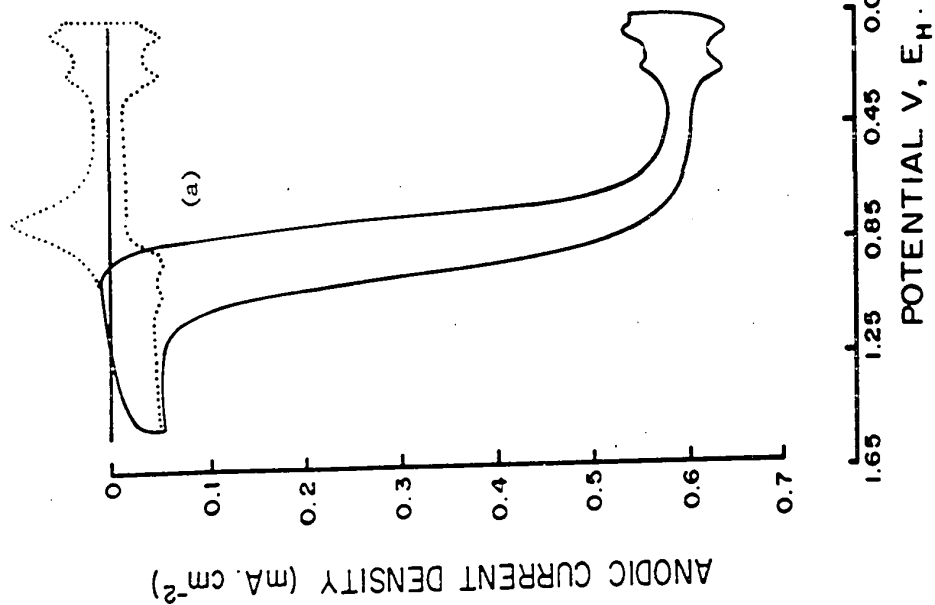
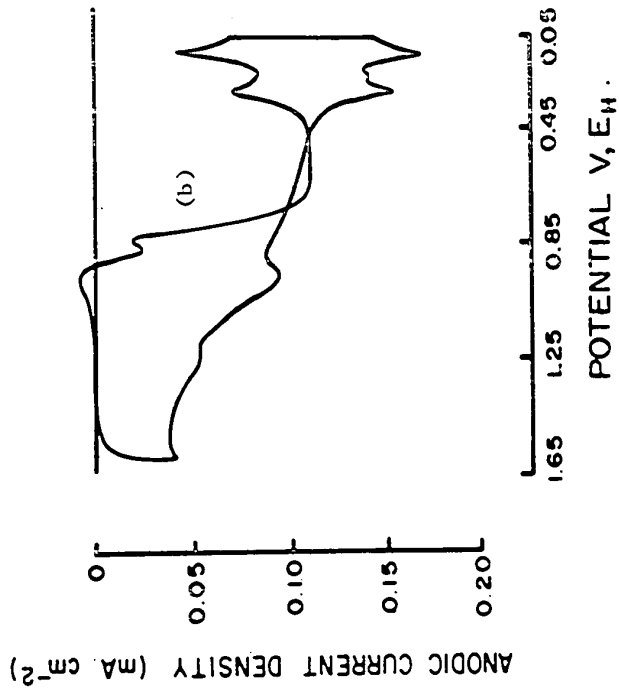
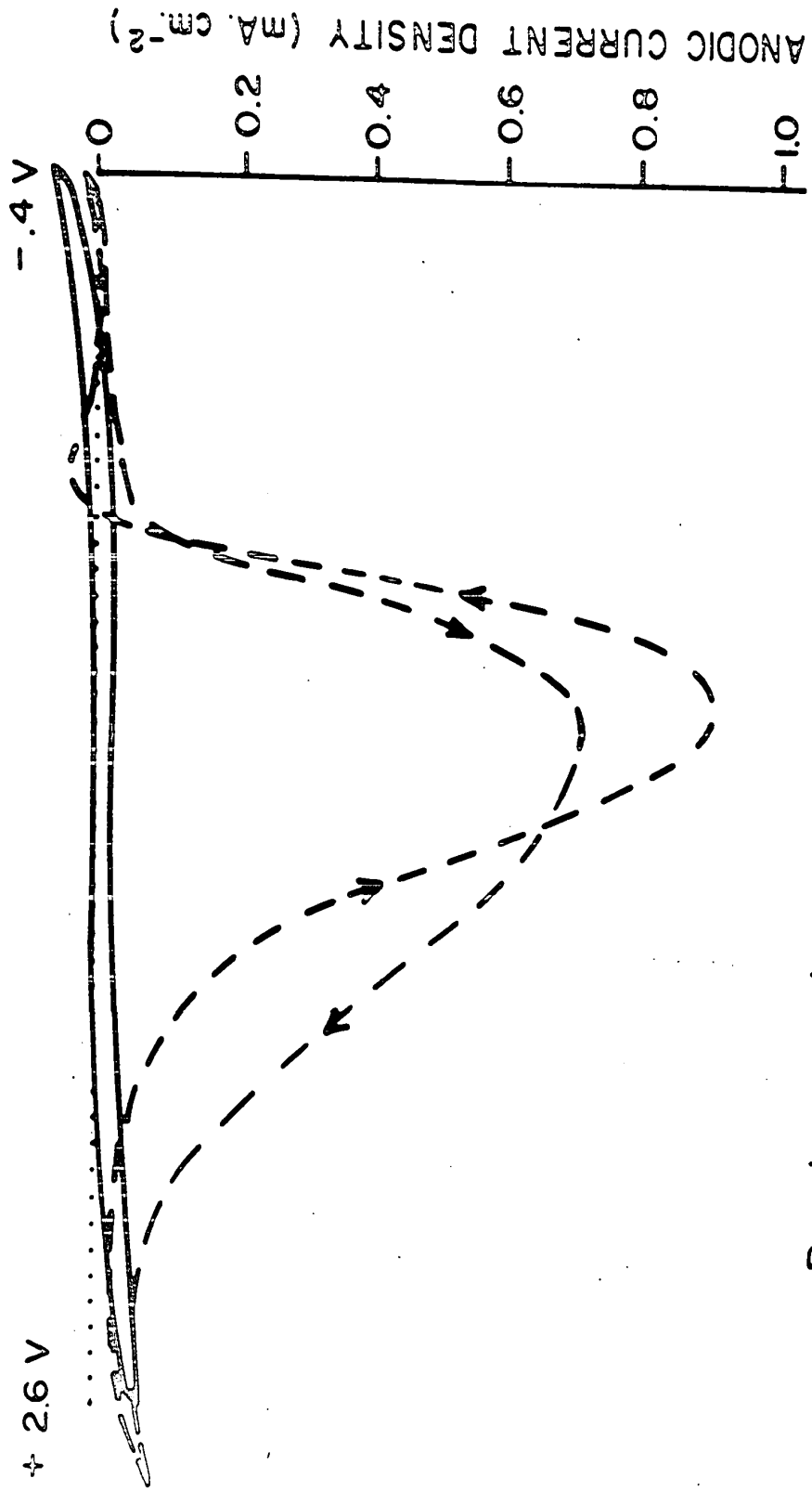


Fig. 61. (a) Potentiodynamic i - V profile for molecular hydrogen oxidation at Pt in 1N H_2SO_4 at electrode rotation rate of 4900 r.p.m. and $(dV/dt) = 50 \text{ mV sec}^{-1}$. Also shown is the background sweep obtained in the absence of hydrogen.
 (b) As in (a) but at a stationary platinum electrode, background not shown.



— Background
 --- H₂

Fig. 62. Potentiodynamic i-V profile for molecular hydrogen oxidation at platinum in anhydrous acetonitrile containing 0.5M NaClO₄, (dV/dt) = 600 mV sec⁻¹. Also shown is the sweep obtained in the absence of hydrogen.

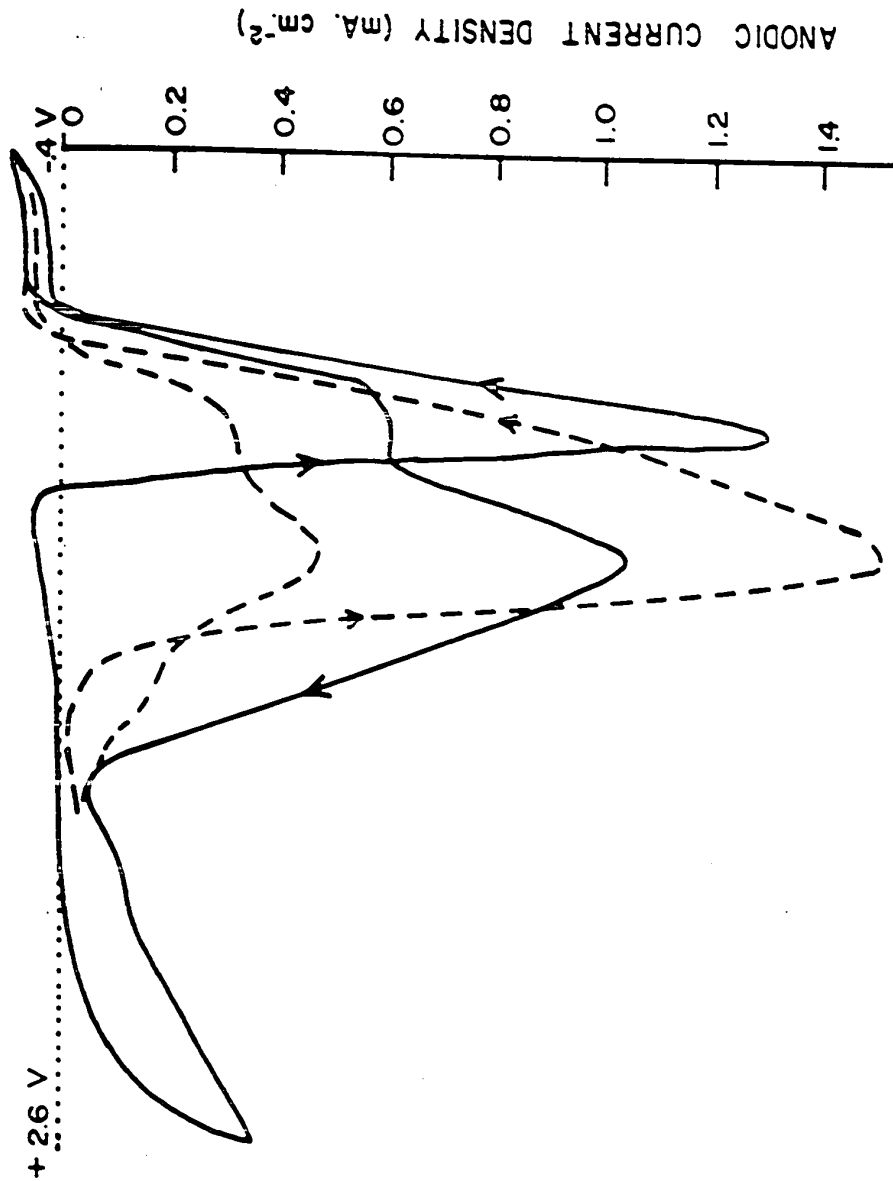
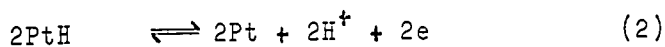
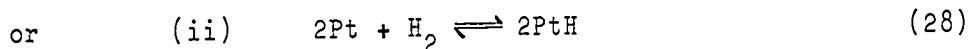
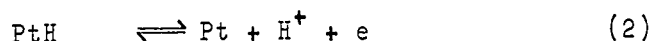
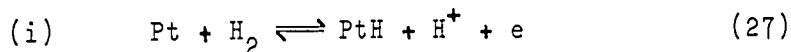


Fig. 63. Potentiodynamic *i*-V profiles at 600 mV sec⁻¹ for molecular hydrogen oxidation at platinum in anhydrous acetonitrile containing 0.5M NaClO₄ and 1.0% (ca. 0.5M) water in two potential ranges:
 ----- -0.4 to 1.6 V, EH
 _____ -0.4 to 2.6 V, EH

which is obviously too low an anodic potential for significant oxide formation in the 1% aqueous acetonitrile system. Thus, oxidation of molecular hydrogen at platinum in acetonitrile offers a sensitive, in situ test for the extent surface oxide formation and hence the presence of traces of water in the system.

The very sharply defined potential for oxide reduction in acetonitrile with 1% water when H₂ is present is to be contrasted with that for the case where no molecular hydrogen is involved, as discussed above (Fig. 60). The presence of molecular hydrogen in the system must hence provide a ready source of protons at the electrode by either of the following pairs of reactions:



As soon as free platinum sites become available by reduction of surface oxide with solution protons ($\text{PtOH} + \text{H}^+ + e \rightarrow \text{Pt} + \text{H}_2\text{O}$), an autocatalytic process will tend to occur with oxidation of molecular hydrogen on the free Pt sites providing further protons. The fact that molecular hydrogen is very reactive at platinum even in anhydrous acetonitrile may indicate one of two things: (a) molecular hydrogen, while unreactive at an oxide covered platinum surface, is

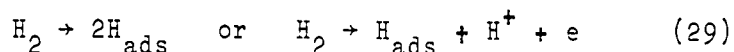
reactive at a surface covered with acetonitrile; (b) even in anhydrous acetonitrile there are still available free platinum sites for hydrogen oxidation and since this is a rapid faradaic process, relatively few free sites would be required to sustain large currents^{*}. In regard to the latter point, such a theory would favor mechanism (i) above where only one free site is required for hydrogen oxidation compared with the requirement of two neighboring sites for mechanism (ii). In connection with (a) above, another explanation for the molecular hydrogen reactivity might be based on the supposition that adsorbed acetonitrile can act as a mediator in the reaction, i.e., adsorbed acetonitrile could be reduced by molecular hydrogen but become rapidly reoxidized electrochemically if the potential were $>0.4 \text{ V, } E_{\text{H}}$.

(e) Oxidation of molecular hydrogen in aqueous solutions

Molecular hydrogen oxidation in aqueous solutions will be discussed here because of the connections with its oxidation in non-aqueous solvents. Fig. 61b shows a potentiodynamic sweep for H_2 oxidation at a stationary platinum electrode. The cathodic and anodic hydrogen adsorption and desorption peaks at platinum appear to arise independently of

* It was shown above (p.103) that even at full coverage by acetonitrile, the platinum surface may still have ca. 33% of the sites available because of the geometry of acetonitrile adsorbed on the electrode surface. However, it must be noted that although this value of 33% was also found experimentally, the system contained much smaller concentrations of acetonitrile (ca. $5 \times 10^{-3} \text{ M}$) than are to be found in the non-aqueous systems under consideration here.

the overall kinetic current for molecular hydrogen oxidation, i.e., a large overall molecular hydrogen current ($H_2 \rightarrow 2H^+ + 2e$) can pass and the anodic or cathodic partial processes ($H_{ads} \rightleftharpoons H^+ + e$) simply add or subtract component currents, to or from, respectively, the overall molecular H_2 current. A closer comparison of the H electrosorption peaks, with and without molecular hydrogen oxidation, revealed that the cathodic charge was somewhat diminished relative to the anodic H charge in the presence of molecular hydrogen. This could arise on account of a small contribution from the molecular hydrogen reaction to the atomic hydrogen coverage without passage of charge for its cathodic deposition, viz.



Since the contribution of the above processes to the ordinary hydrogen adsorption charge is very small (approximately 5% to the cathodic charge), these reactions of molecular hydrogen at platinum are less reversible than the usual atomic hydrogen electrosorption processes involving charge transfer with the solution species H_3O^+ . In the atomic hydrogen region, almost all of the adsorbed hydrogen resulting from the first stage of molecular hydrogen oxidation (reaction (29)) would be rapidly ionized from the surface since the equilibrium coverage with adsorbed hydrogen results mainly from the more reversible reaction $Pt + H_3O^+ + e \rightleftharpoons PtH + H_2O$.

(f) Oxidation of formic acid in acetonitrile

Formic acid was found to be inactive at a platinum electrode in anhydrous acetonitrile over the potential range 1.40 to 0.05 V, E_H , i.e., where it is normally very reactive in aqueous solutions (Fig. 2). A faradaic reaction arises at potentials more anodic than 1.5 V, E_H ; however, it is not known if this reaction is one involving formic acid and platinum surface oxide formed because of the water introduced into the system with addition of the formic acid. The reaction is not oxygen evolution since no molecular oxygen reduction current is observed, even after periods of holding the potential at the anodic end of the sweep. Formic acid oxidation is only observed at lower potentials (i.e. 0.20 to 0.65 V, E_H) when enough water is present in the system to give rise to surface oxide formation (Fig. 64). On the cathodic sweep, formic acid oxidation gives the characteristic anodic current when the surface oxide is partially reduced and free Pt sites are recovered. Fig. 64 shows a comparison between i - V profiles in the system with two different concentrations of water and it is seen that the reactivity of formic acid is enhanced in both regions of oxidation with increased water content in accord with the view that extent of surface oxidation of platinum depends on water concentration.

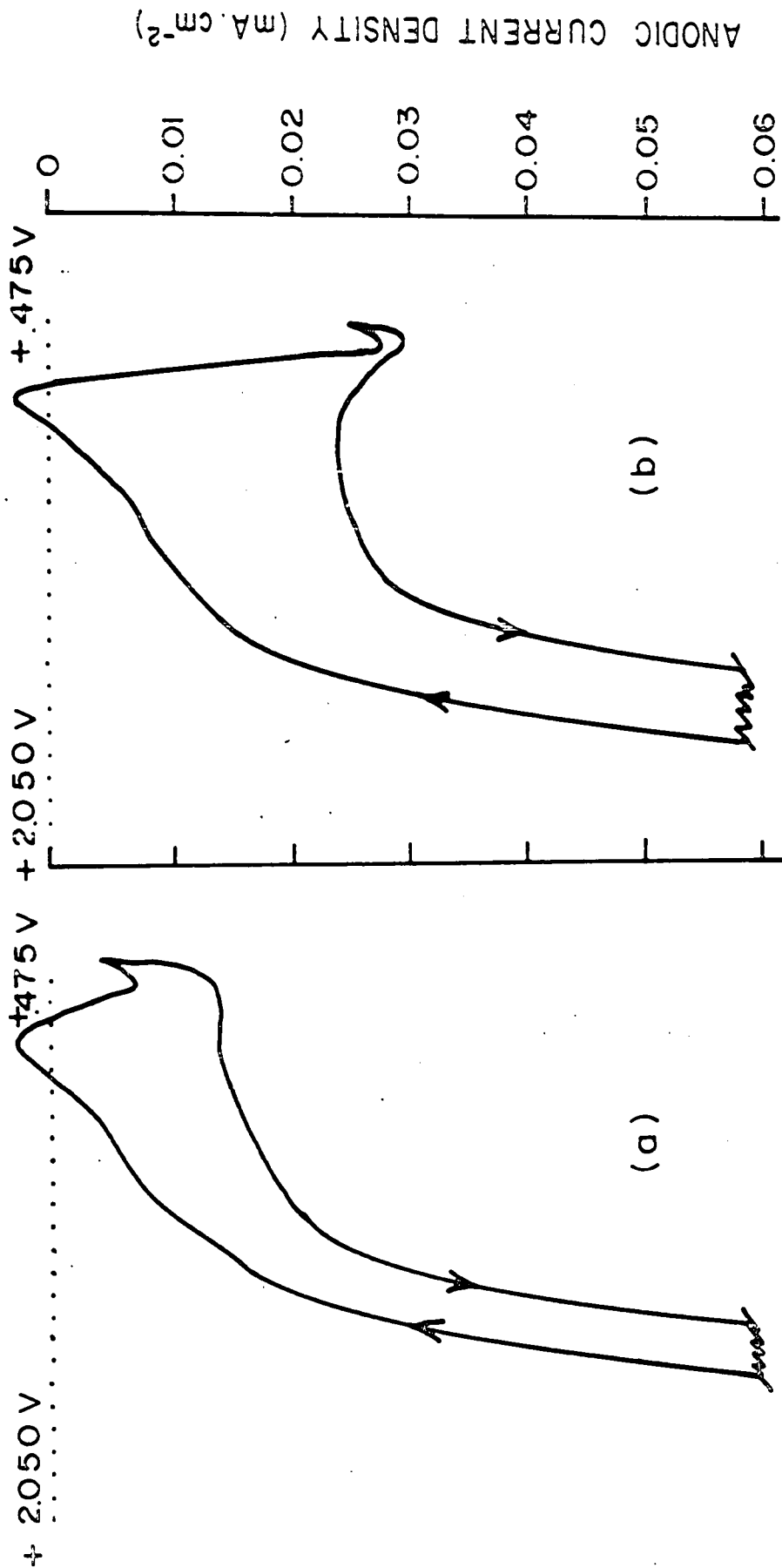


Fig. 64. Potentiodynamic i-V profiles for 0.25M HCOOH at Pt in acetonitrile/0.5M NaClO₄ with two concentrations of water: (a) 0.1M H₂O (.2%); (b) 1.0M H₂O (2%). (dv/dt) = 50 mV sec⁻¹.

(g) Oxidation of formaldehyde and methanol
in acetonitrile

The oxidation behavior of formaldehyde at platinum in nominally anhydrous acetonitrile is complicated, a small oxidation current passing in the first anodic sweep after addition of formaldehyde, but in subsequent sweeps the oxidation is completely inhibited. Because of this complex behavior in acetonitrile, formaldehyde was not studied extensively. Similarly, addition of methanol to a nominally anhydrous acetonitrile solvent system resulted in no oxidation activity at platinum, Fig. 65.*

(h) Conclusions from the work in nominally
anhydrous acetonitrile

The difference in reactivity of the three organic compounds mentioned has already been correlated (Part III) with the number of free platinum sites required for their dissociative adsorption and eventual oxidation. The fact that methanol oxidation is completely inhibited in anhydrous acetonitrile is in accord with the observations of Bagotsky and Vasiliev (17) that its adsorption at platinum requires at least three free sites in appropriate geometrical positions for dissociation of the three methyl H atoms. In the case of formaldehyde, somewhat more activity may be anticipated since

* This is in accord with results discussed on p.150 where it was shown that quite small concentrations (e.g. $10^{-2}M$) of acetonitrile in aqueous media result in complete inhibition of electrochemical oxidation of methanol at platinum.

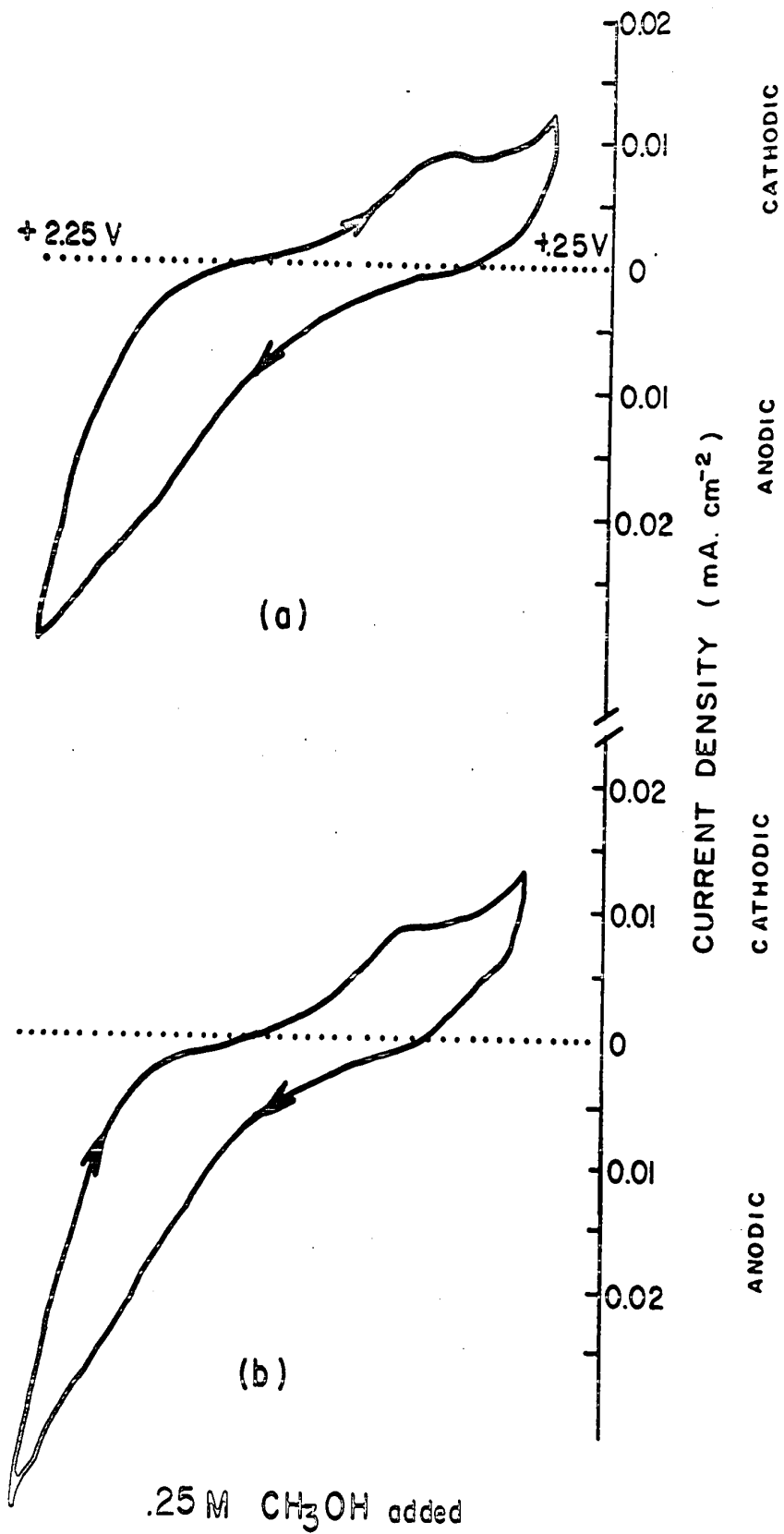
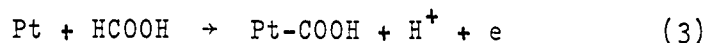
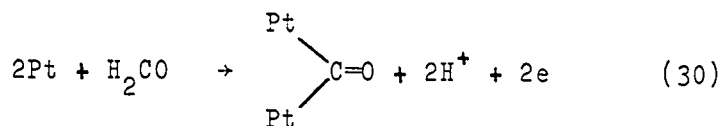
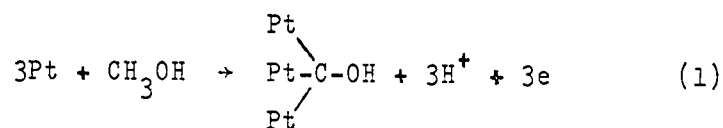


Fig. 65. Potentiodynamic i-V profiles for acetonitrile/0.5M NaClO₄ in the absence of (a) and in the presence of (b) 0.25M methanol, CH₃OH. (dV/dt) = 50 mV sec⁻¹.

only two free platinum sites are required for dissociative adsorption. The much greater activity of formic acid in the nominally anhydrous acetonitrile would, by this argument, be associated with the requirement of only one free platinum site for adsorption. The three dissociative adsorption reactions of interest are as follows:



This approach may, however, be oversimplified since space-filling models (see p.175) shows that although the adsorbed formic acid residue (-COOH) is presumably only adsorbed on one Pt site (or lattice hole), it occupies an area on the surface roughly equivalent to three Pt atoms. A somewhat different explanation of the observation with formic acid and methanol would be that formic acid can displace acetonitrile from the surface (see p.177) while methanol cannot. Different reaction mechanisms may also play a role, i.e. large oxidation currents for formic acid can be sustained by a small fraction of free Pt surface while this same fraction will give only small oxidation currents for the much slower reaction of methanol. Probably all three possibilities play a role. Support for the importance of site requirements

comes from the relatively high reactivity of H_2 which may be associated with the step $H_2 + Pt \rightarrow PtH + H^+ + e$ (requiring only 1 site) rather than $H_2 + 2Pt \rightarrow 2PtH \rightarrow 2Pt + 2H^+ + 2e$ requiring two adjacent sites.

(i) Summary of the results of non-aqueous studies

- (i) In non-aqueous acetonitrile media, the potential range over which the platinum surface is inert towards faradaic and pseudo-faradaic processes extends up to ca. 3.0 V, E_H ; however, this condition is partly due to the significant adsorption of acetonitrile on the platinum surface and subsequent blocking of the normal reactions at platinum even when some water is present.
- (ii) The reduction of platinum surface oxide in nominally anhydrous acetonitrile (and even with solutions containing 5M H_2O) is a diffusion controlled reaction because of the small concentration of protons in solution. Addition of a proton source such as an acid results in the usual behavior for reduction of platinum surface oxide.
- (iii) Although oxidation of molecular hydrogen on platinum is inhibited by surface oxide formation, the reaction readily occurs on a surface at which acetonitrile is adsorbed. As a consequence, oxidation of molecular hydrogen at platinum in anhydrous acetonitrile continues up to ca. 3.0 V, E_H with the range being lowered in the presence of water.

- (iv) Oxidation of molecular hydrogen at platinum in aqueous acid media during a potentiodynamic sweep does not significantly alter the shape of the atomic hydrogen adsorption/desorption peaks. This can be explained in terms of the greater reversibility in the case of electrochemical proton discharge in comparison with the adsorption and oxidation of molecular hydrogen.
- (v) Methanol displays no electroactivity in an acetonitrile solvent system, even in the presence of substantial amounts of water, as expected from the results given earlier (Fig. 46). Formic acid does display a small degree of activity when water is present in the system.

CLAIMS TO ORIGINAL RESEARCH

The following claims are made to original research which has been discussed in this thesis:

- (i) The adsorption of acetonitrile on platinum from aqueous H_2SO_4 solutions has been examined in detail with regard to the effects which this adsorption has on the normal surface reactions at platinum, i.e. hydrogen and oxygen adsorption in aqueous media. The electroactivity of the adsorbed acetonitrile has been extensively studied and a reaction mechanism was proposed for the reduction and oxidation of the adsorbed nitrile in the different potential regions at platinum.
- (ii) A technique has been developed to separate charge components associated with reaction of adsorbed acetonitrile in the H region from those of H deposition or ionization. This has been called the kinetic relaxation technique since it employs a method whereby the response of the various reactions to a rapidly changing potential signal is studied. It was only with the use of this method that true acetonitrile and hydrogen reaction charges could be established and the proposed acetonitrile reaction mechanism confirmed.
- (iii) A series of ten other nitriles was studied with regard to their effect on atomic hydrogen adsorption at platinum.
- (iv) At high concentrations of acetonitrile, adsorption of

another species was indicated, this species inhibiting the reduction-oxidation reactions of acetonitrile.

Its identity was postulated.

- (v) A new effect, in the form of an anodic current transient, arises when organic sulfur molecules such as thiourea and dimethylsulfide adsorb on platinum surfaces which are either partially or fully covered by adsorbed hydrogen. It was proved that the anodic transient charge arises from the displacement, by way of ionization, of chemisorbed hydrogen by the sulfur molecules. This effect was compared with, and shown to be quite different from, that which arises upon adsorption of methanol at platinum in the double-layer region. The anodic hydrogen displacement effect was also found with acetonitrile, benzonitrile and benzene; however, it was more complicated in these cases because of possible reduction of the adsorbed organic molecules.
- (vi) The effects of various concentrations of acetonitrile on the oxidation of methanol and formic acid at platinum in aqueous media were carefully studied. Acetonitrile was observed to activate the FA_1 reaction of formic acid, and the mechanism of this activation was studied in considerable detail. A mechanism was proposed for the activation in terms of the effects of acetonitrile on a blocking species, p , which is the formic acid poison. A new possibility was given for the identity of the p species with reference to the experimental results.

- (vii) Adsorbed mercury was also found to activate the FA_1 reaction at platinum, and the critical coverage with mercury was established experimentally and explained in terms of a model.
- (viii) The effect of adsorption of ordinary solution impurities on the FA_1 peak current was also studied at some length with an explanation of the results.
- (ix) The reaction of methanol, formic acid and hydrogen at platinum in non-aqueous acetonitrile media was studied. The inactivity of methanol and formic acid was explained in terms of the results in Part I. Molecular hydrogen oxidation in non-aqueous acetonitrile occurred over a much larger range of potential than was observed in aqueous media. It was shown that this last result is associated with the absence of oxide formation in non-aqueous acetonitrile media.
- (x) The reduction of platinum surface oxide in nominally anhydrous acetonitrile was studied and the reaction was found to be diffusion controlled even at 5M H_2O because of the small concentration of protons in solution.

REFERENCES

1. J. O'M. Bockris and H. Wroblowa, J. Electroanal. Chem., 7, 428 (1964).
2. B. E. Conway and J. O'M. Bockris, J. Chem. Phys., 26, 532 (1957); M. W. Breiter, Trans. Faraday Soc., 61, 749 (1965).
3. F. Will and C. A. Knorr, Zeit. fur Elektrochem., 64, 258 (1960).
4. B. E. Conway, Rev. Pure and Appl. Chem., 18, 105 (1968).
5. B. E. Conway and H. A. Kozłowska, in course of publication (1972).
6. A. K. N. Reddy, M. Genshaw and J. O'M. Bockris, J. Electroanal. Chem., 8, 406 (1964).
7. F. P. Bowden and E. K. Rideal, Proc. Roy. Soc. London, A120, 59, 80 (1928).
8. A. N. Frumkin and A. I. Slygin, Acta Physiochim. U.R.S.S., 3, 791 (1935); 4, 991 (1936).
9. P. J. Lingane, Anal. Chem., 39, 485 (1967).
10. D. G. Peters and R. A. Mitchell, J. Electroanal. Chem., 10, 306 (1965).
11. J. J. Lingane, J. Electroanal. Chem., 1, 379 (1960).
12. B. E. Conway, E. Gileadi and H. A. Kozłowska, J. Electrochem. Soc., 112, 341 (1965).
13. H. A. Kozłowska and B. E. Conway, J. Electroanal. Chem., 7, 109 (1964).

14. P. Dolin and B. V. Ershler, Acta Physicochim. U.R.S.S., 13, 747 (1940).
15. A. Eucken and B. Weblus, Z. Elektrochem., 55, 115 (1951).
16. M. Breiter, Trans. Symp. Electrode Processes, Philadelphia, Pa., 1959 (1961), 307; see also J. Electrochem. Soc., 109, 42 (1962); and Electrochim Acta, 7, 533 (1962); and J. Electroanal. Chem., 7, 38 (1961).
17. V. S. Bagotsky and Y. B. Vasiliev, Electrochim. Acta, 12, 1323 (1967).
18. O. A. Khazova, Y. B. Vasiliev and V. S. Bagotsky, Elektrokimiya, 1, 82 (1965); V. S. Bagotsky and Y. B. Vasiliev, Electrochim. Acta, 11, 1439 (1966).
19. M. W. Breiter and S. Gilman, J. Electrochem. Soc., 109, 622, 1099 (1962); S. Gilman, Trans. Faraday Soc., 62, 466 (1966); M. W. Breiter, Electrochim. Acta, 7, 533 (1962); M. W. Breiter, J. Phys. Chem., 69, 3377 (1965).
20. Hira Lal, O. A. Petrii and B. I. Podlovchenko, Elektrokimiya, 1, 316 (1965).
21. R. E. Smith, H. B. Urbach, J. H. Harrison and N. L. Hatfield, J. Phys. Chem., 71, 1250 (1967).
22. S. S. Sedova, Y. B. Vasiliev and V. S. Bagotsky, Elektrokimiya, 4, 1113, 1221 (1968).
23. S. B. Brummer, J. Phys. Chem., 69, 562, 1363 (1965); see also S. B. Brummer and A. C. Makrides, J. Phys. Chem., 68, 1448 (1964).
24. M. W. Breiter, Electrochim. Acta, 8, 447, 457 (1963).

25. J. Giner, *Electrochim. Acta*, 9, 63 (1964); 8, 857 (1963).
26. S. B. Brummer, *Elektrokhimiya*, 4, 243 (1968); see also *J. Electrochem. Soc.*, 113, 1041 (1966).
27. Y. B. Vasiliev and V. S. Bagotsky, *Toplivniye elementy*, p.108, *Izd. Nauka*, Moscow (1964).
28. N. Minakshisundaram, Y. B. Vasiliev and V. S. Bagotsky, *Elektrokhimiya*, 3, 193, 283 (1967).
29. A. Kuhn, H. Wroblowa and J. O'M. Bockris, *Trans. Faraday Soc.*, 63, 1458 (1967).
30. J. O'M. Bockris, H. Wroblowa, E. Gileadi and B. J. Piersma, *Trans. Faraday Soc.*, 61, 2531 (1965).
31. D. Gilroy and B. E. Conway, *J. Phys. Chem.*, 69, 1259 (1965).
32. B. E. Conway, J. Wojtowicz and D. Gilroy, *Proc. 2nd International Congress on Fuel Cells, S.E.R.A.I., Brussels, 1967*.
33. H. Wroblowa, B. J. Piersma and J. O'M. Bockris, *J. Electroanal. Chem.*, 6, 401 (1963).
34. A. N. Frumkin and E. A. Aikazyan, *Dokl. Akad. Nauk. SSSR*, 100, 315 (1955).
35. E. A. Aikazyan, *Zh. Fiz. Khim.*, 33, 1016 (1959).
36. S. Schuldiner, *J. Electrochem. Soc.*, 115, 897 (1968); 115, 362 (1968); 116, 767 (1967).
37. A. I. Shlygin and G. A. Bogdanovskii, *Zh. Fiz. Khim.*, 31, 2428 (1957); 34, 57 (1960).

38. B. E. Conway, E. Gileadi and M. Dzieciuch, *Electrochim. Acta*, 8, 143 (1963); E. Gileadi and B. E. Conway, Chapter 5, *Modern Aspects of Electrochemistry*, Vol. III, London (1964).
39. J. Salt, G. Horanyi and F. Nagy, *Acta Chim. Hung.*, 63, 385 (1970).
40. P. I. Dolin, D. V. Kokovlina et al., *Dokl. Akad. Nauk. S.S.S.R.*, 144, 1081 (1962); 147, 649 (1962).
41. Y. M. Volifkovich, Y. B. Vasiliev and V. S. Bagotsky, *Elektrokhimiya*, 5, 1462 (1969).
42. F. C. Anson, *Anal. Chem.*, 33, 934 (1961).
43. F. C. Anson and D. M. King, *Anal. Chem.*, 34, 362 (1962).
44. A. J. Appleby, *J. Electroanal. Chem.*, 24, 97 (1970).
45. A. J. Appleby, *J. Electrochem. Soc.*, 117, 328 (1970).
46. A. Damjanovic and J. O'M. Bockris, *Electrochim. Acta*, 11, 376 (1966).
47. A. N. Frumkin and A. I. Slygin, *Acta Physicochim. U.R.S.S.*, 3, 791 (1935); J. Pearson and J. A. V. Butler, *Trans. Faraday Soc.*, 34, 1163 (1938); D. Gilroy and B. E. Conway, *Can. J. Chem.*, 46, 875 (1968).
48. J. Wojtowicz, N. Marincic and B. E. Conway, *J. Chem. Phys.*, 48, 4333 (1968); J. Wojtowicz, D. Gilroy and B. E. Conway, *Proc. 2nd International Conference on Fuel Cells, S.E.R.A.I., Brussels, 1967*.
49. I. Langmuir, *Trans. Am. Electrochem. Soc.*, 29, 125 (1916); M. I. Temkin, *Zh. Fiz. Khim.*, 15, 296 (1941).

50. B. E. Conway and E. Gileadi, *Trans. Faraday Soc.*, 58, 2493 (1962).
51. M. W. Breiter, *Electrochim. Acta*, 7, 601 (1962).
52. M. W. Breiter, *J. Electrochem. Soc.*, 109, 425 (1962).
53. B. E. Conway and A. K. Vijh, *J. Org. Chem.*, 31, 4283 (1966).
54. B. E. Conway and A. K. Vijh, *Z. Anal. Chem.*, 224, 160 (1967); 224, 149 (1967).
55. M. Fleischmann and D. Pletcher, *Tetrahedron Letters*, 60, 6255 (1968).
56. C. D. Russii, *Anal. Chem.*, 35, 1291 (1963).
57. K. K. Barnes and C. K. Mann, *Anal. Chem.*, 32, 1474 (1967).
58. B. E. Conway, N. Marincic, D. Gilroy and E. J. Rudd, *J. Electrochem. Soc.*, 113, 1144 (1966).
59. J. F. K. Wilshire, *Aust. J. Chem.*, 16, 432 (1963).
60. J. F. O'Donnel and C. K. Mann, *J. Electroanal. Chem.*, 13, 157 (1967).
61. W. Heiland, E. Gileadi and J. O'M. Bockris, *J. Phys. Chem.*, 70, 1207 (1966).
62. T. Osa, A. Yildiz and T. Kuwana, *J. Am. Chem. Soc.*, 91, 3994 (1969).
63. R. F. Dapo and C. K. Mann, *Anal. Chem.*, 35, 677 (1963).
64. M. T. Melchoir and A. H. Maki, *J. Chem. Phys.*, 34, 471 (1961)
65. J. P. Billon, *Bull. Soc. Chim. (France)*, 923 (1961).
66. G. Caquis, J. P. Billon, J. Ransen and Y. Thibaud, *Comptes. Rend.*, 257, 2128 (1963).

67. G. J. Hoytink, Disc. Faraday Soc., 45, 14 (1968).
68. R. A. Marcus, J. Chem. Phys., 43, 2654 (1965).
69. D. M. Hercules, Science, 145, 808 (1964).
70. J. R. Jezorek and H. B. Mark, Jr., J. Phys. Chem., 74, 1627 (1970).
71. J. Badoz-Lambling, Mises au Point de Chimie Analytique, Series 11, p.8 (1963).
72. S. Wawzonek and M. E. Runner, J. Electrochem. Soc., 99, 457 (1952).
73. J. F. O'Donnell, J. T. Ayres and C. M. Mann, Anal. Chem., 37, 1161 (1968).
74. J. F. Coetzee, G. P. Cunningham, D. K. McGuire and G. R. Padmanabham, Anal. Chem., 34, 1138 (1962).
75. G. A. Forcier and J. W. Oliver, Anal. Chem., 37, 1147 (1965).
76. N. S. Moe, Acta Chem. Scand., 21, 1389 (1967).
77. J. E. McClure and D. L. Maricle, Anal. Chem., 39, 236 (1967).
78. J. W. Loveland and G. R. Dimeler, Anal. Chem., 33, 1196 (1961).
79. J. Vedel and B. Trémillon, J. Electroanal. Chem., 1, 241 (1959/60); J. J. O'Connor and I. W. Pearl, J. Electrochem. Soc., 111, 335 (1964).
80. J. P. Billon, J. Electroanal. Chem., 1, 486 (1959/60).
81. C. Papon and J. Jacq, Bull. Soc. Chim. (France), 1, 13 (1965).

82. Yu. M. Tyurin and G. F. Volodin, *Elektrokhimiya*, 5, 1203 (1969).
83. T. C. Franklin and R. D. Sothorn, *J. Phys. Chem.*, 58, 951 (1954).
84. B. E. Conway, H. A. Kozłowska, B. MacDougall and B. V. Tilak, Proc. 2nd International Conference on Fuel Cells, 1968, S.E.R.A.I., Brussels, 1969.
85. M. Ohta, *Bull. Chem. Soc. Japan*, 17, 485 (1942).
86. M. J. D. Low and P. L. Bartner, *Can. J. Chem.*, 48, 7 (1970).
87. K. F. Purcell and R. S. Drago, *J. Am. Chem. Soc.*, 88, 919 (1966).
88. B. Swanson and D. F. Shriver, *Inorg. Chem.*, 9, 1406 (1970).
89. A. Zecchina, E. Guglielminotti, S. Coluccia and E. Borello, *J. Chem. Soc., A*, 2196 (1969).
90. M. F. Farona and N. J. Bremer, *J. Am. Chem. Soc.*, 88, 3735 (1966).
91. R. E. Clarke and P. C. Ford, *Inorg. Chem.*, 9, 227 (1970).
92. O. M. Oranskaya and V. N. Filimonov, *Dokl. Phys. Chem.*, 194, 675 (1970).
93. O. M. Oranskaya, V. N. Filimonov and Ya. E. Shmulyakovskii, *Kinetika i Kataliz*, Vol. II, 727 (1970).
94. J. Tafel, *Zeit. physik. Chem.*, 50, 641 (1905).
95. B. E. Conway, *Theory and Principles of Electrode Processes*, Ronald Press, New York (1965).

96. B. E. Conway and E. Gileadi, *Can. J. Chem.*, 42, 90 (1964); see also *J. Chem. Phys.*, 39, 3420 (1963).
97. S. Srinivasan and E. Gileadi, *Electrochim. Acta*, 11, 321 (1966).
98. J. E. B. Randles, *Trans. Faraday Soc.*, 44, 327 (1948); A. Seuick, *Coll. Czech. Chem. Commun.*, 13, 349 (1948).
99. P. Delahay, *New Instrumental Methods in Electrochemistry*, Interscience Publishers, Ltd., London, 1954.
100. J. C. P. Mignolet, *Disc. of Faraday Soc.*, 8, 105 (1950).
101. T. Biegler, D. A. J. Rand and R. Woods, *J. Electroanal. Chem.*, 29, 269 (1971).
102. S. Gilman and M. W. Breiter, *J. Electrochem. Soc.*, 109, 622, 1099 (1962).
103. V. S. Bagotsky and Y. B. Vasiliev, *Electrochim. Acta*, 11, 1439 (1966); S. Gilman, *J. Phys. Chem.*, 66, 2657 (1962); 67, 78, 1898 (1963); 68, 70 (1964).
104. H. Dahms and M. Green, *J. Electrochem. Soc.*, 110, 1075 (1963).
105. E. Gileadi, L. Duic and J. O'M. Bockris, *Electrochim. Acta*, 13, 1915 (1968).
106. E. Gileadi, B. T. Rubin and J. O'M. Bockris, *J. Phys. Chem.*, 69, 3335 (1965).
107. J. O'M. Bockris and A. K. N. Reddy, *Modern Electrochemistry*, Vol. 2, Plenum Press, New York (1970).
108. V. V. Sobol, A. A. Dmitrieva and A. N. Frumkin, *Electrokhimiya*, 3, 928 (1967).

109. B. E. Conway, H. A. Kozłowska and W. Sharp, D.R.B. Report on Grant No. N.G.R. 52-093-001, June (1971).
110. K. J. Vetter and D. Berndt, Z. Electrochem., 62, 378 (1958); see also K. Dietz and R. Gohr, Electrochim. Acta, 8, 343 (1963); S. Gilman, Electrochim. Acta, 9, 1025 (1964).
111. K. B. Wiberg and K. A. Saegerbarth, J. Am. Chem. Soc., 79, 2822 (1957); see also J. E. Coleman, C. Ricciuti and D. Swern, J. Am. Chem. Soc., 78, 5342 (1956).
112. J. N. Butler, Adv. Electrochem. and Electrochem. Eng. (eds. Delahay and Tobias).
113. B. E. Conway and M. Dzieciuch, Can. J. Chem., 41, 21, 38 (1963); see also J. J. MacDonald and B. E. Conway, Proc. Roy. Soc. London, A269, 419 (1962).
114. D. J. G. Ives and G. J. Janz, Reference Electrodes, Theory and Practice, Academic Press, New York, 1961.
115. J. J. MacDonald and B. E. Conway, Proc. Roy. Soc. (London), A269, 419 (1962); see also B. E. Conway, Proc. Roy. Soc. (London), A256, 128 (1960).
116. A. K. Vijh, Ph.D. Thesis, University of Ottawa (1966).
117. B. MacDougall, H. A. Kozłowska and B. E. Conway, J. Electroanal. Chem., 32, 477 (App.15)(1971).
118. F. Veatch, J. D. Idol, F. S. Jaworowski and L. S. Szabo, Hydrocarbon Process Petrol Refiner, 43, 177 (1964).
119. B. E. Conway, B. MacDougall and H. A. Kozłowska, Trans. Faraday Soc., in press (1972).

120. B. E. Conway and L. Laliberté, Symposium on Optical Studies of Adsorbed Species, Faraday Society (1970) London.
121. D. Gilroy and B. E. Conway, Can. J. Chem., 46, 875 (1968).
122. P. Stonehart, H. A. Kozłowska and B. E. Conway, Proc. Roy. Soc. London, A130, 541 (1969).
123. R. P. Eischens and W. A. Pliskin, Adv. in Catalysis, 10, 1 (1958).
124. S. B. Brummer and K. Cahill, Disc. Faraday Soc., 45, 67 (1968).
125. X. de Hemptinne and K. Schunk, Annal. Soc. Sci. Bruxelles, 80 III, 289 (1966); see also Memoires Acad. Roy. Belg., Classe des Sciences, 32, 1 (1961).
126. S. Gilman, Trans. Faraday Soc., 62, 481 (1966).
127. E. Oikawa, K. Mori and G. Saito, Bull. Soc. Chim. Japan, 39, 1182 (1966; see also E. Oikawa and Shu Kambara, J. Polymer Sci., 2, 649 (1964).
128. J. J. Conn and A. Taurins, Can. J. Chem., 31, 1211 (1953).
129. S. Gilman, J. Phys. Chem., 67, 78 (1962).
130. H. F. Halliwell and S. C. Nyburg, Trans. Faraday Soc., 59, 1126 (1963).
131. A. A. Balandin, Zeit. Phys. Chem., B2, 289 (1929); also 33, 167 (1929).
132. D. L. Smith and R. P. Merrill, J. Chem. Phys., 52, 5861 (1970).

133. M. A. V. Devanathan and M. Selvaratnam, *Trans. Faraday Soc.*, 56, 1820 (1960).
134. H. Binder, G. Sanstede and A. Köhling, *Nature*, 214, 268 (1964); see also *J. Electroanal. Chem.*, 17, 111 (1968).
135. B. E. Conway and M. Dzieciuch, *Can. J. Chem.*, 41, 21, 55 (1963).
136. V. S. Bagotskii and Y. B. Vasiliev, *Electrochim. Acta*, 9, 869 (1964); also *Elektrokhimiya*, 6, 157 (1970).
137. C. W. Fleischman, G. K. Johnson and A. T. Kuhn, *J. Electrochem. Soc.*, 112, 602 (1964).
138. A. H. Taylor, R. D. Pearce and S. B. Brummer, *Trans. Faraday Soc.*, 66, 2076 (1970).